THE UNIVERSITY
of EDINBURGH

TWIST1: a Subtle Modulator of Neural Differentiation and Neural Tube Formation

Paul Andrei Nistor

THE UNIVERSITY
of EDINBURGH

A thesis submitted in fulfilment of requirements for the degree of
Doctor of Philosophy

to

MRC Centre for Regenerative Medicine,
College of Medicine and Veterinary Medicine
University of Edinburgh

2013

I declare that this thesis is of my own composition. The work presented in this thesis is my own, unless otherwise stated. The work described in this thesis has not been submitted for any other degree or professional qualification.

Paul Andrei Nistor

“Nicio limită nu este eternă, dar etern este o limită.”

Titu Maiorescu

“No boundary stands forever, but forever stands a boundary.”

Titu Maiorescu

ABSTRACT

The central nervous system is formed from epiblast precursor cells through Neurulation. Neural induction can be studied in its main aspects in vitro. However, the process is poorly understood, especially in regard to when and how a cell becomes specified, and then committed, to be a neural cell. It is, on the other hand, well established that neural formation requires absence or, inhibition of the BMP signalling both *in vivo* and *in vitro*.

ID1 is a direct target of BMP signalling with major influence on *in vitro* neural differentiation. A cDNA library screen, looking for transcription factors negatively regulated by ID1, reported TWIST1, along with only two other proteins. *Twist1* expression is upregulated during *in vitro* neural differentiation. Furthermore, targeted deletion of *Twist1* has dramatic consequences on anterior neural development. *Twist1* knock-out mice fail to form the closed neural tube in the prospective brain, followed by exencephaly and, early embryonic death.

In this thesis I investigate the influence on in vitro neural differentiation of a TWIST1 constitutively active form, insensitive to ID1 inhibition. I report that this transcriptionally active TWIST1 accelerates neural differentiation, in vitro and, biases it, towards dorsal phenotypes. I provide, for the first time, evidence for *Twist1* expression in the neural tissue, observed weakly in a restricted domain, temporally and spatially, in the dorsal part of the neural tube. I propose a new model for TWIST1 influence at this level. I also investigate how TWIST1 actions depend on levels of expression and dimer choice. I found that, TWIST1 can exert its neural modulating actions only at low levels, as high levels divert a cell fate towards non-neural lineages.

ACKNOWLEDGEMENTS

My biggest thanks go to Sally and all the people in her lab. First I want to thank Sally, for trusting me with a budding project, which now has evolved into a family of related projects. For her soft manner doubled with uncompromising scientific rigour. For her constant support throughout my PhD equally distributed in moments of excitement and despair. There is no part of this thesis where her influence is not strongly felt. My colleague Matt I want to thank for his patience with which he listened to all my complaints and, for his unique expertise with genes from which I richly benefited. I want to thank Chia-Yi for her extensive experience with almost all conceivable lab techniques, experience she presently shared with all those interested and, sometimes even with those not interested. When Guillaume came to our lab, it felt like opening the window wide on a spring day. The scented wind blew strong to all corners of our minds, scattering about piles of old papers and unsettling the dust. I too was moved by his determination to bring mathematical precision to the noisy realm of biology. Amy is the "youngest" member of our lab, but by the time I finished working on my project she had already become an embryo expert and I quickly learned to value her advice. Last, but not least I want to thank Owen. He gave us the bHLH factors potentially regulated by IDs in ES cells. Without him there would have been no TWIST1 and no TWIST1 thesis.

I thank Charles, my co-supervisor, for finding time in his busy schedule for valuable discussions. It is very unlikely to find someone better than him at extracting the essential and conveying it in a clear manner, which everybody can understand.

I thank Ian for original ideas and advices. I guess that I should be most grateful to him for setting up a cutting edge lab where expertise on so many domains could be easily found, a source I did not hesitate to tap. From Nick and Alessia I got advices regarding proteins, from Nicola and Frederick I got molecular biology insights, from Rodrigo I learned to tame the epiblast stem cells, and Dougie taught me a thing or two about the art of generating new cell lines.

Special thanks go to Val and her lab. Val is the kind of scientist that every PhD students dreams of working with, but very few have the chance. Her enthusiasm, skill, insight and modesty are both impressive and contagious. From her and Yali I learned to dissect embryos. They also taught me the even more difficult art of staging them. Filip and Huw taught me the In Situ technique and, Anestis shared with me his insight on the epiblast.

From the large number of people to whom a owe gratitude I want acknowledge the technical staff without whom the activity at the CRM would not be possible. Special thanks should receive Helen and Marilyn who kept the hectic cell culture facility up and running, Carol from the animal facility, someone I never got to meet in person, but who patiently answered all my e-mails and phone calls, Ron for his appreciation of the fragility of the mouse embryo and Valeria for her dedication to our microscopes. I want to thank XinZhi, Sally's lab manager for sorting all problems before they appeared and Anne, Charles's lab manager for going way beyond her duty to help everyone around. Many other people helped me with discussions and support, sharing generously their ideas, expertise and life experience. I thank them, with the deepest regret that space does not allow me to name them all.

Contents

List of Figures

List of Tables

List of Appendices

General Abbreviations

2i	ES cell culture in chemically defined containing Chiron and PD03
Activin	transcription factor made of two Inhba units
ANOVA	analysis of variance
AP	alkaline phosphatase
A-P axis	antero-posterior axis
AVE	anterior visceral endoderm
B27	serum free supplement
BAC	bacterial artificial chromosome
BCIP	5-Bromo-4-chloro-3-indolyl phosphate
bHLH	basic helix-loop-helix
bp	base pair
BSA	bovine serum albumin
CCS	Cell Culture Service
cDNA	complementary DNA
CFU	colony forming unit
Chiron99021	GSK3B inhibitor
CMV	cytomegalovirus
Cre	Cre recombinase
CRM	Centre for Regenerative Medicine
DAM	DNA adenine methylase

DAPI	4',6-diamidino-2-phenylindole
DD	destabilizing domain
DEPC	diethylpyrocarbonate
DH5α	a strain of chemically competent bacterial cells
DI1,2,3	dorsal interneuron1, 2, 3
DIG	digoxigenin
DMEM	Dulbecco's modification of Eagle medium
DMSO	dimethyl sulphoxide
DNA	deoxyribonucleic acid
Dnase	deoxyribonuclease
dNTP	deoxyribonucleotide triphosphate
doTE	clonal ES cell lines containg a Dox inducible TwE construct
doTT	clonal ES cell lines containg a Dox inducible TwTw construct
Dox	doxycycline
dpc	day post coitum
dpn	day post natal
dsRNA	double stranded RNA
DTT	Dithiothreitol
DV axis	dorso-ventral axis
DVE	distal visceral endoderm
EB	embryoid body
EDTA	ethyldiaminotetraacetic acid, disodium salt
EGO	early gastrula organiser
EMT	epithelial to mesenchymal transition (see MET)
EpiSC	epiblast stem cell
ESC	embryonic stem cell
ExE	extraembryonic ectoderm
ExVE	extraembryonic visceral endoderm
F12	Ham's F12 nutrient mixture
FACS	fluorescence-activated cell sorting
FAM	fluorescein amidite
FLAG	Tag octapeptide: DYKDDDDK (1012 Da)
FP	floor plate
FSC	fetal calf serum
G418	geneticin, similar to gentamicin B1
GFP	green fluorescent protein
GMEM	Glasgow minimum essential medium
HEPES	4-(2-hydroxyethyl)-1-piperazineethanesulfonic acid
hESC	human embryonic stem cell
IAA	isoamyl alcohol
IRES	internal ribosomal entry site
ISCR	Institute for Stem Cell Research
LB	L-broth Lauria Bertani
LDS	Nonreducing lithium dodecyl sulfate sample loading buffer
M2	medium for culture of preimplantation stage mouse embryos
MEM	minimum essential medium
MET	mesenchymal to epithelial transition (see EMT)
MGO	mid gastrula organiser
MOPS	3-(N-Morpholino)propane-sulfonic acid
mRNA	mitocondrial ribonucleic acid
N2	chemically defined serum free supplement
NBT	nitro blue tetrazolium chloride
NC	neural crest
NCC	neural crest cells

NSC	neural stem cells
NTMT	alkaline phosphatase buffer
pA	polyadenylation signal
PBS	phosphate buffer saline
PBT	PBS with tween
PCR	polymerase chain reaction
P-D	proximal-distal
PD0325901	selective MAP2K inhibitor
PFA	paraformaldehyde
Pfx	DNA Polymerase from Thermococcus species KOD
POI	protein of interest
PPE	posterior proximal epiblast
PrE	primitive endoderm
PS	primitive streak
qPCR	quantitative polymerase chain reaction
RA	retinoic acid
RIPA	buffer for mamalian cell lysis
RNase	ribonuclease
RP	roof plate
RT	room temperature
rtTA	reverse tetracycline-controlled transactivator
SB431542	TGFbeta/SMAD1 inhibitor
SCS	Saetre-Chotzen syndrome
SDS	sodium dodecyl sulphate
siRNA	small interfering RNA
SOC	Super Optimal broth with Catabolite repression
SPC	subtilisin-like proprotein convertases
SV40	Simian vacuolating virus 40
T7	specific promoter for T7 RNA polymerase
TBE	Tris-borate_EDTA buffer
TBS	Tris buffer saline
TBST	TBS with tween
TetO	tetracycline operator
Top10	a strain of chemically competent bacterial cells
Tris	tris(hydroxymethyl)aminomethane
Tukey HSD	Tukey's Honestly Significant Difference test
TwE	forced dimer formed of TWIST1 and E47
TW-E	active dimer formed of TWIST1 and TCF3
TwTw	forced dimer formed of two TWIST1 factors
TwW-TW	active dimer formed of two TWIST1 factors
UPL	universal probe library
UTR	untranslated region
VE	visceral endoderm

Abbreviations of Genes

Symbol	Other aliaces	Name	Specie
Acvr1	ALK2	activin A receptor, type 1	Mus musculus
Acvr1b	ALK4	activin A receptor, type 1B	Mus musculus
Acvr1c	ALK7	activin A receptor, type 1C	Mus musculus
Adam1		a disintegrin and metallopeptidase domain (meltrin alpha)	Mus musculus
Ahr		aryl-hydrocarbon receptor	Mus musculus
Apc		adenomatosis polyposis coli	Mus musculus
Ascl1	Mash1, bHLHa4(	achaete-scute complex homolog 1 (Drosophila)	Mus musculus
Atf3		activating transcription factor 3	Mus musculus
Atoh1	Math1, bHLHa1-	atonal homolog 1 (Drosophila)	Mus musculus
Bmp4		bone morphogenetic protein 4	Mus musculus
Bmpr1a	ALK3	bone morphogenetic protein receptor, type 1A	Mus musculus
Bmpr1b	Alk6	bone morphogenetic protein receptor, type 1B	Mus musculus
Cd44		CD44 antigen	Mus musculus
Cdh1	E-cad, L-CAM, UVO osteoblas	cadherin 1	Mus musculus
Cdh11	cadherin	cadherin 11	Mus musculus
Cdh2	Ncad	cadherin 2	Mus musculus
Cdh20	Cdh7	cadherin 20	Mus musculus
Cdkn1a	P21	cyclin-dependent kinase inhibitor 1A (P21)	Mus musculus
Cdkn2a	p16	cyclin-dependent kinase inhibitor 2A	Mus musculus
Cer1	Cerr1	cerberus 1 homolog (Xenopus laevis)	Mus musculus
Chrd		chordin	Mus musculus
Chrdl1	neuralin 1	chordin-like 1	Mus musculus
Churc1		churchill domain containing 1	Mus musculus
Ctnna1	alpha E-catenin	catenin (cadherin associated protein), alpha	Mus musculus
Ctnnb1	beta catenin	catenin (cadherin associated protein), beta 1	Mus musculus
ctnnb1b		catenin (cadherin-associated protein), beta	Xenopus laevis
Cx3cl1	neurotact	chemokine (C-X3-C motif) ligand 1	Mus musculus
da		daughterless	Mus musculus
Disp1		dispatched homolog 1 (Drosophila)	Mus musculus
Dkk1		dkk1 homolog 1 (Xenopus laevis)	Mus musculus
Dlx5		distal-less homeobox 5	Mus musculus
Dnajc2	MIDA1	DnaJ (Hsp40) homolog, subfamily C, member 2	Mus musculus
Ebf1	O/E-1, O- 1	early B cell factor 1	Mus musculus
Egfr		epidermal growth factor receptor	Mus musculus
Eomes	Tbr2	eomesodermin homolog (Xenopus laevis)	Mus musculus

ERNI		early response to neural induction ERNI	Gallus gallus
Esrrb		estrogen related receptor, beta	Mus musculus
Fgf2	bFGF	fibroblast growth factor 2	Mus musculus
Fgf4	kFGF	fibroblast growth factor 4	Mus musculus
Fgf5		fibroblast growth factor 5	Mus musculus
Fgf8		fibroblast growth factor 8	Mus musculus
Fgfr1		fibroblast growth factor receptor 1	Mus musculus
Fgfr2		fibroblast growth factor receptor 2	Mus musculus
FKBP1	FKBP12	FK506 binding protein 1A, 12kDa	Homo sapiens
Fn1		fibronectin 1	Mus musculus
Foxa2	HNF-3be Tcf-3b	forkhead box A2	Mus musculus
Foxd3		forkhead box D3	Mus musculus
Fst		follistatin	Mus musculus
Furin	SPC1, PACE	furin (paired basic amino acid cleaving enzyme)	Mus musculus
Fut4	SSEA-1, CD15	fucosyltransferase 4	Mus musculus
Fzd9		frizzled homolog 9 (Drosophila)	Mus musculus
Gata2		GATA binding protein 2	Mus musculus
Gata6		GATA binding protein 6	Mus musculus
Gli1	Zfp-5	GLI-Kruppel family member GLI1	Mus musculus
Gli2		GLI-Kruppel family member GLI2	Mus musculus
Gli3		GLI-Kruppel family member GLI3	Mus musculus
Grem1		gremlin 1	Mus musculus
Gsc		goosecoid homeobox	Mus musculus
Gsk3b	GSK3	glycogen synthase kinase 3 beta	Mus musculus
h		hairy	Drosophila melanogaster
Hes1		hairy and enhancer of split 1 (Drosophila)	Mus musculus
Hesx1	HES-1	homeobox gene expressed in ES cells	Mus musculus
Hey		Hairy/E(spl)-related with YRPW motif	Drosophila melanogaster
hh		hedgehog	Drosophila melanogaster
Hhex	Hex, Hex	hematopoietically expressed homeobox	Mus musculus
Hif1a		hypoxia inducible factor 1, alpha subunit	Mus musculus
Id1		inhibitor of DNA binding 1	Mus musculus
Id2		inhibitor of DNA binding 2	Mus musculus
Id3		inhibitor of DNA binding 3	Mus musculus
Id4		inhibitor of DNA binding 4	Mus musculus
Il1	Il-1	interleukin 1 complex	Mus musculus
Il6	Il-6	interleukin 6	Mus musculus
Inhba		inhibin beta-A, Two INHBA subunits form an ACTIVIN molecule	Mus musculus
Kitl		kit ligand	Mus musculus
Klf4		Kruppel-like factor 4 (gut)	Mus musculus
Lefty1		left right determination factor 1	Mus musculus
Lhx1		LIM homeobox protein 1	Mus musculus
Lif		leukemia inhibitory factor	Mus musculus

Lrp5	LRP7	low density lipoprotein receptor-related protein 5	Mus musculus
Lrp6	crooked	low density lipoprotein receptor-related protein 6	Mus musculus
Mad	MAD, Smad1	Mothers against dpp	Drosophila melanogaster
Map2k	Mek1	mitogen-activated protein kinase kinase 1	Mus musculus
Map2k	Mek2	mitogen-activated protein kinase kinase 2	Mus musculus
Mapk1	ERK	mitogen-activated protein kinase 1	Mus musculus
Mapk1	p38, p38MAP	mitogen-activated protein kinase 14	Mus musculus
Max	MAX	CG9648 gene product from transcript CG9648-RA	Drosophila melanogaster
Msx1	Hox7	homeobox, msh-like 1	Mus musculus
Myc	c-myc	myelocytomatosis oncogene	Mus musculus
Mycn	n-Myc	v-myc myelocytomatosis viral related oncogene, neuroblastoma derived (avian)	Mus musculus
Myf5		myogenic factor 5	Mus musculus
Myod1		myogenic differentiation 1	Mus musculus
Myog	myo	Myogenin	Mus musculus
Nanog		Nanog homeobox	Mus musculus
Ncam1		neural cell adhesion molecule 1	Mus musculus
Nes		nestin	Mus musculus
Neurod		neurogenic differentiation 1	Mus musculus
Neurod	Math3, bHLHa4	neurogenic differentiation 4	Mus musculus
Neurod	Math2, bHLHa2	neurogenic differentiation 6	Mus musculus
Neurog		neurogenin1	Mus musculus
Nkx6-2	Gtx, Nkx6.2	NK6 homeobox 2	Mus musculus
Noda		nodal	Mus musculus
Nog		noggin	Mus musculus
Notch1		notch 1	Mus musculus
Ocln		occludin	Mus musculus
Olig1	bHLHe21	oligodendrocyte transcription factor 1	Mus musculus
Olig2	bHLHe19	oligodendrocyte transcription factor 2	Mus musculus
Olig3	bHLHe20	oligodendrocyte transcription factor 3	Mus musculus
Otx2		orthodenticle homolog 2 (Drosophila)	Mus musculus
Pax3		paired box gene 3	Mus musculus
Pax6		paired box gene 6	Mus musculus
Pax7		paired box gene 7	Mus musculus
Pcsk6	SPC4, Pace4	proprotein convertase subtilisin/kexin type	Mus musculus
per		period	Drosophila melanogaster
Pou5f1	Oct-4, Oc 3/4	POU domain, class 5, transcription factor 1	Mus musculus
Ptch1		patched homolog 1	Mus musculus
Shh		sonic hedgehog	Mus musculus
sim		single-minded	Drosophila

			melanogaster
Smad1		SMAD family member 1	Mus musculus
Smad2		SMAD family member 2	Mus musculus
Smad3		SMAD family member 3	Mus musculus
Smad4		SMAD family member 4	Mus musculus
Smad5		SMAD family member 5	Mus musculus
Smad9	Smad8	SMAD family member 9	Mus musculus
Smo		smoothened homolog (Drosophila)	Mus musculus
Snai1	Sna, Snai	snail homolog 1 (Drosophila)	Mus musculus
Snai2	SLUG	snail homolog 2 (Drosophila)	Mus musculus
Sox1		SRY-box containing gene 1	Mus musculus
Sox2		SRY-box containing gene 2	Mus musculus
Sox3		SRY-box containing gene 3	Mus musculus
Sox9		SRY-box containing gene 9	Mus musculus
Sox10	Sox21	SRY-box containing gene 10	Mus musculus
Sox11		SRY-box containing gene 11	Mus musculus
Stat3		signal transducer and activator of transcription 3	Mus musculus
T		brachyury	Mus musculus
Tbp		TATA box binding protein	Mus musculus
Tcf3	E2A, E12 E47	transcription factor 3	Mus musculus
Tcf4	E2.2	transcription factor 4	Mus musculus
Tcf7		transcription factor 7, T cell specific	Mus musculus
Tcf7l1	Tcf3, bHLHb2	transcription factor 7 like 1 (T cell specific, HMG bc	Mus musculus
Tcf12	HEB	transcription factor 12	Mus musculus
Tcf15	Meso1, paraxis	transcription factor 15	Mus musculus
Tdgf1	cripto	teratocarcinoma-derived growth factor 1	Mus musculus
Tfap2a	AP-2, AP2alpha	transcription factor AP-2, alpha	Mus musculus
Tfap2c	Ap-2.2	transcription factor AP-2, gamma	Mus musculus
Tgfb1		transforming growth factor, beta 1	Mus musculus
Tgfb1		transforming growth factor, beta 1	Mus musculus
Tgfbr1	ALK5	transforming growth factor, beta receptor 1	Mus musculus
Trp53	p53	transformation related protein 53	Mus musculus
Tubb3	betaIII tubulin	tubulin, beta 3 class III	Mus musculus
twi		twist	Drosophila melanogaster
Twist1		twist homolog 1 (Drosophila)	Mus musculus
Vav3		vav 3 oncogene	Mus musculus
Vim		vimentin	Mus musculus
Wnt1		wingless-related MMTV integration site 1	Mus musculus
Wnt3		wingless-related MMTV integration site 3	Mus musculus
Wnt3a		wingless-related MMTV integration site 3A	Mus musculus
Wnt8a	Wnt8	wingless-type MMTV integration site fami member 8A	Xenopus laevis

Zeb1	ZFHX1A Tcf8	zinc finger E-box binding homeobox 1	Mus musculus
Zeb2	ZFHX1B Sip1	zinc finger E-box binding homeobox 2	Mus musculus
Zfp521		zinc finger protein 521	Mus musculus
Zic1		zinc finger protein of the cerebellum 1	Mus musculus
Zic2	Ku	zinc finger protein of the cerebellum 2	Mus musculus
Zic3		zinc finger protein of the cerebellum 3	Mus musculus
Zic5	Opr	zinc finger protein of the cerebellum 5	Mus musculus

I. INTRODUCTION

I1 Overview

Stem cells offer great promise for regenerative medicine. This promise, in all its forms: in vitro generation of transplantable cells and tissues, disease modelling and, drug testing, relies on good control of the differentiation process *in vitro*. While important progress has been made in the recent years, pluripotent cell differentiation control is still far from the desired levels. Reasons for current deficiencies include the complexity of the differentiation process, the insufficient understanding of the *in vivo* differentiation, as well as the fact that, in the embryo and in the culture dish, cells differentiating along multiple lineages coexist in the same location and, seem to be subject to similar inductive signals.

Neural differentiation has been considered as one of the simplest differentiation pathways and thus, ideal for investigating differentiation. Dubbed "the default fate" it was thought that all pluripotent cells are fated to become neural unless instructed otherwise and, the naïve epiblast could be turned to neural fate simply by inhibiting the BMP signalling [Munoz-Sanjuan and Brivanlou, 2002]. Since, according to the default model, the control of neural differentiation is essentially neural fate inhibition by BMP, attention has been turned to the pathways downstream BMP. It was shown that BMP enacts neural inhibition by activating ID proteins, negative regulators of bHLH transcription factors [Ying et al., 2003a]. However, the specific role of IDs in this process is less clear.

A cDNA library screen from the Lowell lab indicated that one of the putative transcriptional targets of IDs in pluripotent cells could be TWIST1, a bHLH factor with roles in gastrulation, somitogenesis, neural tube formation and neural crest specification and differentiation [Barnes and Firulli, 2009]. In this chapter I present a brief literature overview on Stem Cells, followed by a section on bHLH factors with an emphasis on ID proteins. A special section is dedicated to *Twist1* describing its role in development, expression pattern, the pathology linked with *Twist1* mutations

and its molecular mechanism of action. Next, I describe the developmental processes which lead to neural tissue formation in mouse. Parallel formation of non-neural tissues is also briefly described. A particular attention is paid to neural crest, a tissue in which *Twist1* role has long been recognised. Mutant analysis indicated that *Twist1* is involved in correct neural tube formation and dorso-ventral patterning. These processes are described in detail. Finally, I summarize the questions still unanswered regarding *Twist1* role in neural specification and neural tube formation.

I2 Stem Cells

I2.1 Stem Cell Beginnings

The advent of stem cells began with the discovery of a bone marrow population which is able to repopulate the hematopoietic system of irradiated mice [Till and McCulloch, 1961]. Soon after, hematopoietic progenitors could be cultured and differentiated *in vitro*, though they could not be maintained in the undifferentiated state in these conditions [Bradley and Metcalf, 1966]. About the same time bone marrow was shown to be the host of another interesting cell type; this cell, which also has the ability to generate colony forming units (CFUs) *in vivo* and *in vitro*, could be separated from hematopoietic cells by its property of adhering to plastic and could be differentiated into bone, both *in vivo* and *in vitro* [Friedenstein et al., 1968; Friedenstein et al., 1970]. This cell which was later named as Mesenchymal Stem Cell and more recently was suggested to be the pericyte [Schwab and Gargett, 2007; Crisan et al., 2008; Crisan et al., 2011] had been just the first in a long line of tissue stem cells. These cells have limited capacity of self-renewal and, are normally restricted in differentiation to cells belonging to the tissue of origin; however, *in vitro*, their differentiation capacity can be significantly expanded [Serafini and Verfaillie, 2006].

It was only in 1981 that a cell with unlimited self renewal capacity, which was not of malignant origin, could be isolated and cultured [Evans and Kaufman, 1981; Martin, 1981], thus moving the medical research into the Embryonic Stem Cell era.

I2.2 Embryonic Stem Cells

I2.2.1 Mouse ES Cells

Embryonic Stem (ES) cells can be isolated from the Inner Cell Mass of pre-implantation blastocyst; it seems to be possible to propagate these cells indefinitely *in vitro*, while retaining normal differentiation capability and karyotype [Evans and Kaufman, 1981; Martin, 1981]. ES cells can be differentiated in cells belonging to all the three germ layers derived from early epiblast [Smith A.G., 2001], including germ cells [Bradley et al., 1984]. A key feature of ES cells is that they can contribute to all embryonic lineages in chimeras. However, in these conditions their contribution is very limited towards the extraembryonic lineages: primitive endoderm and especially trophectoderm [Beddington and Robertson, 1989]. When transplanted into adult mice ES cells generate teratocarcinomas, often containing cells from two or three germ layers [Evans and Kaufman, 1981; Martin, 1981]. Interestingly, undifferentiated embryonic carcinoma cells can produce embryoid bodies also containing yolk sac and trophectoderm derivates [Kleinsmith and Pierce, 1964].

I2.2.1 Maintaining Pluripotency of ES Cells

Initial derivation and culture conditions involved feeder layers from irradiated fibroblasts [Evans and Kaufman, 1981; Martin, 1981]. Subsequently, it was shown first, that the feeder cells role was to maintain the undifferentiated ES cells by secreting factor tethered to their membrane [Smith and Hooper, 1987] and second, that this factor was leukaemia inhibitory factor (LIF) [Williams et al. 1988, Smith et al. 1988], a member of the interleukin 6 (IL6) family of cytokines [Taga and Kishimoto, 1997]. LIF was reported to act through activation of STAT3 and this process is indispensable for ES cell maintenance under conventional culture conditions [Burdon et al., 1999a; Matsuda et al. 1999]. However, *Stat3* is not required for epiblast formation, as indicated by studies in knock-out mice [Burdon et al., 1999a; Matsuda et al., 1999]. On the other hand, *Pou5f1* has been reported as the necessary factor for ES cell formation and maintenance *in vivo* [Nichols et al., 1998]. Furthermore, NANOG, a divergent homeodomain protein, can maintain POU5F1

levels and bypass STAT3 requirements for ES cell clonal expansion [Chambers at al., 2003]. Of note, *Nanog* is dispensable for formation of pluripotent cells capable of differentiating cells from the three germ layers, but is required for germ cell formation [Chambers at al., 2007].

Another important discovery was the fact that the main anti-differentiating activity of the serum is being held by Bone Morphogenic Proteins (BMPs), and that ES cells can be maintained using LIF and BMPs as the only exogenous instructive signals [Ying et all., 2003a]. The same authors showed that BMPs block ES cell differentiation primarily through ID proteins.

More recent reports indicate that the extrinsic signalling can be by-passed altogether, in ES cell maintenance, provided that mitogen-activated protein kinase (MAPK) pathway and glycogen synthase kinase 3 beta (GSK3B) pathway are inhibited [Ying et al., 2008].

I2.2.3 Human ES cells; Epiblast Stem Cells

Significant differences exist between mouse and human ES cells in culture conditions requirements as well as signalling properties. Consequently, the long time required for isolation of the latter cells [Thomson et al., 1998]. While human ES cells are not responsive to LIF, they can be maintained either with feeder cells [Prelle et all, 1999; Pera et al., 2000] or using conditioned medium from feeder cells [Xu et al., 2001]. Interestingly, they require FGF2 [Kang et al., 2005; Greber et al., 2007] and subsequent activation of MAPK1 pathway, a signalling cascade which induces differentiation in mouse ES cells [Burdon et al., 1999b].

Recently, pluripotent self renewing cells were derived from mouse epiblast of post-implantation embryos. These cells were named Epiblast Stem Cells [EpiSCs], after their origin; unlike mouse ES cells that depend on LIF for their self renewal., EpicSCs rely on FGF and ACTIVIN, resembling human ES cells [Brons et al., 2007; Tesar et al., 2007]. Moreover, the similarity with hES cells and divergence between mouse ES and EpiSCs was also confirmed at the level of differentiating instructive signals [Vallier et al., 2009]. For instance, the authors found that in the case of mEpiSCs inhibition of ACTIVIN/NODAL signalling leads to rapid loss of

pluripotency markers and induction of neural differentiation, as in the case of hESCs, and that a three step protocol, developed for induction of mesoderm and definitive endoderm from hESC could be successfully used in the case of mEpiSCs but not mESCs [Vallier et al., 2009].

I3. Basic Helix-Loop-Helix Family of Transcription Factors

The basic Helix Loop Helix (bHLH) family represents a large group of transcription factors involved in many developmental pathways such as lineage commitment, differentiation, proliferation, sex determination in organisms ranging from yeast to human [Massari & Murre, 2000].

The importance of bHLH domains were first appreciated in *Tcf3* (also known as E2A) gene products (E12 and E47 proteins), which were discovered by their ability to bind to E-boxes [Murre et al., 1989]. At that time, *Myod1* and *Myc* in mouse and *daughterless*, *achaete-scute* and *twist* in Drosophila had already been discovered, though the relation between them was not yet clear [Davis et al., 1987; Hayward et al., 1981; Caudy et al., 1988; Campuzano et al., 1985; Thise et al., 1987]. The E-boxes had been previously identified as DNA cis elements present in immunoglobulin enhancers [Ephrussi et al., 1985].

bHLH proteins have two functionally distinct domains comprised in a highly conserved region of approximately 60 amino acids. At the N-terminal end of the region there is the basic domain which binds DNA in the major groove at the E consensus sequence [Jones S., 2004]. The second domain, placed at the C-terminal end of the region, consists mainly of hydrophobic residues and it acts by facilitating protein-protein interaction, resulting in dimerization of the bHLH factors. This motif contains two amphipathic α-helixes separated by a short loop and it spans for approximately 50 amino acids [Atchley & Fitch, 1997; **Fig I1**].

Figure I1. bHLH domain strucure and its interaction with DNA.

A bHLH heterodimer binds DNA at the major groove. H1-first helix, H2-second helix, before H1, the short basic region can be observed. Source: Jones S, 2004

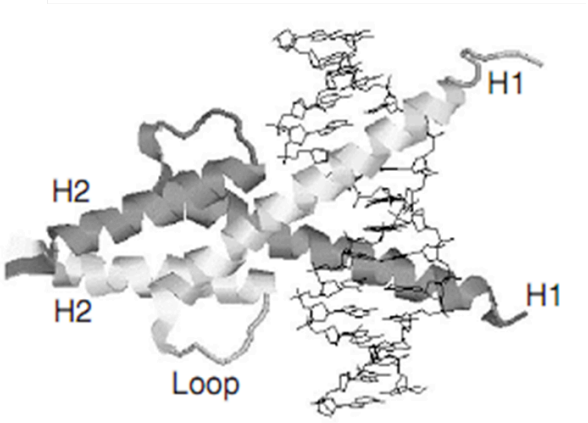
H1
H2
H2
H1
Loop

However DNA binding by the basic region and consequently activation of target genes requires as a first step homo- or hetero-dimerization through the HLH region.

On the contrary, in the absence of basic region the HLH dependent dimerization is not disrupted [Voronova & Baltimore, 1990]. This feature is employed by ID proteins (dominant negative bHLH like proteins, that lack the basic motif) to drive passive inhibition of their binding partners [Benezra et al., 1990].

I3.1 bHLH Superfamily Classification

The transcription factors belonging to the large bHLH family were classified based on their tissue distribution, dimerization capabilities and DNA-binding specificities into 7 classes (I to VII) [Murre et al., 1994]. Subsequently, a phylogenetic classification was proposed, dividing the bHLH proteins into 4 classes (A to D) [Atchley and Fitch, 1997], with two more classes (E and F) added later [Ledent et al., 2002], Table I1.

Class I bHLH proteins is represented by E proteins, it includes E12, E47, TCF12 (also known as HEB), TCF4 (also known as E2.2) and DAUGHTERLESS. E12 and E47 represent spliced variants of *Tcf3* gene. These proteins are expressed promiscuously throughout many tissues, can form homo- and hetero- dimers and bind DNA to the E-box sites alone.

Class II includes protein like MYOD, MYOGENIN, ATONAL, NEUROD1; they have a tissue restricted pattern of expression and do not form homodimers with very few exceptions (notably TWIST1). They form heterodimers with the E proteins and hence bind to the E –boxes [Massari & Murre, 2000]. Class I and II form phylogenetic group A.

Class III include the MYC family and is characterized by the presence of a leucine zipper motif after the second helix of the bHLH domain.

Class IV include proteins like MAD and MAX. These proteins can contain a leucine zipper motif, form homodimers, or heterodimers with other members of the class, or with MYC. Together, class III and IV form phylogenetic group B. It is believed that, group B hold the ancestral sequence of bHLH [Jones, 2004].

Classification of bHLH proteins by sequence			
Phylogen group	Description	Classification according Murre et 1994	Examples of classif proteins (family names)
A	Bind to CAGCTG or CACCTG	I, II	MYOD1, TWIST
B	Bind to CACGTG or CATGTTG	III, IV	MAD, MAX, MYC
C	Bind to ACGTG or GCGT Contains a PAS domain	VII	Single-minded (SIM), a hydrocarbon recep (AHR)
D	Lack a basic domain and hence not bind to DNA but form prote protein dimers that function antagonists of group A proteins	V	ID
E	Bind preferentially to N-b sequences CACGCG or CACGA Contain an orange domain, involv in dimerization and DNA binding	VI	HAIRY
F	Contain an additional COE doma involved in dimerization and DI binding		EBF1

Table I1. Comparison between two bHLH classifications. Adapted from Jones S., 2004

Class V, are the dominant negative ID proteins and they form evolutionary group D.

Class VI, contain an Orange domain and a proline in their basic domain. The Orange domain might be involved in transcription repression as well as dimerization. This class include HAIRY, HEY, HES proteins; form phylogenetic group E, bind preferentially to N-boxes and were initially assigned by Atchley and Fitch to group B [Atchley & Fitch, 1997; Jones, 20004].

Class VII include transcription factors like aromatic hydrocarbon receptor (AHR), hypoxia inducible factor (HIF), Single-minded and Period. These proteins contain a PAS (Period-AHR-Single-minded) domain (260-310 aa) carboxy-terminal from the second helix, which is involved in dimerization. This class form phylogenetic group C [Massari & Murre, 2000; Jones, 2004].

I 3.2 ID Negative Factors of bHLH Transcription Regulation

Soon after the discovery of HLH as a homology domain between multiple transcription factors [Davis, et al., 1987], the first *Id* was identified in a cDNA library screen in murine erythroleukemia cells, using a probe homologous to the second helix common for *Myc*, *Myod1* and *Myog* [Benezra et al., 1990]. In mammals there are 4 ID proteins: IDl, ID2 [Sun et al., 1991], ID3 [Christy et al., 1991], and ID4 [Riechmann et al., 1994].

The expression pattern of these transcripts has been investigated in embryogenesis starting at early gastrulation [Duncan et al., 1992; Wang et al., 1992; Evans and O'Brien, 1993; Jen et al., 1996]. Briefly, *Ids* start by being expressed in extraembryonic tissues. Then, as gastrulation proceeds, they become highly expressed throughout epiblast and its derivates. Later on, expression decreases and becomes tissue specific [Wang et al., 1992]. From the 4 described Ids; *Id1*, *Id2* and *Id3* have a significantly overlapping expression, but different than that of *Id4*. *Id1*, *Id2* and *Id3* are expressed at sites with active morphogenic activities, while *Id4* is expressed in more mature tissues, with the notable exception of developing CNS where all *Id* genes are expressed [Jen et al., 1996]. During gastrulation, *Id1* and *Id3* are expressed in the epiblast and its derivates, while *Id2* is expressed in trophectoderm. Subsequently, *Id1*, *Id2* and *Id3* are expressed in neural crest, neural crest derived mesoderm and paraxial mesoderm. They are expressed highly at sites of chondrogenesis, but not in dermatome or myotome [Wang et al., 1992, Evans and O'Brien 1993, Jen et al., 1996]. Regarding neural differentiation, neural precursors express all *Ids*, while in mature neurons *Id4* becomes the main *Id* player [Nagata and Todokoro, 1994; Jen et al., 1996].

The studies presented here were performed at late developmental stages relative to an eventual role for ID proteins in pluripotent cells *in vivo* and early differentiation events. While it is difficult to perform such studies in the developing early embryo, single cells analysis indicated that *Id1* and *Id2* are upregulated during *in vitro* outgrowth from ICM [Tang et al., 2010] and *Id2* was found to be the earliest marker of the outer cell domain (prospective trophoblast) [Guo et al., 2010].

I3.2.1 IDs Mechanism of Action

One of the best described mechanism of actions for IDs is their binding to TCF3 proteins and preventing formation of active dimers with tissue specific bHLH factors like MYOD1 [Jen et al., 1992; Kurabayashi et al., 1994; Peverali et al., 1994]. TCF3 bind ID proteins with higher affinity than MYOD [Goldfarb et al., 1996], and IDs bind TCF3 with higher affinity than MYOD [Loveys et al., 1996]. Interestingly, ID proteins were shown to block function and DNA binding of some non-bHLH transcription factors as well, like the retinoblastoma protein, or PAX factors [Iavarone et al., 1994; Shoji et al., 1995; Yates et al., 1999; Roberts et al., 2001].

I3.2.2 Ids Induction by BMP

TGFB signalling has two branches. On one branch TGFB, ACTIVIN and NODAL bind to TGFBR1 (TGFb receptor 1, also known as ALK5), ACVR1B (Activin A receptor type 1B, also known as ALK4) and ACVR1C (Activin A receptor type 1C, also known as ALK7); this will induce activation of SMAD2 and SMAD3. On the other branch BMPs/GDFs bind BMPR1A (BMP receptor 1A, also known as ALK3), BMPR1B (BMP receptor 1B, also known as Alk6) and ACVR1 (activin A recptor type 1, also known as ALK2); this will induce activation of SMAD1, 5 and 9 [Miyazono and Miyazava, 2002; Ruzinova and Benezra, 2003].

BMP can induce *Id* through activation of SMAD1/SMAD5 [Hollnagel et al., 1999; Korchynskyi and ten Dijke, 2002; Lopez-Rovira et al., 2002]. Unlike BMP, TGFB1 activates SMAD2/SMAD3 together with a transcriptional repressor ATF3. ATF3 cooperates with SMAD3 and represses *Id* expression [Kang et al., 2003]. However, in some cellular context TGFB1 can induce *Id* genes [Hacker et al., 2003; Sugai et al., 2003; Ruzinova and Benezra, 2003] or have a biphasic effect, activating or repressing *Ids* depending on TGFB1 concentration [Goumans et al., 2002]. The described induction/repression has been reported for *Id1*, *Id2* and *Id3*. It is unclear if the less studied *Id4* is subject to similar regulation.

I3.2.3 IDs Regulate E Protein Activity

Tcf3 knockout mice are born at lower frequency than expected Mendelian ratio. The new-borns, which survived, presented with growth retardation, no B-lymphocyte formation and, most of them died in the first 2 weeks postnatally. The few who survived, presented a high incidence T cell lymphoma after three months of life [Bain et al., 1994; Zhuang et al., 1994; Yan et al., 1997]. *Id1* knockout mice are born at the expected ratio and show no obvious anomalies, suggesting compensation from other Id proteins. Generation of *Tcf3*/*Id1* compound knockouts partially rescued growth retardation and reduced survival at, and after birth compared to *Tcf3* single knockouts. However, the absence of B cell and later formation of T cell tumours could not be influenced [Yan et al., 1997]. Together these data indicate that ID proteins bind to TCF3 as well as to other members of the E protein class (TCF4 and TCF12) and that reducing the overall levels of ID proteins by knocking out *Id1* (in *Tcf3*-/- background) releases some of the negative pressure on other E proteins, partially rescuing growth retardation. On the other hand, proper B and T cell differentiation seem to be strictly dependent on TCF3 activity [Yan et al., 1997].

I3.2.4 *Ids* in Development: Insights from Knock-out Studies

Mice knockout for *Id3* like those for *Id1* are born normally and show no overt developmental anomalies. However, unlike *Id1*, *Id3* knockout present haematological perturbation in B and T cell lineage differentiation [Pan et al., 1999]. Strikingly, *Id1/Id3* compound knockout are not viable and they die at 13.5 dpc of cranial haemorrhages. Starting at 11.5 dpc these embryos show growth retardation, and notably smaller brains, with fewer proliferating cells. Marker analysis showed expanded domains of *Atoh1* (also known as Math1), *Neurod4* (also known as Math3) and *Neurod6* (also known as Math2) indicating premature neuronal differentiation [Lyden et al., 1999].

Id2 knockout mice are born normally, but subsequently show retarded growth with increased neonatal lethality. Phenotypically, they present megacolon and absence of the Payer plates and lymph nodes. On the hematologic lineage complete alymphoplasia and important reduction in natural killer cell number were observed

[Yokota et al., 1999]. Furthermore, female mice *Id2*$^{-/-}$ have a defect in mammary gland pregnancy associated expansion, and they are never able to foster their pups [Mori et al., 2000]. Interestingly, in chick overexpression of *Id2* on embryo surface induces transformation of the ectoderm overlaying the neural tube into neural crest and overgrowth and premature neurogenesis of the neural tube [Martisen and Bronner-Fraser, 1998].

Id4 knockout mice survive postnatally, but they present significantly smaller brains compared to wild type. The reduction in brain size starts to be noticeable at 11.5 dpc and, it was accompanied by precocious differentiation of early cortical progenitors, as indicated by increased expression of *Tubb3* (bIII-tubulin) and *Neurod1* [Yun et al., 2004]. Furthermore, *Id4* is involved in mammary gland cell proliferation in response to estrogen or progesterone by inhibiting MAPK14 [Dong et al., 2011], suggesting a redundant role with *Id2*.

ID proteins role in blocking differentiation and sustaining proliferation, already discussed in neural development, has been shown in many other contexts, physiological and pathological [Norton JD, 2000; Ruzinova and Benezra, 2003]. ID proteins delay senescence by suppressing CDK1A (also known as p21) and CDK2A (also known as p16) cyclin dependent kinase inhibitors [Ohtani et al., 2001;Ouyang et al., 2002; Prabhu et al., 1997]. Furthermore, ID proteins are upregulated in many cancers and this phenomenon is associated with poor prognosis [Israel et a, 1999; Lyden et al., 1999]. Since IDs main role is to bind and sequester E proteins it is thought that this mechanism is employed for cell cycle control as well. However, there are some problems with this hypothesis. First, proposing that IDs act by sequestering E proteins and preventing them to form active dimers does not clarify which active dimers would be involved in a particular process. Second, it has been shown that at least in some cases IDs use different pathways; for instance only repression of CDK1A but not CDK1B is TCF3 dependent [Prabhu et al., 1997; Ohtani et al., 2001]. Furthermore, in erythroleukaemia cells, ID1 associate with DNAJC2 (also known as MIDA1) and helps rather than prevents DNAJC2 specific DNA binding [Inoue et al., 1999].

I4 Twist1 in Mouse Development

I4.1 Twist1 Expression in Mouse Embryogenesis

I4.1.1 Twist1 Expression in The Pre-Implantation and Early Post-Implantation

Twist1 transcripts are first detected after implantation in the ectoplacental cone by in situ hybridization [Stoezel et al., 1995]. More recently q-PCR data shows that the gene is transcribed at low levels in ES cells and its expression increases during differentiation [Aiba et al., 2009; Schulz et al., 2009]. However, our preliminary data [Aliaxandra Radzisheuskaya] indicate that mRNA for *Twist1* can be detected only at very low levels in mouse blastocyst, and that it increases to significant levels in embryos starting at 7.5 dpc.

In the primitive streak embryo (7 – 7.5 dpc) *Twist1* is expressed weakly in "ectodermal cells of the embryo proper and subjacent mesoderm at the side of primitive streak formation" [Stoetzel et al., 1995]. Interestingly, these findings could not be confirmed by other researchers who found *Twist1* signal in the mesoderm, only at some distance from the primitive streak with intense labeling for the anterior mesodermal cells [Füchtbauer, 1995]. At this stage *Twist1* is expressed more abundantly in extra-embryonic ectoderm derived from ectoplacental cone [Stoetzel et al., 1995], and in extra-embryonic mesoderm lining the exocoelom as well as in the allantois [Stoetzel et al., 1995; Füchtbauer, 1995].

I4.1.2 *Twist1* Expression in The Somitic Embryo

At 8 dpc *Twist1* is expressed in the head mesenchyme, somites and somatic part of the lateral plate [Stoetzel et al., 1995; Füchtbauer, 1995]. "In the unsegmented paraxial mesoderm it is detectable only in the most anterior region which will form the next somite" [Füchtbauer, 1995]. At this stage *Twist1* expression is no longer detected in ectoplacental cone [Stoetzel et al., 1995] but it continues in extra-embryonic mesoderm, amnion and allantois [Stoetzel et al., 1995; Füchtbauer, 1995].

It is not expressed in ectoderm or embryonic endoderm, nor in the non-somitic mesoderm or in the tail [Stoetzel et al., 1995; Füchtbauer, 1995].

As the somitogenesis progresses the *Twist1* signal becomes restricted to the ventral medial half of the anterior somites, which will give rise to sclerotome [Füchtbauer, 1995]. At 8 – 8.5 dpc *Twist1* is strongly expressed in the first branchial arches. At 9 dpc it appears in the anterior limb rudiment [Stoetzel et al., 1995; Füchtbauer, 1995]. At 9 – 9.5 dpc "the sclerotome cells continue to express *Twist1*, but now the signal is again detected in the dermatomyotome thus, leaving only, as a small stripe, the *Myf5* expressing myotome without *Twist1* expression". [Füchtbauer, 1995]. Now, the signal appears in the posterior limb (at the time of the third and fourth branchial arch formation. The level of expression decreases in the first and second branchial arches [Stoetzel et al., 1995].

Twist1 is not expressed in the early myocardium, but it is detected between 10 – 13 dpc in the atrioventricular cushion [Stoetzel et al., 1995; Füchtbauer, 1995]. It is excluded from the areas of myogenic and chondrogenic differentiation but it is strongly expressed close to chondrogenic differentiating cells. It is also expressed in the mesenchyme underlining the epidermis with a gradual reduction of the message "with increased distance from the epithelium" [Füchtbauer, 1995].

Twist2 shows a very high degree of conservation with *Twist1* in the bHLH domain and has been reported to act in a redundant manner with TWIST1 [Sosic et al., 2003]. However, *Twist2* expression in the embryo has only been reported at later stages, starting with 10 dpc [Li et al., 1995]. Interestingly, a gene trap experiment detected *Twist2* at the ES cell level [Tanaka et al., 2008].

I4.2 *Twist1* Mutants

I4.2.1 *Twist1* Null a Lethal Phenotype

Twist1 null mice die at 11.5 dpc. Their neural tube fails to close in the cranial region, resulting in exencephaly. Focal haemorrhages are consistently observed at this level.

In *Twist1* null embryos cranial neural tube cannot initiate fusion. However, the neural folds in the trunk region and hindbrain caudal of rhombomere 4 close and form the neural tube [Chen and Behringer, 1995; **Fig I2**]. The defects observed in the cranial neuroepithelium were preceded by mesenchyme abnormalities. The mesenchymal cells in this region presented an abnormal round morphology, with reduced cellular contacts and increased extracellular space [Chen and Behringer, 1995]. Gene expression analysis by in situ hybridization of *Twist1* null mutants showed that "the loss of TWIST1 function in the head mesenchyme impacts on dorsoventral but not the anteroposterior patterning of the cephalic neural tube" [Soo et al., 2002].

Figure I2. *Twist1* null a lethal phenotype.

Twist1 null embryos display severe malformations during gastrulation. White arrow indicates the open neural tube. Black arrows point to the underdeveloped limb buds. Source: Chen & Behringer, 1995

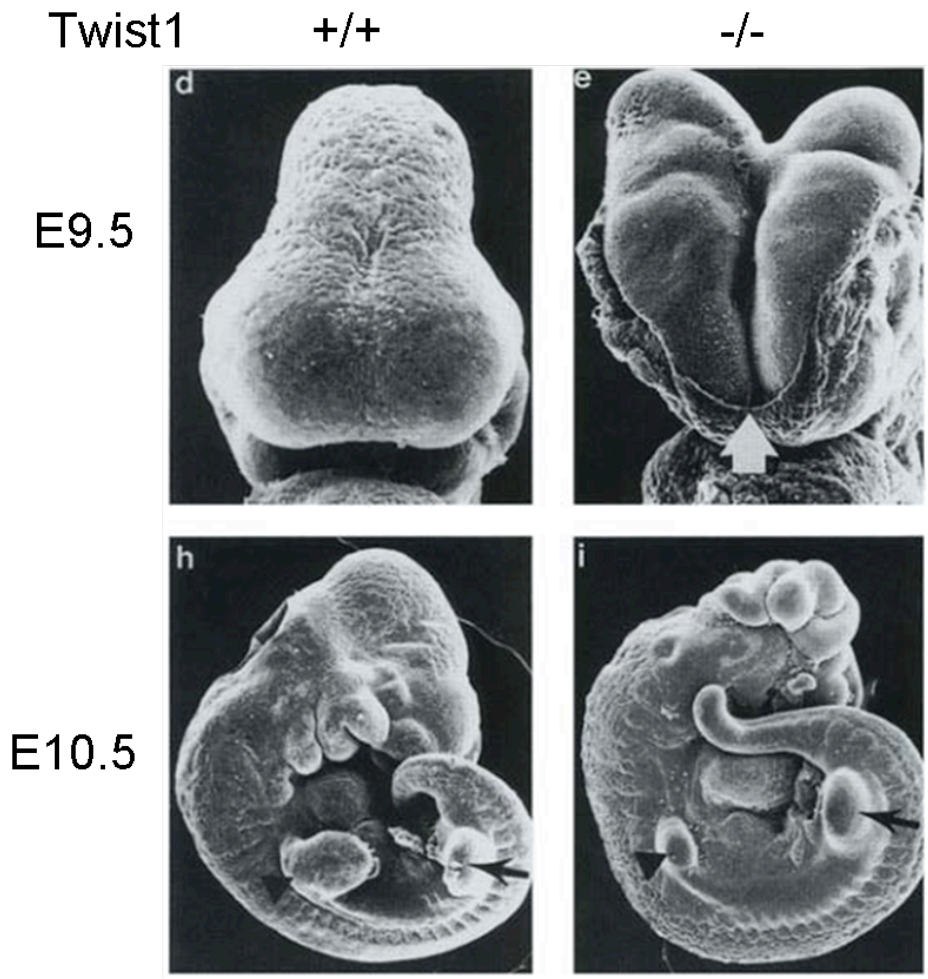
Twist1
+/+
-/-
E9.5
E10.5
d
e
h
i

I4.2.2 Mesenchymal Anomalies in *Twist1* Null Embryos

The mandibular arches in the *Twist1* null embryos were straight and disorganization (similar to that in the forebrain) was observed in the branchial arches mesenchyme [Chen and Behringer, 1995]. The neural crest cells migrating towards the first and second branchial arches were not restricted to the subectodermal mesenchyme, but invaded the paraxial mesenchyme [Soo et al., 2002]. The impaired homing ability appeared to be the consequence of non-autonomus *Twist1* cell effects, as wild type neural crest cell scattered widely in the cranial mesenchyme, when transplanted into *Twist1* null embryos [Soo et al., 2002]. Moreover, *Twist1* knockout induced downregulation of *Cdh11* (involved in cell-cell adhesion). Taken together, these results indicate that alteration in mesenchyme cell adhesion contributes to defective migration and that "*Twist1* is required in the paraxial mesoderm for proper guidance of neural crest cell migration" [Soo et al., 2002].

The overall growth of the *Twist1* null embryos was similar to that of their wild-type litter mates until day 10.5 dpc. However, large pools of blood could be found in the region of the unfused neural tube. At 11.5 dpc all mutant embryos were dead. It is presumed that death was due to multiple cranial focal hemorrhages and that the integrity of the blood vessels was affected by the disorganization of the surrounding mesenchyme [Chen and Behringer, 1995].

I4.2.3 *Twist1* Knock-out Induces Somite Disorganization

Twist1 is normally expressed at high levels in the newly formed somites, but these structures were formed in all *Twist1* null embryos and seemed superficially normal [Chen and Behringer, 1995]. However, the somatic cells were less well segregated and packed than the wild type ones, and the individual domains were less distinct. *Myog* expression at the appropriate time in the myotome indicated that *Twist1* is not required for initial steps of somite differentiation [Chen and Behringer, 1995]. Interestingly, teratoma experiments indicate that tumors generated from *Twist1* mutant ES cells contain less cartilage, extremely low levels of trabecular bone, and scarcely any muscle or tooth buds [Soo et al., 2002]. Significant numbers of apoptotic

cells were detected in *Twist1* null somites, especially in the sclerotome suggesting that *Twist1* might be required for cell growth and survival [Chen and Behringer, 1995].

I4.2.4 Saetre-Chotzen Syndrome – a Human Genetic Disease Linked to *Twist1*

Unlike homozygous null mutants, heterozygous *Twist1* mutants live into adulthood and present an incompletely penetrant and variable phenotype that resembles human Saetre-Chotzen syndrome (SCS) [Bourgeois et al., 1998]. This syndrome is classified as acrocephalosyndactyly type III and consists of a variable phenotype whose main features are: asymmetrical craniosynostosis, flat forehead, straight nasal bridge, ptosis, low hairline, facial asymmetry, small round ears, mild syndactyly of the second interdigital space, short thumbs and broad hallux, or hallucal duplication [Reardon and Winter, 1994].

The great phenotypic variability of *Twist1* heterozygous mutations is in stark contrast to the uniform lesions of homozygotes. In humans, the severity of the syndrome does not seem to correlate with the specific genetic defect. In patients with both mild and severe symptoms various point mutations have been identified as well as large gene deletions. The only correlation could be found with intellectual deficits, which are rarely found in SCS, but so far, when they appeared, they were only found in patients with large gene deletions [Gripp et al., 2000].

I4.2.5 Mapping *Twist1* Gene to SCS Syndrome

The history of human SCS syndrome and what was initially unrelated genetic mouse research, is most intriguing. The initial cases of the syndrome were reported in the first part of the XX century [Saethre H., 1931; Chotzen F., 1932]. The variability of the symptoms led to a lengthy controversy which lasted for more than 50 years regarding the precise features and classification of SCS. A review in 1994 shows, that by that time, the syndrome was loosely linked to deletions in the chromosome 7: “The precise location of and extent of deletion required for craniosynostosis is the focus of some debate among cytogeneticist, some favouring 7p15 as the likely critical area and

others considering the 7p21 region to be more important" [Reardon and Winter, 1994]. However, no later than 1995 the first *Twist1* null mouse was produced [Chen and Behringer, 1995], by 1997 the first heterozygouse mutant was analysed [Bourgeois et al., 1998] and even before that genetic tool was made public the link between human *Twist1* mutations and SCS was reported [Ghouzzi et al., 1997].

I4.2.6 Heterozygous Mice for *Twist1* Deletion

While *Twist1* null heterozygous mice are viable and fertile, there is some pre and perinatal lethality as 40% wild type mice were recovered instead of the predicted Medelian ratio of 33% [Bourgeois et al., 1998]. Mutant mice have accelerated or delayed ossifications in some bones of the skull. At day 7 dpn (days post-natal) the parietal and frontal bones have grown more rapidly in mutants while the supraoccipital bone was already formed and ossified at day 17.5 dpc in wild type, but not in mutant mice. However this difference was mostly recovered by 7 dpn with only 5% reduction in size for heterozygous mutants at that time point [Bourgeois et al., 1998]. Another finding is that 59% of the mutants present hallux duplication on either one or both hindfeet with a supernumerary condrification center present at 13.5 dpc. All heterozygotes with hallux duplication presented skull abnormalities. In rare cases face asymmetry was observed due to deviation of nasal septum and palate bones [Bourgeois et al., 1998].

I4.3 Molecular Mechanisms for TWIST1 Activity

TWIST1 belongs to a class of bHLH transcription factor that forms active dimers with E proteins. TWIST1, E proteins and ID proteins are expressed in calvarial mesenchyme [Rice et al., 2000]. In a protein-protein interaction revealed by non-reducing PAGE electrophoresis it was shown that TWIST can also form homodimers, albeit not with as high an affinity as TWIST-E (TW-E) heterodimers. Moreover, ID proteins compete with TWIST1 for dimerization with E proteins, thus favoring the TWIST1-TWIST1 (TW-TW) dimers [Connerney et al., 2006]. Interestingly, in humans *Twist1* haploinsuficiency generation of craniosynostosis is mimicked by mutations in the fibroblast growth factor receptors (*Fgfr2*) [Bellus et al.,

1996] and there is some indication that TWIST1 regulates *Fgfr2* expression. In *Twist1* heterozygous mice *Fgfr2* expression is expanded into the mid suture [Rice et al., 2000], as well as the phosphorylation of MAPK1 in response to FGFR2 activation [Connerney et al., 2008]. TW-TW and TW-E dimers were found to have opposing activities. Thus, TW-TW but not TW-E induces expression of FGFR2 in 10T1/2 cells, while TW-E blocks induction of FGFR2 expression by BMP7 [Connerney et al., 2006]. Based on these data, the authors concluded, that in *Twist1* heterozygouse mice the balance between TW-TW and TW-E dimers is shifted in favor of TW-TW formation.

I4.3.1 TWIST1 Induces Epithelial to Mesenchymal Transition

TWIST1 has been associated with epithelial to mesenchymal transition (EMT) both in development and in pathological processes. In Drosophila TWIST ortholog induces EMT in the migrating cells from the ventral furrow, a process essential for mesodermal specification [Hay E.D., 1995]. EMT is also essential for cancer cell progression through metastasis and in mouse mammary cancer cell lines *Twist1* mRNA expression correlated with tumor invasion and metastasis [Yang et al., 2004]. When *Twist1* was expressed in MDCK (a non malignant cell line) it was observed that the cobblestone-like morphology of the epithelial cells was replaced by a spindle-like fibroblastic appearance, with reduction in cell-cell contacts. This process correlated with the loss of epithelial markers: CDH1 (also known as E-cadherin), CTNNA1 and up-regulation of mesenchymal markers: CDH2 (also known as N-cadherin), VIM and FN1 [Yang et al., 2004].

I4.3.2 TWIST1 an Antiapoptotic Molecule

MYC and MYCN are oncoproteins that are expressed at high levels in many types of cancer and have been shown *in vitro* to stimulate both cell growth and apoptosis [Evan et al., 1992; Fulda et al., 1999]. It is considered that the activation of apoptosis is a fail-safe mechanism against carcinogenesis and that only cancer cell that are able to suppress this mechanism can form successful tumors, with a poor prognosis for the patient. In human neuroblastoma cells, it was shown that, MYCN is activated only if *Twist1* is expressed in the same time and, downregulation of *Twist1*

by siRNA induces rapid cell death through TRP53 (also known as p53) pathway [Valsesia-Wittmann et al., 2004]. TWIST1 inhibits MYC induced apoptosis in rat cells by downregulating *Cdkn2a* which is an apoptotic effector up-stream of *Trp53* [Maestro et al., 1999]. Together these data show that TWIST1 has antiapototic activity in early embryo development and that it might be involved in mesenchymal cell migration. It can be inferred that one of its actions is to block apoptosis induced by loss of cell-cell contact, a necessary step prior to cell migration, and that cancer cell use these feature abnormally up-regulating *Twist1* expression.

I5 Early Development in Mouse

I5.1 Epiblast Patterning: Proximal vs. Distal

In the pre-gastrulating embryo the epiblast monolayer is fated to generate all the future embryonic tissues plus the extra-embryonic mesoderm and the amnion ectoderm [Gardner and Rossant, 1979]. However, even at this early stage, the embryo patterning has already begun with the formation of a Proximal-Distal (P-D) gradient of morphogenic molecules: NODAL, BMP and WNT. All these molecules have their highest activity in the proximal part of the epiblast. The net result of this gradient is the formation around 5.0-5.5 dpc of the Distal Visceral Endoderm (DVE) which underlines the distal most part of the epiblast [Rossant and Tam, 2009]. The fate of DVE will be to migrate proximally in the next 12 hours, turning into Anterior Visceral Endoderm (AVE). The side where DVE/AVE migrates becomes the anterior region of the embryo, with the opposite region becoming posterior [Arnold and Robertson, 2009]. DVE was identified as a thickening of the visceral endoderm (VE), due to the fact that endoderm cells in this region adopt a columnar morphology [Thomas et al., 1998; Rivera-Perez, 2003]. Furthermore, DVE is characterized by expression of specific markers: *Hhex*, *Lefty1* and *Cer1*; while other markers like *Otx2*, *Gsc*, and *Foxa2* are also expressed in the Node, another region with organizer activity in the mouse [Zernicka-Goetz M., 2002].

I5.1.1 DVE Formation: Nodal Signalling

NODAL, a TGF beta ligand, which binds to ACVR2B, has a twofold role in early epiblast and primitive endoderm (PrE). In early epiblast the role of NODAL is to maintain its undifferentiated status, since in *Nodal* knockouts, the epiblast prematurely acquires a neural fate [Brennan et al., 2001; Camus et al., 2006] and the epiblast expresses both *Nodal* and its co-receptor *Tdgf1* (also known as cripto) from preimplantation stages (3.5-4.5 dpc) [Mesnard et al., 2006; Granier et al., 2011]. As the epiblast mass increases under NODAL influence, the embryo shape becomes more cylindrical and the portion of the PrE at the midline is placed further away from Extra Embryonic Ectoderm (ExE) influences. Here is where DVE forms and surgical ablation of posterior ExE at 5.5 dpc leads to a dramatic expansion of the DVE/AVE in the next few hours, while in explants cultured with posterior ExE, DVE markers domain is significantly reduced [Rodriguez et al., 2005; Richardson et al., 2006]. Furthermore, if *Nodal* or *Smad2* are mutated DVE is not patterned within the PrE [Brennan et al., 2001] and removal of ExE is not sufficient to rescue DVE in *Nodal* mutants [Mesnard et al., 2006].

Interestingly, NODAL downstream gene and, DVE marker, *Lefty1* is expressed asymmetrically in the PrE before implantation and it was suggested that the Anterior-Posterior axis might originate at this early time point [Takaoka et al., 2006]. However, while the early expression of *Lefty1* as well as that of *Hhex* (PrE and DVE marker) was confirmed in the PrE of the preimplantation embryo, both these markers are downregulated immediately after implantation, only to be re-expressed, together with *Cer1*, at 5.5 dpc at the moment of DVE formation, [Mesnard et al., 2006]. Thus, even though it is possible that the early expression of *Lefty1* could have patterning influences on epiblast and/or PrE, it seems that the key structure: DVE, only forms after implantation.

It is noteworthy, that even though NODAL signalling is required for DVE formation, one of the inhibitory influences from which DVE is protected, by being placed at a safe distance from ExE, might be NODAL itself. This can be inferred from the fact that within the epiblast/PrE NODAL signalling is the lowest in the vicinity of DVE [Beck et al., 2002], an activity gradient which is achieved in spite of

NODAL being expressed uniformly throughout the epiblast. How does this happen? NODAL is first secreted as a pro-protein which requires cleavage from the subtilisin-like proprotein convertases (SPC), FURIN (also known as SPC1) and PCSK6 (also known as SPC4 or Pace4), and if the SPC cleavage site in NODAL is mutated AVE markers *Cer1* and *Hesx1* are absent [Guzman-Ayala et al., 2004]. SPC expression in the epiblast has not been reported, but they were found in the trophectoderm and PrE before implantation (4.5 dpc). After implantation their expression becomes more restricted, namely to the ExE and the visceral endoderm of the extraembrionic compartment (ExVE) (5.5 dpc) [Mesnard et al., 2006]. Furthermore, NODAL uncleaved form is sufficient to induce secretion of SPCs in ExE and NODAL acts through FGF4 to maintain the ExE niche [Guzman-Ayala et al., 2004; Ben-Haim et al., 2006]. Thus, at 5.5 dpc, when DVE appears, active NODAL is formed in proximal part of the epiblast from where it diffuses to the rest of the epiblast and VE. It is also possible the SPCs diffuse as well and cleave NODAL throughout the epiblast, but either way the highest concentration of active NODAL must be in the proximal region.

I5.1.2 DVE Formation: BMP and WNT Signalling

Another type of signalling molecules expressed chiefly in the proximal epiblast at E5.5 are *Wnts*. NODAL activates BMP signalling in ExE from where BMP induces *Wnt3* expression in the proximal epiblast. Furthermore, *Wnt3* activates the proximal epiblast enhancer element within the *Nodal* locus [Ben-Haim et al., 2006] and *Catnnb1* (also known as β-catenin) signalling induces *Tdgf1* (also known as Cripto, a NODAL coreceptor) [Morkel et al., 2003], thus establishing a positive feedback loop. In *Catnnb1* mutants (where canonical WNT signalling is disrupted), DVE is formed albeit incompletely, thus *Cer1* and *Lhx1* are expressed in the distal part of the VE, but *Hhex* is not; subsequently DVE fails to migrate anteriorly [Huelsken et al., 2000]. If a *Catnnb1* negative regulator: adenomatous polyposis coli (APC) is disrupted in embryos, DVE fails to form [Chazaud and Rossant, 2006]. Together, these data indicate that a precise level of Wnt activation is required for correct embryo patterning at the time of DVE formation. On the other hand, it is also possible that WNT directly blocks DVE, and thus limits its expansion towards proximal VE, while positively influencing DVE formation only indirectly through NODAL [**Fig I3**].

Figure I3. DVE formation as a result of a signalling network in the gastrulatimg embryo.

DVE, characterised by expression of Lefty1 and Cer, forms in the distal most part of the visceral endoderm and, will migrate to the prospective anterior. DVE fromation is dependent on the interplay between BMP, WNT and NODAL signalling.
Source: Rossant & Tam, 2009.

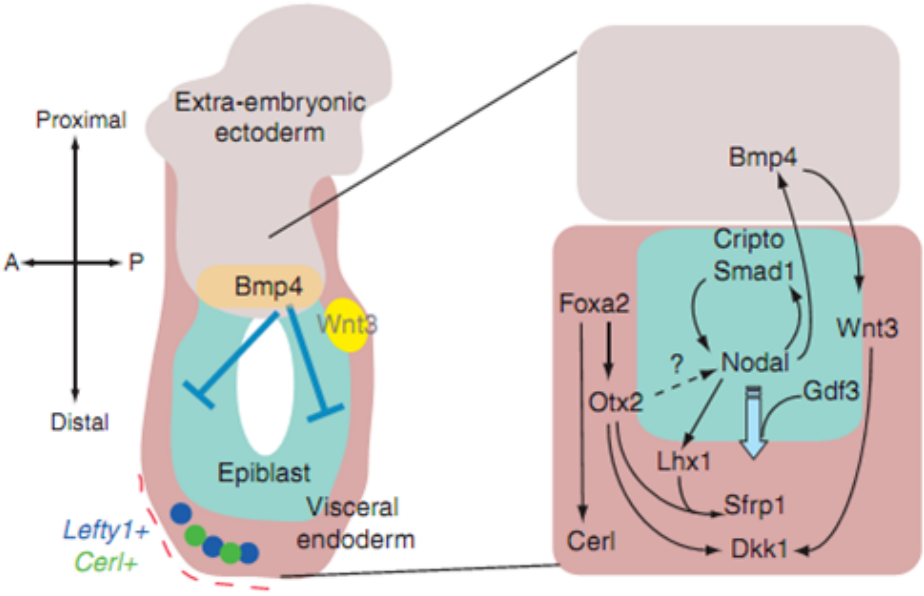
Proximal
A
P
Distal
Extra-embryonic
ectoderm
Bmp4
Wnt3
Epiblast
Visceral
endoderm
Lefty1+
Cerl+
Bmp4
Cripto
Smad1
Foxa2
Wnt3
?
Nodal
Gdf3
Otx2
Lhx1
Sfrp1
Cerl
Dkk1

I5.1.3 DVE Migration: Generation of Anterior Identity

In the next hours after its formation DVE migrates towards the anterior side of the embryo, thus becoming AVE [Rivera-Perez, 2003; Srinivas et al., 2004]. It is unclear at this point how the decision of which side is anterior is being made, in other words, if AVE is being "called" to a prepatterned anterior, or if AVE "decides" where anterior is, simply by it migrating there. However, it was noted, that at the time of its formation DVE is already asymmetrical, with *Lefty1* and *Cer1* being expressed at slightly higher levels towards the prospective anterior [Yamamoto et al., 2004].

As previously stated, WNT and CTNNB1 (beta catenin) constitutive signalling blocks AVE migration. Furthermore, in *Otx2* mutants a similar effect of impaired AVE migration was observed [Kimura-Yoshida et al., 2005]. One of OTX2 function is to induce expression of *Dkk1*, a WNT antagonist and, forced expression of *Dkk1* or, knocking out one allele of *Ctnnb1* can rescue the AVE phenotype [Kimura-Yoshida et al., 2005]. This would indicate a general requirement for WNT downregulation, without clarifying what are the determinants for the anterior-posterior (A-P) axis. Since CER1 is a NODAL, BMP and WNT antagonist [Picolo et al., 1999], perhaps its higher expression towards the prospective anterior provides the directional cues, while still not being strong enough to completely block WNT without help from other antagonists.

It should be noted, that NODAL/SMAD2 signalling induces *Foxa2* and *Lhx1* transcription factors, which trigger production of BMP, WNT and NODAL antagonists like: DKK1, LEFTY1 and CER1 [Perea-Gomez et al., 1999; Waldrip et al., 1998; Arnold and Robertson, 2009]. It cannot be ignored that BMP, WNT and NODAL signalling characterize the posterior proximal epiblast (PPE). Thus, another possibility would be that the A-P axis forms under antagonistic cues from AVE and PPE and that each is established where the signal of the other is weakest, following a series of positive and negative feedback loops [Perea-Gomez et al., 2002; Ang and Costam, 2004].

I5.2 Primitive Streak

I5.2.1 Primitive Streak: General Description

Starting at 6.0 dpc gastrulation begins with the formation, in the next few hours, in the PPE, of the primitive streak (PS), under the influence of NODAL, BMPs and WNTs which are now confined to this region. This combined signalling determines differentiation of the epiblast in this region towards mesoderm, while anterior epiblast is maintained undifferentiated by AVE [Rivera-Perez and Magnuson, 2005]. Next, PS extends distally having at its anterior tip the organizer/node, up until 7.5 dpc when the node lies at the distal tip of the embryo, approximately above the position where DVE once stood in the visceral endoderm [Robb and Tam, 2004]. The epiblast cells which ingress through the anterior most part of PS give rise to anterior axial mesoderm: prechordal plate, anterior part of the notochord and the node [Arnold and Robertson, 2009, Yamanaka et al., 2007]. The anterior axial mesoderm is a source of NODAL, BMP and WNT antagonists, thus reinforcing the protective signals from AVE. Furthermore, cells ingressing through PS at this level, also migrate in the endodermal layer, partially displace and intermingle with AVE cells and form anterior definitive endoderm (ADE) [Kwon et al., 2008]. Under the combined influence of AVE/ADE, Node and mesoderm, the anterior epiblast undergoes neural differentiation in the medial region while, the lateral region differentiates towards surface ectoderm.

I5.2.2 Primitive Streak: Inducing Signals

TGF beta signalling:

NODAL, now located in the PPE region is, as mentioned previously, the master determinant of PS formation, by indcing BMP4 in the ExE, which in turn activates WNT signalling in PPE [Ben-Haim et al., 2006]. It is noteworthy that in *Nodal* null mutants, posterior markers: *T* (alsow known as Brachyury), *Fgf8* and *Wnt3* are absent [Brennan et al., 2001; Ben-Haim et al., 2006] and, PS and consequently mesoderm don not form [Conlon et al., 1994]. Furthermore, if the SPC cleavage site in NODAL is mutated, PS markers expression *T*, *Fgf8* and *Wnt3* is severely reduced and/or not confined to the PS/prospective mesoderm region [Guzman-Ayala et al., 2004].

The importance of BMP signalling in PS formation is stressed by the fact that *Bmp4* null mutants fail to gastrulate and do not express *T* [Winnier et al., 1995]. Furthermore, mesoderm formation is under the influence of TGF beta signalling, with ACTIVIN A treatment inducing anterior mesoderm formation, while BMP is important for generation of posterior and ventral mesoderm, including hematopoietic progenitor formation [Johansson and Wiles, 1995; Finley et al., 1999].

WNT signalling:

The first marker to show proximal posterior regionalization is *Wnt3* which is expressed in this region at 5.75 dpc, before AVE has finished its anterior migration [Rivera-Perez and Magnuson, 2005]. The importance of this signalling molecule is underscored by the fact that mutating it alone is sufficient to block formation of PS and its derivates: mesoderm and notochord [Liu et al., 1999]. The same effect on this developmental structure can be generated by mutating *Ctnnb1* [Huelsken et al., 2000], or both WNT co-receptors: *Lrp5* and *Lrp6* [Kelly et al., 2004]. Furthermore embryos lacking *Wnt3a*, as well as embryos knockout for *Lrp6* only, have a milder posterior phenotype consisting of axis truncation [Takada et al., 1994; Pinson et al., 2000]. Together these data confirm the importance of WNT signalling for PS formation and development, wile pointing to WNT3 as the key WNT for the discussed stage and location.

FGF signalling:

Another signalling molecule downstream NODAL/SMAD2 is FGF8 [Waldrip et al., 1998] and, in *Fgf8*, or *Fgfr1* mutants PS forms but cells fail to leave the epiblast to ingress and to generate the mesodermal layer [Sun et al., 1999; Yamaguchi et al., 1994].

I6 *In Vivo* and *In Vitro* Neural Induction

I6.1 Neural Induction; a Job for an Organizer

After the generation of the PS neural tissue is formed in the anteriorly specified epiblast under the influence of the organizer, which has the ability to induce a secondary axis including a nervous system when transplanted to ectopic position in the embryo. This property has been conserved for many vertebrates: amphibians [Spemann and Mangold, 1924]; fish [Oppenheimer, 1936]; birds [Waddington, 1933] and mammals [Waddington, 1936].

Following many decades of intense efforts, and only after the advent of molecular biology it could be determined that the organizer neural inducing signals consist of antagonists of BMP, WNT and NODAL signalling [De Robertis E.M, 2009]. However, in the mouse the concept of an organizer proved to be more complex when notochord and anterior mesoderm were shown to be important in neural induction (vertical signals) [Sharpe and Gurdon, 1990; Ruiz I Altaba and Melton, 1989, Frohman et al., 1990] as well as the node and adjacent ectoderm (horizontal signals) [Ruiz I Altaba A., 1990; Ruiz I Altaba A., 1992; Keller et al., 1992].

When the first morphologically recognizable mouse organizer, the node, was transplanted to lateral epiblast of late streak embryos, it induced a secondary axis lacking anterior structures [Beddington R.S., 1994]. Corroborating with this, it was found that in *Foxa2* mutant mice, where the node is absent, anterior neural structures form relatively correctly patterned [Ang and Rossant, 1994; Klingensmith et al., 1999]. Thus it appeared that in mouse another structure assumed the role of anterior organizer, with the most likely candidate being AVE, which secretes BMP inhibitors. This was confirmed, when mouse AVE heterotopically transplanted to chick could induce formation of forebrain, a property not shared by the chick AVE [Knoetgen et al., 1999]. Interestingly, mouse and rabbit nodes can induce a full axis in chick, demonstrating that the absence of induced anterior structures in mice is not an intrinsic deficiency in the mouse node [Knoetgen et al., 2000].

Nevertheless, a small group of cells placed immediately anteriorly to the distal tip of PS, secretes BMP antagonists long before the formation of the node [Robb and Tam, 2004]. Thus when this region from early streak embryos, dubbed early gastrula organizer (EGO) was transplanted to lateral epiblast of late streak embryos it could induce a secondary axis, but it too was lacking the anterior structures. On the contrary, when the distal PS of mid streak embryos, mid gastrula organizer (MGO) was transplanted it could induce a full secondary axis [Tam et al., 1997]. As already described, AVE signalling is strengthened by cells from PS forming the anterior axial mesoderm and ADE. Anterior mesoderm induces *Otx2* in adjacent cells, while posterior mesoderm represses it [Ang et al., 1994]. Fate mapping revealed that the majority of these cells ingress from the anterior PS of mid gastrula stage [Kinder et al., 1999; Kinder et al., 2001]. Thus, while posterior notochord is a node derivative, anterior notochord forms by condensation of cells of the anterior axial mesoderm, which are already placed between the AVE and prospective anterior neural tissue at the time of node formation [Yamanaka et al., 2007].

I6.2 Modelling Neural Induction

I6.2.1 The "Default Model"

An essential observation regarding *in vitro* manipulation of neural induction, before the first identification of organizer secreted molecules [Smith and Harland, 1992; Sasai et al., 1994; Hemmati-Brivanlou and Melton, 1994; Bouwmeester et al., 1996], was that in Xenopus, animal cup explants form epidermis, unless the cells are dissociated, in which case they form neural tissue [Grunz and Tacke, 1989]. Later it was proposed that this phenomenon is due to dilution of BMP signalling when cells are dissociated [Hemmati-Brivanlou and Melton, 1994; Wilson and Hemmati-Brivanlou, 1995]. Furthermore, BMP inhibitors or depletion of multiple BMP ligands leads to conversion of the entire ectoderm into neural tissue even in the absence of the organizer [Lamb et al., 1993; Reversade et al., 2005]. Thus, the idea of the default model was born, according to which the default fate of all epiblast cells is to become anterior neural cells and active inhibition of this pathway, by BMP, is required for the

generation of other cell types [Munoz-Sanjuan and Brivanlou, 2002; Levine and Brivanlou, 2007].

I6.2.2 A Chick Strikes at The Default Model

The first serious challenge to the "Default Model" came from work in chick. While in Xenopus, BMP antagonist Chordin is sufficient to induce CNS formation in ecotdermal explants [Sasai et al., 1995], the same is not true in chick embryos [Streit et al., 1998]. It was found that in order to respond to BMP antagonists, chick epiblast need to be exposed to FGF8 signalling, which transiently induces an Early Response to Neural Induction gene (*Erni*) [Streit et al., 2000]. The *Erni* upregulation in the prospective neural plate starts before gastrulation and it has been proposed to be under the control of FGF8, a molecule secreted by the Node. In an attempt to explain how *Erni* can be induced before Node formation, it was proposed that a group of prospective Node cells express *Fgf8* before gastrulation and, that this is the source of neural priming signal [Streit et al., 2000].

I6.2.3 The Default Model Counterattacks on All Fronts

A possible explanation would be that work on two model organisms revealed an evolutionary change: namely that in lower vertebrates neural induction is solely dependent on BMP inhibition, while in higher vertebrates the mechanism is more complex. However, this does not seem to be the case, since in mouse, loss of *Bmpr1a* leads to conversion of the entire epiblast to anterior neural tissue and, inhibition of FGF signalling does not block neural induction [Di-Gregorio et al., 2007]. The default model is strengthen by the evolutionary development of redundancy in BMP inhibitors and, while downregulation of single BMP antagonists in Xenopus has minimal consequences, depletion of *Fst* (follistatin), *Chrd* (chordin) and *Nog* (noggin) together "results in catastrophic failure in dorsal development" [Khokha et al., 2005]. Furthermore, in mice, deletion of both *Chrd* and *Nog*, which are secreted from the node but not AVE, leads to impairment of forebrain formation [Bachiller et al., 2000].

The defenders of the Default Model further charged, by showing that in Xenopus cell dissociation does not work through reducing BMP signalling, which

continue in an autocrine fashion, but by activating FGF signalling. However, this FGF/MAPK acts by phosphorylating and inhibiting SMAD1. Thus, FGF is just another BMP antagonist [Kuroda et al., 2005]. Moreover, IGF, another neural inducer [Pera et al., 2001], works by the same mechanism of MAPK dependent SMAD1 phosphorylation and, IGF and FGF signalling integration at SMAD1 level is required for CHRD induction of neural fate [Pera et al., 2003]. In chick, FGF was also found to be required for acquisition of neural fate through inhibition of BMP [Wilson et al., 2000] and in salamanders lateral epiblast can be induced to neural by MAPK1 pathway [Hurtado and DeRobertis, 2007].

I6.2.4 The Default Model Under The Scrutiny of *In Vitro* Investigation

Similarly to Xenopus dissociated animal cup cells, mouse ES cells cultured at low density in minimal conditions rapidly and spontaneously undergo neural differentiation [Tropepe et al., 2001; Smukler et al., 2006]. Furthermore, while removal of BMP is sufficient for ES cells to progress towards neural, differentiation along this line cannot progress if FGF receptor is blocked and this cannot be rescued by inhibiting BMP signalling [Ying et al., 2003b]. The requirement for FGF signalling is restricted to a time within the first 24h of ES cells differentiation and could be as short as just 1h [Stavridis et al., 2007]. This observation was correlated with chick data showing that FGF inhibition only blocks neural induction before the late streak stages [Stavridis et al., 2007] and in Xenopus, Fgf is required in pre-gastrula stages [Delaune et al., 2005]. Moreover, another key player, NOTCH, increased neural differentiation of ES cells and inhibition of this pathway resulted in a major reduction, although not complete block, of neural differentiation [Lowell et al., 2006].

I6.2.5 Neural Induction: The Field Is Getting Crowded with Players

The cooperation between Fgf and Bmp inhibitors in Xenopus neural induction is not a new finding [Lamb and Harland, 1995]. Interestingly, a more recent report showed that Xenopus Bmp inhibition can induce neural formation only in the presence of Fgf signalling; that Bmp inhibition induces *fgf4* and that, Bmp inhibition further induce some neural genes like *zic1*, while Fgf4 induce a different set of neural

genes one example being *zic3*. *Zic1* and *zic3* are both required for neural specification [Marchal et al., 2009]. Induction of a different set of neural genes by Bmp inhibition and Fgf activation has since been confirmed [Rogers et al., 2011]. It is of note that in the future years a much more complicated picture could emerge. For instance, it was showed, that while *Sox3* is uniformly expressed in the mouse developing central nervous system (CNS), its expression is nevertheless dependent on multiple molecular regulators, with a regional characteristic pattern [Brunelli et al., 2003].

This intensive research on neural induction established beyond any question the central role played by BMP inhibition in the process. It also provided strong evidence for the fact that while the final outcome, i.e. the CNS of different vertebrates may look very different; the mechanisms of initial neural specification are evolutionarily conserved.

Thanks to the large body of work we have now a more complete understanding of the process, mainly concerning the early requirement for FGF signalling, which complements BMP inhibition, as well as the fact, that other pathways like IGF and NOTCH integrate into a final tightly regulated neural induction. It seems that all these data strengthens rather than challenges the default model. Surely, the default model could have never been understood as the absence of all signalling pathways. In order for an alternate model to be proposed it should have been shown not only that other signalling present at the level of undifferentiated cells is important for the induction, but also, that in the embryo, an extrinsic signalling centre for such pathways exists. The closest to come to such evidence was the group of Claudio Stern [Streit et al., 2000; Stern C.D., 2006] who proposed the prospective organizer group of cells as the source of early FGF signalling. However, even though the requirement for such an early signalling is not a matter of controversy, the fact that the FGF8 secretion by those cells is in any way biologically significant, has not been shown. Furthermore, there is no evidence that the intrinsic epiblast cells signalling is not enough to make them responsive to BMP inhibition.

Interestingly, in amniotes epiblast cells undergo extensive polonaise movements prior to gastrulation and, these movements have been characterized as having a precise pattern [Voiculescu et al., 2007]. It is thus possible that all prospective neural plate cells are primed before gastrulation, by passing in the proximity of prospective

organizer cells expressing *Fgf8*, while the later signals from the Node, Notochord, mesoderm and AVE have the role to confirm and stabilize the initial program. However, at this time, the developmental significance of epiblast cell movements is only a matter of speculation.

I6.3 ES Cells as a Model of Neural Induction

I6.3.1 Embryoid Body Technique

Mouse ES cells can be differentiated along multiple cell lineages using the embryoid body (EB) technique. In this method, ES cells are cultured in media without LIF and on a substrate to which they cannot attach and, in these conditions, a low percentage differentiate along neural lineage [Zhuang et al., 1992]. Efficiency of neural differentiation could be increased by adding retinoic acid (RA) after the first 4 days of culture and allowing cells to attach after another 4 days (4-/4+ protocol) [Bain et al., 1995]. A protocol in which RA was maintained only for the first 2 days of differentiation has been attempted as well [Fraichard et al., 1995]. The efficiency was further increased in the 4-/4+ protocol by actively dissociating the embryoid bodies and plating them on laminin coated dishes in serum free defined medium containing DMEM/F12 and N2 supplement [Li et al., 1998].

I6.3.2 Neural Differentiation in Monolayer Technique

Although the use of EB solved the problem of generating large number of neural progenitors/neurons *in vitro*, this method does not allow for the investigation of the critical steps of neural specification. Within the rather complex environment of the embryoid body neural cells are generated following obscure intercellular signalling which can not be easily investigated or controlled. To address this, a monolayer differentiation protocol was proposed, taking advantage of the previously discussed minimal inductive signalling required for neural differentiation. Thus, mouse ES cells were differentiated on cultured dishes, coated with gelatine in a defined media with the N2/B27 mixture. This medium necessarily contains signalling molecules required to help support cell health and survival (e.g. insulin, estrogen,

progesterone), and could in principle contain signals that help promote a neural fate, notably retinoic acid (RA). It was shown to support efficient neural differentiation as assessed by *Sox1* upregulation, a specific marker of neural ectoderm [Wood & Episkopou, 1999]. It was observed that BMP, or serum signalling fully blocks neural differentiation by inducing ID proteins and, that neural differentiation is dependent on autocrine FGF signalling [Ying et al., 2003a; Ying et al., 2003b].

Interestingly, BMP4 blocks FGF dependent MAPK1 activation in ES cells but not in EpiSC. BMP4 also blocks MAPK1 in EpiSCs differentiating towards neural while, in N2B27 BMP stimulates MAPK1 in ES at 24 hours [Zhang et al., 2010]. This indicates that the interplay between BMP and FGF is cell context dependent.

After generating neural stem (NS) cells during 7 days in the monolayer protocol, they can be propagated on laminin under the influence of FGF2 (Conti et al., 2005) and addition of FGF2 in culture (after 7 days) induces markers differentially upregulated during neural conversion like: *Cd44*, *Adam12*, *Cdh20*, *Cx3cl1*, *Egfr*, *Fzd9*, *Kitl*, *Olig1*, *Olig2* and *Vav3* [Pollard et al., 2008]. Furthermore, FGF2 binds to heparan sulphate (HS) on the cell surface, HS sulfation status changes during neural differentiation and, in the absence of HS, ES cells cannot differentiate in the monolayer protocol [Johnosn et al., 2007].

I6.3.3 Neural Differentiation of hESCs

hESC could also differentiate to neurons when allowed to form embryoid bodies [Zhang et al., 2001], however, this method has the already mentioned disadvantage that the signalling pathways involved cannot be either controlled or dissected. hESC can be maintained as undifferentiated monolayer on fibroblast cells, though they have a tendency to differentiate towards primitive endoderm. When BMP signalling was blocked, in these conditions, by addition of NOG, endoderm differentiation was abolished and instead cells differentiated towards neural [Pera et al., 2004]. In defined condition hESC can be cultured on matrigel and, in these conditions they require supplementation of N2/B27 with NOG and FGF2 for induction of a neural cells expressing both *Pax6* and *Sox1* [Yao et al., 2006]. RA which has been shown to be important for neural differentiation of mouse ES cells [Stavridis et al., 2010], only has the role to bias hESC neural differentiation towards a caudal phenotype and this

effect was only observed when starting from early neural rosettes, which are *Pax6*+ and *Sox1*- (first 8 to 10 days) [Li et al., 2005]. When both branches of TGF beta signalling were blocked, using NOG and SB431542 (a ACVR1B and ACVR1C inhibitor) neural cells could be induced efficiently and rapidly; *Pax6* being upregulated between days 5 to 7 and *Sox1*, the earliest marker in these conditions, being upregulated between days 3 to 5 [Chambers et al., 2009]. Interestingly recent reports suggest that FGF2 maintains pluripotency of hESC by inhibiting neural differentiation, in particular the induction of *Pax6* [Greber et al., 2008; Greber et al., 2010]. Furthermore, it was found that the most effective neural induction, with upregulation of *Pax6* between day 3 and 5, can be achieved by a triple inhibition of: BMP/SMAD1 with NOG, TGF-beta/SMAD2 with SB431542 and FGF/MAPK with PD0325901 [Greber et al., 2011].

Taken together, *in vitro* work in mouse and human ES cells confirmed the role proposed in the embryo of BMP inhibition on neural differentiation. It confirmed as well, the importance of FGF signalling, albeit there seem to be contradictions between mouse and humans. However, these could possibly be explained by the concept of a cell on the road to differentiation captured in different stages, with different requirements. As pointed out by the *in vivo* work, FGF stimulation is critical at very early stages. It is possible that after an intermediate stage when FGF is normally downregulated, it is again involved in specification of certain neural types. The possibility cannot be excluded either, that generating neurons in the most rapid way, may not necessarily be the best way. In this context, FGF function could be to prolong the life and expand the pool of progenitors. It should also be noted that the key aspect of BMP inhibition has not been investigated yet beyond its relation with *Id* upregulation.

I6.3.4 Cadherin1 is Downregulated Early in Neural Differentiation

ES cells express CDH1 which functions in maintaining pluripotency and, CDH1 is downregulated during differentiation [Soncin et al., 2009]. Furthermore, CDH1 is reexpressed during fibroblast reprogramming to induced pluripotent cells: in the absence of CDH1 fibroblast cannot be reprogrammed while, expression of *Cdh1* can replace *Pou5f1* during the discussed process [Redmer et al., 2011].

A detailed analysis of ES monolayer neural differentiation indicated a sequential marker dynamic: loss of *Pou5f1*, loss of *Cdh1*, loss of *Fut4* (also known as SSEA-1). The last step coincides with downregulation of *Sox1* and formation of neurons. Furthermore, FGF signalling transiently amplifies the FUT4+ CDH1- population, corresponding to neural progenitor cells [Sterneckert et al., 2010].

Furthermore, during *in vitro* neural differentiation of mouse ES cells CDH1 is lost from the cell surface before the upregulation of *Sox1* [Kamiya et al., 2011].

I6.3.5 *In Vivo* Switch from CADHERIN1 to CADHERIN2 during Neural Differentiation

Epiblast cells differentiating towards neural progenitors switch from CDH1 to CDH2. Initially neural plate is specified in CDH1 positive cells domain, but as neural folds invaginate, at 8.5 dpc, they express CDH2, starting from the deepest region of the neural groove, future floor plate [Hatta and Takeichi, 1986].

This switch from CDH1 to CDH2 is dependent on EMT inducer *Zeb2* (also known as Sip1 – SMAD interacting protein 1, or Zfhx1b) [Van de Putte et al., 2003]. Interestingly, cells ingressing through PS also express CDH2, although later on, this marker is specific to neural derivates, with the exception of the heart and lens [Hatta and Takeichi, 1986].

It is of note that while PS cells undergo a full EMT and migrate away from the epiblast, neural progenitors only upregulate some EMT markers, while remaining a morphological epithelial sheet. Only at the time of neural crest migration, some of these cells will upregulate *Snai2* and break away from epithelial cell to cell contact.

Furthermore, induction of *Zeb2* in the neural plate downstream of FGF/CHURCHILL has been shown to block mesoderm fate at the midline [Sheng et al., 2003]. In hESCs and mouse EpiSCs, *Zeb2* inhibits ACTIVIN/NODAL induced mesoderm fate, without interfering with the maintenance of pluripotency and, *Zeb2* protects neuroectoderm fate agains BMP inhibition [Chnq et al., 2010]. Future research will probably determine if *Zeb2* influence on EMT and, its anti BMP and SMAD activity are two independent or related processes.

I7 Neural Crest at The Border between Prospective Epidermis and Neural Tissue

I7.1 Neural Crest: Overview

Neural crest cells are a vertebrate specific cell type, though evidence for the existence of neural crest like cells has been presented for primitive chordates [Baker and Bronner-Fraser 1997b]. Neural crest cells are specified in the lateral parts of the neural plate, near the border with the surface ectoderm; they delaminate around the time of neural tube closure, migrate extensively and differentiate in a wide range of cells such as peripheral neurons, glia, melanocytes, smooth muscle, cartilage and bone [Baker and Bronner-Fraser 1997a].

Neural crest cells were first identified by their ability to migrate from the dorsal edge of the neural folds (the crest) [His, 1868; Hörstadius, 1950; Weston, 1963]. However, putative neural crest markers are detected prior to this event. A synopsis of such molecules is presented below.

I7.2 Neural Crest: Markers

***Dlx5*:**

One of the earliest detected markers in mouse is the neural crest associated homoeobox gene *Dlx5*, a transcription factor known to interact with MSX1 [Yang et al., 1998]. It is expressed in mouse at the anterior neural ridge (ANR) at late streak stages and marks the lateral edges of the anterior neural plate, presumptive neural crest, at the head fold stage. This later signal disappears soon after the neural tube closure, while the one in the ANR continues [Yang et al., 1998]. Furthermore, fate map indicates that the ANR *Dlx5* domain does not generate any neural crest cells [Cajal et al., 2012]. In Xenopus it marks the neural/ectoderm border, as well as participating in determining its formation [McLarren et al., 2003].

***Tfap2a*:**

Tfap2a (also known as AP2 alpha) was found in mouse to be expressed starting at 8.5 dpc in neural crest and its main derivates, including sensory ganglia and facial mesenchyme. *Tfap2a* is also expressed at lower levels in the ectoderm [Mitchell et al., 1991].

***Msx1*:**

The homeobox gene *Msx1* has been reported in 9.5 dpc mouse embryos in the lateral domain of the trunk neural plate before closure and, in the dorsal-most neural tube after closure [Hill et al., 1989].

***Pax3*:**

The paired box gene *Pax3* is first detected at 8.5 dpc in the dorsal parts of the neuroepithelium with a second expression domain in the developing somites. Subsequently it marks specific brain and spinal cord neurons, as well as neural crest cells in the craniofacial domain, limb mesenchyme and spinal ganglia [Goulding et al., 1991]. More recent reports indicate that *Pax3* is expressed in the epiblast at 6.5 dpc and then, in the anterior neural folds [Basch et al., 2006].

***Pax7*:**

Pax7 is expressed in the epiblast at 6.5 dpc in the future neurectoderm. Later, it is found in the neural folds and, caudal neural folds express *Pax7* but not *Pax3* [Basch et al., 2006]. *Pax7* was also found, to have a second expression domain in the dermatomyotome, with a role in the development of skeletal muscle tissue [Jostes et al., 1990]. Interestingly, *Pax7* null mice are born with defects in cephalic neural crest derivates, but not in the CNS or skeletal muscle [Mansouri et al., 1996] and *Pax7* is required for neural crest specification in chick [Basch et al., 2006].

***Zic* factors:**

Zic genes, the vertebrate homologous of Drosophila odd-paired (*opa*) gene are first expressed at 7.0 dpc in the embryonic mesoderm. At 7.25 dpc *Zic1* and *Zic2* are also expressed in the presumptive dorsal neuroectoderm, with *Zic2* expression becoming more intense in this structure than in the dorsal mesenchyme. At the time of neural tube closure, 9.5 dpc, *Zic1*, *Zic2* and *Zic3* were expressed in the dorsal

midline [Nagai et al., 1997]. In Xenopus, homologs of *Zic1*, *Zic2*, *Zic3* and *Zic5* are all expressed at the neural plate border region and have been found to be important for neural crest development [Nakata et al., 1997; Nakata et al 1998; Nakata et al., 2000]. Mutation of *Zic1*, *Zic2* and *Zic3* in mouse induces neural tube development defects with a weaker effect on neural crest derivates [Nagai et al., 2000]. However, it was later found that *Zic5*, another member of the *Zic* family, with an expression pattern overlapping the previously describes *Zic*s, induces severe defects, if mutated, in facial mesenchyme and facial nerves development [Inoue et al., 2004].

***Foxd3*:**

Foxd3 is a winged-helix transcription factor which has been reported in chick to be expressed in the neural plate at the early primitive streak stage in premigratory neural crest progenitors and to be maintained in migratory neural crest cells until they reach their destination [Yamagata and Noda, 1998], a finding which has been replicated in mouse [Labosky and Kaestner, 1998]. Interestingly, *Foxd3* has also been reported as a molecular switch between neural crest and neuronal fates, differentiating it form other neural crest markers like *Msx1/2*, *Zic1-3*, *Pax3*, *Pax7* which are also expressed in a subset of neurons. Furthermore, FOXD3 can induce neural crest delamination independent of SNAI2 [Dottori et al., 2001].

***Snai1*:**

Snai1 has been shown to be expressed at 8.5 dpc (7 somite stage) in head and trunk migrating neural crest cells. Subsequently, it was expressed in mesenchymal derivates from both neural crest and mesoderm, but not in neuronal neural crest derivates [Smith et al., 1992].

***Snai2*:**

Snai2 is detected in migratory, but not pre-migratory neural crest cells and, its deletion did not impair formation, migration or differentiation of these cells [Jiang et al., 1998].

Sox9* and *Sox10

Sox9 is one of the earliest markers to be expressed in neural crest precursor cells in chick and mouse [Sauka-Spengler and Bronner-Fraser, 2008, Lee and Saint-

Jeanette, 2011] and its expression is followed somewhat later by *Sox10* [Haldin and LaBonne, 2010]. *Sox9* is also required for subsequent neural crest migration [Cheung et al., 2005], while *Sox9* and *Sox10* can both induce formation of ectopic neural crest [Cheung et al., 2003; Kelsh, 2006; Haldin and LaBonne, 2010].

Wnt1

Wnt1 is expressed only in development and is restricted to CNS, marking the prospective midbrain. Around neural tube closure it is detected dorsally, at the midline and, its expression preceded delamination of the neural crest cells. It can be used as a marker of delaminating neural crest cells although, it is rapidly downregulated in these cells [Echelard et al., 1994; Chai et al., 2000].

It is challenging to infer the moment of neural crest induction based on the marker analysis. First, none of the markers is neural crest specific, i.e. expressed only in neural crest cells. Secondly, neural crest is specified within the neural plate and it is unclear what is the sequence of events which turn some of the neural plate cells into neural crest. Thirdly, all the presented markers partially overlap spatially and temporarily making it difficult to generate a map of prospective neural crest, or even neural tube.

A relatively recent study [Puelles et al., 2005] compared the markers reported in the literature for neural or non-neural ectoderm with a carefully generated fate map of stage 4 chick embryos. They found that no marker corresponds precisely to neural or non-neural fates, but rather the "non-neural ectoderm apparently grades over into neural ectoderm in a step-like fashion", by partially overlapping marker expression patterns.

I7.3 Neural Crest Induction Revealed by Fate Mapping

A recent study investigated the fate map of the anterior epiblast and found that it can be divided into three regions: proximal, distal and intermediate. The cells from the proximal region (most rostral) populate only surface ectoderm. Majority of the

proximal cells populate the neuroectoderm, while a minority distributed to ventral ectoderm of the anterior prosencephalon, with no contribution to the surface ectoderm. Progenitors from the intermediate region generate a wide variety of cells [Cajal et al., 2012]. Neural crest cells were found in clones originating from distal and intermediate region, but not the proximal one. The most rostral limit of neural crest progenitors was found at the level of the prospective forebrain just caudally of the optic pit and outside the most anterior limit of Tfap2c (also known as AP2.2) [Cajal et al., 2012].

Corroborating marker analysis with clonal fate maps a clearer picture emerges, while the exact steps and signals of neural crest induction still remain to be uncovered. It is more likely that rather than being defined by precise marker domains, neural crest is determined by the interplay of ectodermal and neural signals and represents an area of extended potency, as indeed, it has been named as the fourth germ layer [Hall, 2000]. Interestingly, when early chick epiblast explants of stage 3-4 were cultured on collagen gels, only those from the medial region, prospective border, were able to generate migratory cells, which could differentiate into melanocytes [Bash et al., 2006]. This indicates that neural crest competence is determined before upregulation of any known neural crest marker and before induction of the neural plate.

I7.4 Signals Inducing Neural Crest Fate

When neural crest induction was investigated in chick, it was found that, juxtaposition of non-neural ectoderm and presumptive neural plate induces formation of neural crest cells. Moreover, both epidermis and neural plate can contribute to neural crest [Selleck and Bronner-Fraser 1995]. Grafting exp in Xenopus showed that neural crest can be induced by an interaction between neural plate and epithelium and both structures are able to generate neural crest cells [Mancilla and Mayor, 1996].

Regarding signalling molecules which may be involved in neural crest specification, BMPs, WNTs and FGFs have been proposed as main palyers [Milet and Monsoro-Burq, 2012].

In Xenopus progressively higher levels of BMP induce Neural plate, neural crest and non-neural ectoderm respectively [Marchant et al., 1998]. The neural crest threshold BMP level, is believed to be determined by interplay of BMP and BMP inhibitors and, the authors propose ectoderm as the source of BMP and mesoderm as the source of BMP inhibitors [Marchant et al., 1998].

Based on Xenopus work as well, other authors proposed a "Two signal model" [La Bonne and Bronner-Fraser, 1998] where low levels of Bmp provide an initial., weak specification of neural crest fate, which is then stabilised by a second signal., proposed to be either Wnt8a or Fgf4. As a source for this second signal non-neural ectoderm and/or underlying mesoderm were considered [La Bonne and Bronner-Fraser, 1998]. Further workindicated that Fgf4 or Fgf8 are the predominant signals, being able, unlike Wnt8a, to induce neural crest even in the absence of Bmp inhibition [Monsoro-Burq et al., 2003]. However, more recent work pinpointed Wnt8a as the neural crest inducing signal secreted from mesoderm, with Fgf8 acting indirectly by activating Wnt8a. Furthermore, the underlying mesoderm secrets Chrd, a Bmp antagonist, which works in conjunction with Wnt signalling to specify neural crest [Hong et al., 2008; Steventon et al., 2009]. However, these findings have again been challenged by further work showing direct FGF signalling requirement in the epiblast for correct patterning of the neural plate/neural crest, in chick [Stuhlmiller and Garcia-Castro, 2012]. Together, these studies provide strength to the idea of the importance of BMP, WNT and FGF signalling in the discussed process, while indicating that all these molecules might be acting in a complex manner, at multiple check-points during neural crest specification.

I7.5 Neural Crest Delamination: The First Overt Manifestation of an Undercover Cell

After induction neural crest cells delaminate from the neural folds/neural tube and migrate to perform their function. This process takes place throughout the length of the neural tube with the exception of the rostral most parts [Nichols D.H., 1981; Couly and Le Douarin, 1985; Couly and Le Douarin, 1987; Le Douarin et al., 2012]. It has also been reported that neural crest migration participates in actual closure of the neural tube [Davidson and Keller, 1999].

Interestingly the manner of migration varies along the rostro-caudal axis, as well as between different species. In the cranial region, neural crest delaminate in an abrupt collective process, while at the trunk level they delaminate individually, over a period of time, in a dripping fashion [Erickson and Weston, 1983; Theveneau et al., 2007]. Moreover, in rostral trunk regions neural crest delaminate just before the respective somite formation, while in more caudal regions the delamination is delayed in relation to somitogenesis [Clay and Halloran, 2010, Theveneau and Mayor, 2012]. Interestingly, neural crest delamination is timed similarly in respect to the neural tube closure in all species, at the trunk level, but not at the cranial level. In the former delamination takes place after the neural tube has closed in all species examined, while in the latter it does so before closure in Xenopus, mouse and human, but not in chick [Nichols D.H., 1981; Nichols D.H., 1987, Sadaghiani and Thiebaud, 1987, Theveneau et al., 2007].

I8 Dorso-Ventral Neural Tube Patterning

I8.1 Neural Tube Patterning; Ventral Signals

Neural tube is patterned by two streams of opposing signals: BMP and WNT from the dorsal and, SHH (sonic hedgehog) from the ventral.

The ventralmost part of the neural tube is formed by the Floor Plate (FP), which can be morphologically recognised as a thin strip of cells and, can be molecularly characterized by expression of *Foxa2* and *Shh*. It is thought that signals from the notochord induce the FP, as shown by the fact that notochord implants ectopically induce FP in the lateral neural tube [van Straaten et al., 1985; Yamada et al., 1991].

I8.1.1 FOXA2 and SHH in Control of The Neural Ventral Patterning

One of the first factors to be expressed in the presumptive notochord is *Foxa2* (also known as HNF3β). It is required for proper formation of the notochord and for subsequent expression of *Shh* in this structure [Echelard et al., 1993; Ang & Rossant, 1994]. Furthermore, expression of *Shh* in the notochord induces its own expression in the floor plate [Chiang et al., 1996; Dale et al., 1997]. Interestingly, *Shh* also induces *Foxa2* in the ventral parts of the neural tube [Echlart el, 1993, Liu et al., 1998] and ectopic expression of the *Foxa2* can ventralize more dorsal regions [Sasaki & Hogan, 1994, Liu et al., 1998]. Thus FOXA2 and SHH cooperatively establish the neural tube ventral signalling centre.

I8.1.2 Neural Tube Patterning: The Work of Morphogenes

The equivalent of the FP in the dorsal part of the neural tube is the roof plate. In between these two plates the neural tube is patterned with progenitors of different neuronal types precisely located on the DV axis [Ribes and Briscoe, 2009]. It is thought that this patterning is achieved by graded morphogen signals from the two sources, ventral and dorsal. For instance, the cleaved form of SHH, which has signalling functions, was found to extend through a narrow region in the ventro-lateral domain, beyond the FP [Marti et al., 1995] and, different concentration of this

peptide are required for the induction of floor plate and motor neuron respectively [Roelink et al., 1995]

I8.1.3 Hedgehog Signalling: Releasing The Inhibition

SHH is first produced as a pre-protein followed by post-translational modifications: first the C-terminal portion is cleaved by autocatalysis [Lee et al., 1994,], followed by addition of cholesterol at the C-terminus [Porter et al., 1996] and palmitoilation at the N-terminus [Pepinsky et al., 1998]. The cholesterol modified Shh can be secreted from the cell by the transmembranar protein Dispatched1 (DISP1) [Burke et al., 1999]. After reaching the target cell SHH binds its receptor Patched1 (PTCH1) [Marigo, 1996a; Stone et al., 1996; Fuse et al., 1999] and releases the inhibitory action PTCH1 has over Smoothened (SMO) [Martin 2001], which then is responsible for all SHH intracellular activity [Frank-Kamenetsky et al., 2002; Chen et al., 2002]. In support of this model, deletion of *Ptch1* is sufficient to induce hedgehog signalling in the absence of hedgehog ligands [Goodrich et al., 1997].

I8.1.4 GLI Factors: The Ultimate Hedgehog Effectors

Activation of SMO induces the dissociation of a microtubule associated multiprotein complex, with the release of GLI transcription factors and activation of hedgehog target genes [Lum et al., 2003; Ruel et al., 2003; Ogden et al., 2003]. SHH performs its actions through GLI proteins (members of the zinc-finger transcription factors) and it has been shown that their activation can fully replace SHH in neural tube patterning [Stamataki et al., 2005].

In mouse there are three *Gli* genes [Hui et al., 1994, Hughes et al., 1997], GLI1 is an activator of SHH pathway target genes, while GLI2 and GLI3 have both activator and repressor domains [Dai et al., 1999; Sasaki et al., 1999]. The repressor activity of GLI2 and GLI3 is induced by proteolysis of the C-terminal domain and this process is blocked by SHH [Sasaki et al., 1999, Wang et al., 2000]. *Gli1* expression is induced by SHH and consequently it is expressed in a ventral to dorsal gradient [Lee et al., 1997]. *Gli3* expression is induced by WNT and repressed by SHH and it is expressed in a dorsal to ventral gradient [Alvarez-Medina et al., 2008;

Yu et al., 2008; Marigo et al., 1996b, Bucher et al., 1997]. *Gli2* is expressed throughout the neural tube independent of SHH activity.

Since *Gli2* expression is not dependent on SHH it is thought to be the first GLI factor to mediate SHH activity [Bai et al., 2002], its deletion results in the absence of floor plate [Ding et al., 1998; Matise et al., 1998]. GLI1 can mimic SHH function, including ectopically induction of *Foxa2* [Hynes et al., 1997], but its deletion does not result in an overt phenotype [Park et al., 2000; Bai et al., 2002]. Together these data suggest that GLI2 can compensate for GLI1 but not the other way around.

I8.1.5 Hedgehog Signalling Regulation: Negative Feed-back

The fact that 2 out of 3 GLI factors have repressing functions indicate that the negative feed-back is one of the key mechanisms that prevent SHH signalling to be induced too far from its source. It is of note that GLI3 is thought to work mainly as a hedgehog repressor and its expression is negatively regulated by SHH [Yu et a, 2008]. Furthermore, in a negative feedback loop SHH transcriptionallly activates hedgehog pathway repressor *Ptch1* [Tabata and Kornberg, 1994; Marigo and Tabin, 1996; Goodrich et al., 1996] and all GLI proteins can bind to the *Gli* binding site in the *Ptch1* promoter [Agren et al., 2004].

I8.1.6 *Gli* Mutants Altered Neuronal Fate on the D-V Axis

In *Gli3* mutants intermediate neural tube neurons are expanded dorsally [Persson et al., 2002] and neurons with ventral telecephalic identity develop ectopically in the dorsal telecephalon [Tole et al., 2000], while $Shh^{-/-}$ $Gli3^{-/-}$ double deletion significantly rescues the absence of the ventral neurons from the $Shh^{-/-}$ single mutant [Litingtung and Chiang, 2000]. This would suggest that one of the main functions of SHH is to suppress GLI3 repressor activity. However, even though in the $Shh^{-/-}$ $Gli3^{-/-}$ most of the ventral neurons are rescued, they are not correctly distributed in their respective domains, but rather, they are intermingled [Litingtung and Chiang, 2000]. Interneural mixing has also been observed in $Gli3^{-/-}$ $Smo^{-/-}$ compound mutants [Wijgerde et al., 2002] as well as in mutants lacking all *Gli* genes [Bai et al., 2004, Dessaud et al., 2008].

I8.2 Neural Tube Patterning; Dorsal Signals

I8.2.1 Specification by BMP

One of the first signals involved in dorsal patterning is BMP [Liem et al., 1995]. As I discussed in the previous chapters, inhibition of BMP signalling is required for induction of the neural plate, while a low level of BMP will induce neural border and neural crest fates. Using mouse ectodermal epiblast explants it was shown that, in this system, BMP can inhibit forebrain fate only until early head-fold stage [Yang and Klingensmith, 2006]. Thus, even before the neural tube is closed, the neural fate has been stabilized against BMP inhibition and, BMP can assume a role in neural tube patterning.

I8.2.2 Evidence for BMP in Neural Tube Patterning: The Chick

The roof plate of chick spinal cord expresses two members of the TGF beta family (BMP4 and ACTIVIN B). It was found that explants of roof plate, as well as BMP4 and ACTIVIN can induce dorsal neurons, while interplay of BMP and ACTIVIN induced different dorsal neurons [Liem et al., 1997]. Further studies showed that another member of *Bmp* family (*Gdf7*) is involved in generation of a specific class of interneurons [Lee et al., 1998] and, that BMP inhibits ventral fates [Mekki-Dauriac, et al., 2002]. This latter finding fits well with the report that the notochord and adjacent mesoderm secrete BMP inhibitors [Liem et al., 2000].

I8.2.3 Evidence for BMP in Neural Tube Patterning: The Mouse

BMP signals from the roof plate induce expression of the transcription factor *Lmx1a*, which acts by withdrawing progenitors from the cell cycle and preventing upregulation of *Atoh1* [Chizhikov and Millen, 2004]. *Atoh1* is required for generation of DI1 progenitors [Gowan et al., 2001]. Interestingly, *Lmx1a* mutants do not develop roof plate [Milloning et al., 2000] and dorsal interneurons fail to form [Milloning et al., 2000].

BMP2 and BMP4 contain a N-terminal basic amino-acid core, important for heparin sulphate (HS) binding. If this basic sequence is mutated BMP can act at greater distances [Ohkawara et al., 2002]. In mice, an inducible BMP4 transgene with a mutation in this region results in a ventral expansion of the dorsal marker *Pax7* compared to control, non-mutated transgene [Hu et al., 2004].

Bmpr1a is expressed ubiquitously in the neural precursors and acts to promote proliferation and induce a dorsal fate. *Bmpr1b* is express only in the dorsal part of the neural tube after 8.75 dpc downstream BMPR1A and its upregulation is inhibited by SHH. BMPR1B induces neuronal terminal differentiation [Panchision et al., 2001].

In the *Bmpr1a* and *Bmpr1b* double knockouts, DI1 neurons are absent, DI2 neurons domain is significantly reduced and, DI3 and DI4 domains are shifted dorsally [Wine-Lee et al., 2004].

Deletion of *Bmpr1a* by *Pax3*-Cre, induces reduction in the number of delaminating neural crest cells, reduction of dorsal marker *Atoh1* domain and failure of neural tube closure at the level of hindbrain in 40% of the cases. By contrast deletion through *Wnt1*-Cre showed none of these effects, indicating a requirement for *Bmpr1a* before neural tube closure [Stottmann and Klingensmith, 2011]. Furthermore, the authors found no influence on *Bmpr1b* expression, in conflict with previous reports [Panchision et al., 2001].

In summary, this body of evidence indicate that neural progenitors are at all times sensitive to BMP influence, as shown by continuous and ubiquitous presence of *Bmpr1a* [Panchision et al., 2001]. Before neural fold stages BMP would negatively interfere with the neural fate, but neural progenitors are protected by the BMP inhibitors secreted from the notochord, mesoderm, AVE and Node [Sharpe and Gurdon, 1990; Ruiz I Altaba A., 1990; Yang and Klingensmith, 2006]. As the neural folds rise to approach each other and, the lateral part of the neural plate becomes dorsal, this region is less protected by the ventral BMP inhibitors. From this moment on BMP participate in induction of the roof plate, dorsal interneurons and neural crest cells. Interestingly, roof plate, induced by LMX1A is formed by non-dividing cells. However, neither neural crest cells, nor DI1 progenitors are postmitotic at this stage and, they can both be found in the roof plate. It is unclear if these cells migrate to the floor plate from adjacent regions, or if LMX1A induce only a subset of roof plate cells. What is clear is that while LMX1A blocks dorsal interneuron fate, it is

permissive for neural crest fates [Chizhikov and Millen, 2004]. Nevertheless, there is strong evidence to suggest that BMP is directly involved in neural tube patterning, beyond induction of the neural crest. The importance of this pathway was further stressed by the fact that Bmp activity in zebrafish was found to regulate D-V patterning at all A-P levels, including the most anterior ones which do not form neural crest [Barth et al., 1999].

I8.2.4 Opposing View: BMP Inhibition in The Dorsal Neural Tube

In contrast with these observations recent studies showed that at least in chick and at least in the cephalic region, dorsal BMP inhibition rather than activation, governs neural tube patterning [Creuzet S.E., 2009]. Thus, cephalic neural crest cells (forming the roof plate at this level in chick) express BMP antagonists GREM1 and NOG and, ablation of this cell population results in anencephaly, secondary to *Fgf8* downregulation [Creuzet et al., 2006; Creuzet S.E., 2009]. Treatment with dsRNA against *Grem1* and *Nog* can replicate the phenotype in intact embryos and treatment with NOG of the CNC ablated embryos significantly rescued the phenotype, both morphologically and in *Fgf8* expression [Creuzet S.E., 2009].

Moreover, an older study showed that, after ablation of the dorsal region of the chick neural tube, the correct DV patterning can be re-established in the absence of BMP signalling, provided that the neural tube was closed [Buxton et al., 1997].

In mouse, BMP inhibitor *Nog* is expressed dorsally in the closing neural folds [Anderson et al., 2006]. Its expression is negatively regulated by SHH and in the absence of noggin the neural folds fail to bend and thus to generate a close neural tube. *Zic*2 mutants, which develop severe spina bifida fail to express BMP antagonists *Nog* and *Chrdl1* in the dorsal neural tube [Ybot-Gonzales et al., 2007].

The evidence supporting a BMP role in dorsal neural tube patterning is too strong to be dismissed. On the other hand, *Nog* expression in the same area with *Bmp* must have a functional role. If NOG would simply be limiting spatially the BMP activity its expression would be stronger on the ventral side, which is not the case. It has been previously reported that in chick BMP is important for neural crest

formation only around neural tube closure, a time point when NOG has an inhibitory effect. On the contrary, a few hours earlier neural crest formation can be inhibited by SHH, but not by NOG [Selleck et al., 1998]. Furthermore, it was proposed that "a coordinated activity of NOG and BMP4 in the dorsal neural tube" is required for sequential delamination of the neural crest cells. Thus it was found that NOG negatively regulates NC delamination and that its expression in the dorsal neural tube is higher in caudal regions, where NCCs will delaminate later [Sela-Donenfeld and Kalcheim, 2009]. These studies trigger the hypothesis that waves of BMP and NOG signalling in the dorsal neural tube control various processes like neural crest specification, floor plate induction, dorsal interneuron specification, neural crest delamination.

I8.2.5 Specification by Wnt

In the closing neural tube many *Wnt* agonists are expressed in a complex manner. The pattern is more intricate in the forebrain, indicating a role in regional subdivision. Three *Wnt*s: *Wnt1*, *Wnt3* and *Wnt3a* are restricted to the dorsal neural tube both in the forebrain and spinal cord [Parr et al., 1993].

When WNT signalling was analysed first, it was observed that it has a mitogenic activity within the neural tube, which could be ascribed to WNT1 and WNT3A, but not to other *Wnt*s and no influence on D-V patterning was reported [Dickinson et al., 1994; Megason and McMahon, 2002]. Later is was shown that the mitogenic activity of WNT signalling has patterning consequences as it specifically expands the neural populations induced by BMP in dorsal neural tube of Leghorn spinal cord [Chesnutt et al., 2004]. Subsequently, a more complicate picture emerged from mammalian experiments, where it was proposed that in dorsal neural tube BMP and WNT antagonize each other; BMP blocking WNT dependent proliferation and WNT blocking BMP dependent differentiation [Ille et al., 2007].

Recently, it was shown that WNT and CTNNB1 signalling is important in D-V patterning in chick where it acts in conjunction with BMP. Thus WNT induces DI2 and DI3 neurons through upregulation of *Olig3* cooperatively with BMP signalling and if WNT signalling is blocked, *Olig3* upregulation is also blocked even under

constitutive BMP stimulation [Zechner et al., 2007]. Furthermore, in a zebrafish model, *Wnt* proliferation and differentiation roles in neural tube have been dissected; *Ctnnb1-b* interacting transcription factor *Tcf7* being ascribed patterning roles, while *Tcf7l1* (previously known as Tcf3) was shown to be a major player in *Wnt* dependent proliferation [Bonner et al., 2008]. Furthermore, it was proposed that a key role for WNT in DV patterning is the antagonism of SHH pathway, by inducing expression of *Gli3* and thus, limiting specification of ventral fates in response to SHH [Alvarez-Medina et al., 2008; Ulloa and Marti, 2010, **Fig I4**].

I8.3 Twist1 Role in The Neural Tube Patterning

Twist1 null mice fail to close the neural tube anterior of rhombomere 4 [Chen & Behringer, 1995] followed by a lethal phenotype. Mice heterozygous for *Twist1* have normal CNS development, but display a variable phenotype reminiscent of the human SCS syndrome [Bourgeois et al., 1998; el Ghouzzi et al., 1997] including skull abnormalities, indicating that high levels of *Twist1* are not required for anterior neural tube development, but that they are required for correct neural crest migration and differentiation.

Twist1 is expressed at high levels in the head mesenchyme prior to neural tube closure and onwards but it has not been described in the neural tube [Stoetzel et al., 1995; Fuchtbauer E.M., 1995].

Twist1 neural phenotype has been explained by the influence on the neural tube of the surrounding mesenchyme which leads not only to a failure of closure but also to a perturbation of the dorso-ventral patterning [Soo et al., 2002]. However, the authors of this study presented no data to support a mechanism of *Twist1* expressing mesenchyme on neural patterning and, only inferred this phenomenon based on previously reported *Twist1* expression. Interestingly, a few *Twist1* positive cells have been observed in the neural tube, but those have been labelled as delaminating neural crest [Fuchtbauer E.M., 1995].

Thus at present, no hypothesis has been put forward to explain how *Twist1* expressing mesoderm is influencing neural differentiation, nor is it clear why would the strongest effect be on the dorsal and not the ventral side of the neural tube, which is closest to the mesoderm. Furthermore, it is not known if *Twist1* absence from the neural tissue signifies an incompatibility between *Twist1* transcriptional activity and neural development and no attempt has been made to reconcile the absence of *Twist1* from neural progenitors *in vivo* with the upregulation of *Twist1* during neural differentiation *in vitro*.

Figure I4. Dorso-Ventral neural identities are regulated by the antagonistic interplay between Shh and Wnt.

SHH from the ventral regions induces expression and activity of GLI activator genes, and if this signalling becomes predominant it induces the expansion of ventral neural fates dorsally: left arrow. WNT from the dorsal regions induces expression of GLI repressors, notably GLI3 and if this signalling branch becomes predominant it induces the expansion of dorsal neural fates ventrally: right arrow.
Source: Ulloa and Marti, 2010

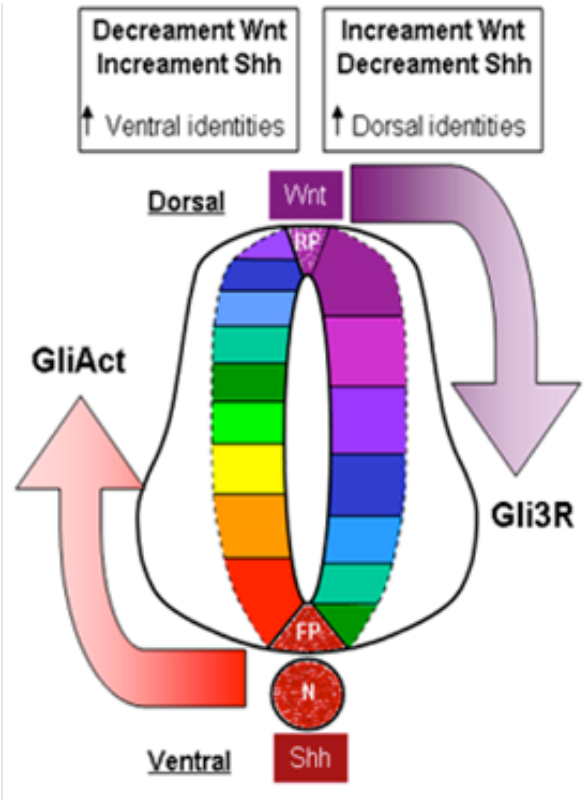
Decreament Wnt
Increament Shh
Ventral identities
Increament Wnt
Decreament Shh
Dorsal identities
Dorsal
Wnt
RP
GliAct
Gli3R
FP
N
Ventral
Shh

I9 Specific Aims of The Thesis

Following the data from the literature presented, I propose the following hypothesis:

General hypothesis:

Twist1 regulates neural differentiation of ES cells and early neural development *in vivo*.

Specific hypotheses:

1) *Twist1* is expressed in during early stages of neural development *in vitro* and *in vivo;*

2) TWIST1 positively regulates neural differentiation;

3) BMPs/IDs suppress differentiation of pluripotent cells in part through repression of TWIST1 activity.

Specific aims:

1. to investigate *Twist1* expression in pluripotent and early differentiating cells;
2. to determine if presence of Tw-E active dimers is compatible with the neural program and can protect it against BMP4 inhibition;
3. to revisit Twist1 expression in the mouse development, specifically in the neural progenitor compartment;
4. to investigate what potential roles TWIST1 could have in neural development.

II. MATERIALS AND METHODS

M1. Molecular biology

M1.1 PCR

M1.1.1 Taq PCR

M1.1.1.1 Taq PCR Materials

Taq DNA polymerase (Qiagen, 2012030) and the reagents provided: 10x PCR Buffer, 10x CoralLoad PCR Buffer, 5x Q-Solution, 25 mM MgCl2.

Other regents: dNTP Mix (Invitrogen, 18427013), Water RNase / DNase free (Gibco, 10977).

M1.1.1.2 Taq PCR method

Taq DNA polymerase was the enzyme used when high proofreading activity was not essential.

PCR was performed according to manufacturer protocol. For PCR products to be revealed immediately on Gel Electrophoresis, 10x CoralLoad PCR Buffer was used. If further purification of the PCR product was required, 10x PCR Buffer was used. 5x Q-Solution was used at concentrations ranging from 0 to 10 µl per 50 ul reaction; usually 5 µl. MgCl2 concentration usually used was 1.5 mM, the concentration present in the 10x PCR Buffer. Each primer was used at a final concentration of 0.5 uM (2.5 ul of a 10 µM solution in water, per 50 µl reaction). 100 to 200 ng total Template DNA was usually used.

Thermal cycling was performed using TProfessional Standard Thermocycler (Biometra). The annealing temperatures were optimized for each primer pair, usually between 55°C and 60°C. Generally between 30 and 35 cycles were used:

94°C – 5 min

30 to 35 cycles:

94°C – 30 seconds

xx°C – 30 seconds

72°C – 1 min per kb

72°C – 5 min

M1.1.2 Pfx PCR

M1.1.2.1 Pfx PCR Materials

Platinum Pfx DNA Polymerase (Invitrogen, 11708) and the reagents provided: 50 mM Magnesium Sulfate, 10x Pfx amplification Buffer, 10x PCRx Enhancer Solution.

Other regents: dNTP Mix (Invitrogen, 18427013), Water; RNase / DNase free (Gibco, 10977).

M1.1.2.1 Pfx PCR Method

Pfx Polymerase was the enzyme used to generate blunt constructs for further cloning.

PCR was performed according to manufacturer protocol. PCRx Enhancer Solution was used at concentrations ranging from 0 to 10 µl per 50 µl reaction; usually 5 µl. Magnesium Sulfate was used at final concentrations varying from 0.75 mM to 2 mM, usually 1 mM. Each primer was used at a final concentration of 0.3 µM (1.5 µl of a 10 µM solution, in water, per 50 µl reaction). 100 to 200 ng total Template DNA was usually used.

Thermal cycling was performed using TProfessional Standard Thermocycler (Biometra). The annealing temperatures were optimized for each primer pair, usually between 55°C and 60°C. Generally between 30 and 35 cycles were used:

94°C – 5 min

30 to 35 cycles:

94°C – 15 seconds

xx°C – 30 seconds

68°C – 1 min per kb

68°C – 5 min

For long primers with annealing temperatures above 68°C the two-step cycling was used:

94°C – 5 min

30 to 35 cycles:

94°C – 15 seconds

68°C – 1 min per kb

68°C – 5 min

M1.1.3 PCR Product Validation by Gel-Electrophoresis

M1.1.3.1 PCR Product Validation by Gel-Electrophoresis Materials

Agarose gel: UltraPure Agarose (Invitrogen, 16500), TBE (see below), SYBR Safe DNA gel stain (Invitrogen, S33102)

Tris-borate-EDTA buffer (TBE): Tris base (Fisher, BP152-1), orthoboric acid (Fisher, 10043-35-3), EDTA 0.5M pH8.0, ultra-pure water. TBE was prepared as a 10x stock solution comprising Tris base 0.45 M, Orthoboric acid 0.45 M and EDTA 10 mM in water. Working solution was prepared by diluting the stock solution 1:20 in water.

Agarose was melted in TBE buffer, 1% final concentration, in a microwave oven. After the mixture was allowed to cool, SYBR Safe DNA gel stain (Invitrogen, S33102) was added at the recommended concentration, 1:10000.

DNA loading dye: Orange G (Sigma, O3756), glycerol (Fisher, 56-81-5), ultra-pure water. DNA loading dye was prepared as a 6x solution comprising OrangeG 0.25% and Glicerol 30% in water.

M1.1.3.2 PCR Product Validation by Gel-Electrophoresis Method

The agarose gel was poured into the mould and allowed to solidify. PCR product was mixed 1:6 with DNA loading dye and loaded on the gel, unless the PCR had been performed using 10x CoralLoad PCR Buffer, in which case the PCR product was loaded directly on the gel. DNA was electrophoresed in 0.5x TBE at 90V for 30 to 90 min depending on the expected size of the band and, visualised using UV trans-illuminator.

M1.1.4 PCR Product Isolation

When the PCR product was to be used in subsequent cloning isolation of the product was performed. For PCR reactions which produced only one band PCR purification was used. For PCR reactions which produced more than one band gel extraction was used. Another method for DNA isolation is precipitation. This method has not been used for PCR products purification, but following other enzymatic manipulations, like digestion. However, the method is presented here for coherence.

M1.1.4.1 PCR Product Isolation – PCR Purification

PCR purification was performed using QIAquick PCR Purification Kit (Qiagen, 28104), according to manufacturer instructions.

M1.1.4.2 PCR Product Isolation – Gel Extraction

DNA was eletrophoresed on an agarose gel as in M1.1.3. For Gel Extraction, the gel was casted into the mould using large combs and, the entire PCR reaction (50 µl) was loaded. After electrophoresis the expected band was cut using a clean scalpel, under UV light. The procedure was optimized for the cutting to be performed in 3 sec or less, so that the risk of introducing DNA mutations due to UV exposure was

minimal. The piece of gel, containing the desired DNA fragment,was placed in a new Eppendorf tube.

DNA was then extracted using QIAquick Gel Extraction Kit (Qiagen, 28704), according to manufacturer instructions.

M1.1.4.3 DNA Precipitation Following Phenol-Chloroform Extraction

Samples of small volume were scaled to 500 µl by adding water RNase, DNase free (Gibco, 10977). Phenol:Chlor:IAA (UltraPure Phenol:Chloroform:Isoamyl Alcohol, Invitrogen, 15593-031) 500 ul was added, mixed and centrifuged 14000 g for 10 minutes. The top, aqueous layer was moved to a new tube. Chloroform (Fisher, C606) 400 µl was added and centrifugation repeated. The top layer was moved to a new tube and precipitated with 40 ul NaAc 3M pH5.2. Ethanol 1 ml was added, mixed and, incubated on dry ice for 30 min, then the sample centrifuged 14000 g for 15 min. Supernatant was discarded and the pellet washed with 70% Ethanol and centrifuged 14000 g for 5 min. Ethanol wash was repeated, then the tubes were air dried and DNA resuspended in Elution Buffer.

M1.1.4.4 Direct DNA Precipitation

Samples of small volume were scaled to 50 µl by adding water RNase, DNase free. DNA was directly precipitated by adding 5 µl NaAc 3M pH5.2. 150 µl ethanol was added and procedure was continued as in M1.1.4.3.

M1.2 Plasmids manipulation

M1.2.1 Plasmid amplification

M1.2.1.1 Plasmid Amplification Materials

Bacterial growth media: LB medium, SOC medium, LB agar

L-broth Lauria Bertani (LB) medium and LB-agar were prepared by the ISCR/CRM Media Service, following standard protocols. **LB** was made by dissolving LB (BD, 244620) 2.5% in water, followed by sterilization through autoclaving. **LB-agar** comprised 1.5% bacto-agar (BD, 214010) in LB.

SOC medium was made in a distilled water solution comprising: Bacto Tryptone 2% (BD 211705), Bacto Yeast Extract 0.5% (BD, 212750), NaCl 10 mM, KCl 2.5 mM, MgCl2 10 mM, MgSO4 10 mM and Glucose 20 mM and, was sterilized by filtration.

Antibiotics: Ampicillin (Calbiochem, 171254), Kanamycin (Calbiochem, 420311), Tetracycline (Sigma, T7660), Chloramphenicol (Sigma, C0378).

All antibiotics were prepared as 1000x stock solutions stored at -20°C.

Ampicillin was prepared as an aqueous solution of 100 mg/ml concentration.
Kanamycin was prepared as an aqueous solution of 50 mg/ml concentration.
Tetracycline was prepared as an aqueous solution of 3 mg/ml concentration.
Chloramphenicol was prepared as an alcoholic solution, in ethanol, of 15 mg/ml concentration.

Antibiotic supplemented media was prepared by adding 1 µl stock solution of the respective antibiotic for 1 ml of medium. LB agar was first melted by heating in the microwave, left to cool down and the antibiotic was added just before the pouring of the plates. Agar plates not used immediately were store at 4°C for up to one month.

Tetracycline supplemented liquid media or plates were protected from light using aluminium foil.

Transfection competent bacterial cells: MAX Efficiency Dh5α Competent Cells (Invitrogen, 18258012), One Shot Top10 Chemically Competent E. Coli (Invitrogen, C404003)

M1.2.1.2 Plasmid Amplification Methods

Plasmidic DNA which either resulted from a ligation reaction (see DNA ligation), or had been previously extracted (see DNA extraction) was incubated on ice for 30 min with the competent cells. For difficult constructs, like TwTw which contained large homology regions, Top10 cell were used.

After incubation, cells were heat shocked for 45 seconds at 42°C, in water bath, and cooled down on ice. Immediately, antibiotic free medium was added and bacteria cells were incubated for 1h at 37°C. In the case of Dh5α 1ml of LB medium was added, in the case of Top10 250 ul of SOC medium was added. Then, 100 µl of bacterial culture was inoculated on one agar plate supplemented with the relevant antibiotic and incubated over-night at 37°C. In the case of plasmids for which the desired ligation was considered a rare event, multiple plates were inoculated.

Next day, individual colonies were picked and inoculated on 5 ml LB supplemented with the same antibiotics and incubated again over-night at 37°C.

M1.2.2 Bacterial DNA Extraction

M1.2.2.1 Bacterial DNA Extraction – Plasmids

Plasmids were extracted from overnight liquid cultures, using Qiagen Plasmid Mini Kit (Qiagen, 12123), according to manufacturer instructions. For low copy plasmids, or large plamids, amplification procedure was modified in the sense that the 5 ml culture was used as starter culture. Subsequently, 250 µl of the starter culture were inoculated into 500 ml medium with the appropriate antibiotics and incubated

overnighta and, plasmidic DNA extracted using Qiagen Plasmid Maxi Kit (Qiagen, 12763), according to manufacturer instructions.

M1.2.2.2 Bacterial DNA Extraction – Artificial Chromosomes

Materials:

Reagents: Tris base (Fisher, BP152-1), HCl (Fisher, H/1200/PB17), EDTA (Fisher, D0450/53), RNase A (Roche, 10109142001 NaOH (Fisher, S/4920/53), SDS (Sigma, 75746), NaAc (Sigma, S2889), Acetic acid (VWR, 20104), Ethanol (VWR, 20821330)), Water RNase / DNase free (Gibco, 10977).

Buffer P1: 15 mM Tris pH8, 10 mM EDTA, 100 µg/ml Rnase A.
Buffer P2: 0.2 M NaOH, 1% SDS.
Buffer P3: 3 M NaAc pH5.2.
Elution Buffer: 10 mM Tris pH8.5

Note: Tris pH was corrected with HCL, NaAc pH was corrected with Acetic acid.

Method:

A 5 ml LB culture was centrifuged 6000 g, for 10 min. The pellet was resuspended in 300 µl buffer P1. Buffer P2 (300 µl) was added, gently mixed and, incubated at room temperature for 5 min. Buffer P3 (300 µl) was added gently mixed and the lysate was incubated on ice for 5 min. The mixture was centrifuged for 10 min at 14000 g 4°C. The supernatant was carefully moved to a new tube and centrifugation repeated. The supernatant was carefully moved to a new tube, 800 µl ice-cold isopropanol added and incubated on ice for 15 min. The mixture was centrifuged at 14000 g for 15 min. Supernatant was discarded and the pellet washed with 70% Ethanol and centrifuged 14000 g for 5 min. Ethanol wash was repeated, then the tubes air dried and DNA resuspended in Elution Buffer.

M1.2.3 Plasmid digestion

After extraction, plasmids were digested using relevant enzymes in the buffers provided by the manufacturer, using the recommended conditions. For validation of the presence of the expected cutting sites in the plasmid at the appropriate position typically 100 to 200 ng of DNA were digested in a 10 µl reaction. For further cloning 1 to 5 µg of DNA were digested in a 50 µl reaction. The amount of enzyme used varied between 1x and 10x recommended amount based on predicted activity. Digestion time was typically 1 to 3 hours, except for NEB time saver enzymes for which digestion time was reduced at 10 to 20 minutes. For enzymes with high star activity digestion time was reduced below 1 hour and 1x amount of enzyme was used. In the case of plasmids used for transfection by electroporation 100 µg of plasmid was digested in a 1 ml reaction, incubated overnight.

Plasmid digested fragments which were used in further cloning were isolated using gel extraction method (see M1.1.4.2).

Plasmids linearized for transfection in Eukaryotic cells were purified by direct DNA precipitation (see M1.1.4.4).

M1.2.4 Plasmid Generation

M1.2.4.1 Plasmid Generation from PCR Constructs

Blunt end PCR products generated by Pfx PCR (see M1.1.2) were purified and then isolated by PCR purification (see M1.1.4.1). A plasmid was generated using Zero Blunt TOPO PCR Cloning Kit (Invitrogen, 450245), according to manufacturer instructions.

Following amplification and extraction the construct was usually digested using convenient cutting sites present in the vector and ligated to generate new plasmids.

M1.2.4.2 Plasmid Generation by Fragment Ligation

Fragments with compatible ends, generated by enzymatic digestion (see M1.2.3) and isolated by gel extraction (see M1.1.4.2) were ligated using T4 DNA Ligase (NEB, M0202), according to manufacturer instructions.

The DNA fragments concentration was calculated so that a ratio vector: insert of 1:3 was achieved. The vector was considered to be the DNA fragment containing the origin of replication and the selective gene and, thus, able to form a viable plasmid if self ligated. The reaction was usually performed at room temperature for 2 hours, or at 4°C overnight.

The resulting plasmid was amplified by transfection to competent cells (see M1.2.1)

M1.2.4.3 Plasmid Generation from Bacterial Artificial Chromosomes by Recombineering

Generation of Recombineering Competent Cells.

Bacterial cells containing the relevant Bacterial Artificial Chromosome (BAC) were electroporated with the pSC101-BAD plasmid as described below. All DNA used for electroporation of bacterial cells was resuspended in water as opposed to Elution buffer, which was the usual procedure.

BAC containg cells were cultured expanded in Chloramphenicol supplemented medium (as in M1.2.1). 30 μl of an overnight culture were inoculated in 1 ml LB selective medium and incubated at 37°C for a few hours, until turbidity reached OD 0.6. Then, the culture was put on ice, transferred to the cold room, and washed 3 times with water, using centrifugation 14000 g for 1 min. Cells are resuspended in 100 μl water, moved to a 0.1 cm electroporation cuvette and pulsed at 1.8kV. Immediately, warm SOC medium 1 ml, was added and cells incubated for 1 hour at 30°C.

Agar plates supplemented with Chloramphenicol and Tetracycline were inoculated as in M1.2.1.2. and incubated at 30°C overnight in dark.

Inserting a Modification into The BAC by Recombineering.

Recombineering competent bacterial cells produced as described above were cultured in medium supplemented with Chloramphenicol and Tetracycline. The electroporation procedure was repeated, with the plasmid of interest, containing 60 bp homology sequence flanking the region with the desired modification of the wild type chromosome and a Kanamycin resistance cassette [Fig M1].

After electroporation bacterial cells were inoculated on agar plates supplemented with Chloramphenicol and Kanamycin and, incubated at 37°C overnight.

Producing a Final Plasmid by Recombineering.

Using the modified BAC cells the above two steps were repeated using in the second step a low copy plasmid containing an Ampicillin resistance cassette flanked by reverse 60 bp homology sequence which corresponds in the BAC with 60 bp sequencing flanking the entire region desired to be retrieved [Fig M2]. The 60 bp sequence were introduced by PCR as in M1.1.2.

After the first electroporation bacteria cells are plated on medium supplemented with Chloramphenicol, Kanamycin and Tetracycline, or just Kanamycin and Tetracycline and, incubated at 30°C in dark. After the second electroporation bacteria cells are inoculated on medium supplemented with Ampicillin and incubated at 37°C. Subsequently the plasmid is isolated as in M1.2.2.1.

Figure M1. Genetic modification of the BAC

Schematic representation of the strategy for introducing a modification in a gene of interest in a BAC. Map not to scale.

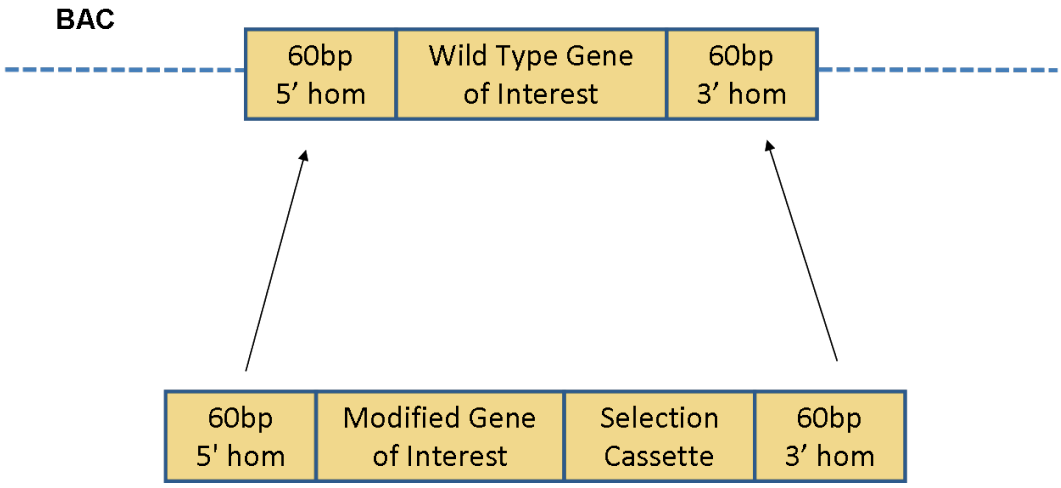
BAC
60bp
5' hom
Wild Type Gene
of Interest
60bp
3' hom
60bp
5' hom
Modified Gene
of Interest
Selection
Cassette
60bp
3' hom

Figure M2. Plasmid containing a genetic modified locus generation

Schematic representation of the strategy to retrieve the modified locus in a low copy plasmid. Homology arms typically represent a genetic region of a few kb flanking the gene of interest which will direct homologous recombination in the eukaryotic cell. Solid blue lines represent schematic stretch of the DNA to allow visualisation of the alignment between the 2 homologous 60 bp sequences. Map not to scale

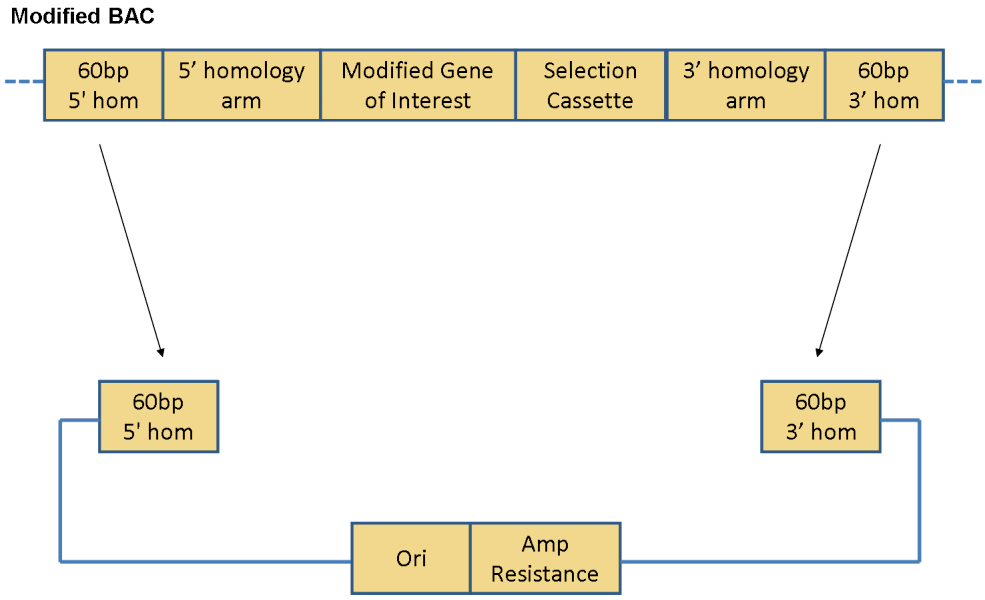
Modified BAC
60bp
5' hom
5' homology
arm
Modified Gene
of Interest
Selection
Cassette
3' homology
arm
60bp
3' hom
60bp
5' hom
60bp
3' hom
Ori
Amp
Resistance

M1.2.5 Sequencing The Newly Generated Plasmids

Newly generated plasmids were sequenced by BigDye reaction using appropriate primers. For plasmids generated by digestion – ligation method sequencing focused around the restriction sites. For plasmids generated from construct resulting from PCR reactions the sequencing covered the PCRed fragment.

Sequencing was set as a 6 µl reaction in water, containing 200 to 500 ng plasmidic DNA with 0.3 ul of 10 µM primer. The analysis was performed by the GenePool Sequencing Service at the University of Edinburgh.

M1.2.6 Plasmid Sequence Analysis

All plasmid sequence analysis for identifying useful cutting sites, primer design, and plasmid map generation were performed using: ApE- A plasmid Editor v2.0.36, copyright © 2003-2009 M. Wayne Davies. Optimal primer sequence was designed using: Primer3, Release 2.2.3, SourceForge; http://primer3.sourceforge.net/. The final oligonucleotide properties were confirmed using the online source: Oligo Calc: Oligonucleotide Properties Calculator; http://www.basic.northwestern.edu/biotools/ oligocalc.html.

M1.3 Generation of Specific Constructs and Plasmids

M1.3.1 FKBP Inducible System

All bHLH constructs used had been previously cloned by Owen Davies in the lab of Dr. Sally Lowell in plasmids containg a SV40 origin of replication with the construct expressed under pCAG promoter. The *FKBP* plasmid [Banaszynski at al, 2006] was obtained from the lab of Dr. Keisuke Kaji. It contained multiple unique restriction sites after the modified *FKBP* sequence. However, none of these restriction sites were compatible with the restriction sites flanking the bHLH contructs in the

bHLH SV40 pCAG plasmids. For this reason convenient restriction sites were introduced by PCR as in M1.1.2.1.

The forward primer was identical for all constructs containing the EcoRV restriction site a 21 nucleotide spacer, meant to introduce a flexible linker between the FKBP and the bHLH factor, and a Flag sequence, which was thus introduced before the bHLH factor. The reverse primer was unique for each bHLH factor containing the last 24 nucleotides of respective gene, a second TGA end and, a Not1 restriction site, all reverse complemeted; see Table M4. Note: EcoRV and NotI sites exist in the TOPO plasmid after the locus for blunt fragment insertion, but these extra cutting sites would produce an extra small fragment easily separated by electrophoresis. This cloning strategy, as well as the primers involved, were designed by Owen Davies.

M1.3.2 Tetracycline Inducible System

For this approach the constructs cloned in the SV40-pCAG plasmids described in M1.3.1 were used. The constructs were cloned in a plasmid where the gene of interest was transcribed downstream a TetO promoter with the Puromycin selection cassette under the influence of Pgk promoter. The strategy used was restriction digest on convenient sites, followed by ligation (M1.2.4.2), without any PCR required. The bHLH fragment was digested using XhoI – NotI digestion. The TetO containing plasmid was digested using PspXI – NotI digestion. The PspXI and XhoI digestion produce compatible ends which, upon ligation, generate a new XhoI, but not PmsXI site [Fig M4]. In this manner plasmids for the following bHLH constructs were produced: Twist1, Twist1-E and Twist1-Twist1.

The resulting construct was subcloned into a TOPO vestor as in M1.2.4.1, sequenced as in M1.2.5, digested using EcoRV – Not1 sites and ligated into the FKBP plasmid as in M1.2.4.2. In this manner plasmids for the following bHLH constructs were produced: Twist1, Twist1-E, Twist1-Twist1, Tcf15, Tcf15-E, Neurod1, Neurod1-Neurod1. The plasmid for Twist1-E is shown in Fig M3 for exemplification.

Figure M3. Inducible FKBP TwE plasmid

Schematic representation; PCR introduced cloning sites EcoRV and NotI are shown.

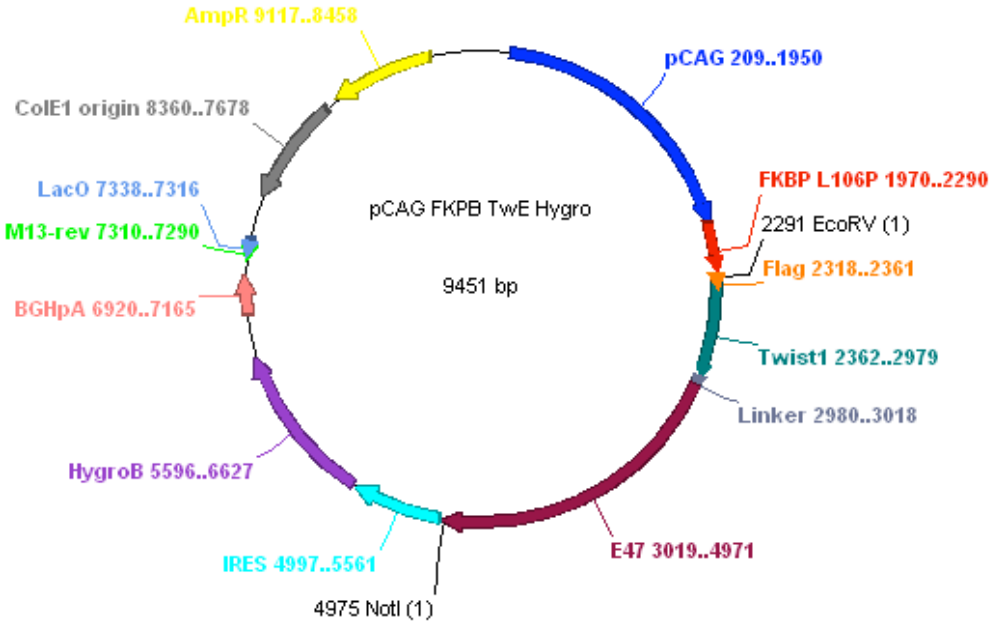
AmpR 9117..8458
pCAG 209..1950
ColE1 origin 8360..7678
FKBP L106P 1970..2290
LacO 7338..7316
pCAG FKPB TwE Hygro
2291 EcoRV (1)
M13-rev 7310..7290
9451 bp
Flag 2318..2361
BGHpA 6920..7165
Twist1 2362..2979
Linker 2980..3018
HygroB 5596..6627
E47 3019..4971
IRES 4997..5561
4975 NotI (1)

Figure M4. Strategy for generating TetO bHLH plasmids

The original plasmid could not be usefully XhoI digested, due to multiple XhoI sites in the TetO promoter. For this reason a PspXI site located after the TetO promoter was used. Agter ligation with a XhoI generated end a XhoI site is produced, position 6294 on the map.

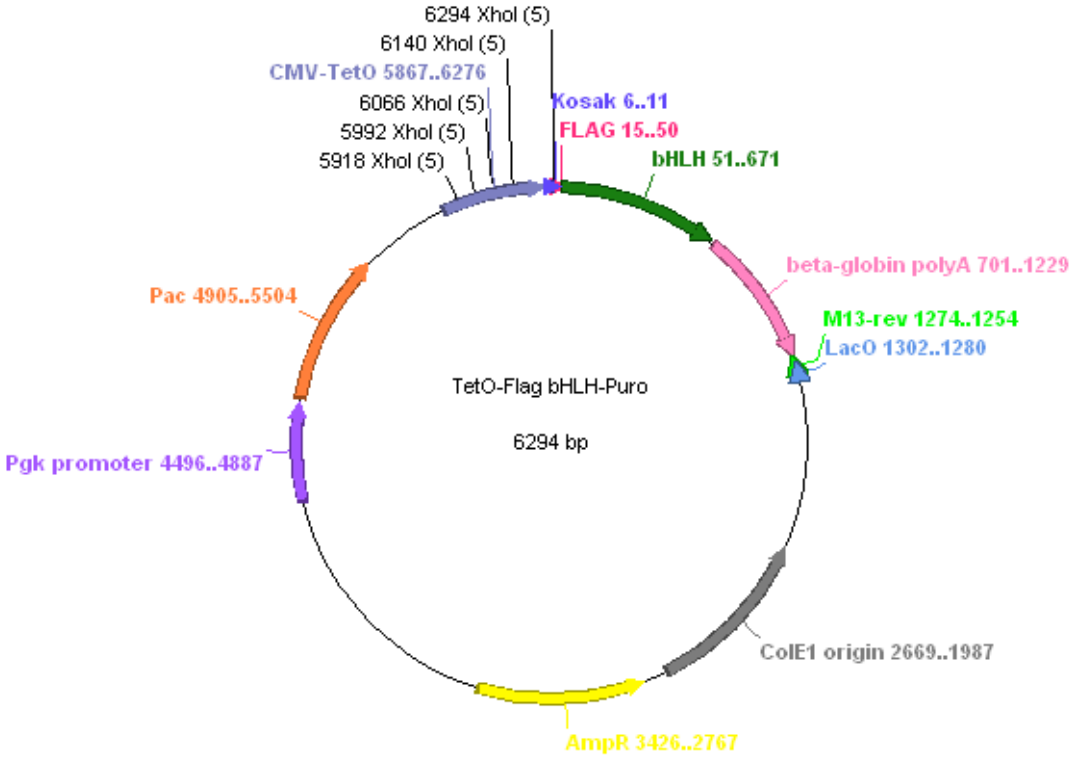
6294 XhoI (5)
6140 XhoI (5)
CMV-TetO 5867..6276
6066 XhoI (5)
5992 XhoI (5)
5918 XhoI (5)
Kosak 6..11
FLAG 15..50
bHLH 51..671
beta-globin polyA 701..1229
M13-rev 1274..1254
LacO 1302..1280
Pac 4905..5504
TetO-Flag bHLH-Puro
6294 bp
Pgk promoter 4496..4887
ColE1 origin 2669..1987
AmpR 3426..2767

M1.3.3 *Twist1* RNA probe for In Situ Hybridization

BAC was extracted from clone bMQ-350m18 (Geneservice), as described (M1.2.2.2). PCR primers were designed to amplify a 0.8 kb fragment in the 3' UTR region of *Twist1* gene [Fig M5]. The fragment was amplified as in M1.1.2.1, subcloned into TOPO as in M 1.2.4.1, sequenced using the M13 primers as in M1.2.5. Sequencing revealed that clone WOTO2 contained a correct insert which could produce a RNA probe complementary to *Twist1* mRNA using the T7 promoter site in the TOPO vector. Clone WOTO1 was in the opposite orientation and required the use of SP6 promoter, situated on the other side of the construct [Fig M6]. In the following procedures WOTO2 was used.

To produce the RNA probe, first WOTO2 was linearized at the BamH1 site [Fig M6] as in M1.2.3. 10 µg of Plasmid were digested with 30 units of BamH1 (NEB, R0136S) using buffer 3 and BSA provided; reaction was incubated overnight at 37°C.

The complete linearization was checked by electrophoresis on agarose gel, as in M1.1.3.2 and DNA was extracted by using Phenol – Chloroform as in M 1.1.4.3.

The linearized and purified DNA was used as template for T7 RNA polymerase (Roche, 10881767001) and the reagents provided: 10x transcription buffer, dNTPs (DIG-UTP) and RNase inhibitor, according to manufacturer protocol. 1 µg of DNA was used in a 20 µl reaction incubated at 37°C for 2 hours.

The template DNA was removed by DNA digestion using DNaseI (Promega, M6101) and the reagents provided: reaction buffer and STOP solution, according to manufacturer protocol.

A small aliquot (1 µl) of the reaction solution, before and, after DNase step was checked by electrophoresis on agarose gel, as in M1.1.3.2 to confirm the presence of RNA and complete removal of DNA.

Figure M5. *Twist1* RNA probes

Schematic representation of the RNA probe for in situ hybridization. Presented are the probe from Wolf et al, 1991 and WOTO2 used in the present work. The WOTO2 probe spans over the corresponding genomic sequence between 188 and 1062 bp after the end of the *Twist1* coding sequence. Map approximately to scale.

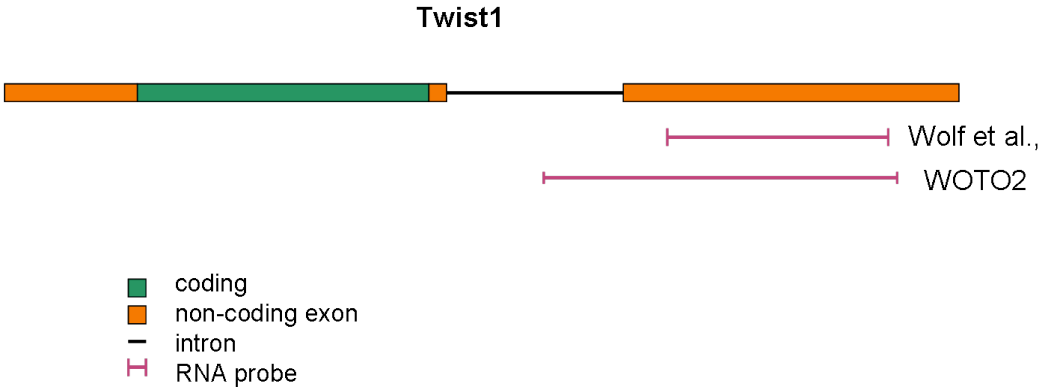
Twist1
Wolf et al.,
WOTO2
coding
non-coding exon
intron
RNA probe

Figure M6. Plasmid for generation of *Twist1* RNA probe

BamHI cutting site is shown, where, after linearization of the plasmid, the RNA elongation stops. RNA is produced under the T7 promoter.

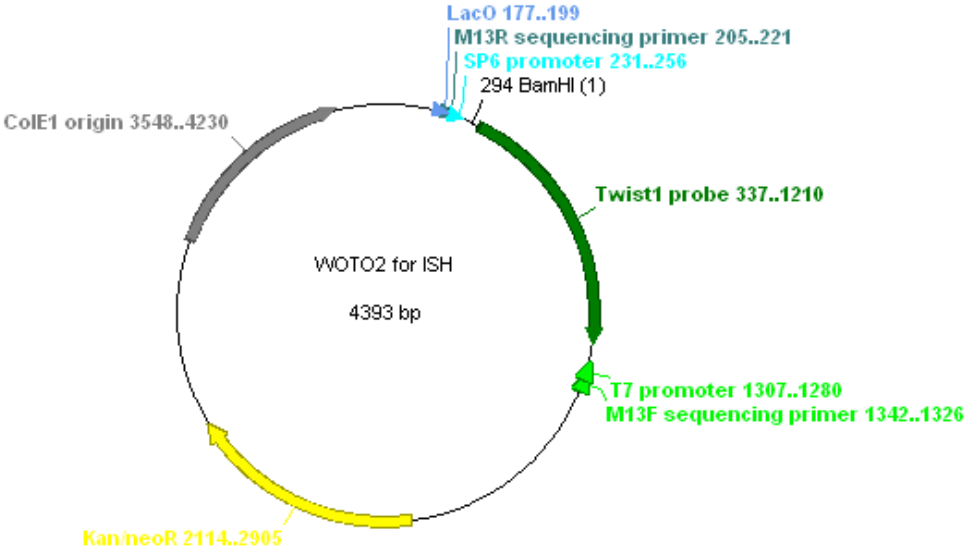
LacO 177..199
M13R sequencing primer 205..221
SP6 promoter 231..256
294 BamHI (1)
ColE1 origin 3548..4230
Twist1 probe 337..1210
WOTO2 for ISH
4393 bp
T7 promoter 1307..1280
M13F sequencing primer 1342..1326
Kan/neoR 2114..2905

The RNA was purified using RNeasy Mini Kit (Qiagen, 74106). The reaction was resuspended in 400 µl lysis buffer (provided) and from this point the extraction was performed according to manufacturer protocol. The labelled RNA was aliquoted in RNase free PCR tubes containing 1.5 µg RNA each and stored at -80°C.

M1.3.4 *Twist1*-Venus Plasmid for Generation of Reporter Cell Lines

M1.3.4.1 Twist1-Venus Plasmid – General Strategy

A strategy was devised to generate *Twist1* reporter ES cell lines. In this strategy [Fig M1 and M2] the *Twist1* coding sequence was modified by inserting the coding sequence for Venus, followed by a double selection cassette, which was flanked by Frt sites [Fig M7].

Venus construct is driven under the *Twist1* promoter, its translation being directed by a Synthetic IRES augmented by 10 repeats of the Gtx gene IRES, which have been shown to amplify gene expression [Chappell et al, 2000] and to be useful in reporter cell lines [Tanaka et al, 2008].

The selection cassette consists of Neomycin resistance gene under the Pgk promoter and the Thymidine kinase gene under the MC1 promoter. After clonal cell lines are selected under Neomycin resistance, the selection cassette can be removed by transient transfection with a Flipase expressing plasmid and cells which failed to undergo the recombination event can be eliminated by treatment with Ganciclovir, which is transformed in the toxic compound Gaciclovir triphosphate by Thymidine kinase [Fig M9].

Figure M7. Plasmid for generation of *Twist1* reporter cell lines

Retrieved plasmid from modified BAC; in between the wild type homology arms, Flag, *Twist1* coding sequence, Venus and the selection cassette were introduced. Frt sites for removal of the selection cassette are shown. For electroporation this plasmid was linearized at the XhoI site.

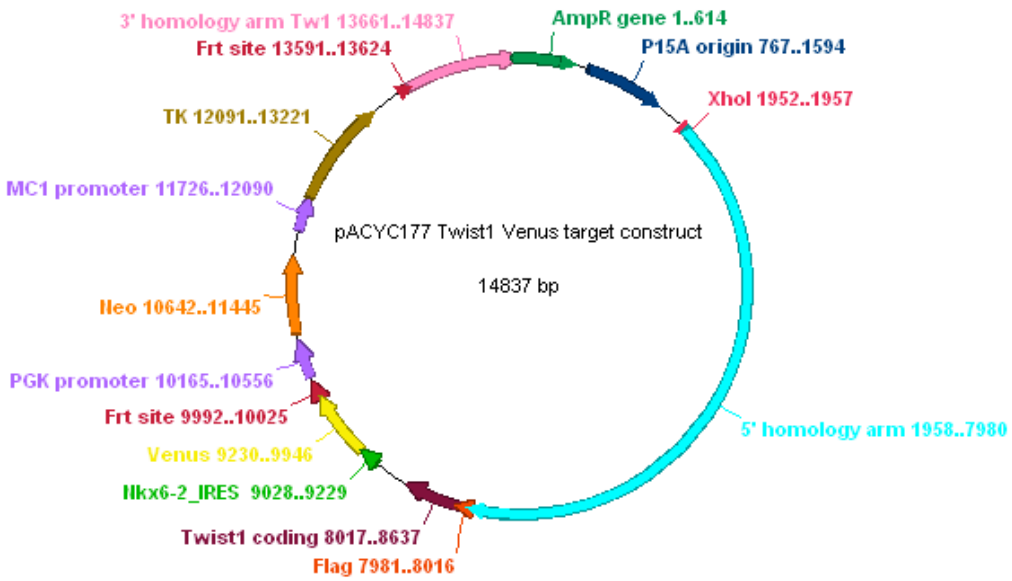
3' homology arm Tw1 13661..14837
Frt site 13591..13624
AmpR gene 1..614
P15A origin 767..1594
XhoI 1952..1957
TK 12091..13221
MC1 promoter 11726..12090
pACYC177 Twist1 Venus target construct
14837 bp
Neo 10642..11445
PGK promoter 10165..10556
Frt site 9992..10025
5' homology arm 1958..7980
Venus 9230..9946
Nkx6-2_IRES 9028..9229
Twist1 coding 8017..8637
Flag 7981..8016

M1.3.4.2 Twist1-Venus Plasmid for BAC Modification

To generate the *Twist1*-Venus construct I started from a NEB193 plasmid which contained the Venus construct downstream an IRES modified as described above. This plasmid had been produced in the lab of Prof. Joshua Brickman by Dr. Maurice Canham. To subclone *Twist1* coding sequence into this plasmid, convenient sites were introduced by PCR starting from SV40 pCAG *Twist1* plasmid similar to M1.3.1. For this purpose primers were designed in the following manner: forward primer contained PacI restriction site, followed by Flag and the first 21 bases of *Twist1*; reverse primer contained AgeI restriction site followed by the last 24 bases of *Twist1*; see Table M4. The new plasmid was generating following the procedures described in M1.2.4.1, M1.2.3 and M1.2.4.2 [Fig M8].

Furthermore, the selection cassette was digested from another plasmid provided by Maurice Canham, in order to be subcloned into NEB193_*Twist1*-Venus using the BamH1 restriction site [Fig M9]. The digested fragments were isolated as in M1.1.4.2.

Since this digestion used the same restriction sites at both ends of the constructs the vector containing the origin of replication (NEB193_*Twist1*-Venus) was dephosphorilated using Rapid Alkaline Phosphatase (Roche, 04898133001) and the buffer provided according to manufacturer protocol. The DNA was purified as in M1.1.4.1 and the vector and the selection cassette were ligated as in M1.2.4.2.

Figure M8. Generation of *Twist1-Nkx6-2*_IRES-Venus construct

Flag-*Twist1* coding sequence was introduced into the NEB193 plasmid, following addition of convenient cutting sites PacI and AgeI, shown. BamHI is the site where the selection cassette would be introduced.

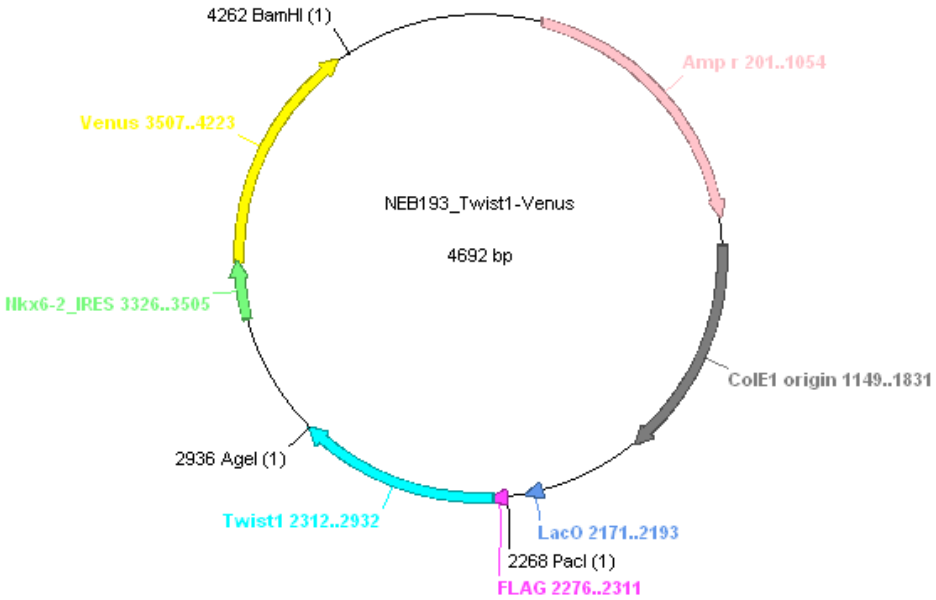
4262 BamHI (1)
Amp r 201..1054
Venus 3507..4223
NEB193_Twist1-Venus
4692 bp
Hkx6-2_IRES 3326..3505
ColE1 origin 1149..1831
2936 AgeI (1)
Twist1 2312..2932
LacO 2171..2193
2268 PacI (1)
FLAG 2276..2311

Since the presented method involved ligation of two fragments with identical ends at both sides any orientation was possible. To test for this I made use of a second Age1 restriction site present in the selection cassette. As can be observed from the map in Fig M9, if the selection cassette had been inserted in the forward orientation, AgeI digestion would have produced a fragment of approximately 1.5 kb and another fragment close to 7 kb in size. However, if the selection cassette had been inserted in the opposite orientation, the AgeI digestion would have produced two fragments closer in size of 3.5 and 4.5 kb respectively. Five clones were checked by this method and clones 1 and 3 had the insert in the forward orientation. In the following experiments clone 1 was used.

M1.3.4.3 Inserting Twist1-Venus Plasmid into BAC

To generate the construct for BAC modification PCR primers were designed containing 60 bases of genomic Twist1 sequence immediately before and after the coding sequence followed by 21 bases homologous to the limits of the region to be recombined, containing the first 21 nucleotides of Flag and the last 21 nucleotides ending with the second Frt site; see Table M4. In this manner a 5.5 kb fragment was PCR amplified as described in M1.1.2 using the two step cycling.

The PCR fragment was isolated using the gel extraction procedure (M1.1.4.2), and resuspending the DNA in water followed by DPN1 digestion (NEB, R0176S) using NEBuffer 4, according to manufacturer protocol. The DPN1 only cuts DAM methylated DNA, not affecting the PCR product, but removing eventual traces of plasmid template, which could induce bacterial cell survival in the absence of desired recombination. The remaining DNA was purified as in M1.1.4.1 with resuspension in water.

Figure M9. Plasmid for BAC modification at the *Twist1* locus

The plasmid contains Flag-*Twist1*, followed by *Nkx6-2*_IRES-Venus and the selection cassette flanked by Frt sites. BamH1 sites were the selection cassette was cloned in are shown. AgeI site were used to check the orientation of the selection cassette.

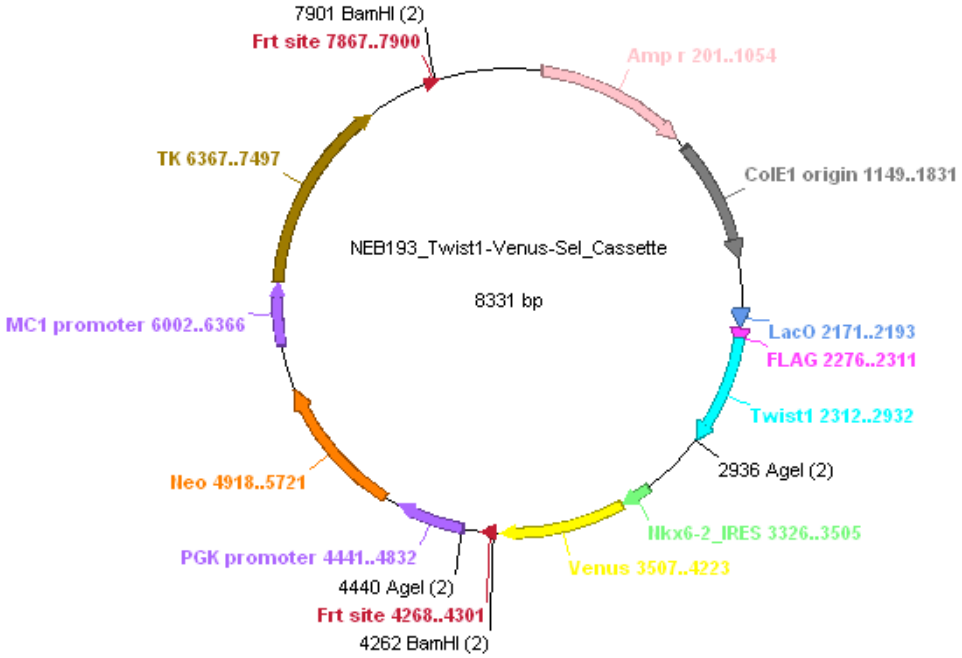
7901 BamHI (2)
Frt site 7867..7900
Amp r 201..1054
TK 6367..7497
ColE1 origin 1149..1831
NEB193_Twist1-Venus-Sel_Cassette
8331 bp
MC1 promoter 6002..6366
LacO 2171..2193
FLAG 2276..2311
Twist1 2312..2932
2936 AgeI (2)
Neo 4918..5721
Ilkx6-2_IRES 3326..3505
PGK promoter 4441..4832
Venus 3507..4223
4440 AgeI (2)
Frt site 4268..4301
4262 BamHI (2)

The construct was elctroporated into BAC clone bMQ-350m18 (Geneservice) as in M1.2.4.3.1 and M1.2.4.3.2. The recombination event was checked by colony PCR for 5 clones following the procedure in M1.1.1 with the exception that one isolated bacterial colony, for each clone, from agar plate, supplemented with Chloramphenicol and Kanamycin was used instead of purified DNA. The PCR primers used were designed to be complementary to the BAC just outside the expected recombination event and, within *Twist1* and selection cassette respectively. Clones 1 and 3 produced bands of the expected size.

To further confirm the recombination event, the above described PCR products were subcloned as described in M1.2.4.1, except that in this case TOPO TA Cloning Kit was used (Invitrogen, 450641). The resulting plasmids were sequenced as in M1.2.5 using M13 primers.

M1.3.4.4 Generation of Twist1-Venus Plasmid for Homologous Recombination

To retrieve the modified fragment a low copy plasmid, pACYC177 generated by Dr. Andrew Smith was used. Using this plasmid as template, a DNA fragment was PCR amplified as in M1.3.4.3. Forward primer contained 60 bases at the 5' end of *Twist1* homology arm followed by XhoI site and 20 bases upstream BamHI site in the pACYC177 plasmid. The reverse primer contained 60 bases at the 3' end of *Twist1* homology arm followed by 22 bases positioned 55 bases downstream plasmid origin of replication. In order for the homology regions to be aligned with the BAC the forward primer was designed forward in respect to the pACYC177 sequence, but was reverse complemented in respect to the genomic region. On the other hand the reverse primer was reverse complemented in respect to the pACYC177 sequence but contained a forward sequence in respect to genomic DNA. The 60 bases regions were designed as to encompass the homology arms used for targeting Twist1 locus used by Chen and Behringer, 1995. The strategy to produce the final construct is described in Fig M10.

Figure M10. *Twist1*-Venus for homologous recombination

Strategy for retrieving the modified *Twist1* locus from the BAC and generation of the final targeting vector. 5' homology arm represent 6 kb upstream *Twist1* coding sequence. 3' homology arm represent 1.2 kb downstream *Twist1* coding sequence. *Twist1*-Venus represent the insertion of Gtx-IRES-Venus downstream *Twist1* coding region. Neo represents Pgk-Neomycin resistance. TK represents MC1-Thymidine kinase. Map not to scale.

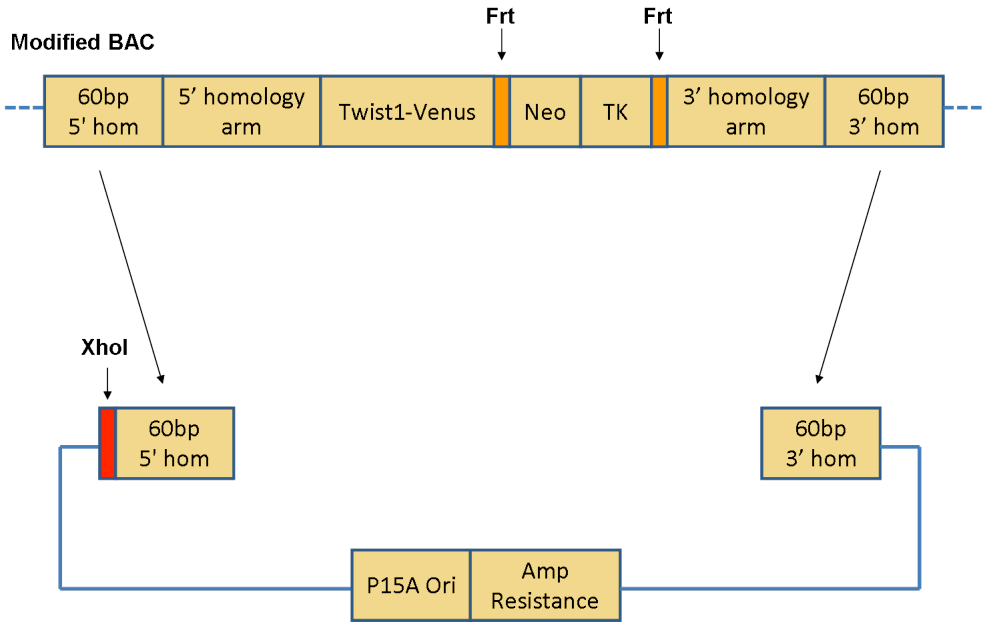
Modified BAC
Frt
Frt
60bp
5' hom
5' homology
arm
Twist1-Venus
Neo
TK
3' homology
arm
60bp
3' hom
XhoI
60bp
5' hom
60bp
3' hom
P15A Ori
Amp
Resistance

The final construct presented in Fig M7 was linearized using the unique restriction site Xho1 as in M1.2.3 digestion for electroporation.

However, at this point careful sequencing of the original NEB193 plasmid containing the Venus, carried by my colleague Mattias Malaguti, revealed a fatal point mutation which generated a BamH1 restriction site between the end of Venus and the beginning of the polyadenilation signal which was designed to terminate the *Twist1*-Venus mRNA. Thus the polyadenilation signal sequence had been lost in the first BamH1 restriction digest, of the original plasmid.

If the vector produced in this manner had been used for gene targeting a single mRNA would have been generated for *Twist1*-Venus and Neomycin resistance gene in a polycistronic sequence. However, after the elimination of the selection cassette at Frt sites the elongation would have terminated at the *Twist1* polyadenilation site at the end of the second non-coding exon. Regrettably, the introduction of Venus before the end of the first exon could influence the splicing site and generate unpredictable splicing events [Fig M11].

For the reasons presented, generation of *Twist1* targeted cell lines was not pursued any further with the above construct. Nevertheless, the work done here showed that the strategy used to introduce a modification into the BAC locus was feasible and that starting from a corrected plasmid the same strategy could produce a viable targeting vector.

Figure M11. *Twist1*-Venus unpredictable splicing event

Schematic representation of *Twist1* locus and its modification to introduce a fluorescent reporter with consideration to RNA splicing. Map approximately to scale.

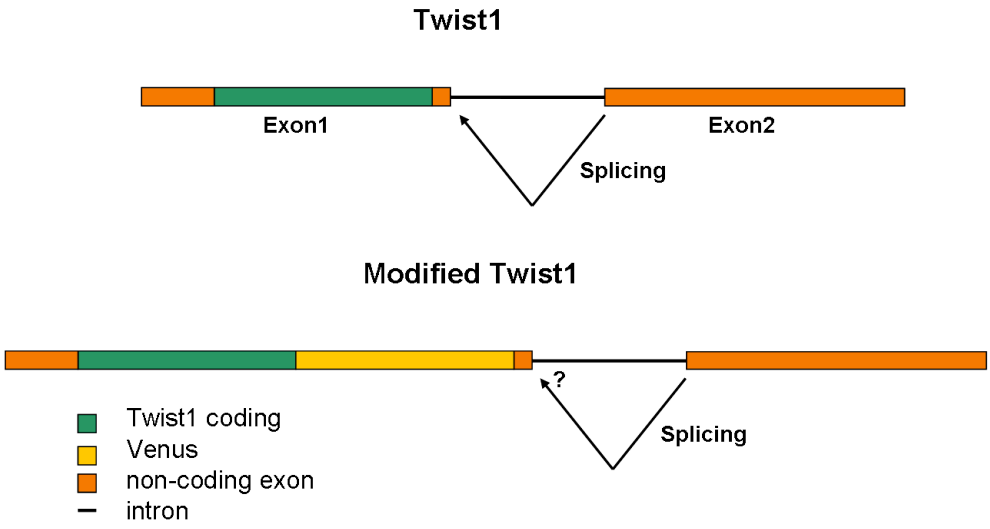
Twist1
Exon1
Exon2
Splicing
Modified Twist1
?
Splicing
Twist1 coding
Venus
non-coding exon
intron

M2. Cell culture

M2.1 Materials, solutions and cell lines

All routine culture procedures and experiments were performed in tissue culture flask/plates (Iwaki or Corning), unless otherwise stated. All flasks, plates, tubes as well as solutions were maintained sterile at all times. Wherever the solutions were made by CRM Cell Culture Service, they are noted as CRM-CCS. For all solution ultra-pure, autoclaved water was used.

M2.1.1 Reagents

Dulbecco's Phosphate Buffer Saline (DPBS), 1x sterile solution, suitable for cell culture (Sigma, D8537)

Gelatine, powder, Type A, for electrophoresis, suitable for cell culture (Sigma, G1890)

Trypsin 2.5%, 10x, without Phenol Red (Gibco, 15090)

Accutase, suitable for cell culture (Sigma, A6964)

Chick serum (Sigma, C5405)

GMEM (Sigma, G5154)

DMEM/F12 (Gibco, 11320)

Neurobasal (Gibco, 21103)

L-Glutamine, 200 mM (Gibco, 25030)

Sodium pyruvate, 100 mM (Gibco, 11360)

MEM Non-essential amino acids, formulated to contain 100x the non-essential amino acids found in the standard Minimum Essential Medium (MEM) (Gibco, 11140)

2-Mercaptoethanol (VWR, 44143-3A)

Foetal Calf Serum (Gibco, 10270, Batch 40F0240K)

Puromycin dihydrochloride, powder, suitable for cell culture (Sigma, P8833)

Hygromycin B, 50 mg/ml (Roche, 843555)

G418 sulphate (PAA, P27-011)

BMP-4, recombinant human (R&D, 314-BP)

Activin, recombinant human, 100% homology with mouse and other mammals for the mature protein (R&D, 338-AC)

FGF2, recombinant human FGF basic (R&D, 233-FB)

PD0325901 (Axon, 1408)

Chiron99021 (Axon, 1386)

LDN193189 (Axon, 1509)

Poly-L-ornithine, 0.01%, mol wt 30,000 to 70,000, suitable for cell culture (Sigma, P4957)

Laminin, 1 mg/ml, from Engelbreth-Holm-Swarm murine sarcoma basement membrane, suitable for cell culture (Sigma, L2020)

Fibronectin, powder, from bovine plasma, suitable for cell culture (Sigma, F4759)

M2.1.2 Solutions

Gelatine: (CRM-CCS) was prepared as 1% solution in water.

Laminin: was diluted in PBS to a final conc of 5 μg/ml.

Fibronectin: was dissolved in warm PBS to a final conc of 7.5 μg/ml.

Trypsin: (CRM-CCS) was prepared as 0.25% Trypsin, 1.3.mM EDTA, 1% Chick Serum in PBS.

Glutamine / pyruvate: (CRM-CCS) as a mixture 1:1 per volume of L-Glutamine and Sodium pyruvate resulting a solution of 100 mM Glut and 50 mM Pyr.

2-Mercaptoethanol: (CRM-CCS) was prepared as a 0.1M solution in water.

LIF: (CRM-CCS) was prepared in house as conditioned medium of Cos7 cells, transiently transfected with a plasmid encoding the human LIF. Medium was collected and LIF activity assayed using CP1 indicator cells. Then, the medium was diluted in PBS to a concentration of 100,000 units/ml.

Puromycin: (CRM-CCS) was prepared as 5 mg/ml solution in PBS.

Hygromycin B: (CRM-CCS) bought as 50 mg/ml and was simply aliquoted.

G418: (CRM-CCS) was prepared as 200 mg/ml active molecule in water, considering the batch activity.

N2 supplement 100x: was prepared as solution in DMEM-F12 containing Insulin (Sigma I-1882) 2.5mg/ml, Apo-transferrin (Sigma T-1147) 10mg/ml, BSA (Gibco 15260-037) 7.5mg/ml, Progesterone (Sigma P8783) 0.002 mg/ml, Putrescine (Sigma P5780) 1.6mg/ml, Na Selenite (Sigma S5261) 3µM.

Standard ES cell medium: was prepared by mixing 500 ml GMEM, 51 ml FCS (final conc 10%), 11 ml Glutamine / pyruvate (100 mM Glut and 50 mM Pyr, final conc 2 mM Glut and 1 mM Pyr), 5.5 ml MEM Non-essential amino acids (100x), 550 µl LIF (100,000 units/ml, final conc 100 units/ml) and 550 µl 2-Mercaptoethanol (0.1 M, final conc 0.1 mM).

N2B27: was prepared by mixing DMEM-F12 with Neurobasal medium 1:1 per volume and supplementing with N2 1:200, B27 1:100 (50x, serum free supplement, Gibco, 17504-044) 1:1000, Glutamine (200 mM, final conc 0.2 mM) and 2-Mercaptoethanol 1:1000 (0.1 M, final conc 0.1 mM).

2i medium: was prepared as N2B27 except Glutamine was increased to 1:200 (1 mM final conc). The medium was supplemented with PD0325901 1µM final conc and Chiron99021 3uM final conc.

Lif + BMP medium: was prepared as N2B27 except Glutamine was increased to 1:200 (2 mM final conc). The medium was supplemented with 1:200 MEM Non-essential amino acids (100x, final conc 0.5x), 1:1000 LIF (final conc 100 units/ml) and BMP4 (final conc 10 ng/ml).

EpiSC medium: was prepared as N2B27 except Glutamine was increased to 1:100 (4 mM final conc) and B27 was increased to 1:50 (final conc 1x). The medium was supplemented with 1:100 MEM Non-essential amino acids (100x, final conc 1x), Activin (final conc 20 ng/ml) and FGF2 (final conc 10 ng/ml).

M2.1.2 Cell lines

E14Tg2a: ES cell line derived from 129/Ola mice.

E14ju: rederived ES cell line from blastocyst of E14Tg2a chimeric mice.

Oct4GIP: Derived from parental line CGR8. Green fluorescent protein (GFP) and Puromycin resistance gene are expressed under the control of the Oct4 promoter [Ying et al, 2002].

46c: E14Tg2A cell line where GFP and Puromycin resistance gene were knocked in the Sox1 locus [Ying et al, 2003b].

Rosa26 rtTA: E14Tg2A_AW2 cell line was generated by Andrew JH Smith and Anna Waterhouse. It contains the coding sequence for the reverse tetracycline-controlled transactivator (rtTA) integrated into the Rosa 26 and expressed from the R26 promoter. The E14tg2A_AW2 cell line will be described in more detail elsewhere [AW, AJHS, S. Lowell in preparation].

M2.2 Cell Culture Procedures

All cell lines were maintained and differentiation experiments performed at 37°C in 7% CO2 humidified atmosphere.

M2.2.1 ES Cell Culture and Maintenance

ES cells were routinely cultured on tissue culture flasks or plates, coated with Gelatine 1% for 30 minutes. Cells were maintained in Standard ES medium and

passaged every two days. To passage, cells were briefly washed with DPBS, and incubated with Trypsin solution at 37°C for 2 to 5 min. The Trypsin was stopped by adding Standard ES medium 10:1 ratio to Trypsin solution, per volume and, centrifuging at 1300 rpm for 3 min. Cells were resuspended in Standard ES media, counted and plated usually at 20,000 cells per cm^2, or at the stated density for each individual procedure.

M2.2.2 Freezing ES Cells

20 million ES cells were detached as in M2.2.1 and resuspended in 5 ml of Freezing Medium, containing 10% dimethyl-sulphoxide (DMSO) and 90% FCS. The cell suspension was aliquoted as 1 ml per cryovial. Vials were placed immediately at -80°C and subsequently transferred to liquid nitrogen after at least 24 hours in the freezer. To thaw, one vial of cells in Freezing medium was quickly thawed at 37°C and cells transferred as soon as possible in Standard ES medium. Then, they were centrifuged at 1300 rpm for 3 min. Cells were resuspended in Standard ES media and plated without counting in one T25 flask.

M2.2.3 2i ES Cell Culture

Tissue culture plates were coated subsequently with Poly-ornithine and Laminin 2h each, at room temperature (RT). Alternatively, second coating was done overnight at 4°C. Cells were maintained in 2i medium and passaged every three days. To passage, cells were briefly washed with PBS and detached using Accutase. Furthermore, a procedure similar to the standard ES cell technique was employed, except serum free medium was used at all times.

M2.2.4 ES Cell Culture in LIF + BMP Medium

Cells were plated on plates coated with Gelatine for 30 min, in Lif + BMP medium and passaged every two days. To passage, the same technique was employed as in M2.2.1, except serum free medium was used at all times.

M2.2.5 EpiSC Culture

Tissue culture plates were coated with Fibronectin for 1h at RT. Cells were initially plated at a density of 200,000 cells per well in a 6 well plate, maintained in EpiSC medium and passaged every two days 1:4. To passage, cells were briefly washed with DPBS and detached using Accutase. EpiSC were pipetted very gently in order to maintain the cells in small clumps rather than dispersing them into single cells, and cells were not counted.

M2.2.6 Neural Differentiation

Tissue culture plates were coated with Gelatine for 1h at RT. Cells were grown in Standard ES medium so that they would reach approximately 70% confluency at the time of passaging. Cells were detached as described in M2.2.1 except that before counting they were washed twice in serum free medium. Then, were plated at a density between 150,000 and 200,000 per well, in a 6 well plate in N2B27. Media was changed every 2 days.

M2.2.7 Induction of Doxycyclin Dependent Transgene

For Doxycyclin dependent transgene induction medium was supplemented with Dox at the time the cells were plated as described above either in Neural Differentiation conditions or in pluripotent conditions of LIF + BMP. The concentration of Dox was either 800 ng/ml or the concentration stated for a particular experiment.

For short induction, 150,000 cells were plated per well in a 6 well plate in LIF + BMP medium and the next day the medium was changed either with LIF + BMP supplemented with Dox, or with N2B27 supplemented with Dox. 9 hours later cells were lysed and RNA extracted as in M3.3.1.

M2.3 Generation of Transgenic Cell Lines

M2.3.1 Lipofection Method

ES cells were plated as in M2.2.1 at a density of 200,000 cells per well in a 6 well plate, in 2 ml Standard ES medium and, allowed to attach for a few hours. Plasmids containing the desired transgene were linearized as in M1.2.3. For transient transfection non-linearized plasmids were used. 1 µg of DNA was diluted in 250 µl GMEM. In a separate tube, 1 µl Lipofectamine 2000 (Invitrogen, 11668) was diluted in 250 µl GMEM and incubated at RT for 5 min. The DNA and Lipofectamine solutions were mixed and, incubated at RT for 20 min to form the transfection complexes. The reaction was then added to the previously plated cells, 500 µl reaction for each well to be transfected. The plate was gently rocked and placed back in the incubator.

M2.3.2 Isolation of Clonal Lines

The next day, cells were passaged without counting using a serial dilution form 1:10 to 1:1000 cells per plating surface. Medium was changed to Standard ES medium supplemented with the relevant antibiotic. The following final concentrations were used: Hygromicin 200 ug/ml, Puromycin 2 µg/ml, G418 200 µg/ml. Medium was changed every two days for the next 1 to 2 weeks, checking microscopically the formation and growth of antibiotic resistant colonies. When colonies grew to be macroscopically visible: 2 to 4 mm diameter, they were transferred to a 96 well plate, one colony per well, using the following procedure.

The position of each macroscopically visible colony was labelled on the plate using a marker. Each marked colony was checked microscopically to confirm that it did not touch or, closely neighboured another colony, in which case its position was crossed with the marker. The remaining colonies were physically removed from the plate in a film of DPBS using a p200 sterile tip. The colony was aspirated into the tip and moved to a round bottom well, of a non-adherent plate, where cells were

dissociated by trypsinization, and then plated in Standard ES medium. Considering that this was a stressful procedure, for the cells, the antibiotic was omitted for the first 24 hours, but added after that time point.

M2.3.3 Electroporation Method

A large number of cells were dissociated as in M2.2.1, washed twice in un-supplemented GMEM, counted and resuspended to a density of 10 million cells per 800 µl DPBS.

100 µg of plasmidic DNA containing the desired transgene was linearized as in M1.2.3. and resuspended in 100 µl water.

100 ul DNA and 800 ul cell suspension were mixed as quickly as possible in a 4 mm gap electroporation cuvette and incubated at RT for 3 min. Cells were electroporated at 3 uF and 0.8 kV, and the time constant was 0.1 or 0.2.

Electroporated cells were plated on 10 cm diameter tissue culture dishes, in Standard ES medium, at densities ranging form 50,000 cells per dish to 1,000,000 cells per dish and incubated at 37°C. The next day medium was changed to Standard ES medium supplemented with the relevant antibiotic. From this moment on the procedure was continued as in M2.3.2.

M3 Preparation of Biological Material for Analysis

M3.1 Cell Fixation for Immunofluorescence

Cells were cultured or differentiated as described in M2. Cells growing on tissue culture plates had the medium removed and fixed using a solution of 4% Paraformaldehyde (PFA, Signma, 158127) in PBS, for 20 min at RT. Cells were washed twice with PBS, maintained in PBS at 4°C and antibody labelled within one month.

M3.2 Fluorescence Activated Cell Sorting (FACS)

Differentiated cells were detached using Cell Dissociation Buffer, enzyme free in PBS (Gibco, 13151-014). Briefly, cells were washed once with PBS and once with dissociation buffer. Then, dissociation buffer was added (3 ml for one T75 flask) and cells incubated at 37°C for 5 min. 10 ml FACS buffer (3% FCS in DPBS) was added and cells detached by gentle pipetting, centrifuged at 1300 rpm for 3 min. Cells were resuspended in 1 to 2 ml FACS buffer and filtered through the Cell-Strainer Cap of a 5 ml Polystyrene Round-Bottom Tube (BD Falcon, 352235) to remove any cell clumps. DAPI was added, to a final concentration of 100 ng/ml, for visualization of non-viable cells.

Sox1 GFP cells and Tomato labelled cells were sorted using FACS Aria II apparatus. Cell fragments, dead cells and duplets were excluded from analysis. Wild type cells were used to set the negative gates. Positive versus negative or high versus low cells were collected in the in separate tubes in FACS medium. Sort quality was assessed by reanalysing sorted populations by FACS and the accuracy exceeded 95% in every instance. Cells were moved as soon as possible on ice and RNA extracted immediately as in M3.3.1 Trizol method, followed by cDNA synthesis.

M3.3 RNA Extraction and cDNA Synthesis

M3.3.1 RNA Extraction

RNA was extracted for cells cultured or differentiated as described in M2, using Total RNA Isolation Mini Kit (Agilent Technologies, 5185-6000) according to manufacturer protocol.

For cells isolated by Flowcytometry Activated Cell Sorting (FACS) RNA was extracted manually using Trizol reagent (Invitrogen, 10296) according to manufacturer protocol. Briefly, 100,000 to 1,000,000 cells isolated by FACS were

centrifuged at 1500 rpm for 5 min and resuspended in 1 ml Trizol. Cells were dissociated and nuclear complexes disrupted by passing 5 times through a seringe fitted with a 26G needle. The suspension was incubated at RT for 5 min. 250 µl Chloroform was added, sample mixed an incubated at RT for 5 min. The sample was centrifuged at 12,000g for 15 min at 4°C. The aqueous phase was moved to a new tube and 650 µl Isopropanol were added and homogenized. The mixture was incubated at RT for 10 min and then, centrifuged at 12,000g for 10 min at 4°C. Supernatant was discarded and the pellet washed with ethanol as in M1.1.4.3 and the RNA resuspended in water.

M3.3.2 cDNA Synthesis

RNA concentration in all samples of one experiment was measured using Nanodrop spectrophotometer. Ideally 1 µg of RNA was diluted in water to a final volume of 10 µl, for each sample. If some samples had a RNA concentration which was lower than 0.1 µg/µl, the final concentration in all samples was scaled accordingly. Samples with RNA concentration lower that 0.01 µg/µl were not included.

cDNA synthesis was performed using M-MLV Reverse Transcriptase (Invitrogen, 28025) according to manufacturer protocol. Included reagents: 5x First-Strand Buffer, 0.1M DTT. Reagents not included: Random Primers (Invitrogen, 48190), 50 ng per reaction, dNTP Mix (Invitrogen, 18427013) 1 µl of 10 mM per reaction, 0.5 mM each dNTP final concentration, RiboLock RNase Inhibitor (Thermo Scientific, E00382), 20 units per reaction.

No-RT control was performed for each sample by not adding the Reverse Transcriptase to the reaction. The absence of significant levels of genomic DNA was confirmed by performing qPCR (see M4.2) using a non-intron spanning pair of primers (*Twist1* coding). The samples were only used if the transcript levels were at least 10^3 times higher in the RT samples compared with No-RT control.

M3.4 Cell Lysis for Western Blot

RIPA buffer: was prepared as an aqueous solution containing: Tris-HCl pH 7.4 50 mM, NP-40 1%, Na-deoxycholate 0.25%, NaCl 150 mM, EDTA 1 mM. and was kept a 4°C.

Pefablock: irreversible serine protease inhibitor (Sigma, 76307), was diluted in water at a concentration of 500 mM (833 µl of water for 1 vial of 100 mg) and kept at 4°C.

Protease inhibitors: cOmplete ULTRA tablets, EDTA free, (Roche, 05892953001). One tablet was diluted in 2 ml water (25x), aliquoted in 50 µl vials and kept at kept a -20°C.

RIPA working buffer was prepared shortly before use by adding to 1 ml of RIPA buffer of: 1 µl Pefabloc 500 mM (final conc 0.5 mM), 1 µl DTT 1M, (final conc 1mM) and, 40 µl 25x Protease inhibitors.

10 million cells were trypsinised as in M2.2.1. and resuspended in 500 µl RIPA working buffer. Cells were rocked at 4°C for 30 min for complete lyses, then 1µl (250 U) Benzonase Nuclease (Sigma, E1014) was added and incubated at RT for 10 min. At this point samples were either stored at -80°C or directly used for Western Blot.

M3.5 Preparation of Embryos for In Situ Hybridization

MF1 wild type mice were housed and mated at the Animal Unit Facility of the ISCR and CRM, in accordance with the provisions of the Animals Scientific Procedures Act (1986). At the stated time points, after mating, pregnant mice were sacrificed by cervical dislocation. Immediately, the mouse was dissected and the uterus containing the embryos was moved to a dish containing sterile M2 medium, with HEPES, suitable for mouse embryos (Sigma, M7167). The embryos were further dissected, using fine forceps, by removing them from the uterine wall. The decidua was removed as well as the Reichert's membranes and, for older embryos, at somitic

stages, the yolk sack and the amnion. After dissection, embryos were moved with a pipette from the M2 medium to a 4% fresh PFA solution, where they were kept overnight. The pipette size was adjusted to the embryo age. Fresh PFA means: stored for maximum one moth at -20°C and thawed the day it was used. For very small embryos: E 6.5 and earlier fixation was shortened at 30 min to 1 hour.

The next day embryos were dehydrated by subsequent incubation in the following solutions at RT: PBT (PBS with 0.1% Tween) twice for 5 min, 25% Methanol in PBT for 5 min, 50% Methanol in PBT for 5 min, 75% Methanol in PBT for 5 min, 100% Methanol twice for 5 min. The embryos were stored in 100% Methanol at -20°C for up to one month.

M3.6 siRNA procedure

RNA silencing was performed using GeneSolution siRNA for Twist1 (Qiagen GS22160) which comprised of the following siRNA constructs: Mm_Twist1_1 – SI00202356, Mm_Twist1_2 – SI00202363, Mm_Twist1_3 – SI00202370, Mm_Twist1_5 – SI02714460. As a negative control AllStars Negative Control siRNA conjugated with Alexa-488 (Qiagen, 1027292) was used. This RNA has no homology with any known mammalian gene and had been validated against non-specific effects on gene expression. siRNA was transfected using HiPerfect Transfection Reagent (Qiagen, 301705) according to manufacturer instructions. Briefly, lyophilized siRNA was resuspended in water to a stock concentration of 10 µM. On the first day of the experiment 200,000 cells (for each condition) were plated in a well of a 6 well plate, coated with gelatine, in N2B27 (serum free). An aliquot of each 10 µM stock solution siRNA was diluted to 2 µM working solution. This included the 4 siRNA Twist1 constructs and the control siRNA. 6 ul of the 2 µM siRNA were mixed with 91 ul N2B27 and 3 ul HiPerfect reagent. Two more control conditions were set: no transfection, and no siRNA were 91 µl of N2B27 were mixed with 3 µl of HiPerfect only. The siRNA transfection reagent mixture was incubated at RT for 5 min and then added dropwise to the culture, followed by a gentle swirl. The final siRNA concentration in the culture medium was 5 nM. Cells were lysed at 24, 48 and 72 hours post transfection, as in M3.3.1. Medium was changed every day.

The optimal siRNA / HiPerfect ratio was determined for the presented culture conditions by incubating various amounts of control siRNA (3 to 12 µl) and HiPerfect (1.5 to 12 µl) and assessing transfection efficiency by flowcytometry based on Alexa488 fluorescence.

M4 Analytical Procedures

M4.1 Immunofluorescence

M4.1.1 Immuno-labelling

Detection of protein expression in adherent culture was performed using specific antibodies. Cells fixed as in M3.1 were blocked and permeabilised using the Block/Perm buffer while rocking for 1 hour at RT. **Block/Perm buffer** contained 3% serum and 0.1% Triton in PBS. Depending on the secondary antibody Goat or Donkey serum was used.

Perm/Block buffer was removed and replaced directly with the relevant primary antibody, at the appropriate, concentration diluted in Perm/Block buffer supplemented with Sodium azide 2 mM. See Table M1 for a list of primary antibodies used. Cells were incubated with the primary antibody for 1 hour at RT while rocking.

Next the primary antibody was removed, cells were washed trice for 10 min at RT in PBS, while rocking. Antibody labelling was repeated with the secondary antibody, diluted usually 1:1000 in Perm/Block buffer; 1 hour at RT while rocking. See Table M2 for a list of secondary antibodies used.

The secondary antibody was removed and cells washed twice in PBS for 10 min at RT while rocking. Nuclei were counterstained using a solution of DAPI 100 ng/ml in PBS for 5 min at RT while rocking. Cells were subject to two final washes with

PBS. For cells differentiated to neurons, where long neurites, loosely attached to the dish were present rocking was very gentle, close to the lowest speed of the machine.

For double marker staining the above procedure was simply repeated. Primary or secondary antibodies were never mixed. The final PBS solution was supplemented with Sodium azide 2 mM and samples were stored at 4°C.

Imaging was performed using an Olympus IX51 inverted microscope with fluorescence and images captured with a Retiga 2000R (QImaging) camera guided by Volocity software version 4.2.0 (Improvision).

M4.1.2 Quantification of Neuron Formation

To quantify neuronal formation pictures of the same field were taken in the blue channel for nuclei stained with DAPI and, in the green channel for neural bodies and processes labelled for TUBB3. To ensure unbiased field selection, fields were chosen in the blue channel based on presence of significant cell numbers.

The total cell numbers in a certain field was assessed automatically following nuclear segmentation using FARSIGHT Nucleus Editing Tool 0.4.4 (Rensselear Polytechnic Institute, http://www.farsight-toolkit.org). The number of cells assessed in each field was between 300 and 1200. TUBBIII positive neurons were counted manually and neurite length was assessed using ImageJ measuring tool (ImageJ 1.47d, Wayne Rasband, National Institute of Health, USA, http://imagej.nih.gov/ij). To assess formation of neurons with “long” neurites 10 random nuclei diameters were measured and the results averaged. An arbitrary threshold of 7 nuclear diameters was set. Neurites shorter than this length were considered as “short” and neurites of this length or exceeding it were deemed “long”. For neurons with more than one neural process the longest process was measured and multiple process lengths were not cumulated. An example of nuclear segmentation and neuronal assessment is given in Fig M12.

Figure M12. Quantification of neuron formation

Nuclear segmentation is shown in (a); each identified nucleus being contoured with a light green line. Neuron counting shown in (b); yellow arrows point towards the cellular bodies of neurons with short neurited, red arrows point towards cellular bodies of neurons with long neurites.

a

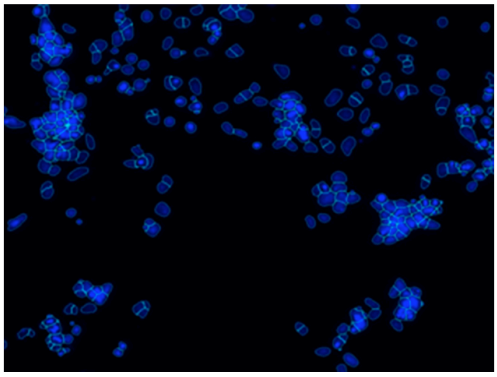

b

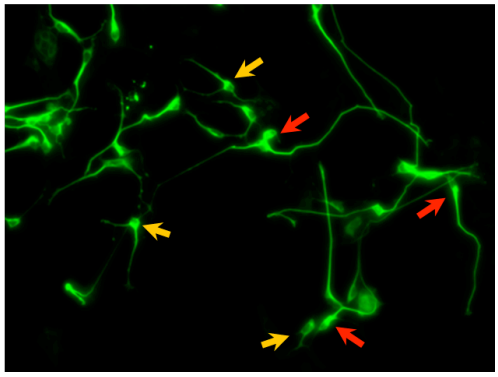

For statistical analysis “R: A language and environment for statistical computing” was used (R Foundation for Statistical Computing, Vienna, Austria. ISBN 3-900051-07-0, URL http://www.R-project.org/). The statistical significance was determined using One-way ANOVA followed by Tukey HSD post hoc test. For analysis the data from two clones was pulled. Error bars represent standard deviation of six microscopic fields for each condition. The data from each clone was not averaged and, each data set was considered an individual sample.

M4.2 Quantitative PCR

Quantitative PCR was performed using cDNA samples produced as in M3.3. LightCycler480 System (Roche) was used with Universal Probe Library (UPL). Briefly UPL is based on 165 short hydrolysis probes which detect 8- or 9-mer motifs that are very prevalent in the transcriptomes. The probes are labelled at the 5' end with fluorescein (FAM) and at the 3' end with a dark quencher dye allowing for fluorescence only upon dissociation of the synthetic nucleotide by polymerase exonuclease activity.

The quantitative PCR was carried in a LightCycler480II apparatus (Roche). The reaction was set in a 384 well plate, in 10 µl reactions, using LightCycler480 Probes Master (Roche, 04887301001) and individual UPL probes (used at 100 nM final conc), purchased from Roche. Amplification primers (used at 200 nM final conc) were designed using Roche online software: http://www.roche-applied-science.com/sis/rtpcr/upl/. A list of primers used and their corresponding probes is presented in Table M3.

Each primer pair was tested against formation of non-specific amplification products in a Taq PCR reaction revealed on a gel. As a template, cDNA from samples where the gene of interest was expected to be expressed was used. The testing for the majority of the primers used in our lab was performed by XinZhi Zhou. New primers were designed in the case of primer pairs which produced more than one band. Furthermore, the single band was subcloned into pGEM-T Easy (Promega, A1360), and six decimal serial dilutions of the resulting plasmid were used to generate a

standard curve for each gene. For all genes the highest standard concentration was of 400 ng/ml. Correction for DNA copy number based on insert size was not performed, given that the insert would not exceed 150 bp, less than 5% of the total plasmid size. R^2 for all standard curves used was of at least 0.9.

The Cp value for each reaction was automatically calculated using the Roche Light Cycler 480 algorithms. Concentration values were also obtained automatically from the Roche Light Cycler 480 software by reporting the Cp values of the samples to the standard curve.

The following cycle conditions were used:

95°C – 5 min
45 cycles:
95°C – 5 seconds
61°C – 10 seconds
72°C – 1 second
40°C – 10 seconds

Acquisition was performed during elongation at 72°C.

Each gene expression was normalized to TBP. For each sample duplicate reactions were performed and the assay repeated if technical replicates showed significant inconsistency. Error bars represent range value between two samples.

Statistical analysis was performed across multiple experiments. For this, the average expression value for each gene in each experiment was arbitrarily set to 1. Error bars represent standard deviation of the mean of the samples from all experiments taken into consideration. Significance was calculated using a paired T-test and p values below 0.05 were considered significant. For this analysis samples with and without Dox treatment were compared and no multiple comparison was performed.

M4.3 Western Blot

M4.3.1 Measuring Sample Protein Concentration

Concentration of total protein from cell lysate obtained as in M3.4 was measured using the Bio-Rad protein assay, based on Bradford method, using a 202.5 ul reaction in transparent 96 well plates (Corning, CLS3085) assessed in Glomax Multi Detection System (Promega).

Briefly, Protein Assay Dye Reagent Concentrate (Bio-Rad, 500-0006) was diluted 1:5 in water. Each protein sample was diluted 1:10 in water. In each well, 200 ul diluted assay reagent were mixed with 2.5 µl diluted sample. Samples were incubated at RT for 20 min and absorbance was measured at 595 nm. Protein concentration was determined against a BSA standard curve. BSA stock solution of 50 µg/µl was serially diluted in water to the following concentrations: 0, 0.75, 1, 5, 7.5, 10 ug/µl. These BSA solutions were treated in the same way as the samples, except that 2.5 ul of RIPA working buffer diluted 1:10 in water was also added, to compensate for sample buffer absorption. An example of standard curve is presented in Fig M13.

M4.3.2 Protein Separation by Weight in Gel Electrophoresis

Based on assayed protein concentration samples were diluted in water to the lowest concentration of the particular batch. 50 µl of diluted samples were mixed with 25 µl 4x NuPAGE LDS Sample Buffer (Novex, NP0008) and 25 µl DTT 1M. Samples were heated at 95°C for 10 min.

10 µl of heat denaturated samples were loaded on a NuPAGE 4-12% Bis-Tris Gel 1 mm 10 wells (Novex, NP0321). In each gel one lane was loaded with 10 µl SeeBlue Pre-Stained Standard (Life Technologies, LC5625). Electrophoresis was performed in a Novex MultiCell gel tank using NuPAGE MOPS SDS running buffer (Novex, NP0001) at 200 V, and not exceeding 120 mA. The samples were run until

the standard ladder was well displayed and the blue dye reached the bottom of the gel, usually 1 to 1.5 hours.

The gel was then removed from its precast case and equilibrated for 15 min in transfer buffer. Transfer buffer was made as an aqueous solution containing 1x NuPAGE Transfer buffer (Novex, NP0006) and 10% Methanol. Amersham Hybond ECL blotting membrane (VWR, RPN203D) was equilibrated in transfer buffer for at least 5 min. The proteins were transferred on the membrane in a Novex MultiCell gel tank at 25 V for 1 hour in transfer buffer.

M4.3.3 Resolving The Protein of Interest on Western Blot

Presence of proteins was checked by briefly staining the membranes with Ponceau S solution, 0.1% in 5% Acetic acid (Sigma, P7170). The Ponceau S was gradually washed with water, until the bands could be clearly seen and, finally, completely removed by adding a few drops of 0.2 M NaOH in water. NaOH was removed by a couple more water washes and the membrane was transferred to blocking solution for 1 hour at RT while rocking. Blocking solutions contained 10% skimmed milk and 0.1% Tween in PBS.

Next the primary antibody was diluted in blocking solution and the membrane was transferred in this solution for 1 hour at RT while rocking. See Table M1 for antibodies and concentrations used. Subsequently, the membrane was washed for at least 1 hour at RT, changing the solution at least three times. Washing buffer contained 1% skimmed milk and 0.1% Tween in PBS.

The procedure was repeated for the secondary antibody; see Table M2.

Finally the membrane was washed twice in PBS and 1 ml of SyuperSignal West Pico Chemiluminescent Substrate (Thermo Scientific, 34077) was incubated on the active site of the membrane, for a few min. Images were captured on Amersham Hyperfilm ECL (VWR, 28906837), which were developed depending on the strength of the signal between 15 sec and 5 min.

Figure M13. Standard curve for protein concentration assay

BSA known concentration serial diluted samples assayed by Bradford method.

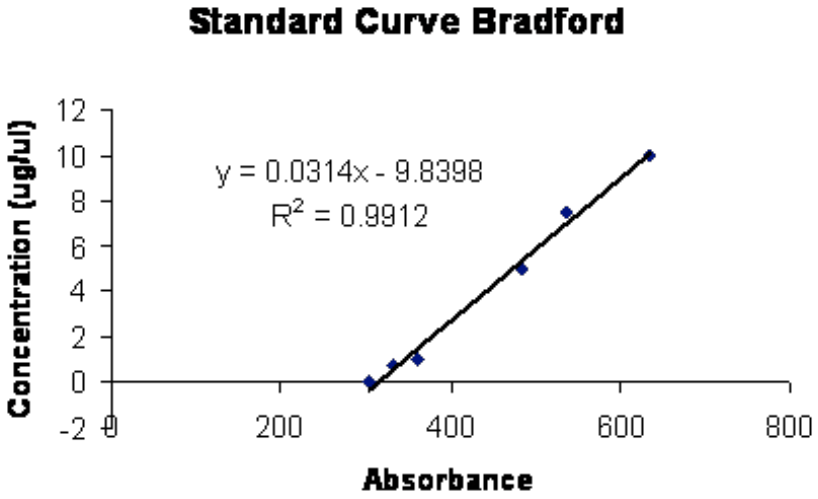
Standard Curve Bradford
Concentration (ug/ul)
12
10
8
6
4
2
0
-2
0
200
400
600
800
Absorbance
y = 0.0314x - 9.8398
R2 = 0.9912

For loading control analysis the membrane was reblotted with anti-alpha-Tubulin (see table M1). The membrane was striped using acidic stripping buffer, which was made as an aqueous solution containing: 1.5% Glycine, 0.1% SDS, 1% Tween, and pH was adjusted to 2.2 with HCl. Membranes for stripping were incubated at RT for 10 min in this buffer while rocking, followed by two washes in PBS 10 min each and 2 washes in PBS-Tween 0.1% 10 min each. The labelling procedure was then repeated starting from blocking.

M4.4 In Situ Hybridization

M4.4.1 Reagents

Anti Digoxigenin-AP (Roche, 11093274910)
Citric acid, anhydrous, cell culture tested (Sigma, C2404)
DEPC (Sigma, 472565)
DIG RNA Labeling Mix (Roche, 11277073910)
DNase I (Promega M6101)
Formamide 37% (Sigma, F1635)
Formamide 99.5 GC (Sigma, F9037)
Glutaraldehide (Sigma, G5882)
Glycine (Sigma, G8898)
Heparin (Sigma, H3393)
Hering sperm DNA (Promega, D1811)
Hydrogen peroxide, 30% (Sigma S216763)
Hydrochloric acid, 36.5-38% (HCl, Sigma, H1758)
Hydrogen peroxide (Sigma, S216763)
Magnesium chloride, anhydrous (MgCl2, Sigma, M8266)
Methanol (VWR, 20846)
Sodium acetate, 3M (NaAc, Sigma 71196)
Paraformaldehyde (PFA, Sigma, 158127)
PBS 10x, cell culture tested (Sigma, P5493)
Potassium chloride (KCl, Sigma, P9333)

Proteinase K (Sigma, P2308)

RNase A (Roche, 10109142001)

RNase free water (Invitrogen, 10977-049)

RNase Inhibitor (Roche 03335399001)

Sheep serum (Sigma, S2263)

SigmaFast BCIP/NBT, tablets (Sigma, B5655)

Sodium chloride (NaCl, Sigma, S7653)

Sodium citrate dihydrate (Sigma, W302600)

Sodium dodecyl sulphate (SDS, Sigma, L3771)

T7 RNA polymerase (Roche 10881767001)

Tween (Promega, H5151)

Yeast RNA, Ribonucleic acid from torula yeast (Sigma, R6625)

M4.4.2 Stock Solutions

PBS: prepared by diluting PBS 10x in RNase free water

PBT: prepared by adding 0.1% Tween to PBS

PFA 4%: prepared by diluting PFA in PBS warmed to 70°C aliquoted, stored at -20°C.

Methanol 25% to 75%: prepared by mixing the appropriate volume of Metahnol with PBT.

Proteinase K: 500x prepared as a solution of 5 mg/ml in PBT. Aliquoted as 50ul containing tubes and stored at -20°C.

SSC: was prepared as an aqueous solution of NaCl 3M, NaCitrate 350 mM and pH was adjusted to 4.5 with Citric acid. DEPC was added, 1:1000, mixed, the solution was left with the cap unscrewed in the fume hood overnight and autoclaved the next day.

Heparin: was prepared as an aqueous solution of 10%, aliquoted as 50 µl containing tubes and stored at -20°C.

SDS solution: was prepared as an aqueous solution of 10% SDS.

NaCl solution: was prepared as an aqueous solution of 5M NaCl.

Tris pH 7.5: was prepared as an aqueous solution of 1M Tris-HCl. pH was adjusted with HCl.

Tris pH 9.5: was prepared as an aqueous solution of 1M Tris-HCl. pH was adjusted with HCl.

TBS: was prepared as an aqueous solution containing NaCl 1.38 M, KCl 27 mM, and Tris pH 7.5 125 mM (1:8 form 1 M solution). Solution was autoclaved.

RNase stock solution: was prepared as an aqueous solution of 1%, aliquoted in 125 µl containing tubes and stored at -20°C.

Sheep serum: was inactivated by heating at 55°C for 30 min. Then it was aliquoted as 1 ml containing tubes and stored at -20°C.

MgCl2: was prepared as an aqueous solution containing 1 M MgCl2. Solution was autoclaved.

PBT pH 5.5: was prepared by adjusting the pH of PBS solution with HCl. Then 0.1% Tween was added.

M4.4.3 Short Term Solutions

Hydrogen peroxide working solution: was prepared by diluting Hydrogen peroxide 30% 1:5 in PBT.

Proteinase K working solution: was prepared by diluting Proteinase K stock solution 1:500 in PBT.

Glycine: was prepared as a solution containing 0.2% Glycine in PBT.

Refix solution: was prepared by adding 0.2% Glutaraldehide to a 4% PFA solution.

Refix labelled embryos solution: was prepared by adding 0.1% Glutaraldehide to a 4% PFA solution.

Long term storage solution: was prepared by diluting 4% PFA to a concentration of 0.1% PFA in PBT

Prehybridization solution: was prepared by diluting SSC 1:4 in a 50% Formamide aqueous solution. Tween was added to 0.1% and Heparin to a final concentration of 0.005%.

Yeast RNA: was prepared as an aqueous solution of 10% RNA.

Hybridization solution: was prepared by adding to the prehybridization solution Yeast RNA 1:100 and Hering sperm DNA 1:100. The probe was denatured for 10 min at 80°C. 1 µg of probe was added to 1 ml hybridization solution

Wash Solution I: was prepared by diluting SSC 1:5 in a 50% Formamide aqueous solution. SDS was added to a final conc of 1%.

Wash Solution II: was prepared as an aqueous solution containing NaCl 500 mM, Tris pH 7.5 10 mM and Tween 0.1%

Wash Solution III: was prepared by diluting SSC 1:10 in a 50% Formamide aqueous solution.

RNase working solution: was prepared by diluting RNase stock solution 1:100 in Wash Solution II (final conc 0.01%)

TBST: was prepared by diluting TBS 1:10 in water and adding Tween to a final conc of 0.1%.

Blocking solution: was prepared by diluting sheep serum 1:10 in TBST.

DIG Label: was prepared by diluting Blocking solution 1:10 in TBST and adding DIG-AP 1:2000.

NTMT: was prepared as an aqueous solution containing NaCl 100 mM, Tris pH 9.5 100 mM, MgCl2 50 mM and Tween 0.1%.

BCIP/NBT: was prepared as an aqueous solution containing 100 mM NaCl, 45 mM MgCl2 and Tween 0.1%. To 10 ml of this solution one BCIP/NBT tablet was added, dissolved in the dark and filtered using a syringe fitted with a 0.45 μm filter. Note: the salts in the solution were calculated so that with the salts in the BCIP/NBT tablet the final desired concentrations would be achieved, namely: Tris pH 9.5 100 mM, NaCl 100 mM and MgCl2 50 mM.

M4.4.4 In Situ Hybridization Procedure

For the following experiments *Twist1* probe generate as described (M1.3.3) was used. As control, previously validated probes for *Pou5f1* and *Tcf15* were used.

Prehybridization procedures

Embryos dissected, fixed and dehydrated, as in M3.5 were rehydrated by 5 min sequential washes in 75%, 50% and 25% Methanol solution respectively, followed by two washes in PBT 5 min each.

Next embryos were bleached in Hydrogen peroxide working solution for 1 hour at RT, followed by three 5 min washes in PBT. Proteolysis was performed by placing

embryos in Proteinase K working solution at RT for times optimized for embryo age. For the embryos used in the experiments presented here proteolysis lasted between 5 and 12 min. Proteolysis was stopped by placing embryos in Glicine solution for 5 min at RT. Glicine was washed in PBT at RT, twice, 5 min each.

Next embryos were refixed by placing them in Refix solution for 20 min. Refix was washed in PBT at RT, twice, 5 min each. Embryos were then placed in Prehybridization solution overnight at 65°C.

RNA probe hybridization

Next day embryos were briefly washed with prewarmed Hybridization solution not containing probe. They were then placed in Hybridization solution with probe, overnight at 65°C.

Next day the embryos were washed twice in Wash Solution I for 30 min at 65°C and once in a 1:1 mixture of Wash Solution I and Wash Solution II for 10 min at 65°C. Then they were washed three times in Wash Solution II at RT for 5 min each and placed in RNase working solution at 37°C for 15 min. RNase step was repeated. Then the embryos were washed at RT for 5 min once in Wash Solution II and once in Wash Solution III. Finally they were washed twice at 65°C for 30 min in Wash Solution III.

DIG labelling

Next embryos were equilibrated in TBST, three washes at RT, 5 min each. Then they were placed in Blocking solution for 5 to 8 hours at RT. Then, embryos were placed in DIG Label overnight at 4°C.

Next day, embryos were washed all day in TBST at RT. First three brief 5 min washes were performed, than multiple 1 or 2 hour washes. Finally, embryos were placed in TBST at 4°C overnight.

Alkaline phosphatase reaction

Next day embryos were equilibrated in NTMT for 3 washes at RT, 10 min each. Then they were placed in BCIP/NBT solution and rocked in dark. Staining

development was checked microscopically at increasingly longer intervals 15 min, 30 min, 1 hour, 2 hours etc, up to 48. When staining was considered sufficient, embryos were removed from the staining solution and washed, still in dark, twice with NTMT for 10 min each and twice with PBT for 10 min each. Then, embryos were placed in the stop solution: PBT pH 5.5 at 4°C overnight.

Next day they were fixed in Refix labelled embryos solution for 1 ht at RT and then placed in Long term storage solution at 4°C.

Whole embryos were imaged using a Nikon AZ100 microscope and images captured with NIS Elements Imaging Software version 4.0 (Nikon Instruments Inc.). For sectioning embryos were embedded in paraffin, after dehydration is ethanol sequential solutions (40%, 70%, 90%, 95% and twice 100%) and cleared in Xylene. Next day, embryos were sectioned at 7 µm thickness in a microtome (Anglia Scientific). Sections were washed twice with Xylene to remove the wax and mounted underneath coverslips in DPX (Agar Scientific). Sectioning procedure was performed by Ronald Wilkie. Sections were imaged using an Olympus BX61 microscope and images were captured with Volocity version 6.1.1 (Perkin Elmer Inc.).

Table M1 primary antibodies:

Antibody name	Specificity	Specie	Dilution used	Source	Technique
ECCD2	CDH1; human, mouse	Rat Monoclonal IgG2a	1:200	Zymed Laboratories, Calbiochem	Immunostain
32/N-Cadherin	CDH2	Mouse IgG1	1:100	BD	Immunostain
Sc-763: E47 N-649	E47; mouse, rat, human Crossreacts with E12	Rabbit, Polyclonal	1:200	Santa Cruz Biotech	Western Blot

BioM2	Flag	Mouse, monoclonal, IgG1	1:1000 1:4000	Sigma-Aldrich	Immunostain, Western Blot
Sc-5279: Oct-3/4 C-10	POU5F1	Mouse, monoclonal, IgG2b	1:200	Santa Cruz Biotech	Immunostain
Rat-401	Nestin; rat, mouse	Mouse, monoclonal, IgG1	1:20	Susan Hockfield, Yale Univ	Immunostain
Tuj1	Neuronal class III β-Tubulin, mammalian	Mouse, monoclonal, IgG2a	1:1000	Covance, R&D Systems	Immunostain
Sc-17320 Sox2	SOX2; mouse	Goat, polyclonal	1:500	Santa Cruz	Immunostain
Anti-Twist1	TWIST1, human, rat, mouse	Rabbit, polyclonal	1:1000	Sigma-Aldrich	Western Blot
Anti-alpha-Tubulin loading control	Alpha-Tubulin, human, mouse, rat, chicken	Rabbit, polyclonal	1:5000	Abcam	Western Blot

Table M2 secondary antibodies:

Specificity	Conjugate	Specie	Dilution	Source	Technique
Mouse IgG1	Alexa-Fuor 488	Goat	1:1000	Molecular Probes A-21121	Immunostain
Mouse IgG1	Alexa-Fuor 594	Goat	1:1000	Molecular Probes A-21125	Immunostain
Mouse IgG2a	Alexa-Fuor 488	Goat	1:1000	Molecular Probes A-21131	Immunostain
Mouse IgG2a	Alexa-Fuor 594	Goat	1:1000	Molecular Probes A-21135	Immunostain
Mouse IgG2b	Alexa-Fuor 488	Goat	1:1000	Molecular Probes A-21141	Immunostain
Mouse IgG2b	Alexa-Fuor 594	Goat	1:1000	Molecular Probes A-21145	Immunostain
Rat IgG	Alexa-Fuor 488	Goat	1:1000	Molecular Probes A-11006	Immunostain
Goat IgG	Alexa-Fuor 488	Donkey	1:1000	Molecular Probes A-11058	Immunostain
Mouse IgG	HRP	Goat	1:25000	Promega V4021	Western Blot
Rabbit IgG	HRP	Goat	1:25000	Promega V4011	Western Blot

Table M3 qPCR primers:

Gene	Forward primer	Reverse primer	Probe #
Cadherin1	ATCCTCGCCCTGCTGATT	ACCACCGTTCTCCTCCGTA	18
Cadherin2	GCCATCATCGCTATCCTTCT	CCGTTTCATCCATACCACAAA	18
Eomes	ACCGGCACCAAACTGAGA	AAGCTCAAGAAAGGAAACATG	9
Esrrb	CGATTCATGAAATGCCTCAA	CCTCCTCGAACTCGGTCA	89
Fgf5	AAAACCTGGTGCACCCTAGA	CATCACATTCCCGAATTAAGC	29
Fgfr2	CCTGCGGAGACAGGTAACAG	CGGGGTGTTGGAGTTCAT	17
Gata2	CACAAGATGAATGGACAGAACC	ACAGGTGCCCGCTCTTCT	75
Gata6	GGTCTCTACAGCAAGATGAATGG	TGGCACAGGACAGTCCAAG	40
Gli1	CAGGGAAGAGAGCAGACTGAC	CGCTGCTGCAAGAGGACT	84
Id1	TCCTGCAGCATGTAATCGAC	GGTCCCGACTTCAGACTCC	78
Id2	GACAGAACCAGGCGTCCA	AGCTCAGAAGGGAATTCAGATG	89
Klf4	CGGGAAGGGAGAAGACACT	GAGTTCCTCACGCCAACG	62
Ascl1	TCTCCTGGGAATGGACTTTG	CGTTGGCGAGAAACACTAAAG	74
Atoh1	TGCGATCTCCGAGTGAGAG	CTCTTCTGCAAGGTCTGATTTTT	69
Msx1	CAGAGTCCCCGCTTCTCC	GTCTTGTGCTTGCGTAGGG	20
Ncam1	GATTTCCAGAGCCCACCAT	CGGAGCTGTCACTCACTGAA	69
Nanog	CCTCCAGCAGATGCAAGAA	GCTTGCACTTCATCCTTTGG	25
Pou5f1	GTTGGAGAAGGTGGAACCAA	CTCCTTCTGCAGGGCTTTC	95
Pax3	AAAAGGCTAAACACAGCATCG	CAATATCGGAGCCTTCATCTG	110
Pax7	GGCACAGAGGACCAAGCTC	GCACGCCGGTTACTGAAC	85
Shh	ACCCCGACATCATATTTAAGGA	TTAACTTGTCTTTGCACCTCTGA	32
Sox1	GTGACATCTGCCCCCATC	GAGGCCAGTCTGGTGTCAG	60
Sox9	GAAGCTGGCAGACCAGTACC	GGTCTCTTCTCGCTCTCGTTC	75
T	ACTGGTCTAGCCTCGGAGTG	TTGCTCACAGACCAGAGACTG	27
TBP	GGGGAGCTGTGATGTGAAGT	CCAGGAAATAATTCTGGCTCA	97

Tcf15	GTGTAAGGACCGGAGGACAA	GATGGCTAGATGGGTCCTTG	104
Twist1	GAGCAACAGCGAGGAGGA	CGACTGCTGCGTCTCTTG	66
Wnt1	TACTGGCACTGACCGCTCT	CTTGGAATCCGTCAACAGGT	25
Zeb1	GCCAGCAGTCATGATGAAAA	TATCACAATACGGGCAGGTG	48
Zeb2	CAAGAGGCGCAAACAAGC	TGCGTCCACTACGTTGTCAT	79
Zfp521	AAGCAAGCGAAACCGAGAT	TTCTGGCCTCTTCTTGCAGT	16

Table M4 cloning primers:

Name	Sequence	Comments
FKBPflg-f	TT**GATATC**ATGACAGGGAGCACAGGAAGT**ATGGATTACAAGGATGACGATG**	FKBP common forward primer. In bold EcoRV site and the Flag sequence
E47-CAG-fl-r	CATGGC**GGCC**GC**TCATCA**CAGGTGCCCGGCTGGGTTGTG	E47 reverse primer for FKBP Twist1-E and FKPB Tcf15-E plasmids. In bold NotI sequence and the 2 stop codons, reverse complemented
Twist1-CAG-r	CATGGC**GGCC**GC**TCATCA**GTGGGACGCGGACATGGACCAGGC	Twist1 reverse primer for FKBP Twist1 plasmid. In bold NotI sequence and the 2 stop codons, reverse complemented
TcF15-CAG-r	CATGGC**GGCC**GC**TCATCA**TCGCCGAGGCCCTCGGAGCGGG	Tcf15 reverse primer for FKBP Tcf15 plasmid. In bold NotI sequence and the 2 stop codons, reverse complemented
NeuroD1-CAG-r	CATGGC**GGCC**GC**TCATCA**ATCGTGAAAGATGGCATTAAGC	Neurod1 reverse primer for FKBP Neurod1 and FKBP Neurod1-Neurod1 plasmids. In bold NotI sequence and the 2 stop codons, reverse complemented
PP015-ISHf	CCCTGGCAAGCAGTTCAGTCC	Forward primer for Twist1 In Situ Hybridization probe, in the 3' UTR

PP016-ISHr	ACCATACTTCCTCTGAAGGAA	Reverse primer for Twist1 In Situ Hybridization probe, in the 3' UTR
PacI-fl-Twist1-f	CATG**TTAATTAA**ATGGATTACAAGGATGACGATGACAAGACAGGTAGT**ATGATGCAGGACGTGTCCAGC**	Forward primer for generation of a Twist1 coding amplicon containing a PacI site for subcloning into NEB193 plasmid. In bold Pac1 site and the beginning of Twist1
BatXI-AgeI-Twist1-r	CATGCCA**ACCGGT**TGG**CTAGTGGGACGCGGACATGGACCAG**	Reverse primer for generation of a Twist1 coding amplicon containing a AgeI site for subcloning into NEB193 plasmid. In bolt the AgeI site and the end of Twist1 reverse complemented
SL223_recTw1F	CTCCTCTGCTCTACCCTCCCCCGTCCCGGCTCCGCGAGGCCGCACGTCGCCGCCCGCGAG**ATGGATTACAAGGATGACGAT**	Forward primer to generate BAC modification, containing 60 nt of Twist1 genomic locus. In bold the first 21 nt of the Flag
SL224_recTw1R	TCCCTGGAGCCGGTCCTTACCTAGGTCTCCGGCCTGCAGAGGGGGTGGGGAGCTCCGCTG**GAATTCGAGCTCGGTACCCGG**	Reverse primer to generate BAC modification, containing 60 nt of Twist1 genomic locus. In bold the last 21 nt of the NEB-Twist construct finishing with the last Frt site, reverse complemented.
SeqRepTwBac350 f	GGGAAGCTGGCGGGCTAGGGC	Forward primer for modified BAC colony PCR recognizing the Twist1 locus up to 6 nt before the start of the 60 nt flanking sequence in the primer SL22_recTw1F.
SeqTw r	CTAGTGGGACGCGGACATGGA	Reverse primer for modified BAC colony PCR recognizing the end of Twist1 coding up to the stop codon, reverse complemented.
SeqRepTwBAC350 r	AACAGGGGACCCGCGGCCTGG	Reverse primer for modified BAC colony PCR recognizing the Twist1

		locus up to 9 nt after the end of the 60 nt flanking sequence in the primer SL224_recTw1R, reverse complemented
A2RF	TGCTAACCCCACATCCTTCT	Recognizes a region close to the end of the selection cassette; designed by Aliaxandra Radzisheuskaya
PP007Twretrieve5	TGAGTCACTCACTGTTAAACTCTCACTGGTATTGTGTTTTTCATAATATCCCCTGATACTC**CTCGAG**GTCACCATCCTGTCGGCTGTG	Forward primer for generation of a retrieval construct from pACYC177 plasmid. In bold is the Xho1 site; underscored is the homology sequence with the pACYC177. See M1.3.3.4 for further details
PP008Twretrieve3	TAAGACTCAGAATTAACTTGGTGGTAAATACTTGTTTGTTTAACTCTAGGGGCATCTAGGACTCACTTTCTGGCTGGATGATG	Reverse primer for generation of a retrieval construct from pACYC177 plasmid. Underscored is the homology sequence with the pACYC177. See M1.3.3.4 for further details

III. RESULTS 1

TWIST1 A PUTATIVE REGULATOR OF NEURAL DIFFERENTIATION

R1.1 Overview

Inhibition of BMP signalling is the key requirement for the progression towards neural differentiation both *in vivo* and *in vitro* [Munoz-Sanjuan and Brivanlou, 2002; Ying et al, 2003a]. Furthermore, BMP downstream target, ID1 is able to replace BMP in blocking neural differentiation *in vitro* [Ying et al, 2003a]. However, our understanding of neural fate regulation by BMP/ID has yet not progressed any further.

Dr Sally Lowell has been interested in finding out what are the signalling pathways affected by IDs in blocking neural differentiation. To this end, Dr Owen Davies, in her lab, performed a Yeast-2-Hybrid assay on a mouse ES cell cDNA library. He found that at the highest stringency level ID1 interacts only with E12 and E47, the two splice variants of *Tcf3* gene [previously known as E2A]. When he then asked, which are the binding partners of these two latter proteins, besides IDs, he found only 3 other proteins TWIST1, TCF15 and NEUROD1; all bHLH factors.

Microarray data, as well as our lab unpublished data showed that *Twist1* is expressed at low levels in ES cells and its expression increases during neural differentiation [Aiba et al., 2009; Lowell lab unpublished data]. *Tcf15* is expressed at higher levels in ES cells, but its expression is downregulated in early stages of differentiation [Aiba et al., 2009; Lowell lab unpublished data]. *Neurod1* is a known neural bHLH factor. However, its action has been reported on later stages, being downstream of *Neurogenin1* [Ma et al, 1996; Talikka et al, 2002]. Taking into consideration these reasons, I inferred that *Twist1* is the candidate gene with the highest chances of being involved in regulating the early stages of neural differentiation.

In this chapter I present evidence for *Twist1* expression in pluripotent and differentiating cell compartments. Furthermore, I test the influence of an ID resistant TWIST1 active form on neural differentiation. Finally, I investigate the requirement for *Twist1* in the process of neural differentiation

R1.2 *Twist1* Marks The Primed Pluripotent Cell Compartment.

Before testing the role of TWIST1 on differentiation I asked the question of its expression in the pluripotent compartment. As stated previously, *Twist1* is upregulated during the transition from ES cells maintained in LIF and Serum, towards neural differentiation. However, *Twist1* expression in the pluripotent compartment was less studied.

To address this point I used the Oct4-GIP cell line produced in the lab of Prof. Austin Smith [Ying et al, 2002]. In this cell line GFP-Ires-Puro is expressed downstream of the *Pou5f1* promoter in a randomly integrated construct. Culturing this cell line, under Puromycin selection, eliminates differentiated cells and, thus removes the confounding issue represented by high expression of differentiation markers in a small number of cells within an ES cell population. For this experiment I compared ES cells, established in 2i conditions, cultured in LIF and Serum or established in EpiSC condition (this cell line has been established in EpiSC conditions by Rodrigo Osorno). *Twist1* expression was compared with the expression of *Fgf5*, a known epiblast stem cell marker. I found that for both *Twist1* and *Fgf5* expression increases from 2I to LIF-Serum to EpiSC conditions [**Fig R1.1**]. However, while for *Fgf5* the most dramatic increase was found between LIF-Serum and EpiSC, over 100 fold [Fig R1.1b and c], for *Twist1* the major increase was between 2I to LIF-Serum almost 50 fold, with a minor further increase to EpiSC [**Fig R1.1a**]. Thus it appears that *Twist1* is most notably upregulated when pluripotent cells are released from the ground state.

Figure R1.1. *Twist1* marks the primed ES cell population.

qPCR for *Twist1* (a) and *Fgf5* (b and c) for pluripotent cells maintained in 2i conditions, ES standard conditions (LIF + Serum) and EpiSC conditions. Expression in 2i has been arbitrarily set to 1. One experiment performed in duplicates is shown. Error bars represent value range.

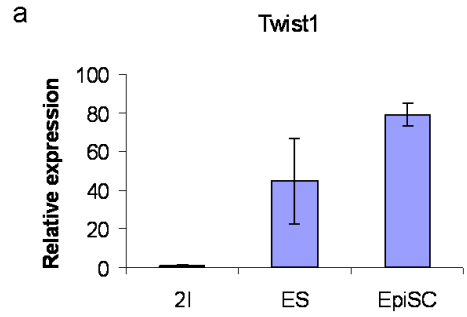
a
Twist1
Relative expression
100
80
60
40
20
0
2I
ES
EpiSC

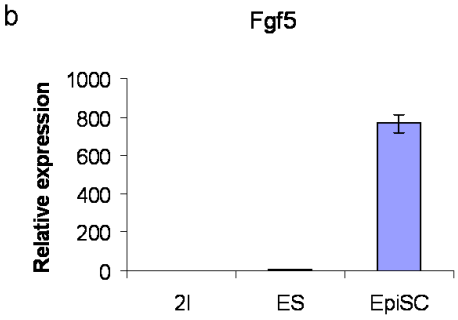
b
Fgf5
Relative expression
1000
800
600
400
200
0
2I
ES
EpiSC

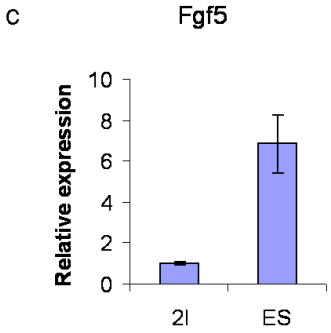
c
Fgf5
Relative expression
10
8
6
4
2
0
2I
ES

R1.3 *Twist1* Is Associated With The Neural Differentiating Population.

Although *Twist1* is upregulated during *in vitro* neural differentiation, it was not thought to be associated *in vivo* with early neural progenitors, but rather it was considered a mesenchymal marker [Soo et al., 2002]. Since neural differentiation *in vitro* is never a perfectly controlled process there is a possibility that *Twist1* upregulation follows its expression in non-neural differentiating cells which are usually present in the culture.

To test for this possibility a Sox1-GFP reporter cell line, called 46c [Ying et al, 2003b] was used. 46c cells were differentiated for 4 days in the monolayer protocol, sorted based on GFP and gene expression assessed by qPCR. (Differentiation, sorting and RNA extraction, for this experiment, were performed by Ms. XinZhi Zhou.)

Zfp521 is a transcription factor shown to be upstream of *Sox1* in neural differentiation [Kamiya et al, 2011] and, is used here along *Sox9,* an early neural and neural crest marker [Cheung and Briscoe, 2003], as control of the neural differentiation. On the other hand, *Gata6* a marker of endoderm and some mesodermal cells [Molkentin J.D., 2000; Fletcher et al, 2006] should not be upregulated during neural differentiation. As expected *Zfp521* and *Sox9* are upregulated in the *Sox1*-high population, compared to *Sox1*-low population, while *Gata6* was expressed at similar levels in both populations indicating that endoderm is not a major route taken by cells which differentiate towards non-neural fates. Furthermore for *Twist1* a small but significant upregulation in the *Sox1*-high population was observed. This result shows that *Twist1* is not preferentially upregulated by non-neural differentiating cells and, supports the idea that *Twist1* could have a role in neural differentiation. *Gata6* was expressed at similar levels in both populations indicating that endoderm is not a major route taken by cells which differentiate towards non-neural fates [**Fig R1.2**].

Figure R1.2. *Twist1* is associated with *Sox1* high population.

qPCR for *Zfp521* (a), *Sox9* (b), *Gata6* (c) and *Twist1* (d) in 46c cells differentiated in N2B27 for 4 days and GFP sorted (XinZhi Zhou). *Twist1* is upregulated in *Sox1* high population along other neural associated markers: *Zfp521* and *Sox9*. On the other hand the primitive endoderm marker *Gata6* is not differentially regulated between samples, indicating that non-neural cells do not progress via an endoderm route. Expression in *Sox1* low samples has been arbitrarily set to 1. For *Zfp521, Sox9* and *Gata6* one experiment performed in duplicates is shown. Error bars represent value range. For *Twist1* triplicate experiment performed in duplicates is shown. Error bars represent standard deviation of the mean; $p = 0.03$. Two qPCR analyses were performed by XinZhi Zhou.

a

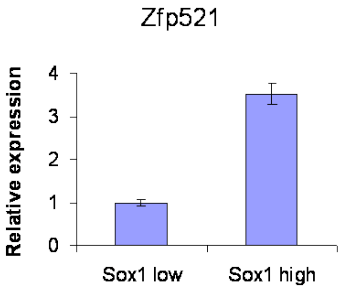
Zfp521
Relative expression
4
3
2
1
0
Sox1 low
Sox1 high

b

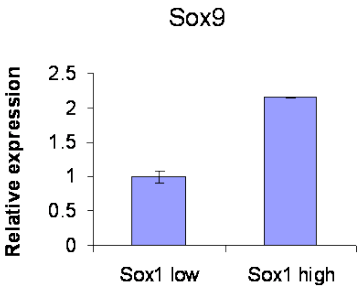
Sox9
Relative expression
2.5
2
1.5
1
0.5
0
Sox1 low
Sox1 high

c

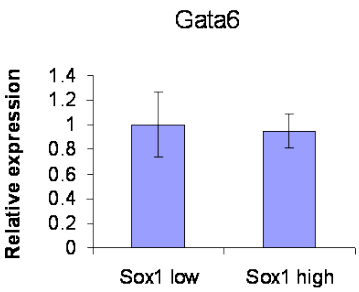
Gata6
Relative expression
1.4
1.2
1
0.8
0.6
0.4
0.2
0
Sox1 low
Sox1 high

d

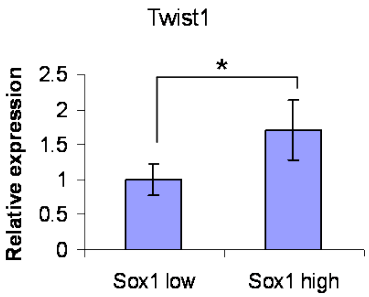
Twist1
*
Relative expression
2.5
2
1.5
1
0.5
0
Sox1 low
Sox1 high

R1.4 Generating TWIST1 Inducible Cell Lines

As it has been previously reported ID proteins bind E proteins and sequester the latter from forming binding partners with other bHLH factors [Jen et al, 1992; Kurabayashi et al, 1994; Peverali et al, 1994]. In the case of TWIST1 the unavailability of E proteins shifts dimer choice probability towards formation of TWIST1-TWIST1 homodimers [Connerney et al, 2006]. Thus TWIST1-E dimers activity would mimic a molecular status of low ID while TWIST1-TWIST1 dimers would mimic a status of high ID activity. A theoretical model of TWIST1 dimer formation in the process of neural and non-neural differentiation is presented in **Fig R1.3.**

In order to investigate the role of TWIST1 and its dimer choice on cell differentiation I set out to generate cell lines with inducible tethered dimers by means of a flexible linker, which have a low sensitivity for competing interactors [Connerney et al, 2006]. **Fig R1.4** explains schematically the strategy of using inducible TWIST1 constructs to dissect the effects of dimmer choice. When TWIST1 monomer is induced it forms dimers with E proteins if they are available. However, if IDs are present at significant levels they sequester the E proteins and TWIST1 forms homodimers. The formation of either dimer results in the activation of its specific target genes [**Fig R1.4a**]. By contrast, if TWIST1 forced homodimer (TwTw) is induced it activates its target genes even if E proteins are available [**Fig R1.4b**]. Moreover, if TWIST1-E forced dimer (TwE) is induced it activates its target genes even in the presence of ID proteins [**Fig R1.4c**]. Thus, TW-E is the active dimer to be considered in regard to the blocking activity of BMP/ID.

The first attempt of producing inducible TwE cell lines involved the FKBP system, where the protein of interest is fused to a form of FKBP1A containing a destabilizing mutation. Thus the entire transgenic construct is effectively targeted for degradation. Protein expression is achieved by treating the cells with the small molecule ligand “Shield”, which binds and masks the destabilizing domain [**Fig R1.5a**].

Figure R1.3. ID1 sequester E proteins from forming active dimers.

Theoretical model on how ID1 acting downstream of BMP can influence bHLH factors dimer choice. The case of TWIST1 is presented

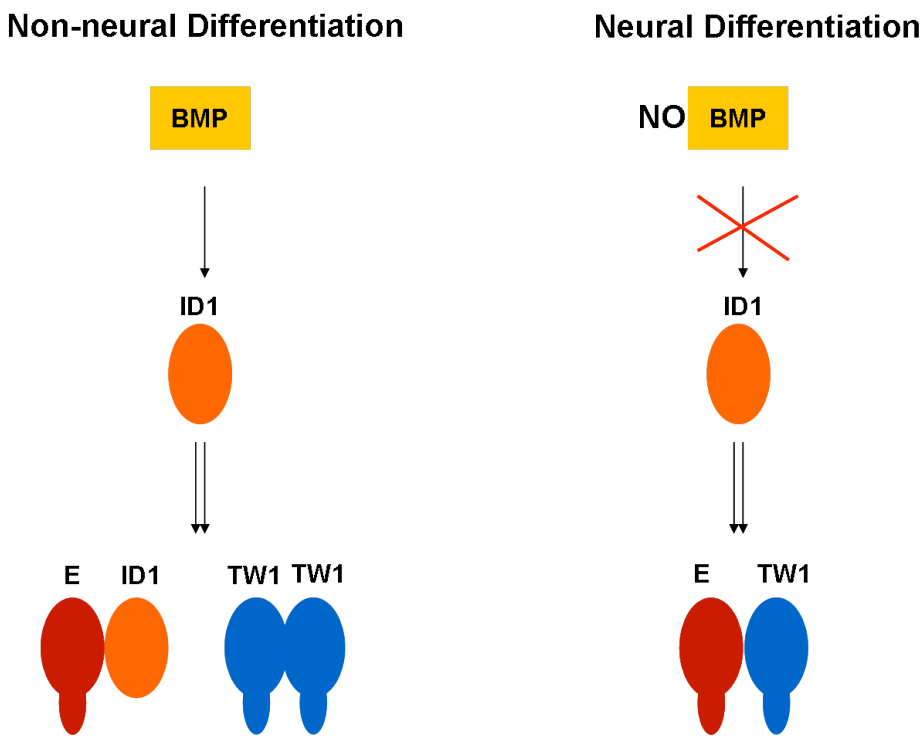
Non-neural Differentiation
BMP
ID1
E
ID1
TW1
TW1
Neural Differentiation
NO
BMP
ID1
E
TW1

Figure R1.4. Schematics of TWIST1 inducible constructs transcriptional activity

Formation of TW-E or TW-TW active dimers results in transcriptional regulation of their respective genes. Induction of TwE or TwTw forced dimers is resistant to dimer choice regulation depending on presence/availability of E or ID proteins.

a

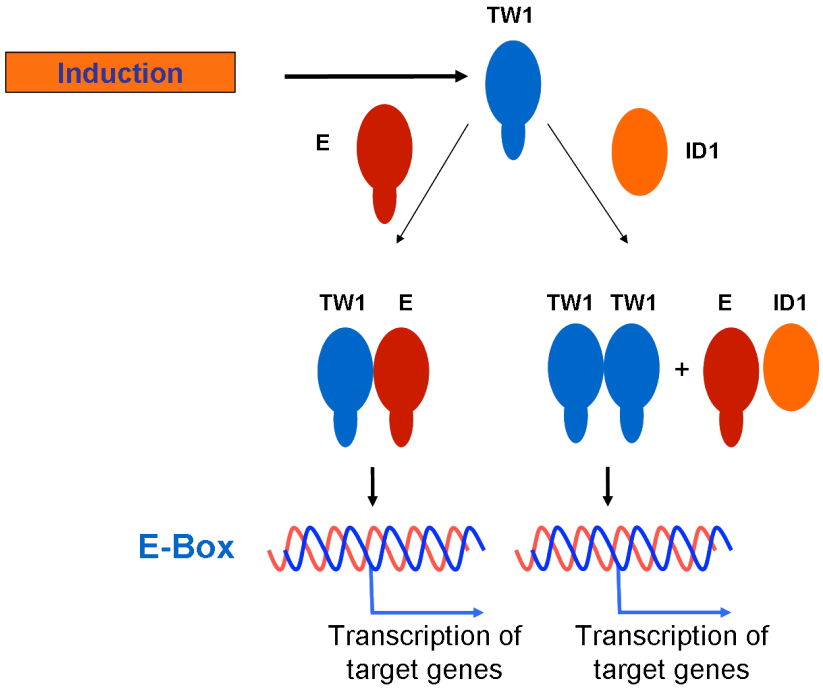
Induction
TW1
E
ID1
TW1 E
TW1 TW1 E ID1
+
E-Box
Transcription of target genes
Transcription of target genes

b

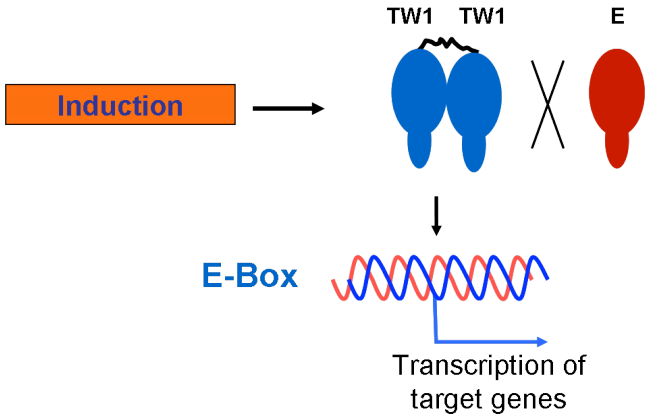
Induction
TW1 TW1
E
E-Box
Transcription of target genes

c

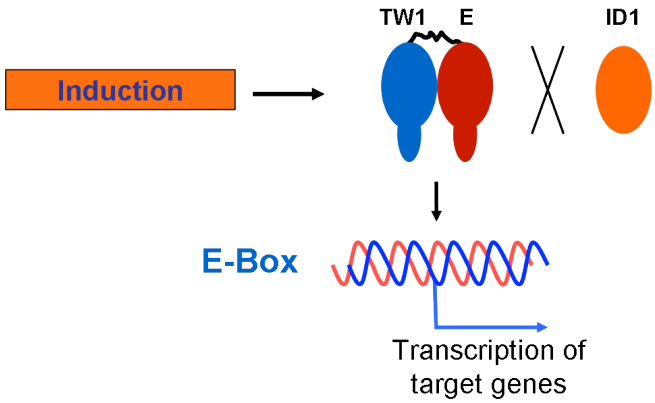
Induction
TW1 E
ID1
E-Box
Transcription of target genes

Figure R1.5. Strategy for conditional control of protein stability

DD = destabilizing domain, here FKBP1A-L106P, POI = protein of interest, here TwE, ligand = small molecule with affinity for DD, here Shield (adapted from Banaszynski at al, 2006) (a). Flag staining of cells transfected with FKBP constructs and induced with Shield for 24 hours. Positive cells could be obtained in transient transfections for TWIST1 monomer and TwE but not for TWIST1 stably transfected cells. However, other constructs, like HES1, can generate inducible cells stably transfected (b). Scale bars represent 50 μm.

a

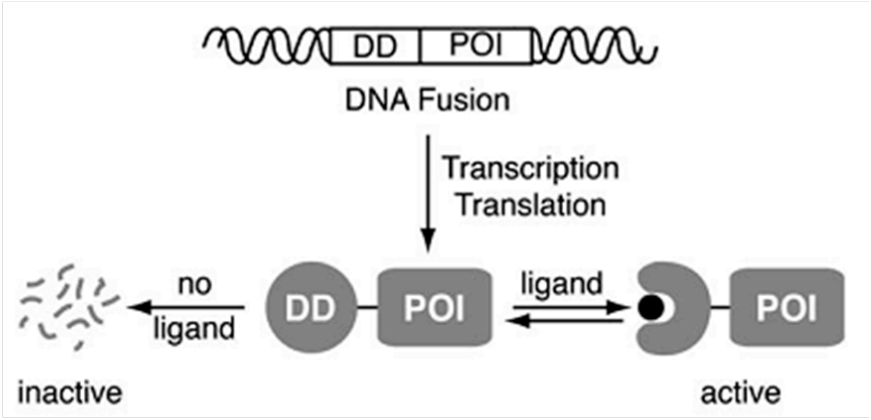

b

Flag stainig after Shld induction

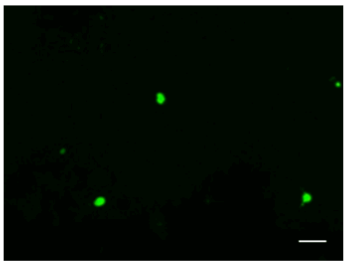

Transient FKBP-Tw

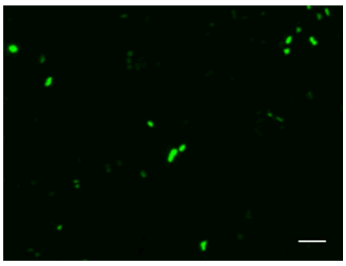

Transient FKBP-TwE

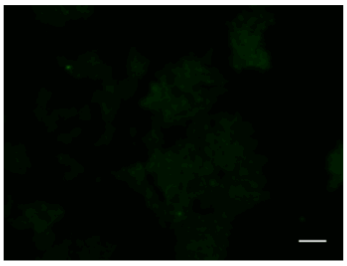

Stable FKBP-Tw

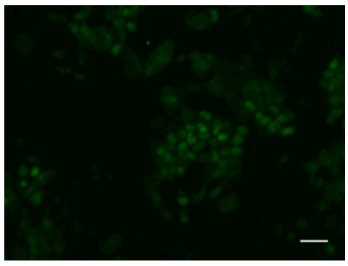

Stable FKBP-Hes1

However, using this strategy no clones expressing the protein of interest could be isolated. Expression could be elicited in transient transfection experiments indicating that the construct was functional [**Fig R1.5b**]. I considered that the most likely explanation was that the transgene was detrimental for cell proliferation in self renewal conditions, while the degradation mechanism was probably not efficient enough to remove the active protein before exerting its effects.

To address this problem I employed a different strategy, where the construct of interest was expressed under the CMV-TetO promoter and transfected into ES cells where the rtTA2^{S}-M2 construct [Urlinger et al, 2000] had been targeted to the Rosa-26 locus. Diagram of the strategy is presented in **Fig R1.6**. rtTA targeted ES cells were a kind gift of Dr. Andrew Smith.

Using this strategy it was possible to isolate clones capable of inducing the TwE transgene, though some of them retained the Puromycin selection cassette while losing TwE. Furthermore, the expression was heterogeneous for all the clones isolated. **Fig R1.7** shows induction at the RNA level [**Fig R1.7a**], Flag immunofluorescence [**Fig R1.7b**] and western blot [**Fig R1.7c**].

R1.5 TwE Accelerates *In Vitro* Neural Differentiation.

When TwE was induced during neural differentiation a striking effect could be observed in the form of premature formation of post-mitotic neurons. Thus, at day3 of differentiation, when TUBB3 just begins to be expressed, by a few cells in the control conditions, it can be observed in a high proportion of the cells in TwE induced sample, taking the shape of long interconnecting neurites [**Fig R1.8**].

While early formation of post-mitotic neurons was striking and unexpected, it could not be considered as an indication that TwE favours neural induction. One possibility was that TwE was only inducing exit from the neural progenitor state.

Figure R1.6. Schematics of Doxycyclin inducible system

Model of the system: Rosa26 = genomic locus constitutively active. rTetR-VP16 = reverse Tet Repressor fused with viral VP16 activator domain. Tet Repressor element is revered in the sense that it was mutated so that its product binds to the TetO sequence only in the presence of Doxycyclin. rtTA = reverse tetracycline controled Trans Activator, the product of rTetR-VP16 element [Urlinger et al, 2000] (a). Diagram of TwE Doxycyclin inducible construct and plasmid (b and c respectively).

a

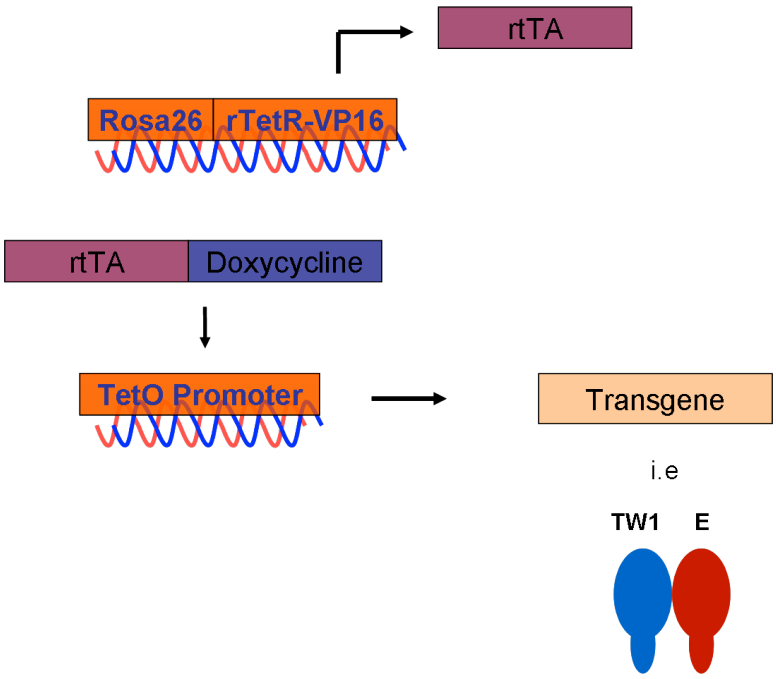
rtTA
Rosa26
rTetR-VP16
rtTA
Doxycycline
TetO Promoter
Transgene
i.e
TW1
E

b


PGK
Puro
pA
CMV-TetO
Flag
Twist1
linker
E47
pA

c

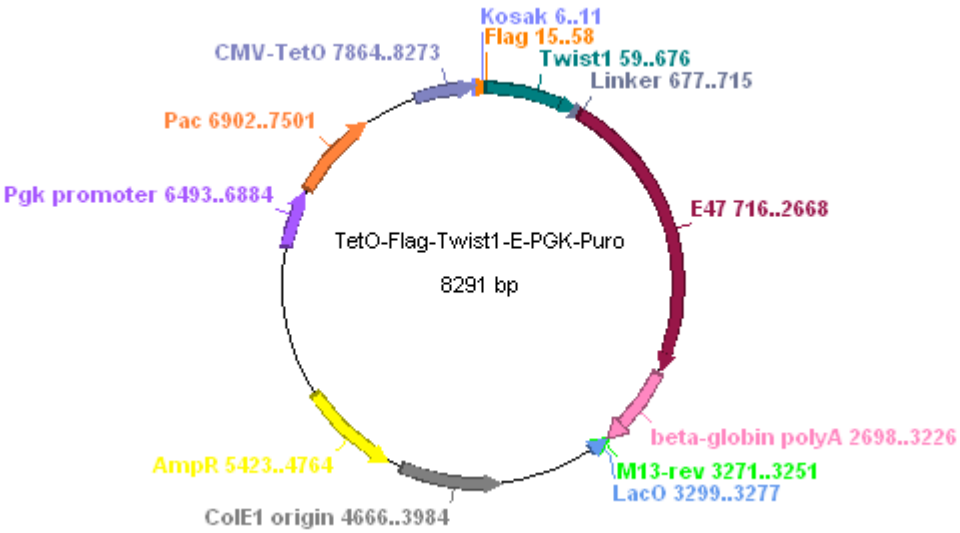
Kosak 6..11
Flag 15..58
Twist1 59..676
Linker 677..715
CMV-TetO 7864..8273
Pac 6902..7501
Pgk promoter 6493..6884
E47 716..2668
TetO-Flag-Twist1-E-PGK-Puro
8291 bp
beta-globin polyA 2698..3226
M13-rev 3271..3251
LacO 3299..3277
AmpR 5423..4764
ColE1 origin 4666..3984

Figure R1.7. Characterization of TwE inducible cell lines

qPCR showing expression of *Twist1* after 48 hours of induction compared to uniduced samples or control non-transfected cells. Expression in parental cell line has been arbitrarily set to 1. One experiment performed in duplicates is shown. Error bars represent value range (a). Immunofluorescence for Flag staining after 48 hours of induction showing typical heterogeneous expression; scale bars represent 50 μm (b). Western blot for 3 clones showing induction of the transgene in clone doTE53 and doTE77 (c).

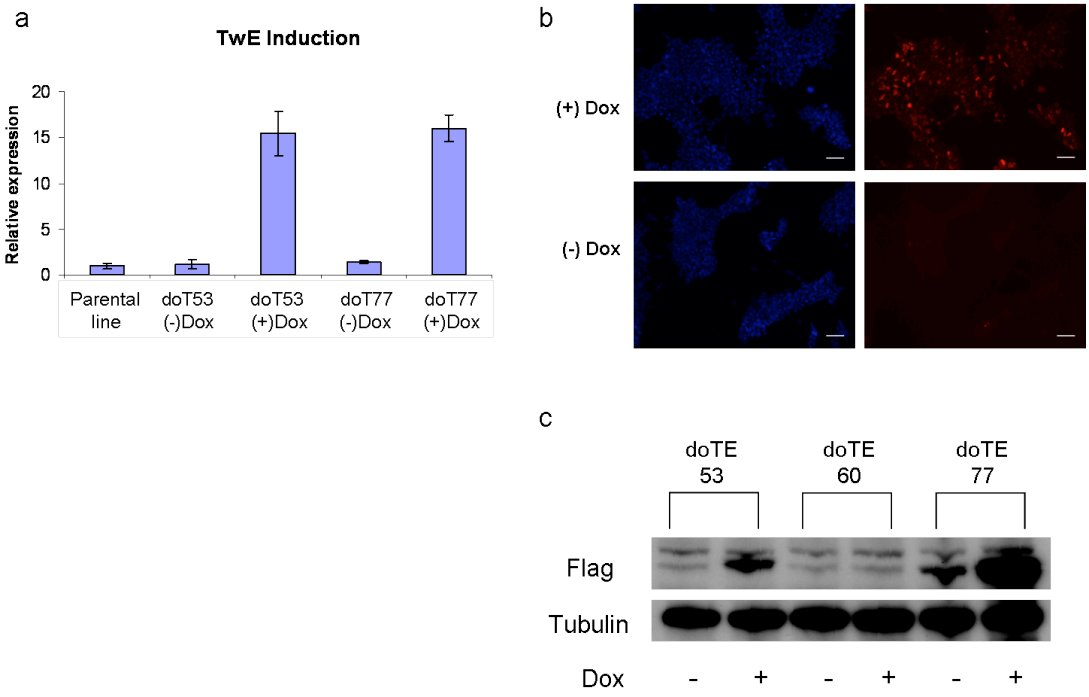
a
TwE Induction
Relative expression
20
15
10
5
0
Parental line
doT53 (-)Dox
doT53 (+)Dox
doT77 (-)Dox
doT77 (+)Dox
b
(+) Dox
(-) Dox
c
doTE 53
doTE 60
doTE 77
Flag
Tubulin
Dox
- + - + - +

Figure R1.8. TwE induces rapid formation of mature neurons

After three days of monolayer neural differentiation in N2B27 TUBB3 positive cell just began to be observed in control –Dox, while being well represented in TwE induced +Dox. Upper panels: phase contrast, lower panels: TUBB3 staining. Scale bars represent 50 μm.

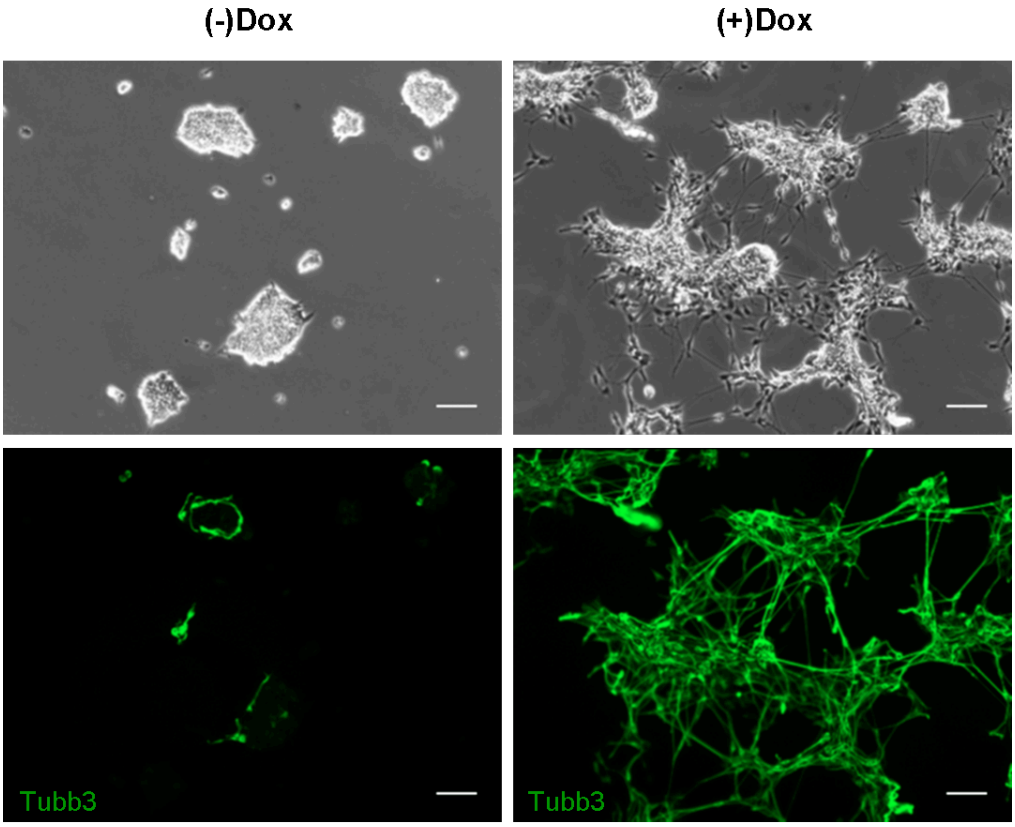

Day 3 of differentiation

Two markers: *Sox1* and *Sox2* could provide useful insights regarding this issue. *Sox1* marks neural progenitor cells both *in vivo* and *in vitro* [Wood & Episkopou, 1999; Ying et al., 2003b]. *Sox2* is expressed throughout the epiblast before gastrulation, but then, is restricted to anterior ectoderm. At the start of somitogenesis, just like *Sox1, Sox2* specifically marks the neural progenitors [Wood & Episkopou, 1999]. During *in vitro* differentiation, at day 4, SOX2 was still strongly expressed by control cells, while in TwE induced it was downregulated already at day 3 and was almost undetectable at day 4 [**Fig R1.9**].

Next, *Sox1* was assessed at the mRNA level. Similar to SOX2, *Sox1* is downregulated prematurely in response to TwE. Interestingly, *Sox1* is also upregulated earlier in TwE induced samples, indicating a possible facilitation of neural induction [**Fig R1.10c**]. However, the upregulation at day 2 is not statistically significant across three experiments, while downregulation at days 4 and 5 is. Increasing the n of repeat experiments could provide statistical significance at day 2 as well, but the present data may indicate that the later downregulation is a more robust phenomenon. *Zfp521* is an early neural transcription factor, reported to act upstream of *Sox1*. There is a trend for its upregulation at all time points in response to TwE, but the differences are not statistically significant [**Fig R1.10b**]. Furthermore the pluripotency marker *Pou5f1* is abruptly downregulated in the presence of TwE, although for this marker more repeat experiments are required in order to assert statistical significance [**Fig R1.10a**].

Nestin is another neural progenitor marker. In the control population it begins to be upregulated at day 4 and, at day 5 produces a strong signal by immunofluorescence. In the TwE induced cells it was slightly upregulated in a few cells at day 3 [Fig R1.11a yellow arrows], however the later upregulation on days 4 and 5 is curbed in this condition [Fig R1.11b and c].

In summary, the data presented here supports the idea that TwE accelerates neural differentiation and forces cellular exit from the neural progenitor state. There is also some indication that TwE facilitates entry in the process of neural differentiation, as shown by a trend of early upregulation of *Sox1*.

Figure R1.9. TwE induction leads to premature downregulation of pluripotent and neural progenitor cell marker SOX2.

Four days of monolayer neural differentiation in N2B27; no Dox induction Day 3 (a) and Day 4 (c), Dox induction Day3 (b), Day 4 (d). From left to right panels represent: phase contrast, DAPI, TUBB3 staining, SOX2 staining. Scale bars represent 50 μm.

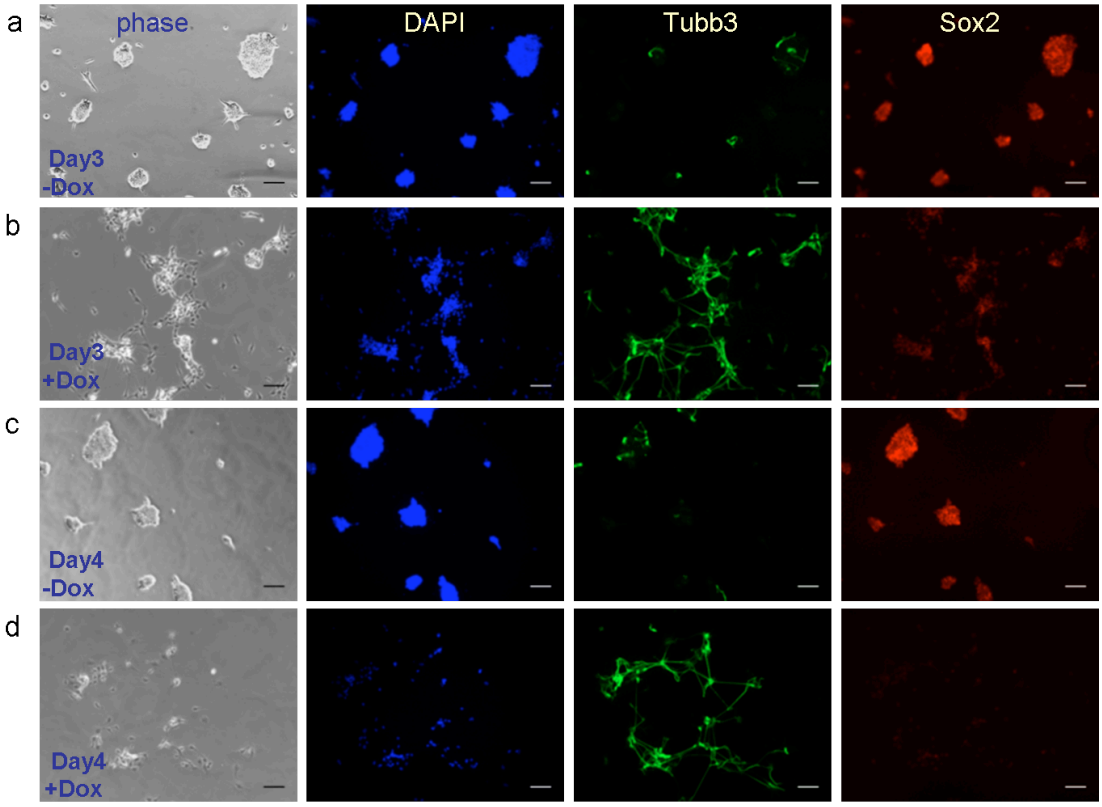
a
phase
DAPI
Tubb3
Sox2
Day3
-Dox
b
Day3
+Dox
c
Day4
-Dox
d
Day4
+Dox

Figure R1.10. TwE accelerates progenitor dynamics during neural differentiation.

qPCR of cells after 4 days of monolayer differentiation in N2B27; *Pou5f1* (a), *Zfp521* (b) and *Sox1* (c). Expression in ES cells has been arbitrarily set to 1. For *Pou5f1* one experiment performed in duplicates is shown. Error bars represent value range. For Zfp521 and Sox1 triplicate experiments performed in duplicates are shown. Error bars represent standard deviation of the mean. For Sox1 at day 3 $p = 0.02$ and at day 4 $p = 0.008$.

a

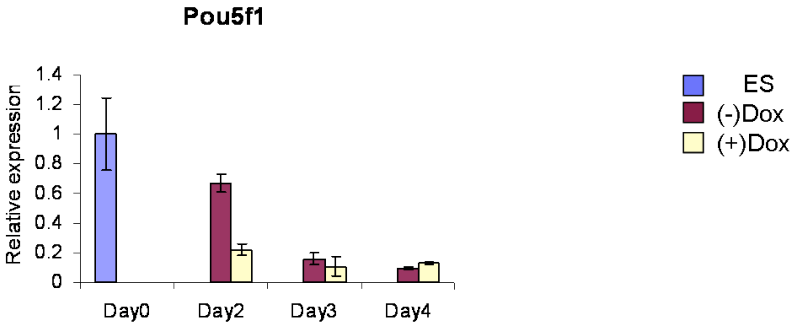
Pou5f1
Relative expression
1.4
1.2
1
0.8
0.6
0.4
0.2
0
Day0
Day2
Day3
Day4
ES
(-)Dox
(+)Dox

b

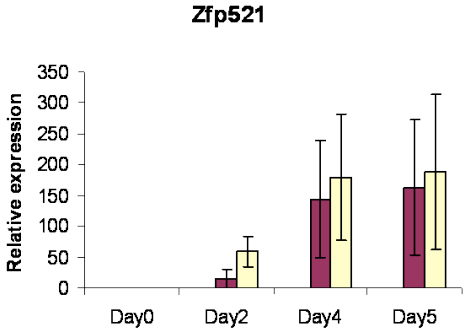
Zfp521
Relative expression
350
300
250
200
150
100
50
0
Day0
Day2
Day4
Day5

c

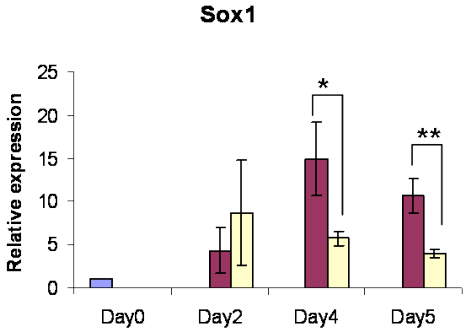
Sox1
Relative expression
25
20
15
10
5
0
*
**
Day0
Day2
Day4
Day5

Figure R1.11. TwE induction negatively influences the upregulation of NESTIN.

Five days of monolayer differentiation in N2B27; no Dox induction left panels, Dox induction right panels, DAPI and NESTIN staining. Day3 (a), Day4 (b) and Day 5 (c). Scale bars represent 50 μm.

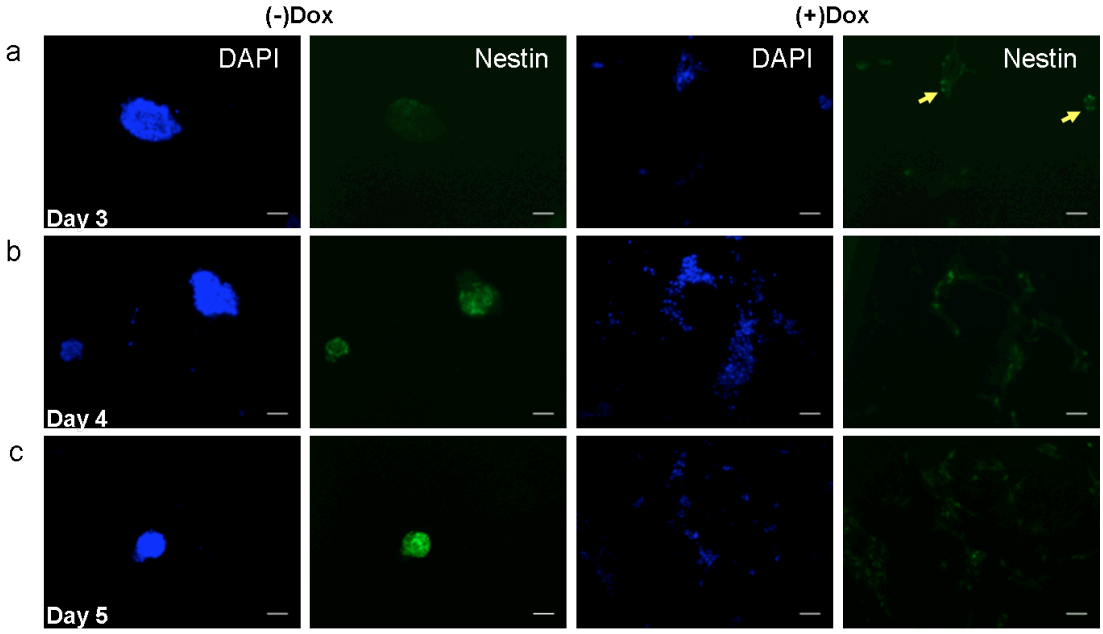
(-)Dox
(+)Dox
a
b
c
DAPI
Nestin
DAPI
Nestin
Day 3
Day 4
Day 5

R1.6 TwE Acts Early on Neural Differentiation.

In the previous sections I showed that TwE influences neural differentiation. However, the evidence to support the notion of TwE acting at the initial stages of neural differentiation is less compelling. To clarify this point an experiment was designed concentrating at the early events of differentiation. Thus, control cells are plated in N2B27 at what is considered to be Day 0 of neural differentiation, similar with previous experiments. To test TwE early roles the transgene was induced with Dox 24 hours prior to differentiation (Day -1), while cells were maintained in ES cell conditions, LIF and Serum. Thus, at Day 0 when differentiation began cells were already expressing the transgene. Dox was maintained for the first 24 hours of differentiation (Day 1) after which it was removed. This condition is compared to Dox stimulation throughout the experiment Day 0 to Day 5 and –Dox control [**Fig R1.12a**].

First, it was tested that the upregulation and downregulation dynamics of the transgene corresponds to the desired features of the experiment. Thus, 24 hours after removal of Dox there was no expression of the transgene either at the RNA [**Fig R1.12b**] or protein level [**Fig R1.12c**]. Furthermore, upregulation dynamics shows that the protein reaches maximum level after 24 hours of induction [**Fig R1.12c**], the time when differentiation began.

Sox1 was upregulated at the highest levels at Day 2 by the early Dox stimulation, while, in these conditions, subsequent downregulation was mitigated, the expression reverting to control levels by day 5. In contrast, Dox stimulation throughout differentiation produced a more modest upregulation of *Sox1* at Day 2 followed by a marked downregulation at later time points [**Fig R1.13a**]. Thus, it appears that TwE action is biphasic: first it facilitates entry to neural differentiation and upregulation of *Sox1* and subsequently, hastens the exit from neural progenitor state, a phenomenon which correlates with *Sox1* downregulation.

Zfp521 was maximally upregulated at Day 2 in early Dox condition as well. However, at later time points it reverted to control level, in the case of early

treatment, while being upregulated by continuous Dox induction [**Fig R1.13b**]. This would indicate that *Zfp521* expression above the control levels is dependent on the transgene at all time points.

Pax3 is expressed in vivo in a subset of dorsal neural progenitors and future neural crest cells [Goulding et al, 1991]. In the present *in vitro* experiment it started to be upregulated at Day 3 of neural differentiation. Interestingly, TwE induction stimulated an early upregulation at Day 2, followed by block of high level upregulation at the later time points. Moreover, at Day2, *Pax3* was maximally upregulated by early Dox treatment. The upregulation at later time points was further augmented by this early treatment [**Fig R1.13c**]. *Pax3* data confirms the biphasic action of TwE, as well as indicating that the transgene has opposing actions on specific markers depending on the cellular context.

Atoh1 is a more mature neural marker marginally induced in the first 5 days of monolayer neural differentiation, but highly upregulated in response to TwE. However, early Dox treatment had no positive influence on this marker upregulation, further stressing the two phase hypothesis [**Fig R1.13d**].

The experiment presented in this section complements the previous experiments, indicating that TwE is able to influence neural differentiation most notably at early time points. Furthermore, it is suggested that only certain neural features can be generated by transiently activating TwE. However, in order to assess statistical significance more repeats are required for this experiment.

Figure R1.12. TwE early induction during neural differentiation experiment

The diagram presents the three conditions used. ES cells were usually cultured in LIF + Serum and transferred to N2B27 when neural differentiation began: Day 0 (green and blue bars). For transgene induction Dox is added when cells were transferred to N2B27 (orange bar). For early induction Dox was added 24 before the start of differentiation and maintained for the first 24 hours of differentiation (pink bar), after which the cells continued to differentiate in N2B27 alone (a). qPCR for *Twist1* for cells during 5 days of monolayer differentiation in N2B27 not induced (-Dox), induced (+Dox) or induced early (+Dox early) as described. Expression in ES cells has been arbitrarily set to 1. One experiment performed in duplicates is shown. Error bars represent value range (b). Western blot for Flag, showing induction and clearance of the protein after Dox removal at the stated time points (c). For this experiment cells were maintained in Serum + LIF.

a

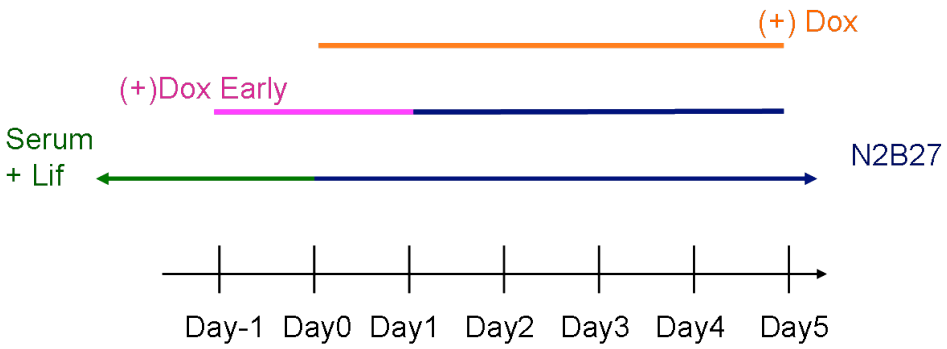
(+) Dox
(+)Dox Early
Serum
+ Lif
N2B27
Day-1
Day0
Day1
Day2
Day3
Day4
Day5

b

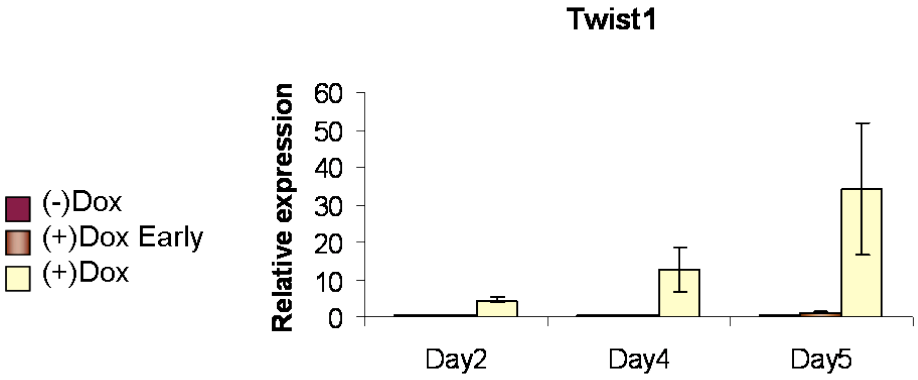
Twist1
(-)Dox
(+)Dox Early
(+)Dox
Relative expression
60
50
40
30
20
10
0
Day2
Day4
Day5

c

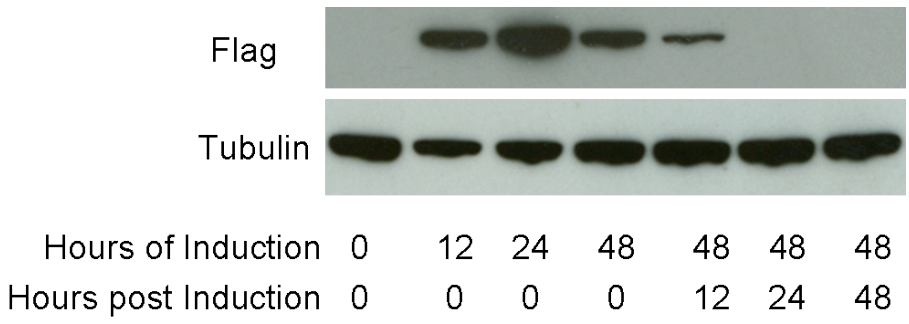
Flag
Tubulin
Hours of Induction 0 12 24 48 48 48 48
Hours post Induction 0 0 0 0 12 24 48

Figure R1.13. TwE accelerates entry to and exit from neural progenitor stage.

qPCR for early or continuous induction of TwE during neural differentiation showing early upregulation of *Sox1* (a), *Zfp521* (b) and *Pax3* (c), followed by later downregulation of *Sox1* (a), *Pax3* (b) and upregulation of *Atoh1* (d). Expression in ES cells has been arbitrarily set to 1. One experiment performed in duplicates is shown. Error bars represent value range

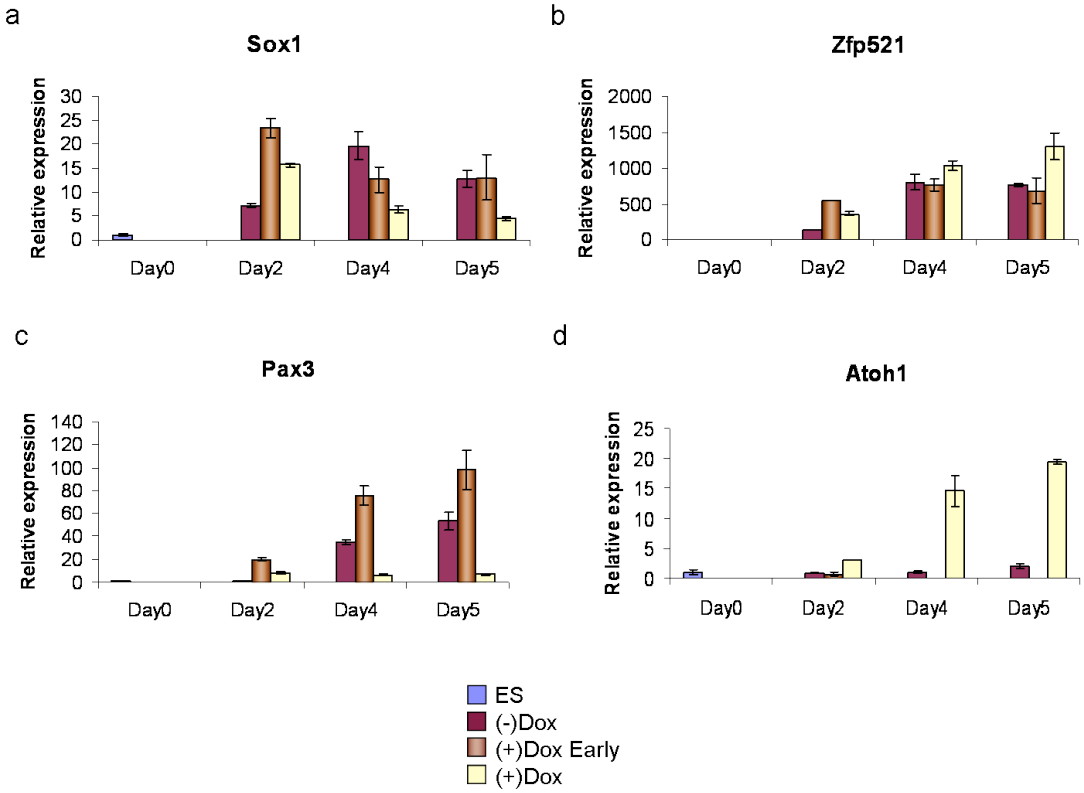
a
Sox1
Relative expression
30
25
20
15
10
5
0
Day0
Day2
Day4
Day5
b
Zfp521
Relative expression
2000
1500
1000
500
0
Day0
Day2
Day4
Day5
c
Pax3
Relative expression
140
120
100
80
60
40
20
0
Day0
Day2
Day4
Day5
d
Atoh1
Relative expression
25
20
15
10
5
0
Day0
Day2
Day4
Day5
ES
(-)Dox
(+)Dox Early
(+)Dox

R1.7 TwE and EMT during Neural Differentiation

When neural folds form, prospective neural progenitors undergo a particular form of EMT, during which CDH1 (E-cadherin) is downregulated but, the morphological epithelial characteristics are maintained. This type of EMT is dependent on *Zeb2* (also known as Sip1) and, this factor is required for neural differentiation [Sheng et al, 2003; Chnq et al, 2010].

On the other hand, TWIST1 is a known EMT effector, being involved in CDH1 downregulation in physiological and pathological processes [Hay E.D., 1995; Yang et al, 2004]. Furthermore, *Ncam1* is an adhesion molecule with a role in neural cell communication [Rutishauser et al, 1988] and neural crest migration [Breau et al., 2006]

During monolayer neural differentiation, *Zeb1*, *Zeb2* and *Ncam1* were upregulated. Upon TwE induction there was a trend of enhanced upregualtion for *Zeb1*, but this was not statistically significant. Furthemore, Zeb2 upregulation was also enhanced, and this was statistically significant across three experiments for days 3 and 4. *Ncam* upregulation was also enhanced but more repeat experiments are required for this marker in order to assess statistical significance [**Fig R1.14**]. In conclusion, TwE stimulates EMT in a fashion consistent with that observed in neural differentiation and, could act upstream of *Zeb2*.

R1.8 TwE Opposes BMP4 During Monolayer Differentiation.

In the work presented so far, I showed that TwE influences neural differentiation, that it may act both on very early stages of entry to the neural progenitor stage, as well as on later stages and that it stimulates EMT in the process. However, my central hypothesis stipulated that BMP signalling block on TW-E dimer formation is part of the process of neural inhibition. I will now investigate whether TwE can rescue the block on neural differentiation imposed by BMP4.

Figure R1.14. TwE upregulates EMT markers during neural differentiation.

qPCR of cells during 5 days of monolayer differentiation in N2B27; *Zeb1* (a), *Zeb2* (b) and *Ncam1* (c). Expression in ES cells has been arbitrarily set to 1. For *Zeb1* and *Zeb2* triplicate experiments performed in duplicates are shown. Error bars represent standard deviation of the mean. For *Zeb2* at day 3 $p = 0.02$ and at day 4 $p = 0.01$. For *Ncam1* one experiment performed in duplicates is shown. Error bars represent value range.

a

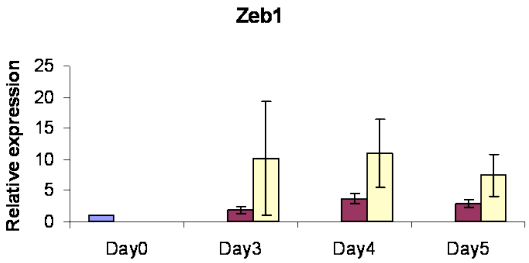
Zeb1
Relative expression
25
20
15
10
5
0
Day0
Day3
Day4
Day5

b

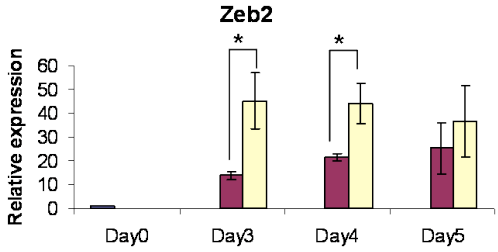
Zeb2
Relative expression
60
50
40
30
20
10
0
*
*
Day0
Day3
Day4
Day5

c

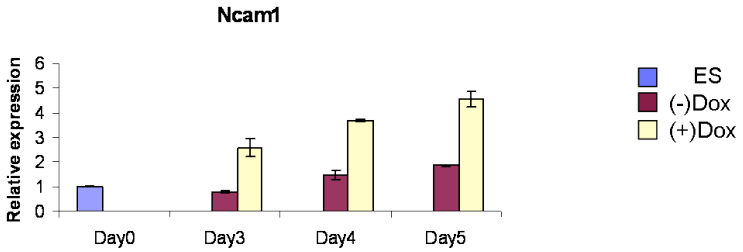
Ncam1
Relative expression
6
5
4
3
2
1
0
Day0
Day3
Day4
Day5
ES
(-)Dox
(+)Dox

Figure R1.15. TwE overcomes BMP4 block on neurite formation.

Cells differentiated for 3 days in N2B27+BMP4 (1ng/ml). Neuron formation as assessed by TUBB3 staining is blocked by BMP4 and rescued by induction of TwE (+Dox). Scale bars represent 50 μm.

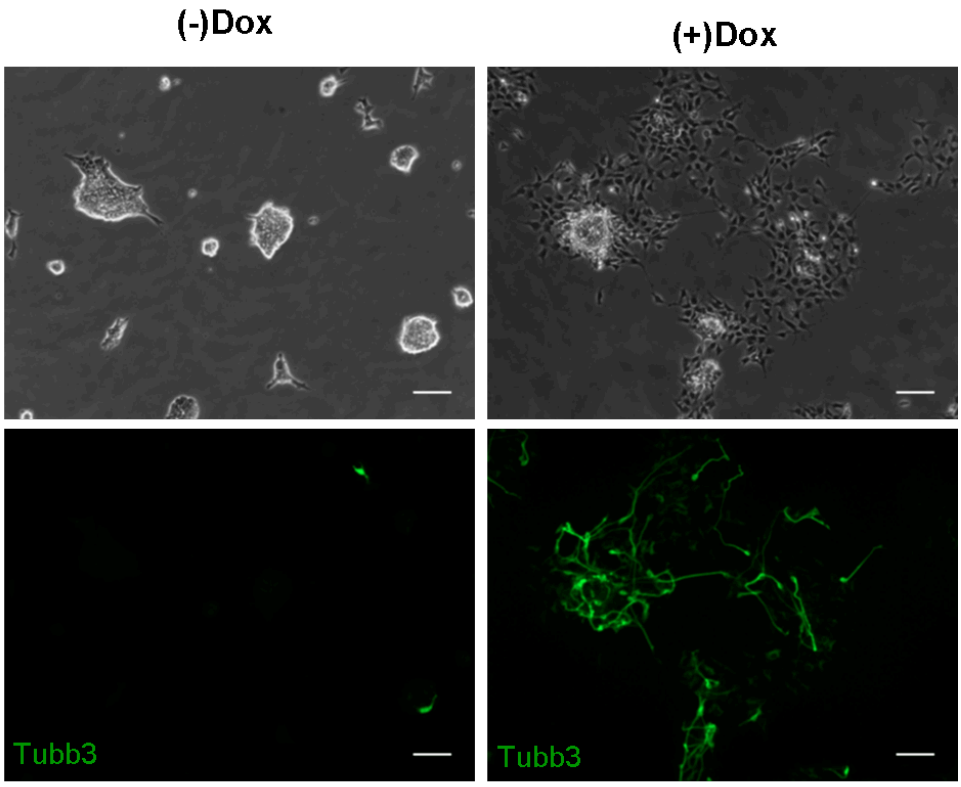

Day 3 of differentiation, 1 ng/ml BMP4

To test this hypothesis, 1 ng/ml BMP4 was added to the medium of cells differentiating in the monolayer protocol, in N2B27. This dose was sufficient to block the neurite formation. However, if TwE is induced, by Day 3, long interconnecting neurites, staining positive for TUBB3, could be readily observed [**Fig R1.15**].

R1.9 TwE Partially Overcomes BMP4 Block on Neural Differentiation.

The experiments presented above indicated that TwE has the ability to overcome BMP4 block on neural differentiation as assessed by formation of TUBB3 neurons. However, when BMP4 dose was increased to 5 ng/ml, TUBB3 positive neurons were no longer apparent in response to TwE induction (data not shown). I asked whether at this dose of BMP4, TwE could rescue neural differentiation as assessed by mRNA markers level. An experiment was designed where ES cells were differentiated for 5 day in N2B27 as a control of neural differentiation. In sister wells neural differentiation was blocked by addition of 5 ng/ml BMP4 while, in the third condition, this inhibition was rescued by activation of TwE.

FigR1.16 shows upregulation of mRNA levels for a number of neural markers, in the course of 5 day of differentiation, as well as the block in upregulation affected by BMP4: *Sox1* (a), *Zfp521* (b), *Pax3* (c), *Sox9* (d) and *Ascl1* (e). Furthermore, *Cdh2* is upregulated during neural differentiation and this is mitigated, albeit not completely blocked by BMP4 [**Fig R1.16f**]. TwE is able to rescue the expression of all the mentioned markers, with the exception of *Sox1* and *Ascl1*, at similar or higher levels compared to those in the control differentiation. It should be mentioned that for *Pax3* expression, the rescue to controls levels is only observed until day 3. After this time point, the levels continue to increase in the control, but plateau in the TwE rescue condition. This is consistent with previous data showing that TwE has a positive influence on *Pax3* only early in differentiation. However, in order to assess statistical significance more repeats are required for this experiment.

Figure R1.16. TwE partially overcomes BMP4 block on neural differentiation.

Cells differentiated for 5 days in N2B27 with or without BMP4 (5ng/ml) and Dox. qPCR analysis shows that BMP4 blocks upregulation of neural markers and this is rescued for most of them by TwE: *Sox1* (a), *Zfp521* (b), *Pax3* (c), *Sox9* (d), *Cdh2* (f) *Tcf15* (g). Expression in ES cells has been arbitrarily set to 1. One experiment performed in duplicates is shown. Error bars represent value range.

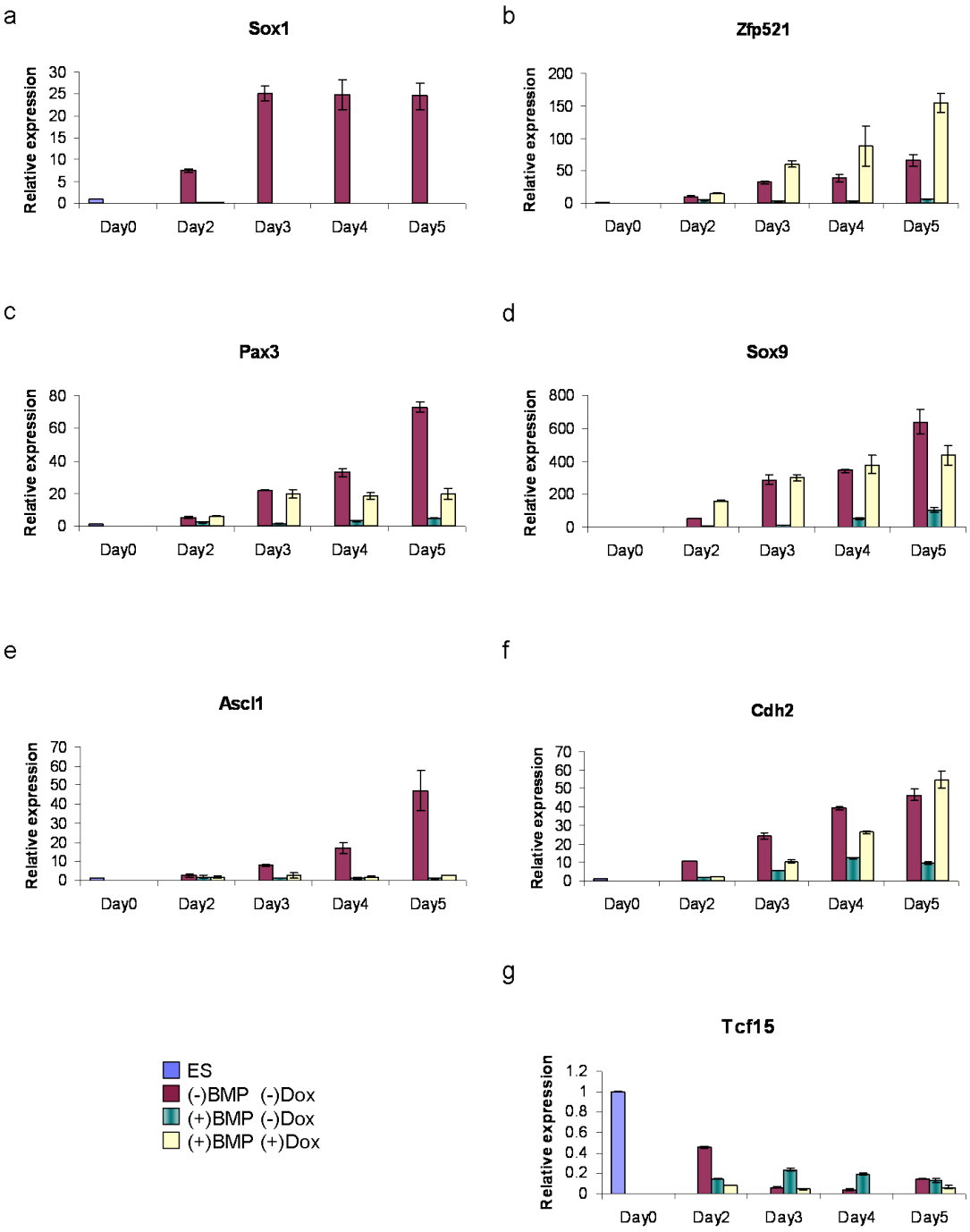
a
Sox1
Relative expression
30
25
20
15
10
5
0
Day0
Day2
Day3
Day4
Day5
b
Zfp521
Relative expression
200
150
100
50
0
Day0
Day2
Day3
Day4
Day5
c
Pax3
Relative expression
80
60
40
20
0
Day0
Day2
Day3
Day4
Day5
d
Sox9
Relative expression
800
600
400
200
0
Day0
Day2
Day3
Day4
Day5
e
Ascl1
Relative expression
70
60
50
40
30
20
10
0
Day0
Day2
Day3
Day4
Day5
f
Cdh2
Relative expression
70
60
50
40
30
20
10
0
Day0
Day2
Day3
Day4
Day5
g
Tcf15
Relative expression
1.2
1
0.8
0.6
0.4
0.2
0
Day0
Day2
Day3
Day4
Day5
ES
(-)BMP (-)Dox
(+)BMP (-)Dox
(+)BMP (+)Dox

The most serious failure in neural rescue by TwE was the lack of *Sox1* upregulation against high BMP levels. The data presented in the previous sections indicated that TwE is able upregulate as well as to downregulate *Sox1*, although the data supporting downregulation was more consistent. In the context of BMP4 inhibition of neural differentiation it indicates that targets other than TwE are stopped from enacting the neural program. The absence of *Sox1* correlates with the TwE failure to upregulate *Ascl1* or to produce overt morphologically recognizable neurons. Interestingly, in vivo *Sox1* is not required for neural differentiation [Malas et al, 2003]. Hence, the lack of neuron formation, is most likely, not a consequence of *Sox1* absence, but rather *Sox1* is a marker of the failure of proper neural differentiation.

However, there is a possibility that *Zfp521*, *Pax3* and *Sox9* do not mark a neural population in this context. *Zfp521* is restricted to the neural compartment in the gastrulating embryo [Kamiya et al, 2011], but has been reported as having a role in mesenchymal cells at later stages [Hesse et al, 2010]. *Pax3*, *Sox9* and *Twist1* are all expressed in the neural crest and somitic compartment [Goulding et al, 1991; Ng et al, 1997; Stoetzel et al, 1995; Fuchtbauer E.M., 1995]. I therefore asked if the cells induced by TwE against BMP could have a profile consistent with somitic like cells. To answer this question I made use of the somitic specific marker *Tcf15* [Burgess et al, 1995]. This marker was expressed at lower levels that in ES cells in all conditions tested, and the lowest levels, at all time points, were found in TwE induced samples [**Fig R1.16g**]. Consequently, the most likely explanation is that TwE induces formation of a cell type expressing a subset of neural and neural crest markers.

To clarify the role TwE has in rescuing neural differentiation, another experiment was set up, where cells were differentiated with or without Dox induction, in the absence of BMP4, 1 ng/ml BMP4 and 5 ng/ml BMP4 respectively. The same markers were tested as in the previous experiment at day 4 of differentiation with the expected results for no BMP4 and 5 ng/ml BMP4 conditions.

Figure R1.17. TwE rescue of neural differentiation depends on BMP4 levels.

Cells differentiated for 4 days in N2B27 with 0, 1 or 5 ng/ml BMP4. qPCR analysis shows that 1 ng/ml BMP4 does not block completely *Sox1* upregulation (a) while having a significant negative effect on all neural markers (a-f). In this conditions TwE can fully rescue the expression of all neural markers except *Sox1*; *Sox1* (a), *Zfp521* (b), *Pax3* (c), *Sox9* (d), *Ascl1* (e) and *Cdh2* (f). Expression in ES cells has been arbitrarily set to 1. For *Sox1*, *Zfp521*, *Pax3*, *Sox9* and *Ascl1* two repeat experiments performed in duplicates are shown. Error bars represent standard deviation of the mean. For *Sox1* with no BMP4 $p = 0.02$, for *Pax3* no BMP4 $p = 0.005$, for *Pax3* with 5 ng/ml BMP4 $p = 0.003$, for *Sox9* with 1 ng/ml BMP4 $p = 0.01$ and for *Sox9* with 5 ng/ml BMP4 p = 003. For *Cdh2* one experiment performed in duplicates is shown. Error bars represent value range.

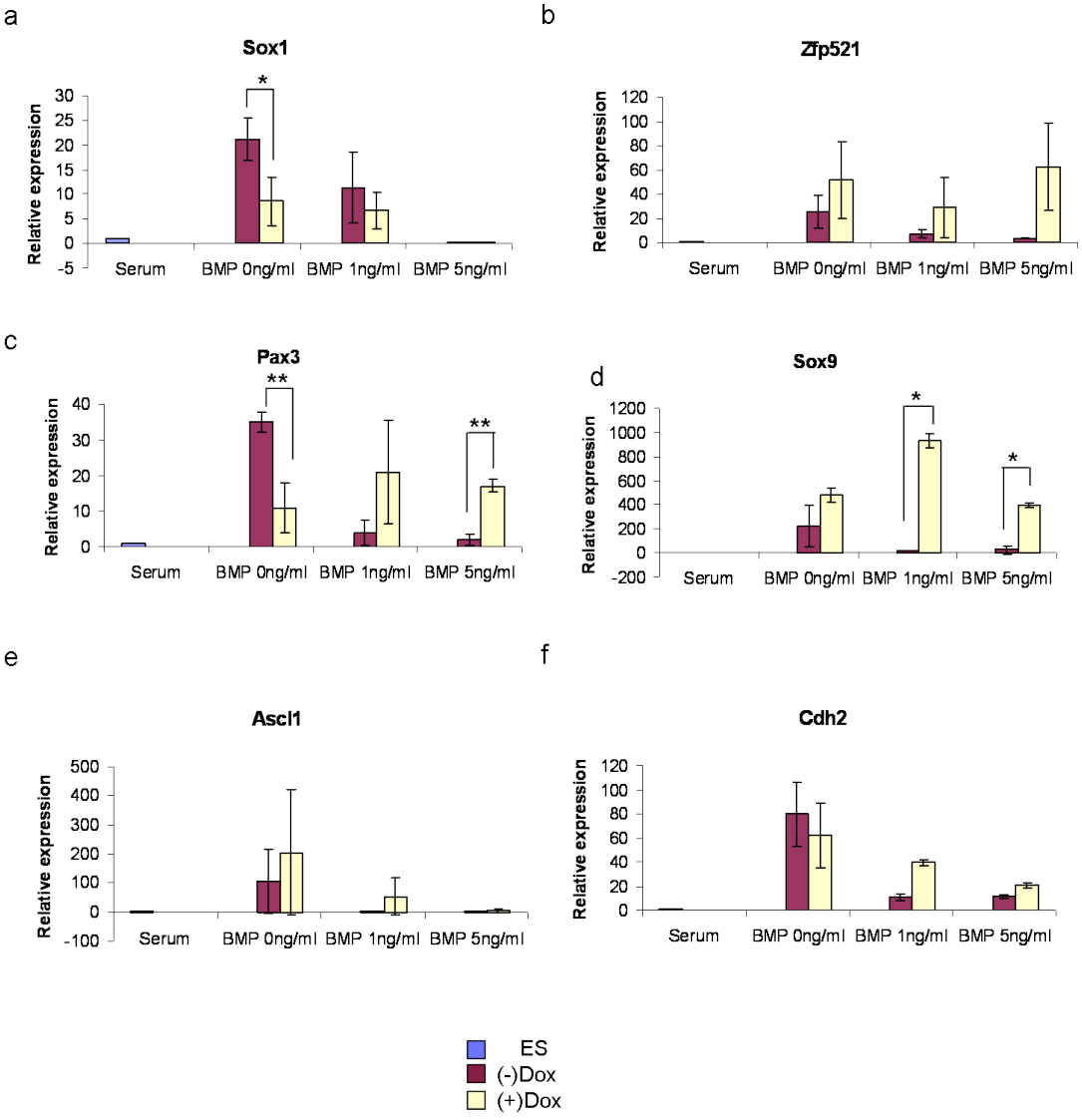
a
Sox1
Relative expression
30
25
20
15
10
5
0
-5
*
Serum
BMP 0ng/ml
BMP 1ng/ml
BMP 5ng/ml
b
Zfp521
Relative expression
120
100
80
60
40
20
0
Serum
BMP 0ng/ml
BMP 1ng/ml
BMP 5ng/ml
c
Pax3
Relative expression
40
30
20
10
0
**
**
Serum
BMP 0ng/ml
BMP 1ng/ml
BMP 5ng/ml
d
Sox9
Relative expression
1200
1000
800
600
400
200
0
-200
*
*
Serum
BMP 0ng/ml
BMP 1ng/ml
BMP 5ng/ml
e
Ascl1
Relative expression
500
400
300
200
100
0
-100
Serum
BMP 0ng/ml
BMP 1ng/ml
BMP 5ng/ml
f
Cdh2
Relative expression
120
100
80
60
40
20
0
Serum
BMP 0ng/ml
BMP 1ng/ml
BMP 5ng/ml
ES
(-)Dox
(+)Dox

In 1 ng/ml condition *Sox1* was permitted, albeit at lower levels compared to no BMP4 and induction of TwE did not seem to have a notable influence on *Sox1* expression. In these conditions, of 1 ng/ml BMP4, the expression of all the other tested neural markers was rescued by TwE, including that of *Ascl1* [**Fig R1.17**]. When statistical significance was assessed, it was observed that *Sox1* is significantly downregulated by TwE in the absence of BMP4, while *Zfp521* upregulation was not statistically significant. *Pax3* was significantly downregulated at day 4 in the absence of BMP4 and significantly upregulated at 5 ng/ml BMP4 dose only. *Sox9* was significantly upregulated in the presence of BMP4 (1 and 5 ng/ml), while *Ascl1* upregulation was not significant in any condition.

In conclusion, it can be noted that TwE ability to rescue neural differentiation against BMP block is dependent on *Sox1* expression. As long as *Sox1* is expressed TwE can rescue neural differentiation, while TwE cannot rescue *Sox1*. On the other hand, in the presence of high BMP4 and no *Sox1* TwE only the expression of some markers common for neural and neural crest progenitors and thus, drives cells towards a phenotype that resembles neural crest.

R1.10 Mesenchymal-like Cells under TwE and BMP4 Influence

R1.10.1 TwE Blocks Primitive Streak fate.

In the previous section I showed that TwE and BMP4 have opposing effects on neural differentiation. On the other hand, BMP4 is one of the key signalling molecules involved in PS formation and essential for *T* (Brachyury) upregulation [Winnier et al, 1995].

When PS markers *Eomes* and *T* were analysed during monolayer neural differentiation it was observed that they undergo only a minor upregulation in control conditions, but this is significantly enhanced by BMP4. This enhancement is blocked by TwE induction, indicating that cells induced in the presence of both BMP and TwE do not turn on the PS program [**Fig R1.18**].

R1.10.2 Not BMP4 but TwE Induces EMT.

In vivo PS formation is accompanied by overt EMT as the epiblast cells begin their migration to form the mesodermal and enodermal germ layers [Arnold and Robertson, 2009]. Interestingly, an EMT event could not be observed in response to 5 ng/ml BMP4 during monolayer differentiation in spite of PS marker upregulation. On the contrary, when cell morphology was analysed, it was observed that until Day3, BMP4 induces formation of tight colonies, more or less indistinguishable from those formed during neural differentiation. Starting on Day 4, the clusters of compact cells begin to be surrounded by large epithelial cells with a polygonal morphology [**Fig R1.19b**, yellow arrows]. On the other hand, in TwE induced samples an early formation of mesenchymal like cells with reduced cellular contacts can be observed [**Fig R1.19a and b**, orange arrows]. By Day 4, these cells cover almost the entire surface of the well. Depending on the experiment, the epithelial polygonal cells in the +Dox condition are either completely absent or greatly reduced.

Previously *Twist1* had been reported to drive loss of CDH1 [Yang et al., 2004]. I was not able to test this feature for TwE during neural differentiation since in this context CDH1 is normally replaced by CDH2. Here CDH1 is maintained by BMP and, TwE influence could be investigated. For this purpose, cells were stained for CDH1 on day 4 of differentiation. In the absence of Dox, polygonal cells stained brightly, CDH1 marking the membrane and, making the points of cellular adhesion readily observable. By contrast, in Dox treated samples CDH1 signal was very weak, it did not localize at the membrane and cellular contacts could not be visualised [**Fig R1.19c**].

These data indicates that in the context of in vitro monolayer differentiation BMP induces markers of PS but fails to generate overt mesodermal cells with mesenchymal characteristics. On the other hand, TwE blocks upregulation of PS markers, but induces formation of morphologically recognizable mesenchymal cells. Furthermore, marker analysis has indicated that these cells had a neural crest like profile as assessed by upregulation of Pax3 and Sox9 [**Fig R1.17c and d**].

Figure R1.18. TwE blocks BMP4 induced primitive streak fate.

Cells differentiated for 5 days in N2B27 with or without BMP4 (5ng/ml) and Dox. qPCR analysis shows that BMP4 induces upregulation primitive streak markers *Eomes* (a) and *Brachyury* (b) and that this event is negatively influenced by TwE. Expression in ES cells has been arbitrarily set to 1, except for *Brachyury* which was unfetectable in ES cells. For this marker Day2 condition (-)BMP (-)Dox which was the lowest detectable condition and was set to 1. One experiment performed in duplicates is shown. Error bars represent value range.

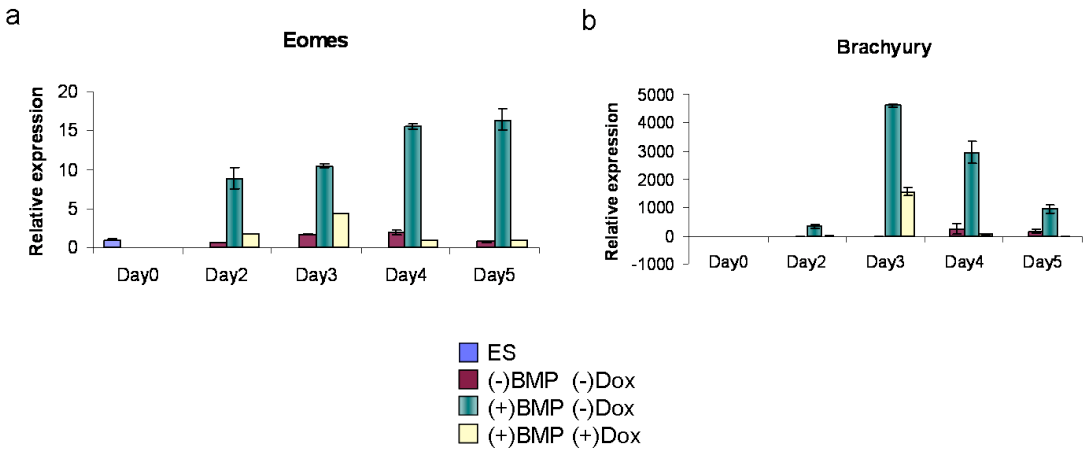
a
Eomes
Relative expression
20
15
10
5
0
Day0
Day2
Day3
Day4
Day5
b
Brachyury
Relative expression
5000
4000
3000
2000
1000
0
-1000
Day0
Day2
Day3
Day4
Day5
ES
(-)BMP (-)Dox
(+)BMP (-)Dox
(+)BMP (+)Dox

Figure R1.19. TwE blocks formation of epithelial cells induced by BMP4.

Cells differentiated in N2B27+BMP4 (5ng/ml) for 3 days (a) or 4 days (b and c). At day 4 BMP4 induces formation of epithelial cells (yellow arrows), but this is blocked by TwE which induces instead formation of mesenchymal like cells starting at day 3 (orange arrows). CDH1 is lost from cell surface in samples where TwE was induced (c). Scale bars represent 50 μm.

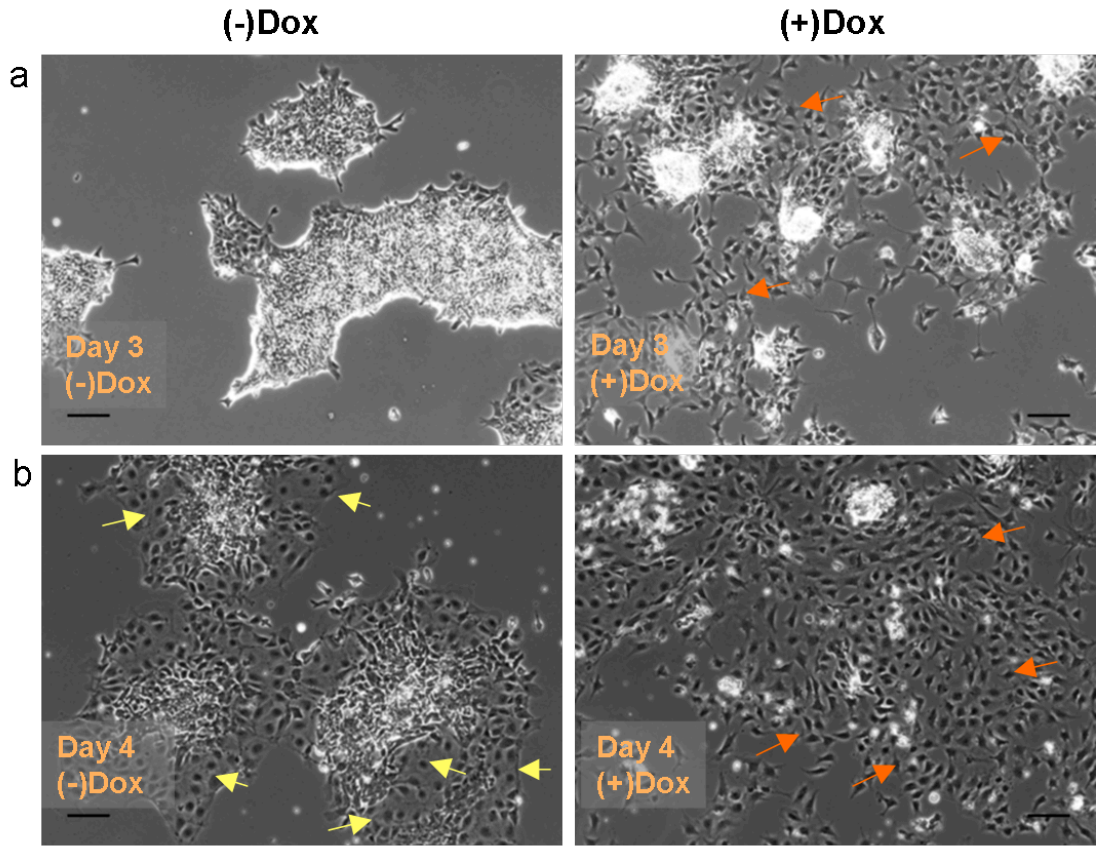

Day 3 and 4 of differentiation; 5 ng/ml BMP4

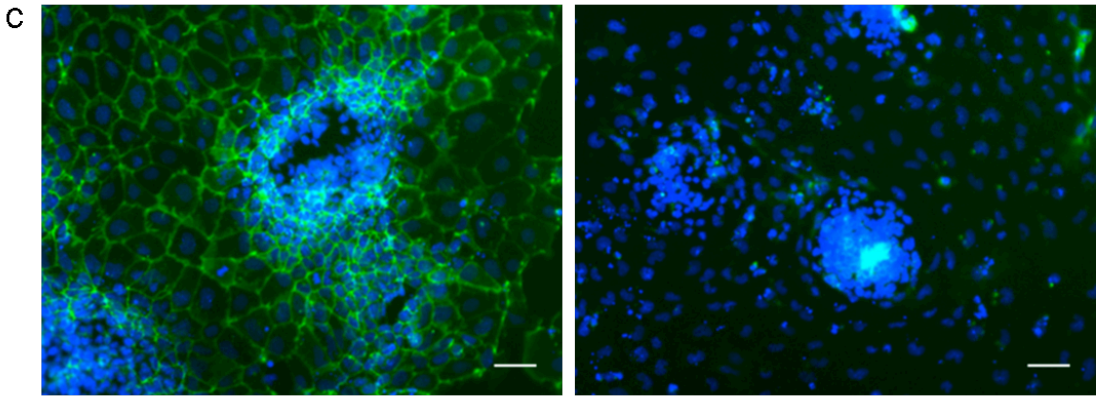

Day 4 of differentiation; Cadherin1 staining, 5 ng/ml BMP4

R1.11 *Twist1* Is Not Required for Early Neural Progression.

After showing that TwE facilitates progression through neural differentiation and can partially rescue this type of differentiation against BMP inhibition, the next question to ask was if Twist1 is required for neural induction.

For this purpose I employed the method of siRNA directed against *Twist1*. Four siRNA constructs were tested and the two with the best knockdown were subsequently used. Cells were transfected with the siRNA according to manufacturer protocol at the beginning of neural differentiation; siRNA used: Twist1 construct1, Twist1 construct4 and Control a siRNA which does not target any known gene. RNA knockdown was good after the first 24 hours, close to 90% and, was gradually lost, cells reverting to levels of *Twist1* close to physiological ones, by day 3 [**Fig R1.20a**]. When early neural markers were tested: *Sox1*, *Zfp521* and *Zeb2* [**Fig R1.20b to d**], it was found that they all progressed through neural differentiation with a dynamic similar to control.

A negative result in a siRNA experiment is hard to interpret, due to the difficulties in estimating what is the knockdown level which should produce phenotypical consequences and, for how long should the knockdown be maintained. On the other hand it is conceivable that BMP blocks multiple targets when inhibiting neural differentiation and the data presented in this chapter supports the notion that if TwE is at all one of the neural inducers, it is not the only one.

Figure R1.20. High levels of Twist1 RNA are not required for neural differentiation.

ES were differentiated for 3 day in the neural monolayer protocol and treated either with control siRNA or with siRNA constructs directed against *Twist1*. qPCR for *Twist1* (a), *Sox1* (b), *Zfp521* (c) and *Zeb2* (d). Expression for each gene in day1 control conditions has been arbitrarily set to 1. One experiment performed in duplicates is shown. Error bars represent value range.

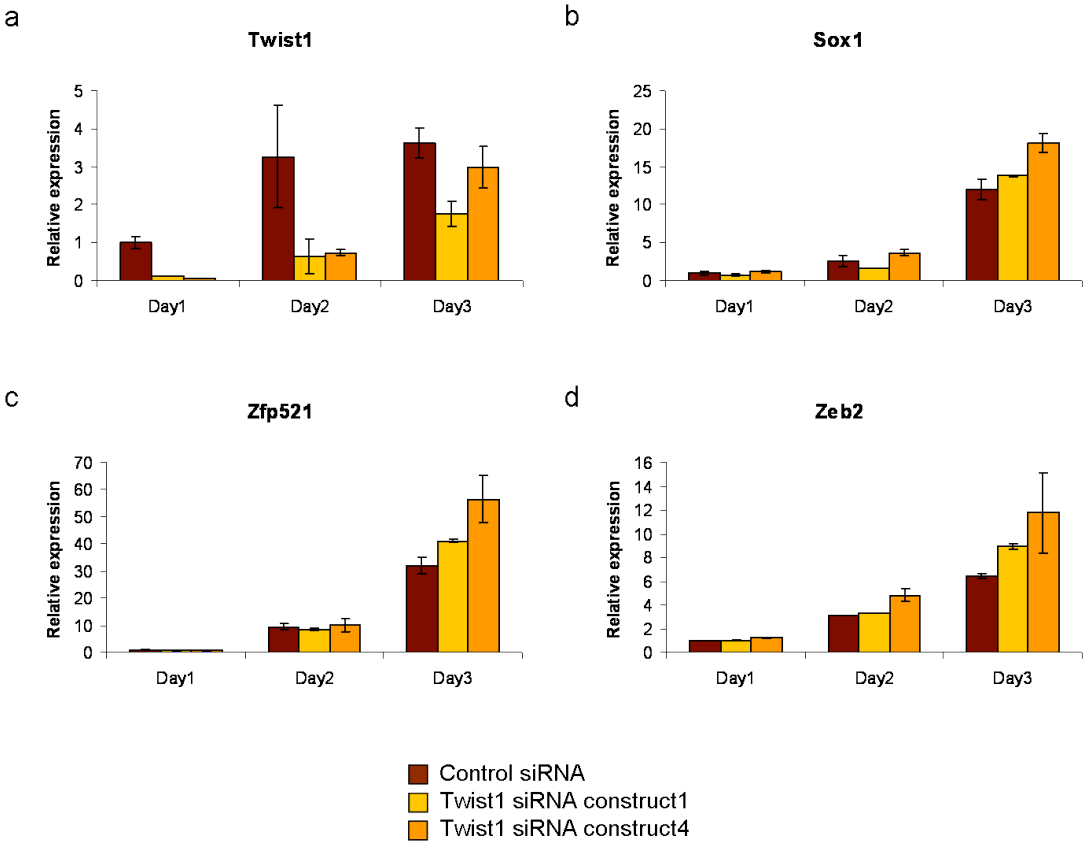
a
Twist1
Relative expression
0
1
2
3
4
5
Day1
Day2
Day3
b
Sox1
Relative expression
0
5
10
15
20
25
Day1
Day2
Day3
c
Zfp521
Relative expression
0
10
20
30
40
50
60
70
Day1
Day2
Day3
d
Zeb2
Relative expression
0
2
4
6
8
10
12
14
16
Day1
Day2
Day3
Control siRNA
Twist1 siRNA construct1
Twist1 siRNA construct4

R1.12 Conclusions

In the present chapter I started from the observations that *Twist1* is expressed in ES cells, that it is upregulated during neural differentiation and that, as a partner of E proteins is a putative target for BMP/ID pathway. I complemented these observations with the notion that within the pluripotent cell compartment it is upregulated at the exit from the ground state and that, later on, it is associated with neural differentiating cells.

By using an ID resistant and inducible active form of TwE I made the striking observation that neural differentiation is accelerated both at the point of entry and exit from neural progenitor state, that TwE enhances an EMT process specific to neural differentiation and that TwE can partially rescue the BMP imposed block on neural differentiation, although this was most striking at low doses of BMP. An important point is that *Zfp521* expression can be fully rescued with no positive influence on *Sox1* [**Fig R1.16a and b**]. It has been previously reported that when overexpressed *Zfp521* rescues *Sox1* expression from BMP inhibition [Kamiya et al, 2011]. It can be inferred that either *Zfp521* requires very high, non-physiological levels to induce *Sox1*, or that TwE induces other phenotypic changes which makes *Sox1* not responsive to *Zfp521* induction

Another interesting observation was the fact that in the presence of BMP, TwE induces the formation of a mesenchymal like cell type which is not generated through a PS intermediate state. Furthermore, to this cell type the choice seems to be open whether to adopt a neural fate or to remain mesenchymal. In recent years a neural-mesenchymal progenitor has been described, residing at the node/streak border, namely, at the edge of BMP signalling [Tzouanacou et al, 2009]. On the other hand it should be noted that neural crest cells are also at a crossroad between neural and mesenchymal fates, that they require BMP signalling and that, TwE induces the upregulation of a number of neural crest markers, both in the presence and in the absence of BMP.

Regarding the initial hypothesis, according to which Tw-E dimer function as a neural inducer, it can be considered that the data presented here serves more to refute than to support it.

First, the fact that TwE accelerates neural differentiation could label TwE as a neural facilitator. However, in vivo, acceleration of neural differentiation has disastrous consequences, usually resulting in smaller brains, improperly patterned [Kageyama et al, 2005]. Thus, it is reasonable to infer that neural induction relies on transcription factors which do not risk accelerating the neural differentiation, and above all, not accelerating the exit from neural progenitor state.

Second, moderately high levels of BMP are able to block neural differentiation in the presence of TwE, at least in certain key aspects.

Third, early neural differentiation can progress unhindered, in the presence of *Twist1* siRNA.

Taking into account the above considerations, it becomes essential to ask whether *Twist1* has a physiological role in neural differentiation in vivo; and what such a role might be. This question will be explored in the next chapter.

Figure R1.21. Schematic Conclusions

TwE might facilitate pluripotent cells entry to the neural program, while strong evidence support the idea that it accelerates the exit from neural progenitor state, towards postmitotic neurons. TwE partially blocks BMP4 activity on neural induction, while strongly opposing BMP4 on EMT.

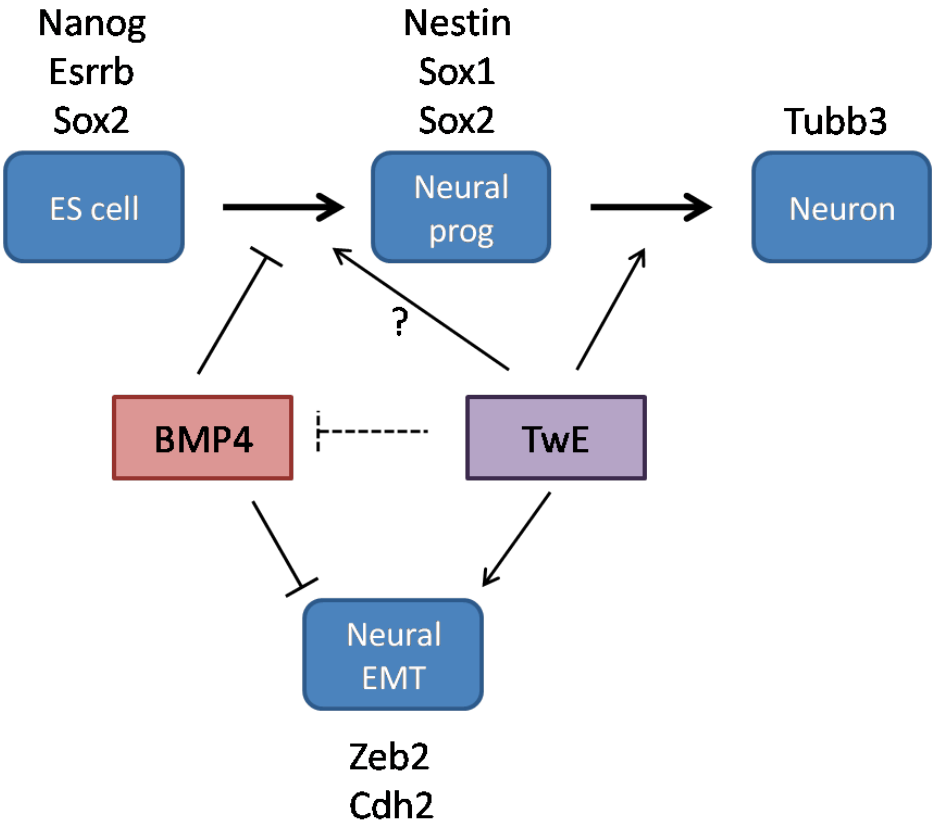
Nanog
Esrrb
Sox2
ES cell
Nestin
Sox1
Sox2
Neural prog
Tubb3
Neuron
?
BMP4
TwE
Neural EMT
Zeb2
Cdh2

IV. RESULTS 2

TWIST1 IN DORSAL NEURAL PATTERNING

R2.1 Overview

As discussed in the previous chapter, BMP and ID inhibit neural differentiation and, one of their putative targets in the process is the TWIST1-E dimer. A constitutively active form of TwE can accelerate neural differentiation and partially rescue neural induction after blockade by BMP. However, it is not easy to infer from the *in vitro* work presented how TwE normally integrates in the general process of neural induction and development.

Interestingly, knockout studies showed that the absence of *Twist1* leads to failure in anterior neural tube closure, followed by severe malformation of the developing brain [Chen and Behringer, 1995]. However, expression studies showed that while *Twist1* is strongly expressed in the head mesenchyme it is absent from the neural tissue [Stoetzel et al., 1995; Füchtbauer E.M., 1995].

A detailed analysis of neural tube development in *Twist1* mutant mice revealed defects of dorso-ventral patterning at the level of anterior neural tube. The study concluded that these defects, which consist mainly of a dorsal expansion of ventral marker domains, at the anterior level, are due to non-autonomous influences from surrounding mesenchyme [Soo et al, 2002]. However, a mechanism for such an influence has not been proposed. Moreover, the ventral neural tissue, which is closest to the mesoderm, develops relatively normally, while the pernicious effects of *Twist1* absence are cast on the dorsal neural tissue. Currently, no explanation has been provided for this phenomenon.

In this chapter I investigate potential *Twist1* roles on dorso-ventral patterning of the neural tube. I investigate *Twist1* expression in the gastrulating embryos, with an emphasis on neural tube and compare the results with the already published data on this issue. Finally, based on *in vitro* mixing differentiation experiments, I propose a

mechanism for non-autonomous influence *Twist1* expressing cells can have on dorsal neural specification.

R2.2. TwE Biases Neural Differentiation Towards Dorsal.

I presented, in the previous chapter, data showing that TwE enhances the expression of neural markers both in the absence and in the presence of exogenous BMP. Furthermore, when these markers were analysed based on their dorso-ventral positioning it was observed that only dorsal markers were upregulated, while the ventral ones were downregulated.

Fig R2.1 presents a synopsis of these markers at day 4 of differentiation in the absence of BMP: *Sox9* (a), *Ascl1* (b), *Atoh1* (c), *Pax3* (d), *Pax6* (e) and *Shh* (f). Dorsal markers like *Sox9*, *Ascl1*, *Atoh1* are upregulated while, *Pax6* which has its domain immediately ventral to the *Ascl1/Atoh1* markers is downregulated. The ventral morphogen *Shh* is downregulated, as well. *Pax3*, which is a dorsal marker, is downregulated, by this has already been explained as a biphasic action of TwE on this marker. Across three repeat experiments only *Atoh1* upregulation and *Pax3* downregulaton was statistically significant. More repeat experiments are probably required to assert statistical significance for the other markers. A diagram of dorso-ventral distribution of these markers from Liu and Niswander, 2005 is presented [**Fig R2.1g**].

While it is possible that all the actions reported for the TwE dimer represent artificial phenomenons, with no physiological significance, it is quite a coincidence that dorsal markers should be upregulated, connecting TwE activity with reported patterning and neural tube closure defects. Therefore a physiological role for Twist1 becomes more likely and I set out to investigate its expression and mechanism of action more closely.

R2.3. *Twist1* Begins to Be Expressed in The Embryo around Gastrulation.

As stated earlier, *Twist1* is expressed in ES and neural differentiating cells. Aliaxandra Radzisheuskaya, in Lowell lab, compared *Twist1* levels of expression in ES cells to those in the whole embryo at different stages and found, that until gastrulation, expression in the embryo is lower than in ES cells, that it reaches the ES cells level between 6.5 and 7.5 dpc and then, continues to increase sharply until 9.5 dpc when it reaches the maximum [**Fig R2.2**].

These data is consistent with the previously reported expression pattern, which showed that *Twist1* expression begins at gastrulation [Stoetzel et al., 1995; Füchtbauer, 1995]. However, it is harder to explain why expression in ES cells should be higher than in peri-implantation blastocyst: 10 fold higher than at 5.5 dpc while, at 4.5 dpc is virtually undetectable. The most obvious explanation would be that some element in the artificial environment of ES cells brings about this expression of *Twist1*. On the other hand, it should be noted that the expression in the blastocyst is more similar with that in 2i conditions, although 2i also represents an artificial context, where pluripotency is maintained by small molecule inhibitors.

R2.4 *Twist1* Is first Expressed at Streak Stages.

To clarify any potential points of controversy, I wanted to confirm *Twist1* expression in early embryos by whole mount in situ hybridization, an analysis which has already been performed in the past [Wolf et al, 1990; Ang and Rossant, 1994; Stoetzel et al., 1995; Füchtbauer, 1995]. An overview of the finding in these studies is presented in Appendix 2, at the end of the thesis.

Figure R2.1. TwE induces a dorsal phenotype during neural differentiation.

qPCR showing expression of *Sox9* (a), *Ascl1* (b), *Atoh1* (c), *Pax3* (d), *Pax6* (e) and *Shh* (f) in ES cells and cells at day 4 of neural differentiation in monolayer protocol. Cells were either not induced: (-)Dox, or induced throughout differentiation: (+)Dox. For each gene the expression in ES cells has been arbitrarily set to 1. For *Sox9*, *Ascl1*, *Atoh1*, *Pax3* and *Pax6* triplicate experiments performed in duplicates are shown. Error bars represent standard deviation of the mean. For *Atoh1* $p = 0.005$, for *Pax3* $p = 0.01$. For *Shh* one experiment performed in duplicates is shown. Error bars represent value range. Schematics of antero-posteriom neural marker distribution in the mouse spinal cord, adapted from Liu & Niswander, 2005. Red circle represents the neural fate closest to the observed marker expression.

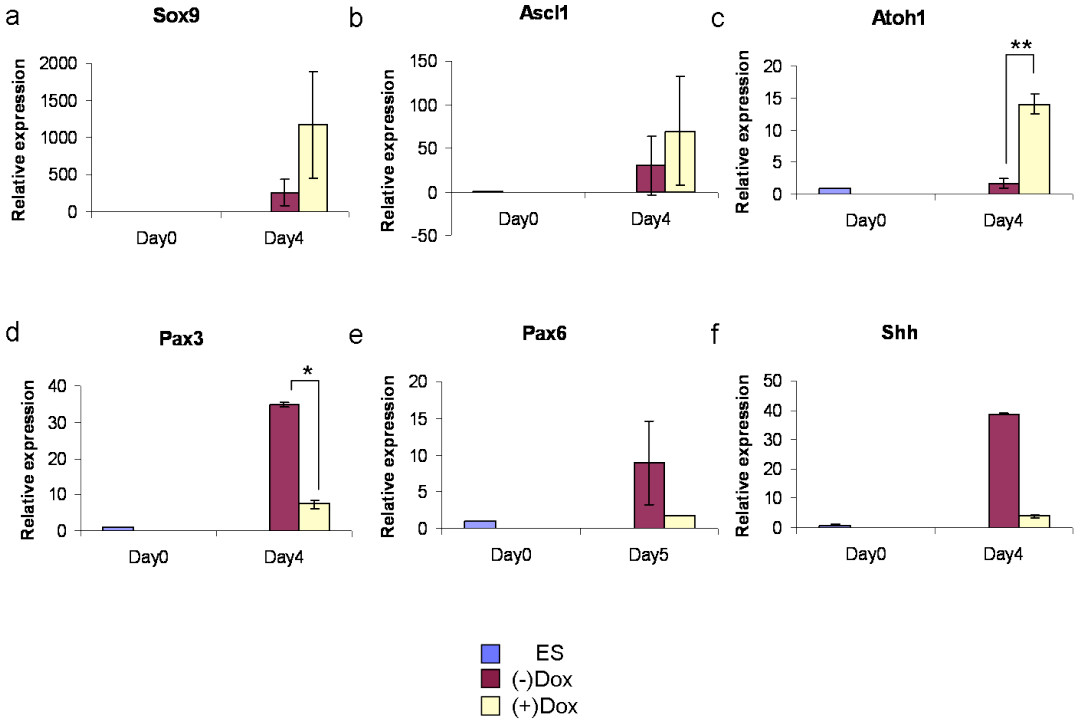
a
Sox9
Relative expression
2000
1500
1000
500
0
Day0
Day4
b
Ascl1
Relative expression
150
100
50
0
-50
Day0
Day4
c
Atoh1
**
Relative expression
20
15
10
5
0
Day0
Day4
d
Pax3
*
Relative expression
40
30
20
10
0
Day0
Day4
e
Pax6
Relative expression
20
15
10
5
0
Day0
Day5
f
Shh
Relative expression
50
40
30
20
10
0
Day0
Day4
ES
(-)Dox
(+)Dox

g

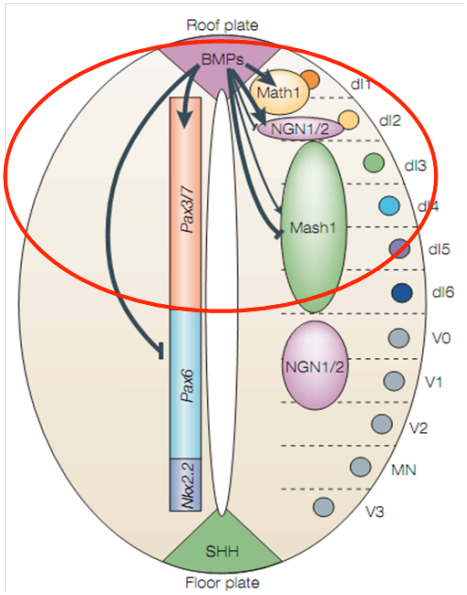
Roof plate
BMPs
Math1
NGN1/2
Pax3/7
Mash1
Pax6
Nkx2.2
NGN1/2
SHH
Floor plate
dI1
dI2
dI3
dI4
dI5
dI6
V0
V1
V2
MN
V3

Figure R2.2 *Twist1* is expressed in ES cells at low levels.

qPCR for *Twist1* for ES cells, whole embryos from 4.5 dpc to 10 dpc and decidua. (Aliaxandra Radzisheuskaya). The expression in ES cells has been arbitrarily set to 1. One experiment performed in duplicates is shown. Error bars represent value range.

a

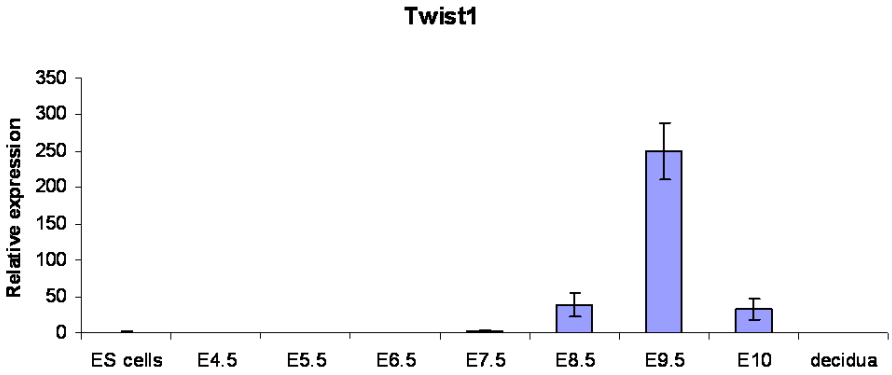
Twist1
Relative expression
350
300
250
200
150
100
50
0
ES cells
E4.5
E5.5
E6.5
E7.5
E8.5
E9.5
E10
decidua

b

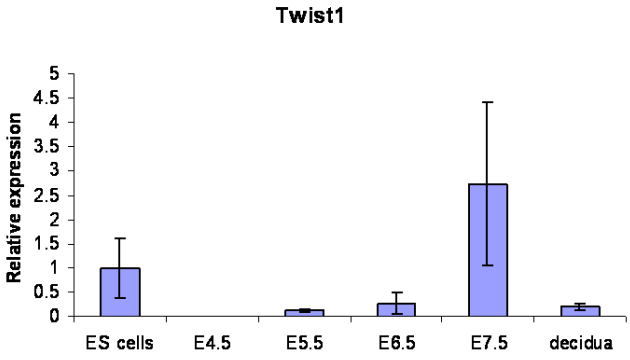
Twist1
Relative expression
5
4.5
4
3.5
3
2.5
2
1.5
1
0.5
0
ES cells
E4.5
E5.5
E6.5
E7.5
decidua

To this end I generated a *Twist1* RNA complementary probe as described in Material and Methods (**M1.3.3**). The probe, of approximately 870bp in length, was design to target the 3'UTR to avoid any conserved regions homologous with other bHLH factors and, encompasses the sequence of the shorter probe described in Wolf et al, 1990.

At 6.5 dpc, pre-streak/early-streak stages the embryo lacks any signal even after being developed for 48 hours [**Fig R2.3a**]. A signal was first observed around 7.5 dpc in mid-streak embryos as weak and diffuse staining, probably of mesodermal cells which migrated through the primitive streak. The signal becomes stronger and more condensed as the embryo progresses towards late streak and early bud stages [**Fig R2.3b**]. As the signal becomes stronger it is apparent, that at these stages, it is restricted to mesoderm of the embryo proper and the allantois [**Fig R2.3e and f**].

As the embryo progresses towards the late bud stage (8.0 dpc), the signal becomes suddenly quite strong. *Twist1* expressing cells accumulate mainly in the anterior mesoderm and allantois [**Fig R2.4a**]. Slightly later (early 8.5 dpc), at the head fold stage, the signal in the prospective head mesenchyme is very strong. In the same time, distal and posterior mesoderm becomes clear. The epiblast, which on the anterior side has now transformed to neural folds, is also clear of any discernable staining [**Fig R2.4b, c and d**]. The black arrow, in **Fig R2.4b**, indicates the proximal/distal limit of the signal. The few positive cells which seem to be posterior and proximal [**Fig R2.4b**, yellow arrow] are an artefact resulted from superimposition of cells from the anterior mesenchyme of an embryo which could not be perfectly aligned for viewing from the lateral perspective. This can be observed better in **Fig R2.4d** which presents the posterior view. Here it is clear that the whole posterior region is devoided of signal. The only other positive region besides anterior mesenchyme and allantois is represented by a bilateral string of extra-embryonic mesoderm connecting the allantois with the embryo proper **[Fig R2.4d**, red arrow].

Figure R2.3. *Twist1* is expressed in the mesoderm starting at mid streak stages.

Whole mount in situ hybridization for Twist1 of post implantation embryos. Pre-streak embryos (a), group of embryos arranges from left to right mid streak to early bud (b) and individual embryos: late streak (c) early bud (d, e and f). Last to pictures present the same embryo: anterior view (e) and lateral view (f). Blue arrows indicate allantois, yellow arrows indicate a patch of positive cells in the mesoderm lateral of primitive streak. Proximal side (prox), distal side (dist). Scale bars represent 50 μm.

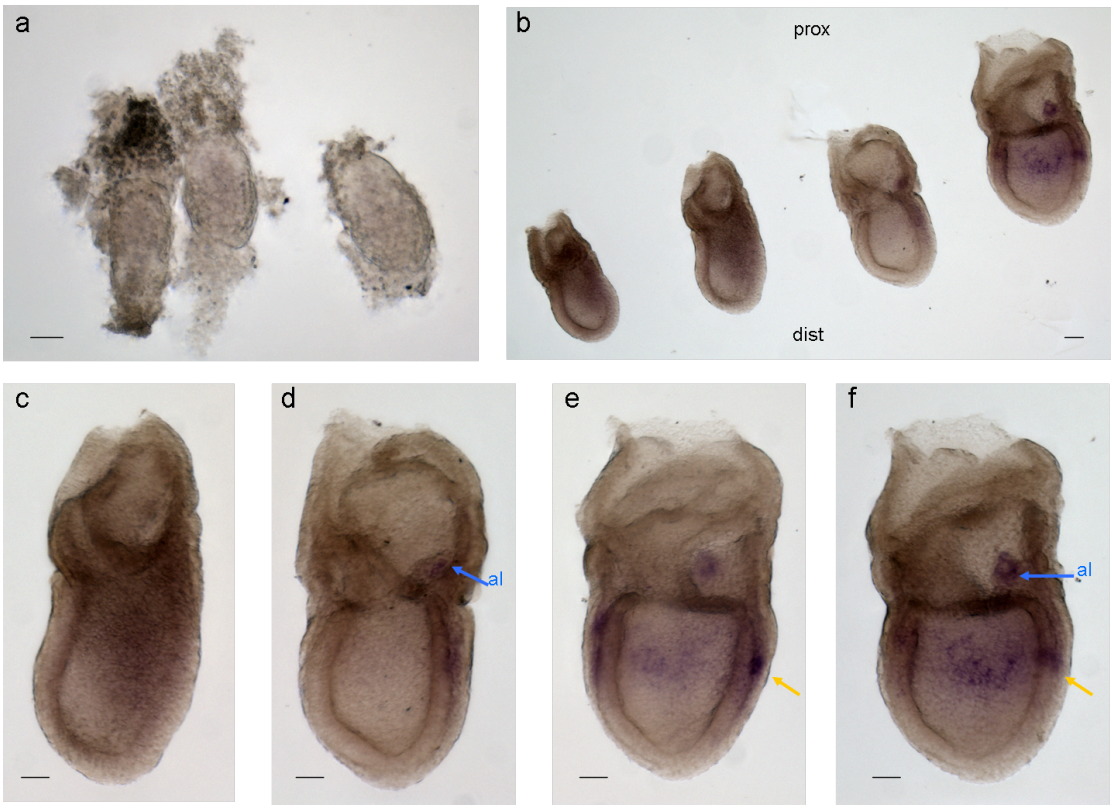
a
b
prox
dist
c
d
al
e
f
al

Figure R2.4. Head mesenchyme the first embryonic domain of high *Twist1* expression.

Whole mount in situ hybridization for *Twist1* of embryos around head fold stage. Late bud stage (a), head fold stage (b, c and d). Head fold stage same embryo lateral view (b), anterior view (c) and posterior view (d). Black arrow marks the anterior distal limit of the *Twist1* signal. Yellow arrow points to lateral mesoderm cells which seem to stretch to the PS. Red arrow shows in posterior view that the only cells which stretch towards posterior underline the extraembryonic amnion. Blue arrow indicates the allantois. Neural folds (nf), head mesenchyme (hf). Scale bars represent 50 μm.

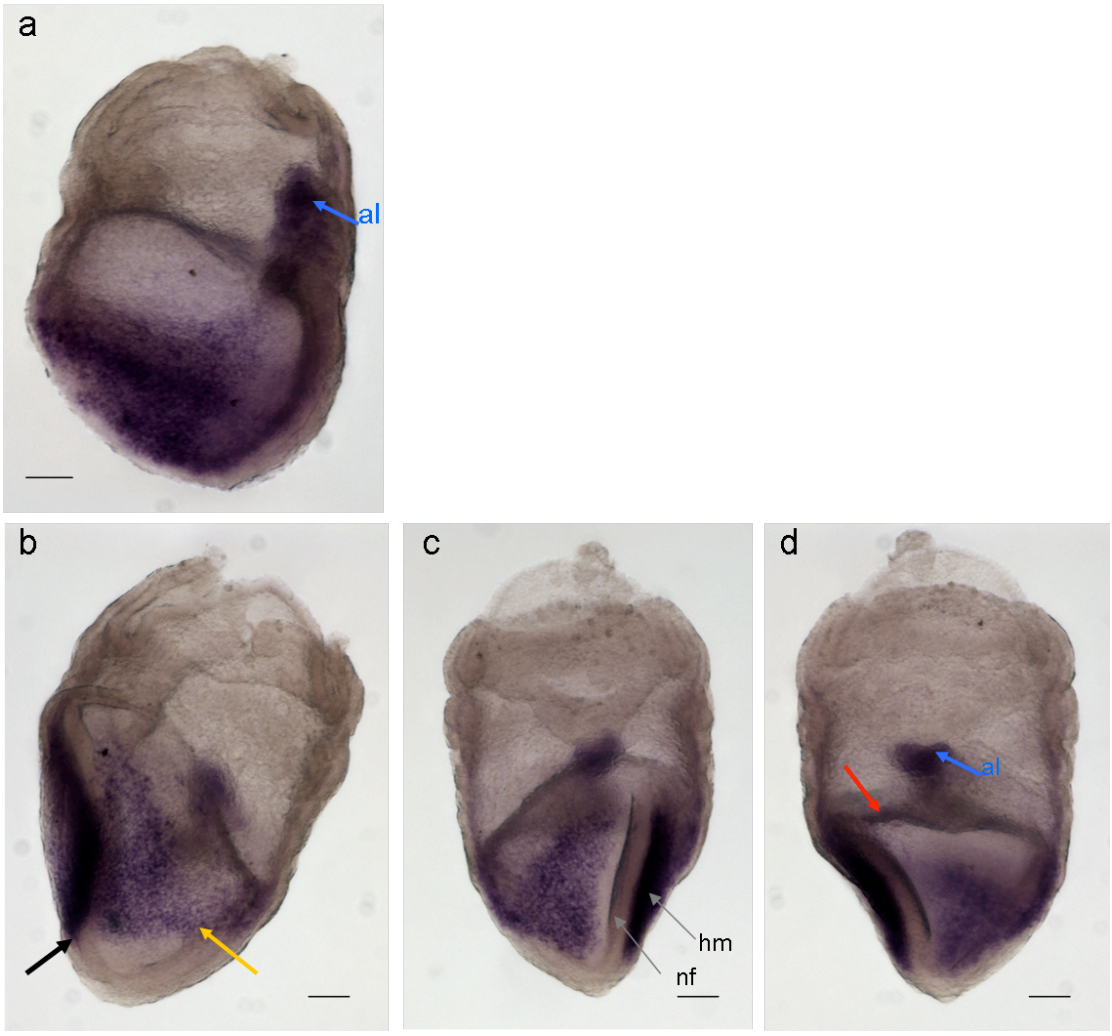
a
al
b
c
hm
nf
d
al

The data presented in this section correlates well with the previous in situ data, as well as with the results from whole embryo RNA expression. Initiation of expression, which has been previously placed at the rather loose time point of 7.5 dpc [Stoetzel et al., 1995; Füchtbauer, 1995] has now been narrowed to the mid to late streak-stage. I was able not only to confirm the strong expression in the anterior, prospective head, mesenchyme, but also to show downregulation, at the head fold stage, of *Twist1* from the posterior mesoderm.

R2.5 *Twist1* Expression in The Primitive Streak Controversy

While *Twist1* expression in the mesoderm is undisputed, the moment when *Twist1* begins to be expressed in a mesoderm cell enjoys less consensus. Füchtbauer, 1995 reported that only cells "at a distance from PS" express *Twist1*, while Stoetzel et al., 1995 reported *Twist1* expression in the PS, see Appendix 2.

When studying *Twist1* expression in embryos of all relevant stages, I could find no evidence that this marker is present in the PS.

First, *Twist1* is upregulated very weakly, after PS formation and, at this point, the staining is not confined or even apparent in PS. Thus, it is clear that at least for the early cells migrating from the PS, *Twist1* upregulation is a subsequent event, which probably correlates with the differentiation of these cells.

Second, at the bud stage, when staining becomes more convincing it is possible to tilt the embryo so that mesodermal signal would appear as located in the epiblast. Yellow arrow in **Fig R2.3e** points to a group of positive cells, which in the frontal view, can be easily identified as mesoderm cells. However, if the embryo is rotated to lateral view, the usual way of imaging embryos, the same signal seems to come from the epiblast [**Fig 2.3f**].

Fig R2.4a shows a late bud stage embryo with what appears to be strong staining in the posterior epiblast. This image is similar with images in the literature on which *Twist1* PS expression claim is based. However, this again, is just

superimposition of lateral planes, as all embryos appear clear when viewed from posterior [**Fig R2.4d**]. Furthermore, if one wants to recognize that signal as real epiblast signal, one would have to consider the fact that immediately adjacent mesoderm cells are negative and hence, infer that mesoderm cells downregulate *Twist1* when migrating from the epiblast. Thus, according to such a theory, *Twist1*, an EMT inducer, would be expressed in the epithelial epiblast and downregulated as soon as mesodermal cells begin their migration.

Third, Füchtbauer, 1995 showed the absence of *Twist1* on transverse sections, while no such sections have been published by the proponents of *Twist1* expression in PS.

Moreover, even in cephalochordate, the evolutionary precursor of vertebrates, *twist* homologue is not expressed "during initial mesoderm formation … unlike in Drosophila" [Yasui et al., 1998]. This suggests that *Twist1* expression later in mesoderm differentiation is a feature conserved in the chordate branch of evolution.

However, since the question of *Twist1* expression in PS is not central to my project, I did not pursue this matter any further, as deciding beyond any doubt would require careful sectioning of all stages from streak to head fold. It is regrettable, though, that most authors, considering *Twist1* as a mesoderm marker accept its expression in PS on insufficient evidence.

R2.6 *Twist1* Expression during Somitogenesis

As somitogenesis begins and the embryo starts to turn, the main difference in *Twist1* expression is represented by the new signal domain which now comes from the somites and the mesoderm cells condensing to form a new somite [**Fig R2.5**]. The distal limit of *Twist1* expression domain, has now transformed into a posterior limit [**Fig R2.5**, **black arrow**; see also **Fig R2.6b**]. The positive extraembrionic mesoderm is connected by two strings of lateral mesoderm, the only portion of the embryo proper which has *Twist1* expressing cells beyond the posterior limit.

Figure R2.5. New *Twist1* domains: somites and lateral mesenchyme.

Whole mount in situ hybridization for Twist1 of embryos at early somitic stages. 3 somite stage (a), 6 somite stage (b and c). C presents lateral view of the embryo in b. Black arrow indicated the caudal limit of Twist1 domain, which corresponds to the point to which somitogenesis has progressed. Red arrow points to the head mesenchyme. Yellow arrow points to neural folds. Blue arrow shows the base of the allantois. Rostral side (rost), caudal side (caud). Scale bars represent 50 μm.

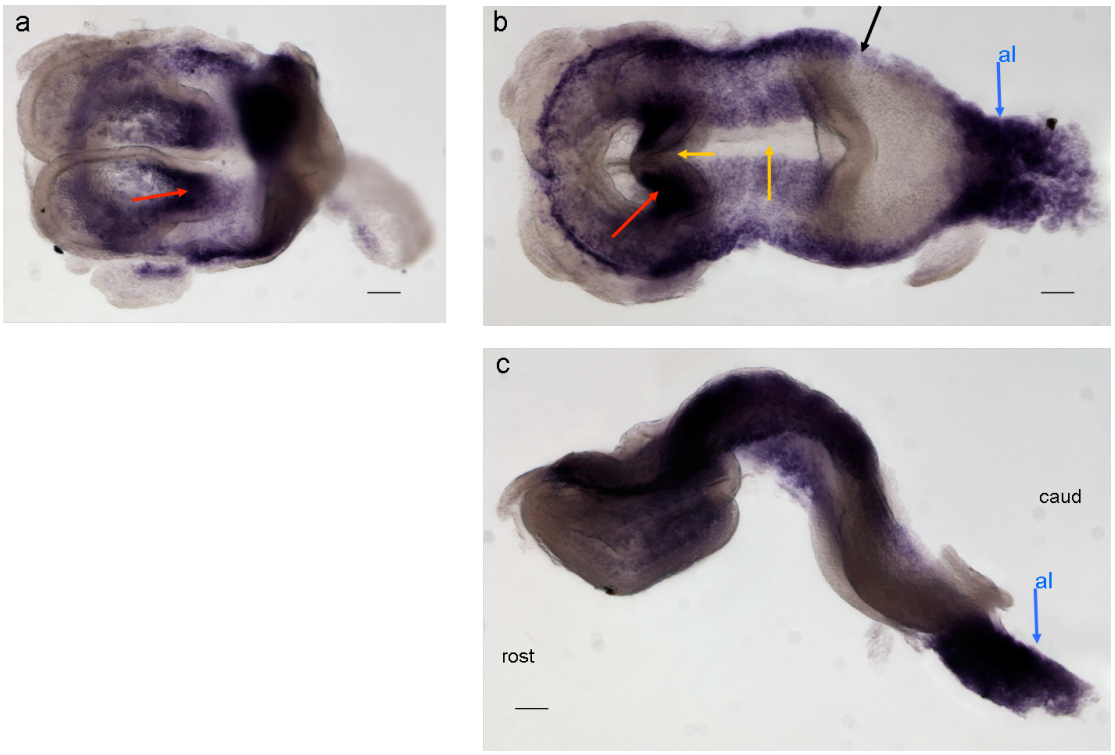
a
b
al
c
caud
al
rost

Head mesenchyme continues to express strongly especially under the neural folds [**Fig R2.5a and b**]. The ectoderm remains negative, including the neural ectoderm.

As the first branchial arch is formed it represents a new domain of *Twist1* expression, where at this stage, the signal is stronger than in any other structure. The ectoderm of the branchial arch is negative and, can be seen as a translucid hallo surrounding the arch [**Fig R2.6** red arrows].

Since the purpose of this experiment was to identify any signal in the neural tissue, which was assumed to be very weak, if at all, or else it would have already been reported, embryos were developed for 48 hours, a time at which most strongly positive structures were saturated. **Fig R2.6b and c** shows two embryos of close age. The embryo in (c) has only been developed for 4 hours. Here the difference in intensity between the fist branchial arch and the rest of the positive structures can be seen more clearly.

Interestingly, all previously reported expression domains can also be distinguished with this shorter developing time. Furthermore, a subset of heart mesenchyme, which is positive for *Twist1* can observed.

At 9.5 dpc [**Fig R2.6d**] the signal continues to be strong without any major changes in the domains of expression.

The body of data presented in this section, largely confirms the previously published information on *Twist1* expression in mouse development. Some clarifications have been produced on small points while, no indication could be obtained regarding *Twist1* expression in the neural tissue at the studied stages in the wholemount analysis.

Figure R2.6. *Twist1* expression remains constant for later stages.

Whole mount in situ hybridization for Twist1 of embryos at mid and late somitic stages. 8.5 dpc turning embryos (a, b and c). 9.0 dpc embryo (d). C presents an embryo developed for shorter time. Black arrow indicated the caudal limit of *Twist1* domain, which corresponds to the point to which somitogenesis has progressed. Red arrow indicates the clear ectoderm surrounding the cells which express *Twist1* at very high levels in the brachial arch. Yellow arrow indicates the *Twist1* positive cells in the heart mesenchyme. Scale bars represent 100 μm.

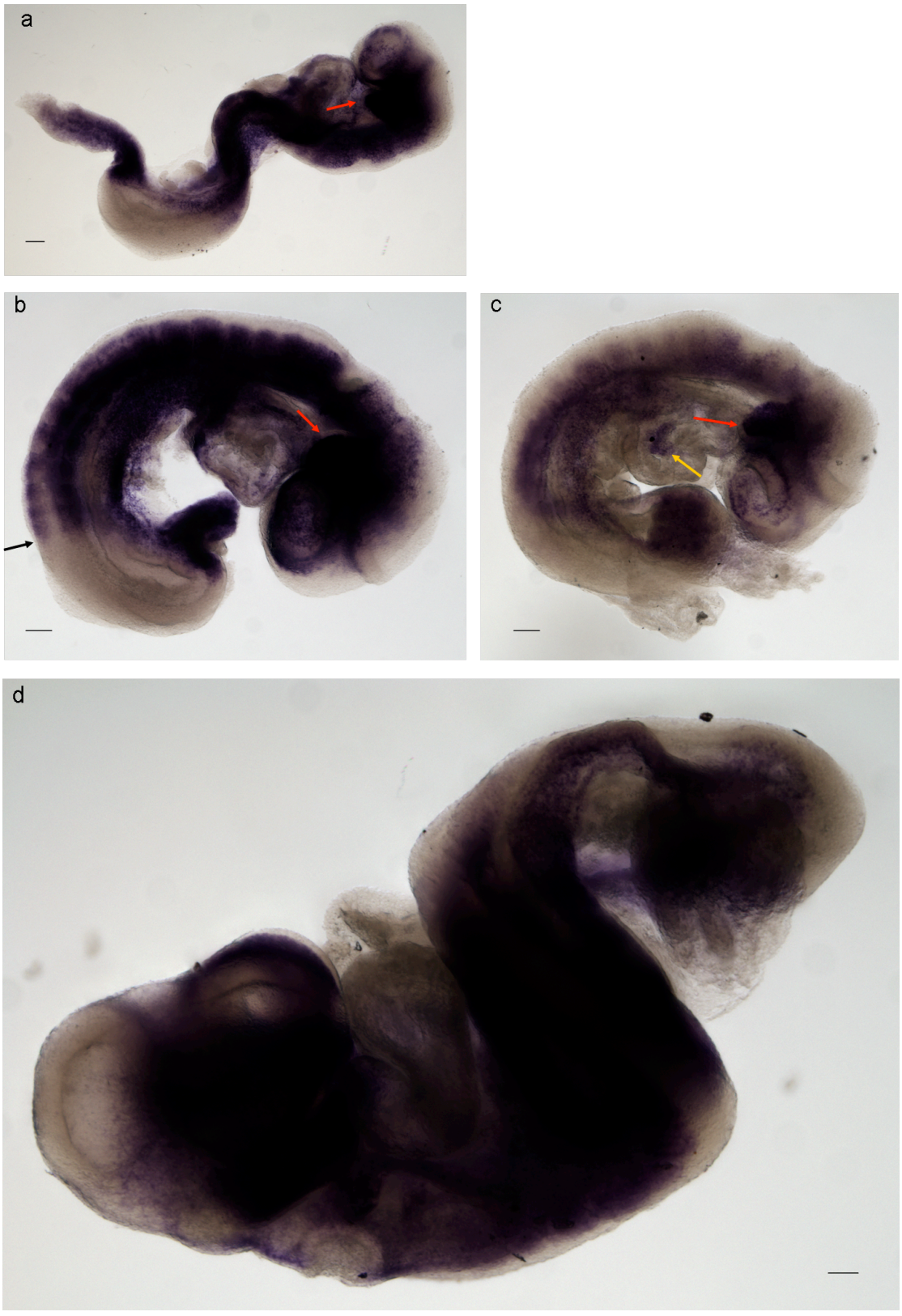
a
b
c
d

R2.7 *Twist1* Is Weakly Expressed in Dorsal Neural Folds.

Since *Twist1* appeared to be not expressed in the neural tube, even by employing the method of extending in situ developing time, transverse embryo sections were imaged to confirm or rule out any possible *Twist1* signal in neural cells. Embryo sectioning was performed by Ronald Wilkie.

One possible problem with whole embryos imaging could have been the fact that the strong mesoderm signal might obscure an eventual weaker signal in the neural tube. This would be overcome as well by imaging sections.

At the bud stage, section imaging revealed *Twist1* expression in the expected domains: extraembryonic mesoderm, and embryonic mesoderm lateral of PS [**Fig R2.7a to g**].

At the somitic stage, expression in the mesodermal compartment is obvious. However, now a second weaker domain can be seen in the neural folds. In more posterior regions [**Fig R2.8a to d**], the signal is so weak it can barely be observed, appearing more like a shadow on the dorsal side. However, at careful examination, this shadow can be clearly distinguished from ventral side which is completely staining free.

As the sectioning plan moves more anteriorly, towards the hindbrain, the signal becomes restricted to the dorsal tip of the folds [**Fig R2.8e to g**]. At this level the signal is more evident and individual positive cells can be distinguished: see **Fig R2.8h** presenting a magnification of the tip of the fold in (g).

A few hours later, after the embryo has turned, the neural folds at the spinal cord level become clear, devoided of any signal [**Fig R2.9a**]. On the other hand, at the brain level, the signal is now limited to the very edge of the neural fold [**Fig R2.9 b to d and h**]. The more posterior regions of the forebrain are the first to close, before the more anterior ones. **Fig R2.9e to g** shows this region as the neural folds are just about to fuse.

Figure R2.7. *Twist1* an early mesoderm marker.

Transverse sections of whole mount in situ hybridization for *Twist1* of early bud embryo. Sections are arranged from proximal to distal: a to g. Posterior side of the embryo is marked with an asterisk. Ectoderm (red arrow), endoderm (yellow arrow). Scale bars represent 50 μm.

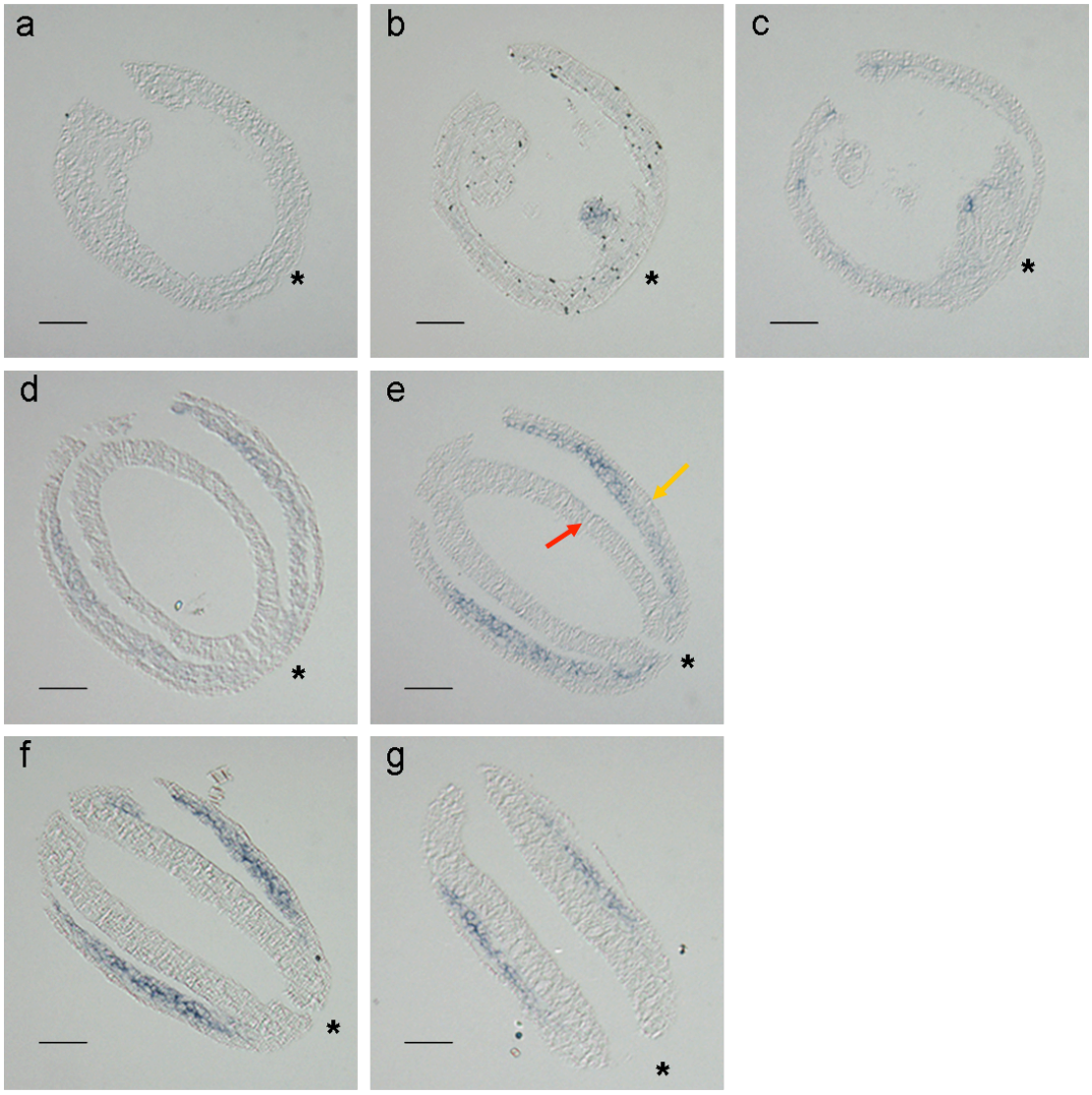
a
b
c
d
e
f
g

Figure R2.8. *Twist1* is weakly expressed in the dorsal neural tube.

Whole mount in situ hybridization for *Twist1* of an 8.5 dpc embryo sectioned from posterior to anterior (a to g) as shown in (i). Magnification of the box in (g) focussing on dorsal neural tube (h). Neural fold (nf, red arrow), somite (so, yellow arrow), head mesenchyme (hm, blue arrow), branchial arch (ba, purple arrow). Scale bars represent 50 μm.

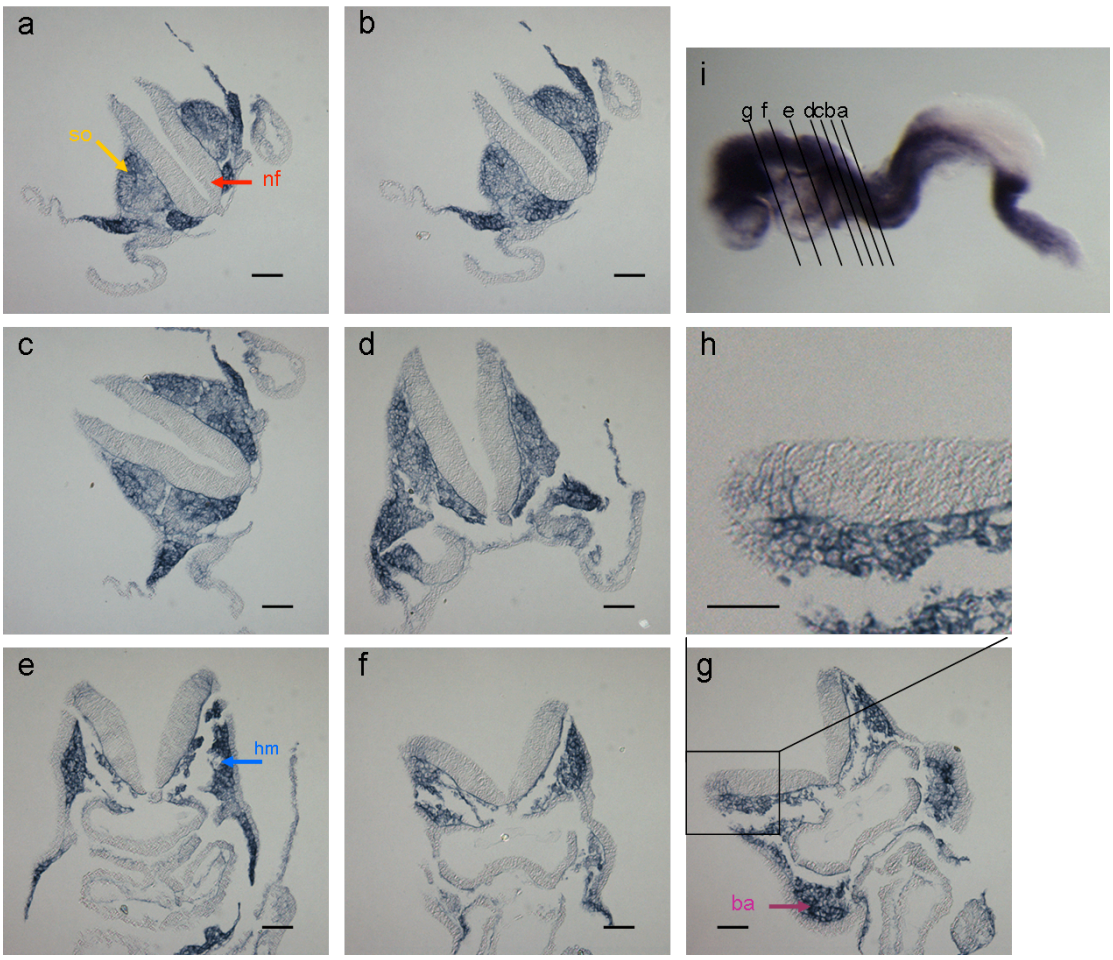
a
so
nf
b
i
g f e d c b a
c
d
h
e
hm
f
g
ba

Figure R2.9. *Twist1* signal localizes to the dorsal edges of the neural folds before closure.

Whole mount in situ hybridization for *Twist1* of an 9.0 dpc embryo sectioned from posterior to anterior (a, b and e) as shown in (i). (b) shows a section through hindbrain and frontbrain presented at a higher magnification in (c and d) respectively. Magnification of the box in (g) focussing on dorsal neural tube (h). Magnification of box showing dorsal neural fold in the hindbrain (h). Consecutive section after (e) restricted to the neural folds (f and g). Forebrain (fb, red arrow), hindbrain (hf, yellow arrow) branchial arch (ba, purple arrow). Scale bars represent 50 μm.

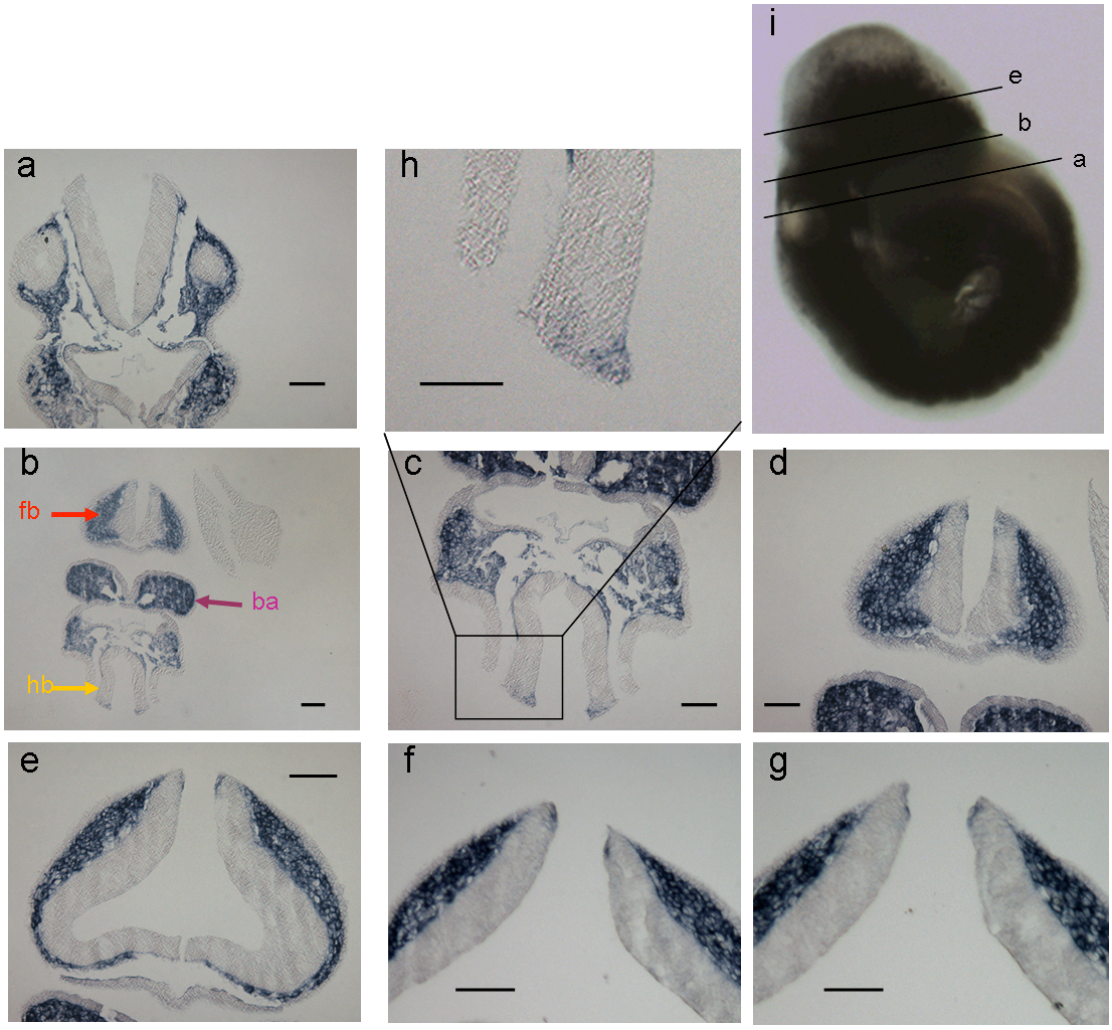
a
h
i
e
b
a
b
fb
ba
hb
c
d
e
f
g

Here *Twist1* signal is slightly stronger, but restricted to just one or two cell in each plane and fold; the cells which most likely are going to be involved in the fusion process.

R2.8 TWIST1 Non Autonomous Roles Tested *In Vitro*

In the previous section I provided evidence for the existence in the neural folds of cells which express *Twist1* at low levels and which are restricted to the dorsal regions. These data make the previously suggested non-autonomous mechanism of action no longer obligatory, while raising new possibilities.

However, a non-autonomous role is still possible: that of the influence of neural cells expressing *Twist1* over neighbouring neural cells, which lack this marker. To test this hypothesis an experiment was designed where a mixture of cells inducible for the active dimer TwE and non-inducible cells were differentiated together.

First, a TwE inducible cell line was labelled with Tomato fluorescent protein localized to the nucleus. For this purpose a plasmid, produced by Frederick Wong in the lab of Prof Ian Chambers, containing a CAG-H2B-td Tomaoto-Ires-Puromycin construct was used. Since the cells I intended to label, the doTE77 line, already contained a Puromycin resistance gene, I replaced the Puromycin selection cassette, with Hygromicin, in the mentioned plasmid, as described in Material and Methods; resulting plasmid is presented in **Fig R2.10a**.

Using this plasmid to transfect TwE inducible cells resulted in generation of double resistant cell lines containing pCAG-Puro-TetO-TwE and pCAG-H2B-Tomato-IRES-Hygro. A cell line, called doTE77T2 which expressed Tomato in every cell was used [**Fig R2.10b**]. This cell line had a similar response to Dox induction during neural differentiation as the parental cell line: doTE77, as judged by premature neurite formation.

Figure R2.10. Tomato labelling of TwE inducible cells

Schematic representation of the plasmid used for labelling TwE inducible cells (a). Subclone T2 of clone doTE77 expresses Tomato in all cells. Fluorescence: left column blue channel, right column red channel (b). Scale bars represent 50 μm.

a

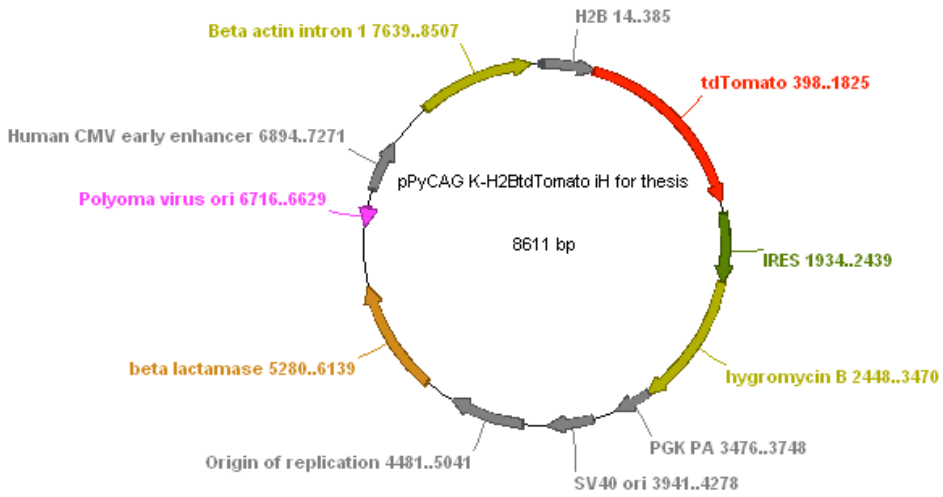
H2B 14..385
Beta actin intron 1 7639..8507
tdTomato 398..1825
Human CMV early enhancer 6894..7271
pPyCAG K-H2BtdTomato iH for thesis
Polyoma virus ori 6716..6629
8611 bp
IRES 1934..2439
beta lactamase 5280..6139
hygromycin B 2448..3470
PGK PA 3476..3748
Origin of replication 4481..5041
SV40 ori 3941..4278

b

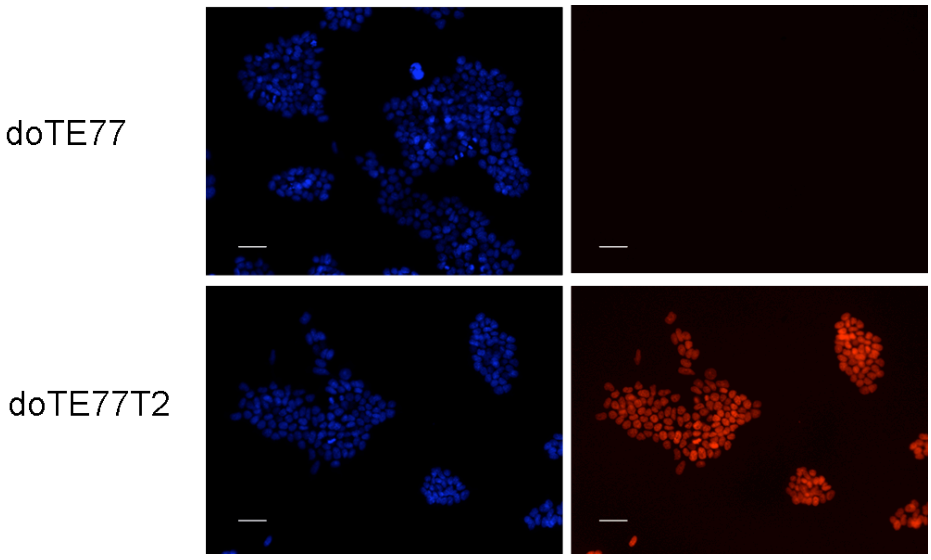
doTE77
doTE77T2

Figure R2.11. Diagram of cell mixing experiments strategy.

TwE inducible ES cells labelled with Tomato, clone doTE77T2 were mixed 1:1 with Sox1-GFP reporter cells, 46c. The mixture of cells was put through neural differentiation in the monolayer protocol for 4 day, a time point at which the majority of 46c cells were expressing GFP. The two population were separated by FACS and, RNA was extracted.

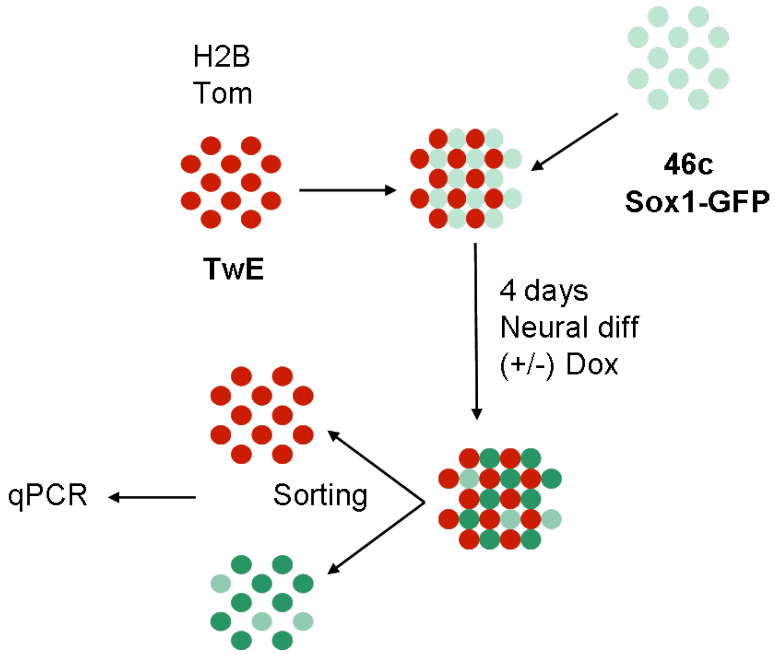
H2B
Tom
TwE
46c
Sox1-GFP
4 days
Neural diff
(+/-) Dox
Sorting
qPCR

Fig R2.11 shows the experimental design for cell mixing differentiation. Briefly, TwE inducible, Tomato labelled cells were mixed with Sox1-GFP, 46c cell line [Ying et al, 2003b], in a ratio of 1:1 in N2B27 with or without Dox. After 4 days of differentiation, the majority of 46c cells express GFP, indicating that they underwent neural differentiation. The two cell lines were once again separated by FACS, based on red fluorescence and, RNA extracted from each cell population.

R2.9 TwE Does Not Accelerate Neural Differentiation Non-Autonomously.

At the first analytic step of the experiment: cell separation based on flow cytometry after 4 days of differentiation, it was observed that the presence of TwE cells did not generally alter the process of neural differentiation in the neighbouring, non-inducible cells. Sox1, as reported by GFP was upregulated in 46c cell line in a similar percentage of cells and at the same level, regardless whether the neighbouring cells were induced or not for TwE [**Fig R2.12**].

However, a subtle but interesting phenomenon was observed at the level of the cells which upregulated Sox1 at very low levels or did not upregulate it at all. When TwE was induced, there was a clearer separation between GFP+ and GFP- cells in the 46c line [**Fig R2.12b and c** black arrows]. This could indicate that TwE expressing cells "help" other differentiating cells to make a decision between neural and non-neural and, is consistent with Twist1 being expressed in cells close to neural/surface-ectoderm border.

Next, neural induction/differentiation markers in the two populations were analysed by qPCR. For TwE inducible cells, the expected pattern for tested markers, as reported in the previous chapter, was observed. On the other hand, no difference for any of the markers was seen for 46c cell line when cultured either with TwE induced or not-induced cells [**Fig R2.13**: *Twist1* (a), *Sox1* (b), *Zfp521* (c), *Atoh1* (d), *Pax3* (e) and *Sox9* (f)].

Figure R2.12. TwE induction does not facilitate non-autonomously neural induction.

Flow cytometry of ES cells differentiated for 4 day in the neural monolayer protocol. Mixed culture of TwE inducible cells labelled with H2B td-Tomato and 46c-Sox1-GFP cells. Pseudocolour blot of uniduced samples (a) and induced samples (b). Ellipses for (a) and (b) indicate populations which were sorted as Tomato positive (green arrows) and Tomato negative (red arrows). Vertical bars in the lower ellipses indicate the GFP 15% lowest and highest population respectively. In induced samples the GFP negative and positive population are better separated (black arrow), but the overall GFP positive population is not shifted. Histogram of the non-red population only (c). Vertical bars indicate gating for the GFP negative, low and high populations respectively. Percentage of GFP neg and GFP low cells in uninduced and induced samples respectively from the histogram (c) are presented in (d). Error bars represent standard deviation of the mean for two replicate experiments.

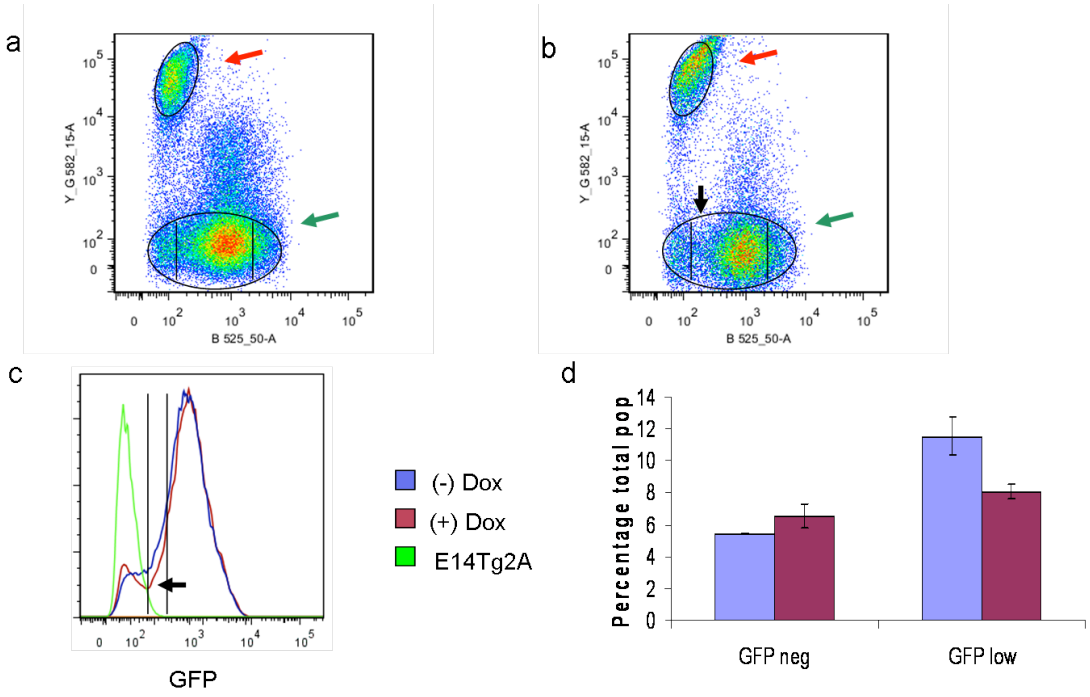
a
b
c
d
Y_G 582_15-A
B 525_50-A
GFP
(-) Dox
(+) Dox
E14Tg2A
Percentage total pop
GFP neg
GFP low

Figure R2.13. TwE does not influence neural differentiation non-autonomously.

qPCR for *Twist1* (a), *Sox1* (b), *Zfp521* (c), *Atoh1* (d), *Pax3* (e) and *Sox9* (f) for sorted TwE inducible and Sox1-GFP reporter cells after 4 days of coculture in neural differentiation conditions. For each gene, expression in Sox1-GFP reporter cells in the Dox not-treated condition has been arbitrarily set to 1. One experiment performed in duplicates is shown. Error bars represent value range.

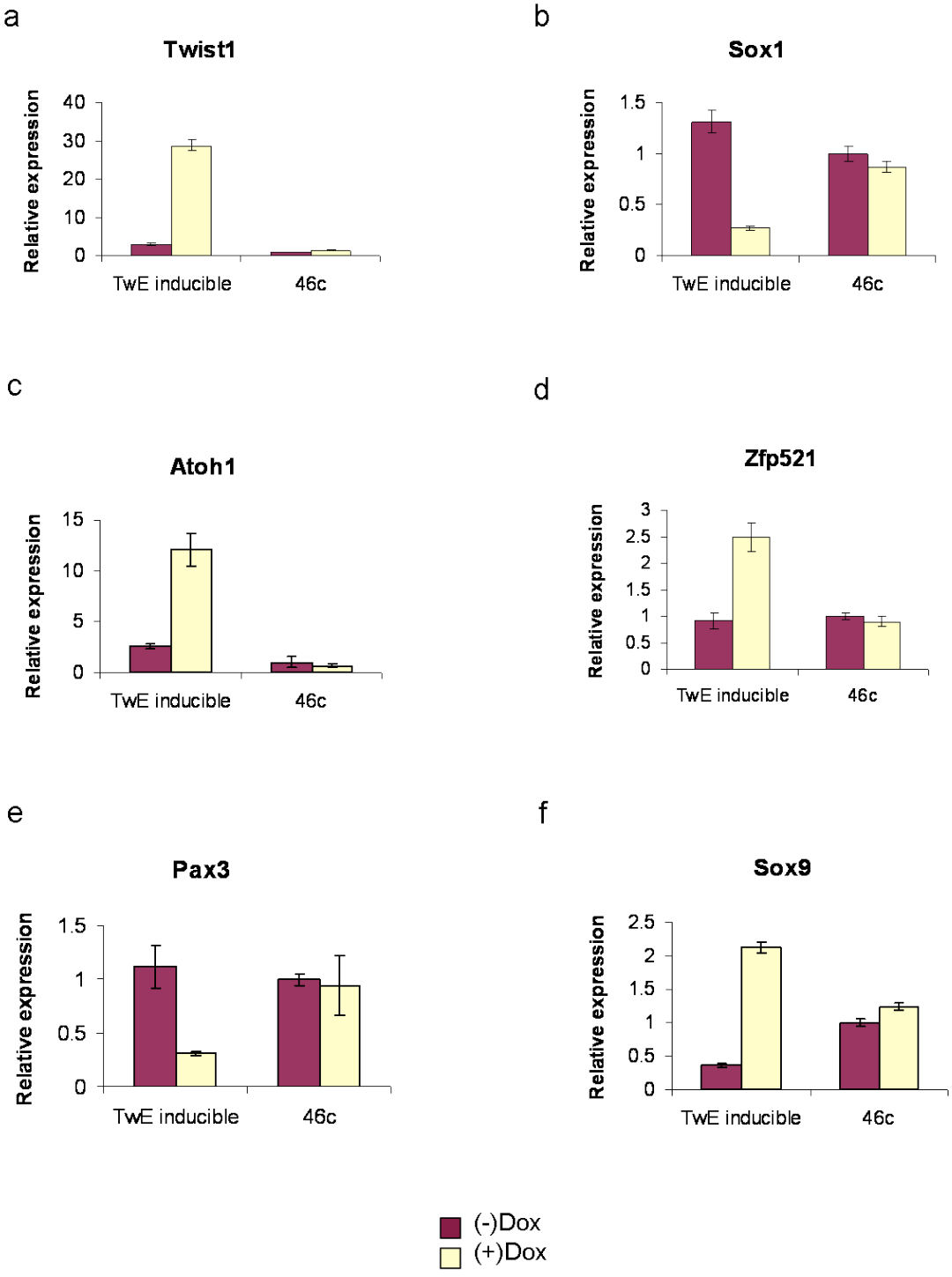
a
Twist1
Relative expression
40
30
20
10
0
TwE inducible
46c
b
Sox1
Relative expression
1.5
1
0.5
0
TwE inducible
46c
c
Atoh1
Relative expression
15
10
5
0
TwE inducible
46c
d
Zfp521
Relative expression
3
2.5
2
1.5
1
0.5
0
TwE inducible
46c
e
Pax3
Relative expression
1.5
1
0.5
0
TwE inducible
46c
f
Sox9
Relative expression
2.5
2
1.5
1
0.5
0
TwE inducible
46c
(-)Dox
(+)Dox

Figure R2.14. TwE does not recapitulate non-autonomously its autonomous influence on neural differentiation.

qPCR for *Sox1* (a), *Zfp521* (c), *Sox9* (c) and *Pax3* (d) for sorted TwE inducible and Sox1-GFP high and low cells after 4 days of coculture in neural differentiation conditions. For each gene, expression in TwE inducible cells in the Dox not-treated condition has been arbitrarily set to 1. Error bars represent standard deviation of the mean for two biological replicates. One experiment performed in duplicates is shown. Error bars represent value range.

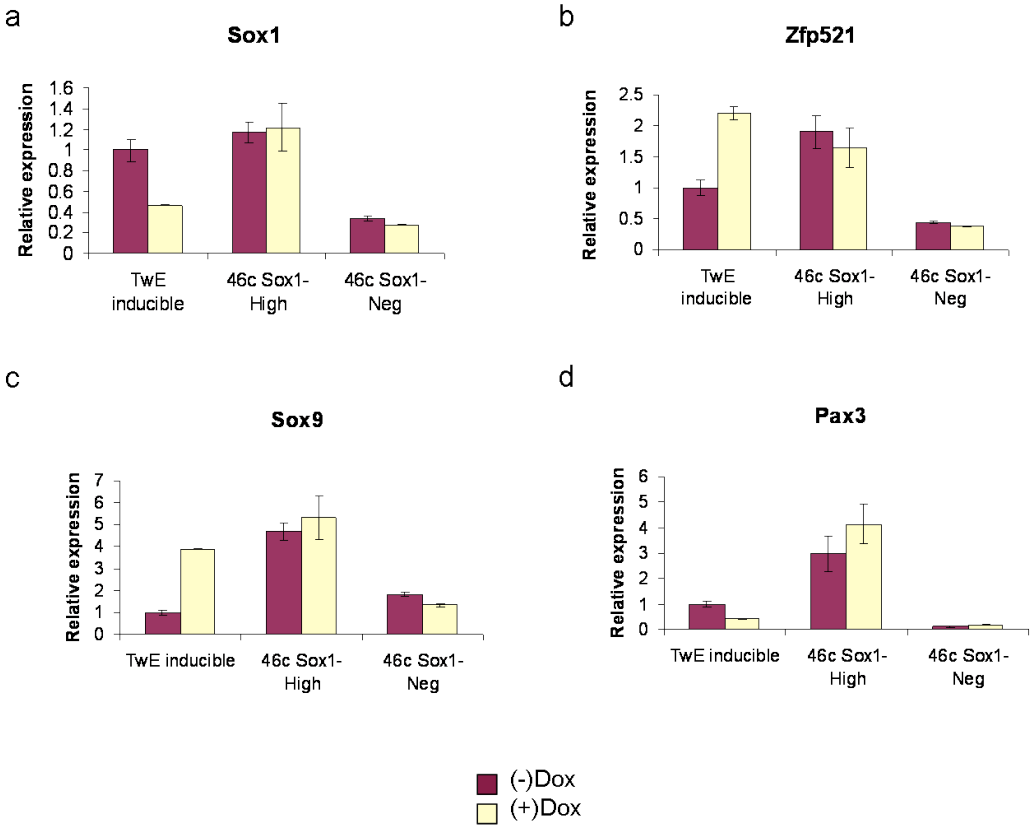
a
Sox1
Relative expression
1.6
1.4
1.2
1
0.8
0.6
0.4
0.2
0
TwE inducible
46c Sox1-High
46c Sox1-Neg
b
Zfp521
Relative expression
2.5
2
1.5
1
0.5
0
TwE inducible
46c Sox1-High
46c Sox1-Neg
c
Sox9
Relative expression
7
6
5
4
3
2
1
0
TwE inducible
46c Sox1-High
46c Sox1-Neg
d
Pax3
Relative expression
6
5
4
3
2
1
0
TwE inducible
46c Sox1-High
46c Sox1-Neg
(-)Dox
(+)Dox

The data indicate that there is no modification in neural progenitor dynamics (*Sox1* and *Zfp521*), no early entry to mature cell phenotype (*Sox1*, *Atoh1*), and no dorso-ventral bias (*Atoh1*, *Pax3* and *Sox9*) induced by TwE on Sox1-GFP cells.

There was a possibility that the absence in marker expression change was due to an upregulation, for instance, in the GFP high population, masked by a downregulation in the GFP low population. To test for this hypothesis a similar experiment was designed, where the Tomato negative cells were sorted based on the 15% highest and lowest GFP expression. In this case, clear differences could be seen between GFP high and low population but not between non-inducible cells differentiated in the presence or absence of Dox [**Fig R2.14**].

This experiment confirms that the presence of TwE expressing cells does not alter *in vitro* neural differentiation in the neighbouring cells.

R2.10 TwE Non-Autonomously Influences Fate-Choice Decisions

Analysis of Sox1GFP expression which indicated that there might be a bias in fate decision [**Fig R2.12**] was somewhat contradicted by qPCR analysis of differentiation markers in sorted populations, which showed no difference in expression of neural marker brought about by non-autonomous expression of *Twist1* [**Fig R2.13**]. There was a possibility that the effect noticed by flow cytometry as a population shift was too small to have any phenotypic significance. However, taking into consideration the *Twist1* expression at the dorsal edge of the neural fold, there was a possibility that, from that position it might influence the fate choice between neural crest and surface ectoderm, and not neural differentiation per se. I therefore, set out next to investigate markers of neural crest and surface ectoderm in this experiment.

Figure R2.15. TwE non-autonomously stimulates the neural differentiating population to adopt a neural crest fate.

qPCR for *Wnt1* (a and c) and *Gata2* (b and d) for sorted TwE inducible and Sox1-GFP high and low cells after 4 days of coculture in neural differentiation conditions. For each gene, expression in TwE inducible cells in the Dox not-treated condition has been arbitrarily set to 1. Error bars represent standard deviation of the mean for two biological replicates. For each graph one experiment performed in duplicates is shown. Error bars represent value range.

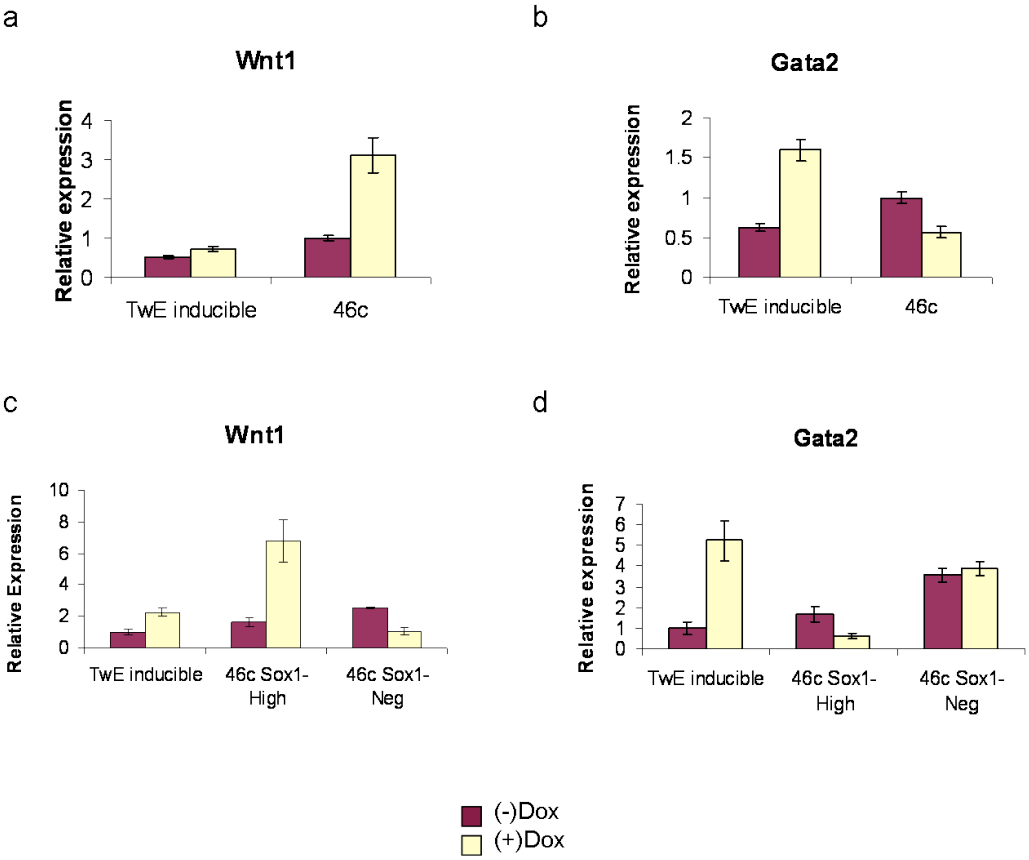
a
Wnt1
Relative expression
4
3
2
1
0
TwE inducible
46c
b
Gata2
Relative expression
2
1.5
1
0.5
0
TwE inducible
46c
c
Wnt1
Relative Expression
10
8
6
4
2
0
TwE inducible
46c Sox1-High
46c Sox1-Neg
d
Gata2
Relative expression
7
6
5
4
3
2
1
0
TwE inducible
46c Sox1-High
46c Sox1-Neg
(-)Dox
(+)Dox

Upregulation of *Wnt1* is one of the most specific markers of neural crest cells which are preparing to delaminate from the neural tube [Echelard et al., 1994; Chai et al., 2000], while *Gata2* is a marker of surface ectoderm [Sheng & Stern, 1999; Basch et al., 2006].

When *Wnt1* was tested I found it to be markedly upregulated in 46c cells differentiated in the presence of TwE expressing cells. On the other hand, *Gata2* was downregulated in 46c line under TwE expressing cells influence [**Fig R2.15a and b**].

Furthermore, when tested against populations separated based on GFP expression, *Wnt1* was found to be specifically upregulated in the neural differentiating cells, but downregulated in cells which failed to turn on *Sox1*. On the other hand *Gata2* was downregulated only in *Sox1* high cells but permitted in *Sox1* low cells [**Fig R2.15c and d**].

Together, these data reveal that TwE expressing cells could have a fate choice influence, consistent with their potential location at the border between neural ectoderm and surface ectoderm. Thus, TWIST1 can non-autonomously upregulate *Wnt1* and suppress *Gata2* in neighbouring neural cells. On the other hand, surface ectoderm cells, which are present close by, have their fate safeguarded by *Wnt1* suppression and *Gata2* expression.

However, upregulation of *Wnt1*, a neural crest marker and, dorsal morphogen, did not induce upregulation of other neural crest markers like *Sox9* or *Pax3*. One explanation is that in the course of the in vitro differentiation there was not enough time for Wnt1 to influence cell fates. However, another explanation could be that *Pax3* and *Sox9* being expressed before *Wnt1* are not downstream the latter gene, or that WNT1 requires other partners, like BMP, absent from the artificial cell culture system, to further induce neural crest markers.

R2.11 Conclusions

In this chapter I started from the observation that TwE induction has a dorsalizing effect on neural differentiation as assessed by marker expression level.

Then, I challenged the idea that *Twist1* is absent from the neural tissue and, showed that it is expressed at low levels in a time and domain restricted manner. It starts by being expressed in the dorsal parts of the neural folds both in the brain and in the spinal cord; expression in the spinal cord being weaker and more diffuse. As the neural folds prepare for the fusion process, *Twist1* expression is lost from the spinal cord and is gradually restricted more dorsally in the prospective brain until only the cells in the fusing margins still express this marker. I showed that this weak and restricted expression cannot be observed in whole embryos and that on sections was only detected due to being purposefully looked for and, by using a staining saturating technique. This may explain why this expression domain has not been reported previously in the literature

Finally, based on in vitro differentiation experiments I proposed a role for *Twist1* expressing cells, concerning cell fate decisions at the border between neural and surface ectoderm. I also showed that although TwE has a dramatic and, one might even call it devastating, effect on neural differentiation in the cells in which it is expressed, it does not seem to have a readily observable effect on neural differentiation in neighbouring cells, at least not for markers tested here.

Twist1 is a well known neural crest marker and in my experiments it mildly increased *Wnt1* expression autonomously and, markedly non-autonomously. A question here rises if *Wnt1* in neural crest cells might be downstream of *Twist1;* in which case *Twist1* should be expressed in neural crest cells before their delamination from the neural tube. The large number of neural crest cell leaving the neural tube stand in stark contrast with the very few cells expressing *Twist1*. On the other hand, it is possible that neural crest cells upregulate *Twist1* at, or around the time of delamination from the neural tube. Since this is a sudden process in the brain I would have missed it in my analysis. A much more detailed investigation of the stages from

neural fold to mid somitogenesis stages would have been required. It should also be noted that *Twist1* can be observed as soon as the neural crest domain forms outside the neural tube, indicating that this marker is either upregulated at the time of delamination or, immediately after.

I propose a mechanism, in which a subset of dorsal neural cells upregulate *Twist1* before anterior neural tube closure, around the time of neural crest delamination. They stabilize the neural program in the neighbouring cells by downregulating *Gata2*, strengthen the dorsal identity by inducing *Wnt1* while autonomously upregulating dorsal markers like *Pax3* and *Sox9*. The later neural crest marker *Sox10* is not upregulated as these cells are not necessarily fated to become neural crest. Then, the cells which are to remain in the neural tube, downregulate *Twist1*, before *Pax3* and *Sox1* would be negatively influenced and, the exit from neural progenitor state risked.

The data presented in this chapter highlights an important question: "why is *Twist1* expressed at much lower levels in neural versus mesoderm tissue?" I will address this question in the next chapter.

Figure R2.16. Schematic Conclusions

Twist1 is expressed in the developing neural tissue in very restricted manner in time and space. Its expression can only be detected after the head fold stage and is lost as soon as the anterior neural folds fuse (a). It is of note that before the fusion of the anterior neural folds, *Twist1* can be observed at the trunk level as well, but the expression in this domain ceases even before the expression in the anterior. In vitro data suggest that active TWIST1 favours neural dorsal fate on the expense of both ventral neural fate and surface ectoderm (b).

a

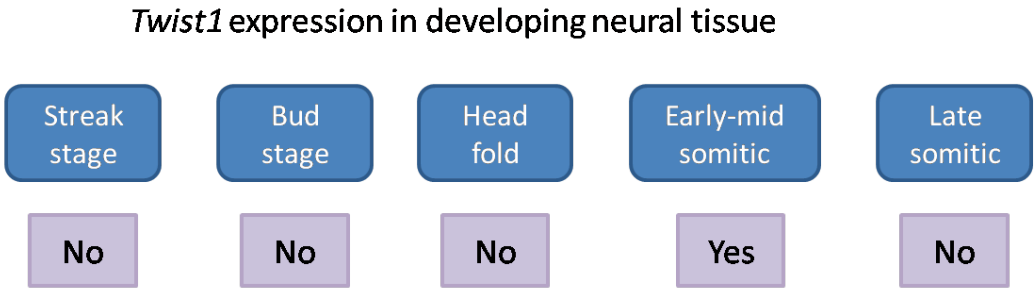
Twist1 expression in developing neural tissue
Streak stage
Bud stage
Head fold
Early-mid somitic
Late somitic
No
No
No
Yes
No

b

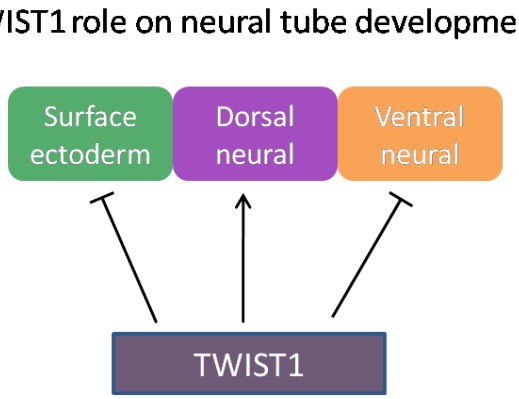
TWIST1 role on neural tube development
Surface ectoderm
Dorsal neural
Ventral neural
TWIST1

V. RESULTS 3

TWIST1 LEVELS OF ACTIVITY DECIDE CELL FATE

R3.1 Overview

Pluripotency is a cellular state which can be maintained indefinitely *in vitro*, but exists only briefly *in vivo*. Both *in vivo* and *in vitro* transcriptional mechanisms exist which allow a cell to follow its developmental program through differentiation [Chambers et al., 2003; Ying et al., 2008]. Such transcriptional effectors should be able to induce differentiation, but are kept inactive in pluripotent cells. In Results_1 I analyzed the possibility that the transcriptionally active TwE functions in the induction of neural differentiation from pluripotent cells. The work had been based on *Twist1* expression in ES and differentiating cells as well as on the notion that in the absence of BMP signalling, TWIST1 partner choice would be biased towards formation of TW-E dimers. Using a cell line in which TwE could be induced at levels comparable with observed *Twist1* upregulation during *in vitro* neural differentiation I noticed an acceleration of neural differentiation in response to TwE. A partial rescue of neural differentiation against BMP4 was also effected by TwE.

Expression analysis in the mouse embryo, as described in Results_2, indicated that *Twist1* is not expressed in pluripotent epiblast cells. One possibility would be that *Twist1* expression in ES cells is simply a cell culture artefact and is not informative in respect to any physiological process. However, there is still a possibility that while not usually involved in early differentiation events, *Twist1* could be recruited to such an end, in special circumstances, as might be the case of *in vitro* differentiation. Either way, *Twist1* presence in ES cells indicates that, at least at certain levels, it can be tolerated without compromising the pluripotency.

Furthermore, at somitogenesis *Twist1* is massively upregulated, over 100 fold compared to ES cells, by whole embryo mRNA levels. When in situ data is taken into consideration it has to be concluded that this upregulation is generated mainly by the mesenchyme. On the other hand, high levels of *Twist1* have not been observed either

in vivo or *in vitro* in pluripotent or neural differentiating cells. High *Twist1* levels could simply be a molecular mark of the mesenchyme. An alternative hypothesis would be that pluripotency cannot be maintained if *Twist1* is expressed beyond a certain threshold. Moreover, the neural differentiation program might be incompatible with high levels of *Twist1*.

Following the above considerations I asked the questions whether:

1. High, but still physiological levels of active *Twist1* are capable of forcing the exit from pluripotency?
2. *Twist1* high levels of activity could bias differentiation away from the neural program towards mesenchyme?

By physiological levels of Twist1 I understand levels of expression not exceeding expression observed in certain cell types, like the mesenchyme.

In this chapter, I analyse the effects of TwE induction at levels, comparable with *Twist1* levels in the mesenchyme, in pluripotent cell differentiation. I show that high expression of TwE is not compatible with maintenance of pluripotency in mouse ES cells and, that neural differentiation is blocked. Finally, taking into consideration the idea that BMP activity could influence TWIST1 dimer choice I analyse the effects of TWIST1-TWIST1 forced dimer (TwTw) in the context of neural differentiation.

R3.2 TwE Forces Differentiation of ES Cells.

R3.2.1 Generation and Characterization of ES Cell Lines Expressing TwE at Relatively High Levels

Expression analysis indicated that during *in vitro* differentiation *Twist1* mRNA levels is upregulated up to 30 fold [Aiba et al., 2009; Lowell lab unpublished data], while in whole embryos, at a time when the mesenchyme form an important part of the embryo, it is upregulated over 100 fold compared with its expression in ES cells

[**Fig R2.2a**]. In order to test the effects of higher TwE levels it was necessary to obtain clones which could be induced to express the transgene at higher levels, which would reflect more closely the expression levels in the mesenchyme. I inferred that the reason behind the difficulty of obtaining TwE high level inducible clones was the potential leakiness of a pluripotency detrimental factor. In order to mitigate this phenomenon, I isolated new clones, supplementing the standard ES cell media with PD0325901, a MAP2K inhibitor. Using this method, I was able to isolate clones which stained brightly, albeit still heterogeneously, when screened for Flag immunofluorescence, with some of them expressing TwE RNA at higher levels than the clone doTE77, used previously [**Fig R3.1**].

R3.2.2 TwE Induced Cells Lose ES Cells Morphological Characteristics

In order to test self renewal in defined conditions, cells were established in N2B27 supplemented with LIF and BMP4, by being cultured in these conditions for two weeks. The cells were passaged every two days. The passage at which Dox was first added was considered passage 1. After 48 hours cells were imaged, trypsinized and, replated in the same conditions. This was considered passage 2. The procedure was continued in the same manner up to passage 4. Details of cell culture procedure are presented in **M2.2.1** and **M2.2.4**.

From the first passage it was observed that cells differentiated in response to TwE induction. After the first 48 hours of treatment two morphologically distinguishable cell populations segregated [**Fig R3.2**]. These populations consisted of cells in tight colonies which resembled pluripotent cells (red arrows), surrounded by small mesenchymal like cells which covered the remainder of the available culture surface (yellow arrows). This feature was initially similar among multiple clones. However, as the cells were passaged, clone doTE155 maintained a relatively stable pool of pluripotent cells forming tight colonies. On the contrary, in the case of clone doTE171 the pluripotent colonies grew smaller and smaller, and died out by passage 4. Other clones displayed a phenotype which was in between these two clones, in the sense that they were able to maintain some tight colonies, but not as efficiently as clone doTE155. Below, these two aforementioned clones are characterised.

Figure R3.1. Screening of Twist-E cell lines selected for high induction

Immunofluorescence for two clones: doTE 155 and doTE 171, after 24 hours of induction showing heterogeneous expression, including brightly stained cells; red staining: Flag, blue: DAPI. Scale bars represent 50 μm (a). qPCR showing expression of *Twist1* after 24 hours of induction compared to uniduced samples Expression in uninduced cell of clone doTE77 has been arbitrarily set to 1. For each clone one experiment performed in duplicates is shown. Error bars represent value range (b). Western blot for 3 clones showing induction of the transgene in response to Dox treatment (c).

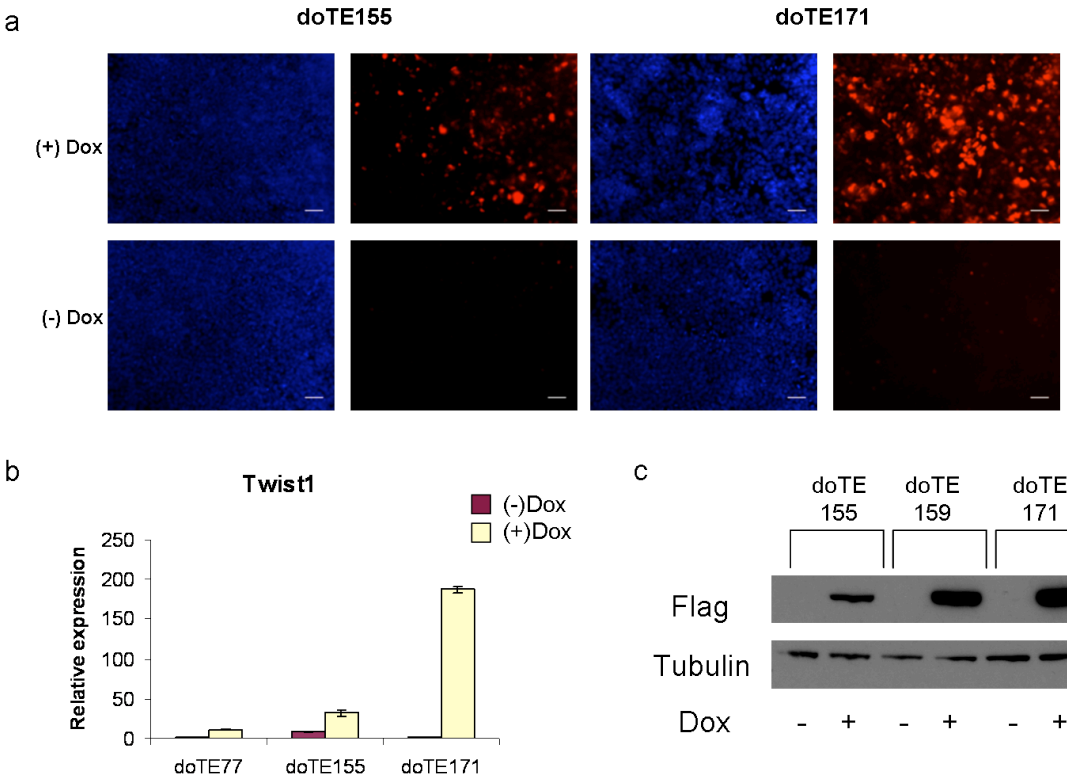
a
doTE155
doTE171
(+) Dox
(-) Dox
b
Twist1
(-)Dox
(+)Dox
Relative expression
250
200
150
100
50
0
doTE77
doTE155
doTE171
c
doTE 155
doTE 159
doTE 171
Flag
Tubulin
Dox
- + - + - +

Figure R3.2. Maintenance of TwE inducible clones is dependent on transgene silencing.

Phase-contrast pictures of cells passaged in self renewal conditions, N2B27 with LIF and BMP4, under continuous Dox induction. Red arrows: colonies of cells with pluripotent morphology, Yellow arrows: young differentiated cells, probably generated from the pluripotent colonies, Green arrows: old differentiated cells, probably generated from parent differentiated cells from the previous passages. Passage 1 +Dox (a), passage 2 +Dox (b), passage 3 +Dox (c), passage 4 +Dox (d), passage 3 -Dox (e), passage 3 parental line +Dox (f). Scale bars represent 50 μm.

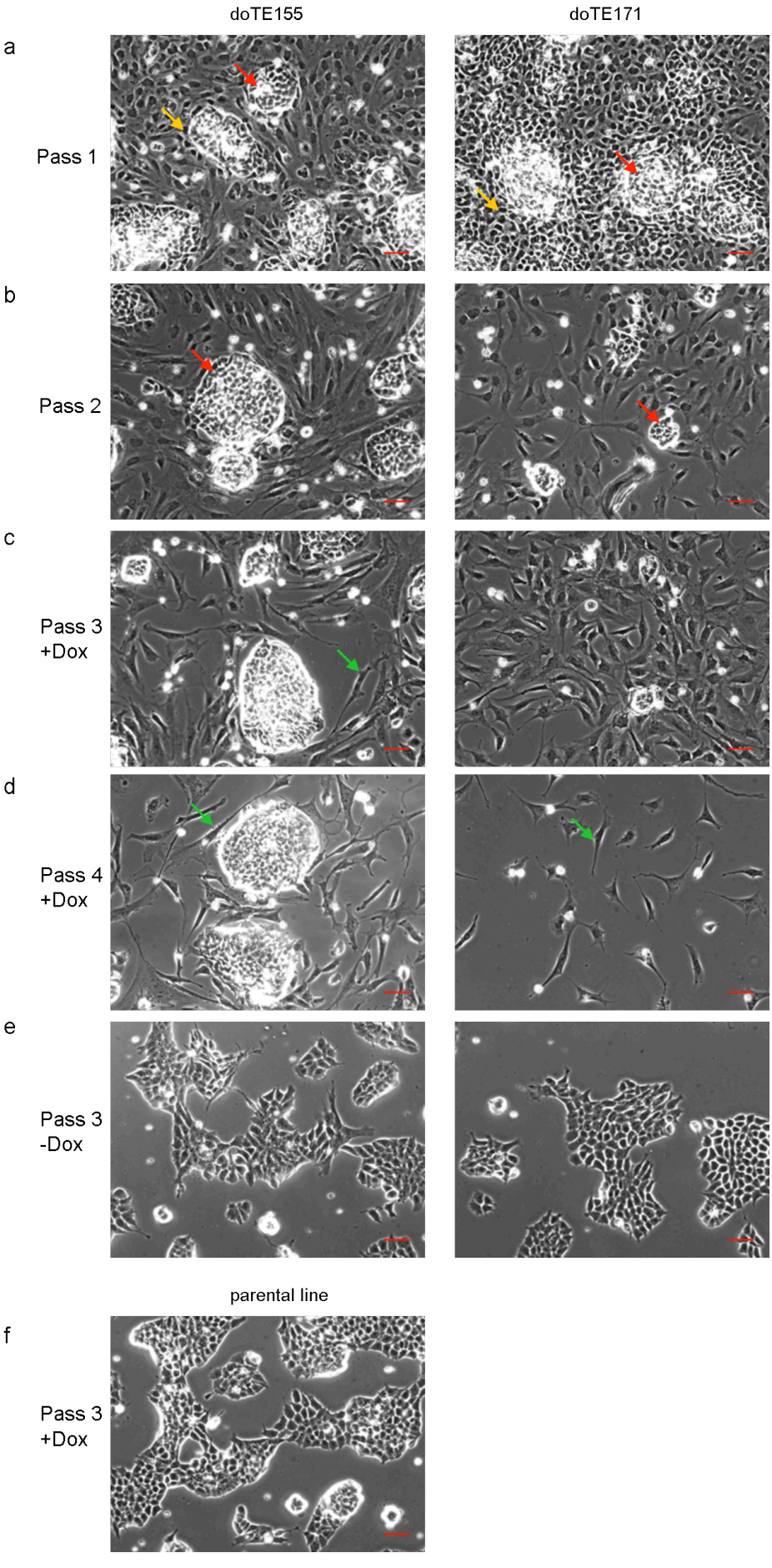
doTE155
doTE171
a
Pass 1
b
Pass 2
c
Pass 3
+Dox
d
Pass 4
+Dox
e
Pass 3
-Dox
parental line
f
Pass 3
+Dox

Careful observation of what seemed to be differentiating cells indicated that they lost their proliferating capacity fairly quickly, as by passage 4 their number was greatly reduced in the case of both clones. Furthermore, these cells suffered a progressive change in morphology: they became larger and more elongated at later passages [**Fig R3.2** green arrows]. The observation that even for clone doTE155 which maintains pluripotent colonies at later passages, the differentiated cells become larger and, small mesenchymal like cells could no longer be seen, indicates that these cells do not differentiate continuously from the pluripotent pool, but that the pluripotent cells adapted and were no longer sensitive to TwE influence.

R3.2.3 TwE Induced Differentiation Is Accompanied by EMT.

TWIST1 is a known EMT effector involved in CDH1 downregulation. Furthermore, CDH1 downregulation is a key event accompanying the differentiation processes during gastrulation and CDH1 is required in mouse ES cells for LIF dependent self renewal. It was reported that CDH1 presence/absence has significant transcriptional effects independent of CTNNB1/TCF transactivation [Soncin et al., 2009; Soncin et al., 2011] and, CDH1 cell to cell contact was found critical for induced pluripotent stem cells generation [Zohn et al, 2006; Chen et al, 2010].

Morphological analysis of cells induced for TwE in N2B27 supplemented with LIF and BMP indicated that an EMT process was associated with TwE induced differentiation. I tested CDH1 expression by immunofluorescence. As expected, only cells from the clusters were positive for this marker while no signal was observed in the dispersing cells [**Fig R3.3**], indicating that only the former cells maintained an epithelial structure.

Figure R3.3. CDH1 is not maintained in cells differentiating under TwE influence.

Immunofluorescence for the first two passages of TwE inducible clones under Dox stimulation; CDH1 – green. Left column phase contrast, right column CDH1/DAPI. Scale bars represent 50 μm.

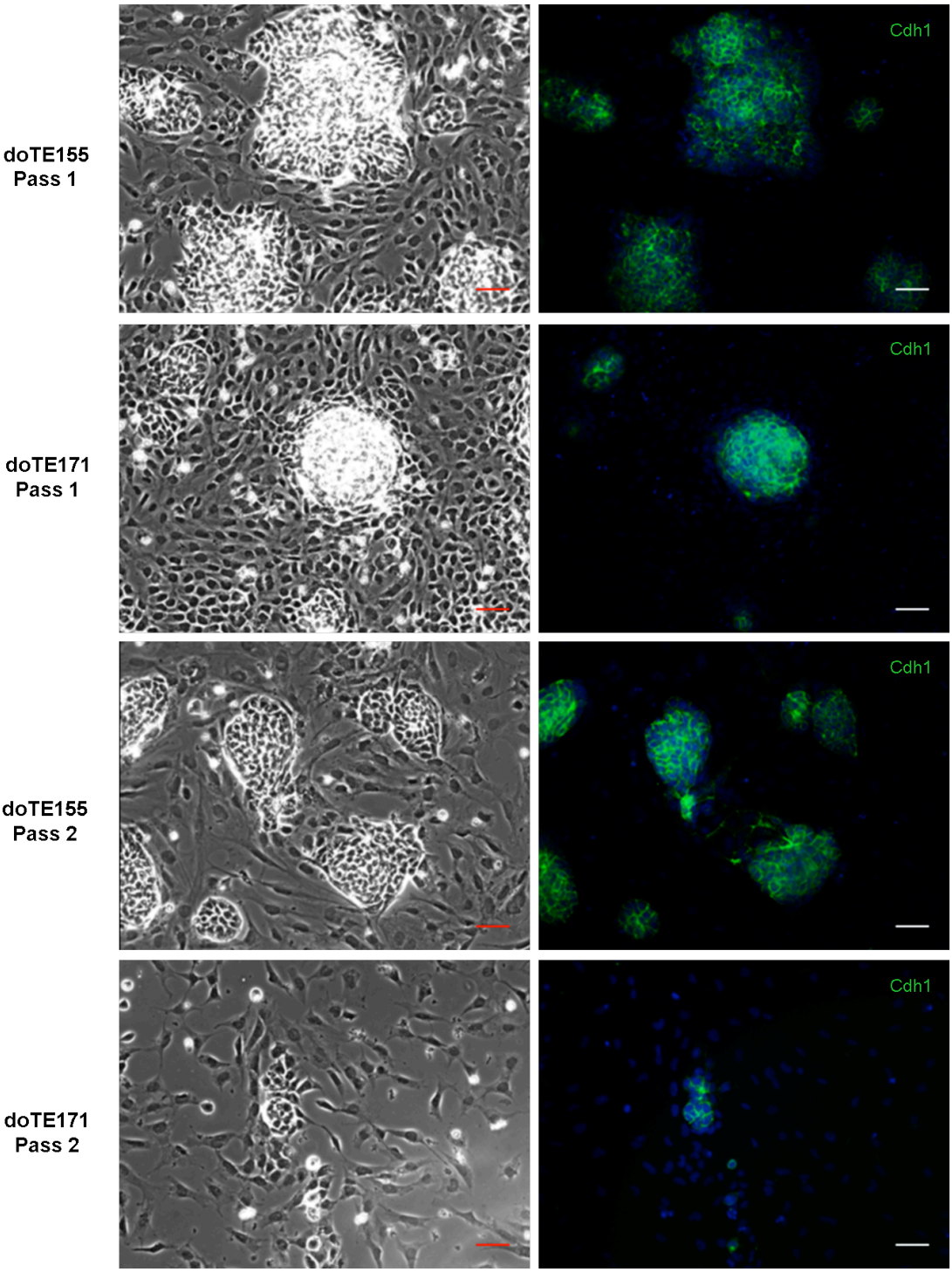
doTE155
Pass 1
Cdh1
doTE171
Pass 1
Cdh1
doTE155
Pass 2
Cdh1
doTE171
Pass 2
Cdh1

R3.3 Pluripotency Can only Be Maintained by Downregulating The TwE Transgene.

R3.3.1 Expression of The TwE Transgene and POU5F1 Pluripotency Factor Are Negatively Correlated.

To further clarify the effects of TwE on pluripotency I stained cells at passage 1 and 2 of Dox induction for Flag and POU5F1. POU5F1 only labelled cells from tight clusters in the case of both clones, confirming the previous assertion that those were the pluripotent cells. Furthermore, for clone doTE155 there was a clear segregation where almost no POU5F1 positive cells stained for Flag. Thus, downregulation of the transgene seems to be instrumental for pluripotency maintenance for this clone. Interestingly, even some of the differentiating cells downregulated the transgene, as indicated by existence of POU5F1(-) Flag(-) cells [**Fig R3.4**]. There is also a possibility that the observed phenomenon is due to selection of the cells do not express the transgen.

On the other hand, some colocalization of POU5F1 and Flag can be seen in the case of clone doTE171 although Flag is weaker in pluripotent cells. Interestingly, the differentiating cells express the transgene more strongly and more uniformly than in the case of doTE155. At any rate, downregulation of the transgene was not enough for this clone to safeguard the fate of pluripotent cells which were rapidly lost [**Fig R3.4**].

R3.3.2 Differentiation Positively Correlates with TwE Level of Induction.

Next, I confirmed the loss of pluripotency by markers RNA expression. For all pluripotency markers tested downregulation is more abrupt in the case clone doTE171 than clone doTE155 [**Fig R3.5a to c**]. It should be noted that *Pou5f1* is maintained above 50% of uninduced population even for doTE171 at passage 2 when very few POU5F1+ cells can be seen by staining, indicating a possible post transcriptional control. *Fgf5* an epiblast marker, in contrast is upregulated and, as expected, more strongly for doTE171 [**Fig R3.5d**].

Figure R3.4. TwE transgene is not maintained in pluripotent cells.

Immunofluorescence for the first two passages of TwE inducible clones under Dox stimulation; Flag – red, POU5F1 – green. Left column phase-contrast, middle column DAPI, right column Flag/POU5F1. Scale bars represent 50 μm.

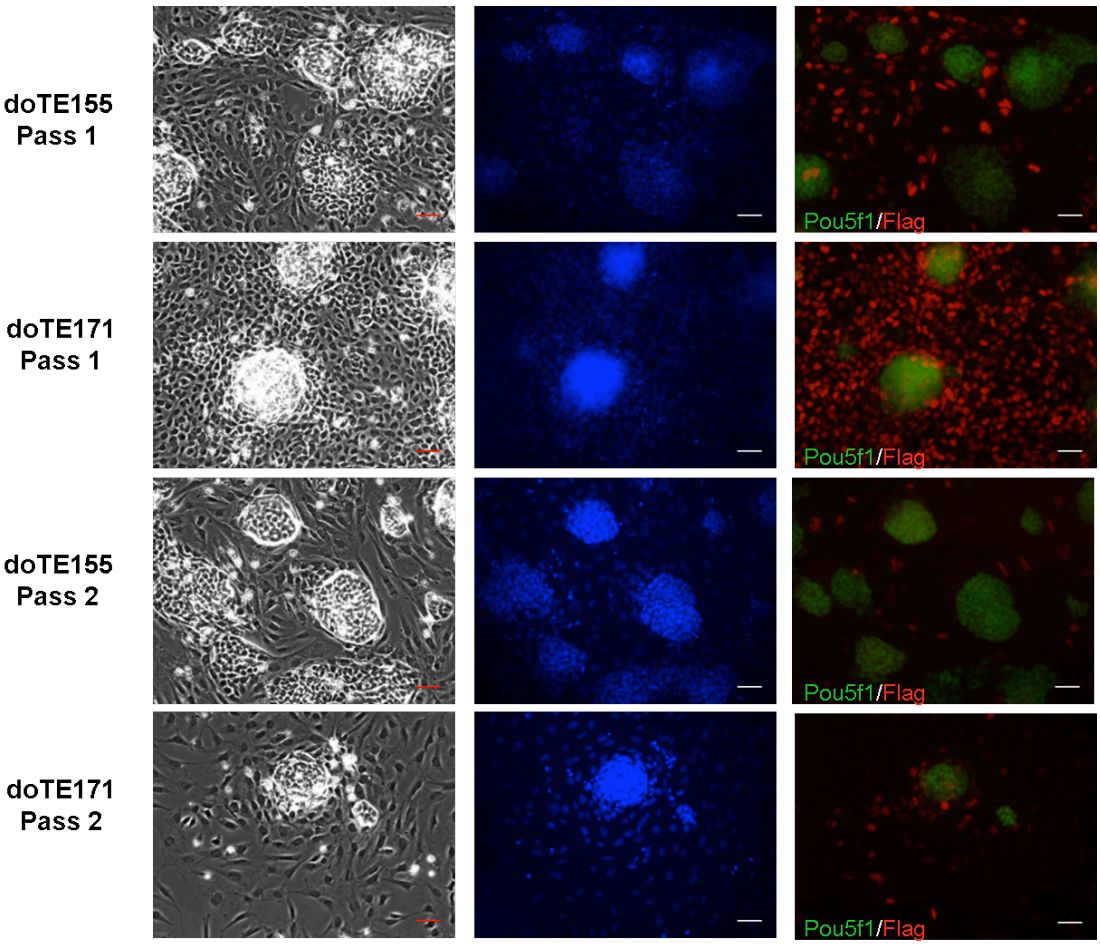
doTE155
Pass 1
doTE171
Pass 1
doTE155
Pass 2
doTE171
Pass 2
Pou5f1/Flag
Pou5f1/Flag
Pou5f1/Flag
Pou5f1/Flag

Figure R3.5. TwE induces transition from pluripotency to differentiation.

qPCR showing expression of ES markers *Pou5f1* (a), *Nanog* (b), *Esrrb* (c), epiblast marker *Fgf5* (d), EMT marker *Zeb2* (e), early neural marker *Zfp521* (f) and neural/neural crest marker *Pax3* (g), while passaging cells in self renewal conditions under the continuous influence of Dox. For each gene the average expression in the two clones before Dox induction has been arbitrarily set to 1. For each clone one experiment performed in duplicates is shown. Error bars represent value range

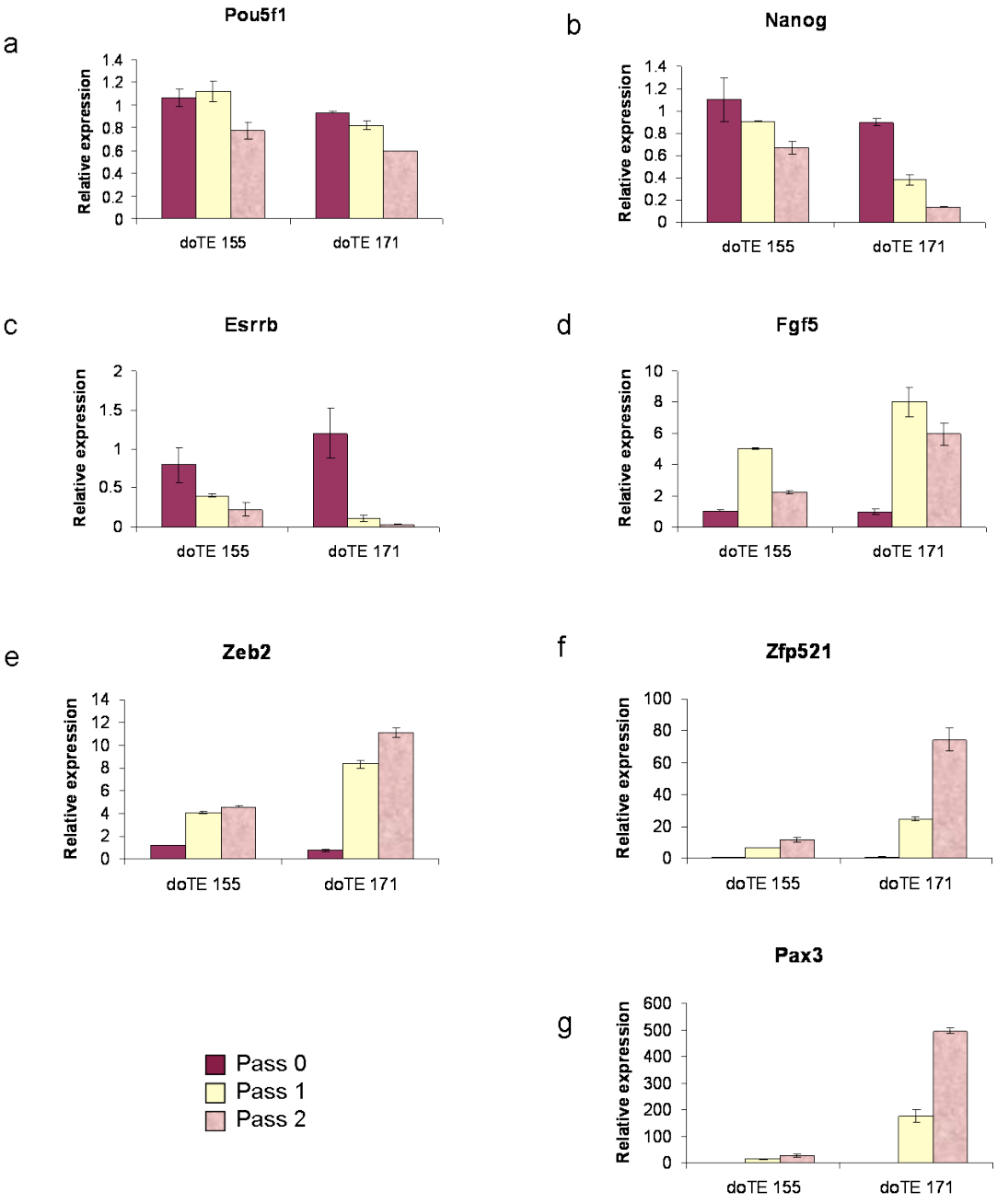
a
Pou5f1
Relative expression
1.4
1.2
1
0.8
0.6
0.4
0.2
0
doTE 155
doTE 171
b
Nanog
Relative expression
1.4
1.2
1
0.8
0.6
0.4
0.2
0
doTE 155
doTE 171
c
Esrrb
Relative expression
2
1.5
1
0.5
0
doTE 155
doTE 171
d
Fgf5
Relative expression
10
8
6
4
2
0
doTE 155
doTE 171
e
Zeb2
Relative expression
14
12
10
8
6
4
2
0
doTE 155
doTE 171
f
Zfp521
Relative expression
100
80
60
40
20
0
doTE 155
doTE 171
g
Pax3
Relative expression
600
500
400
300
200
100
0
doTE 155
doTE 171
Pass 0
Pass 1
Pass 2

When markers, which have been previously shown to be upregulated in clone doTE77 during neural differentiation (*Zeb2, Zfp521, Pax3*), were tested, they were all found to be upregulated in self renewal conditions as well. Furthermore, doTE171 upregulated all these markers at higher levels, indicating a correlation with the level of induction [**Fig R3.5e to g**].

R3.4 Immediate TwE Influences on Gene Expression

R3.4.1 Early TwE Induction

In the previous section I showed that TwE transgene is silenced in a significant number of cells soon after induction: i.e. passage 1 [**Fig R3.4**]. This indicates that at 24 hours, when induction was previously tested important variation in respect to initial levels of induction may have already occurred. Preliminary data indicated that the transgene might be expressed at the protein level already at 6 hours post induction. I estimated, that testing the induction not too long after that time point, a good indication could be obtained regarding baseline induction levels between the two analysed clones.

When TwE expression was tested in self renewal conditions at 9 hour post induction it was observed that the two clones responded similarly to Doxycyclin [**Fig R3.6**], in contrast with induction at 24 hours [**Fig R3.1b**]. This confirms the importance of transgene silencing in clonal response to TwE and indicates that by 24 hours, already important phenotypical changes have occurred.

R3.4.2 Early TwE Response for Pluripotency and Differentiation Markers

Regulation of differentiation by TwE had been assessed in the previous chapters by gene expression at days 2 to 5 of differentiation, when, most likely, the observed effects represented global cell fate changes. Here, I took advantage of the induction at 9 hours to investigate the TwE early response genes.

For this experiment cells adapted in N2B27 supplemented with LIF and BMP4, a condition further called as LIF + BMP, were used. Induction with Dox was performed either in these conditions or in N2B27 alone, which is the same as neural differentiation medium. The experiment is described in material and methods M2.2.7.

R3.4.2.1 Early TwE Influence on Pluripotency

First, I investigated the early effects of TwE induction on pluripotency markers. *Klf4* is one of the earliest markers to be downregulated when ES cells are placed in differentiating condition. In this experiment, TwE had a significant negative effect on *Klf4* in self renewal condition. In differentiating condition, on the other hand, *Klf4* had already been markedly downregulated by 9 hours and, TwE did not influence it any further [**Fig R3.7a**].

Id1 is another anti-differentiating effector which is downregulated at the early steps of differentiation. TwE has a minor effect of upregulation of *Id1* in self renewal conditions. The effect becomes more obvious in differentiating conditions where *Id1* is very low [**Fig R3.7b and c**]. Since ID1 prevents the formation of Tw-E dimers this can be interpreted as a negative feed-back mechanism, through which TwE limits its own effects.

R3.4.2.2 Early TwE Influence on EMT

Next I looked at the EMT process. Previously, I observed that *Zeb2*, is one of the earliest EMT markers to be influenced by TwE [**Fig R1.14b**]. Here this marker is upregulated at 9 hours by TwE both in self-renewing and differentiating conditions [**Fig R3.7d**]. Interestingly, *Cdh1* which is practically eliminated by TwE during differentiation is not influenced during this short induction. Furthermore, *Cdh2* whose upregulation is facilitated by TwE after three days of differentiation, is actually downregulated by 9 hours treatment with Dox [**Fig R3.7e and f**]. Together these data indicate that TwE role on Cadherins is chiefly an indirect one resulting from influences on cell fate rather than on direct gene expression.

Figure R3.6. Early TwE induction

qPCR showing *Twist1* expression after 9 hours induction with Dox in self renewing conditions. Expression in uninduced cells for clone doTE171 has been arbitrarily set to 1. For each clone one experiment performed in duplicates is shown. Error bars represent value range.

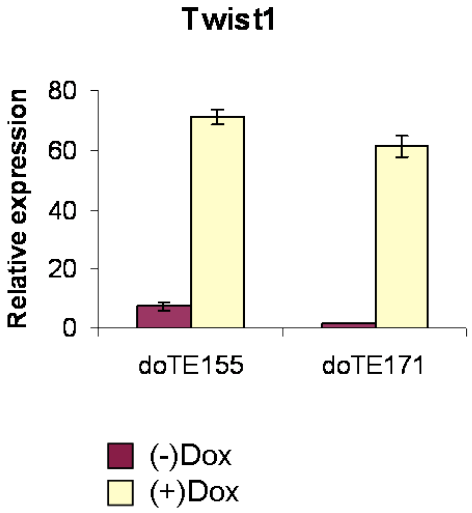
Twist1
Relative expression
80
60
40
20
0
doTE155
doTE171
(-)Dox
(+)Dox

Figure R3.7. TwE early influence on self renewal and differentiation

Cells were induced with Dox 800ng/ml for 9 hours either in self renewal condition N2B27 supplemented with Lif and BMP4 or in differentiation conditions N2B27 alone. qPCR showing expresion of *Klf4* (a), *Id1* (b and c), *Zeb2* (d), *Cdh1* (e) and *Cdh2* (f). In (c) Id1 expression is shown in differentiating conditions alone, for a better appreciation of modulation of the lower Id1 levels in this conditions. For each gene the average expression in the two clones in uninduced self-renewal conditions has been arbitrarily set to 1. For each clone one experiment performed in duplicates is shown. Error bars represent value range.

a

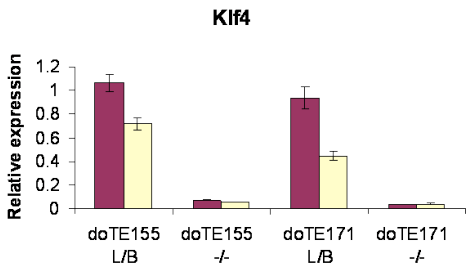
Klf4
Relative expression
1.2
1
0.8
0.6
0.4
0.2
0
doTE155 L/B
doTE155 -/-
doTE171 L/B
doTE171 -/-

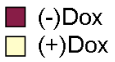
(-)Dox
(+)Dox

b

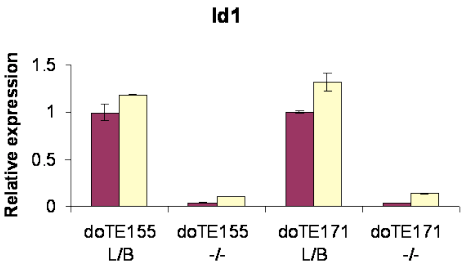
Id1
Relative expression
1.5
1
0.5
0
doTE155 L/B
doTE155 -/-
doTE171 L/B
doTE171 -/-

c

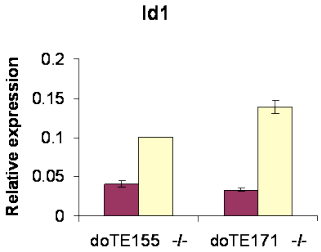
Id1
Relative expression
0.2
0.15
0.1
0.05
0
doTE155 -/-
doTE171 -/-

d

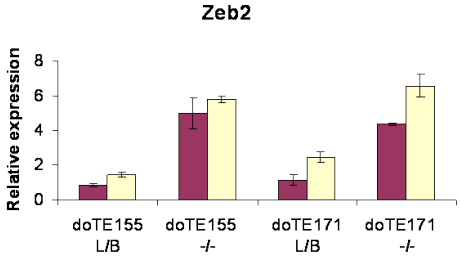
Zeb2
Relative expression
8
6
4
2
0
doTE155 L/B
doTE155 -/-
doTE171 L/B
doTE171 -/-

e

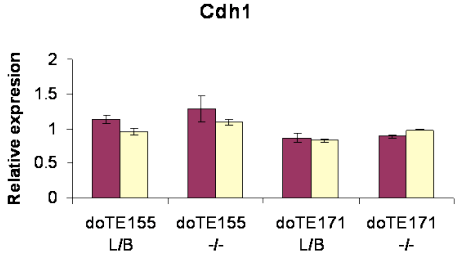
Cdh1
Relative expression
2
1.5
1
0.5
0
doTE155 L/B
doTE155 -/-
doTE171 L/B
doTE171 -/-

f

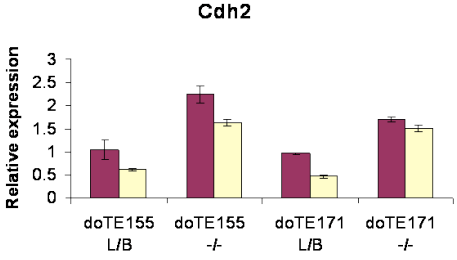
Cdh2
Relative expression
3
2.5
2
1.5
1
0.5
0
doTE155 L/B
doTE155 -/-
doTE171 L/B
doTE171 -/-

R3.4.2.3 Early TwE Influence on Neural Differentiation

Regarding early neural differentiation markers, *Zfp521* is not influenced by TwE in a consistent manner, indicating that for this marker too, any reported influences may be indirect. On the other hand, *Sox1* is downregulated for all clones and conditions tested [**Fig R3.8a and b**]. While this explains the consistent *Sox1* downregulation, I have seen across experiments, it comes into conflict with the notion that *Sox1* downregulation is a later event involved in premature exit from neural progenitor state. Integrating all the results, I conclude, that TwE is most likely a direct negative regulator of *Sox1*, but that this effect could be counterbalanced for a limited time by other changes in cell differentiation. However, TwE negative effect on *Sox1* must in the end win, in the case of continuous TwE induction, resulting in ultimate suppression of this marker. Furthermore, direct *Sox1* downregulation by TwE could also explain why it is possible to rescue the expression of *Zfp521* without rescuing the expression of *Sox1*.

R3.4.2.4 Early TwE Influence on Other Differentiation Markers

In other differentiation systems TwE has been reported to act by influencing *Fgfr2* expression [Connerney et al., 2006]. When short induction of TwE was tested, upregulation of *Fgfr2* expression for all conditions tested was observed [**Fig R3.8c**]. Interestingly, TwE had been found previously to downregulate *Fgfr2* expression [Connerney et al., 2006]. This is an indication that TwE may have repressive or activating roles depending on cell context.

Pax3 is a dorsal neural marker for which I have reported an early TwE role. *Pax3* was upregulated by short Dox induction in all conditions although, the effect in clone doTE171 was strong, while in clone doTE155 was minimal [**Fig R3.8d**].

Gli1 is one of the SHH effectors and has been proposed to be non-cell autonomously regulated by *Twist1* [Soo et al., 2002]. It is negatively influenced by short induction of TwE most notably in self-renewing conditions [**Fig R3.8e**].

Figure R3.8. TwE early influence on neural markers

Cells were induced with +Dox for 9 hours either in self renewal condition N2B27 supplemented with Lif and BMP4 or in differentiation conditions N2B27 alone. qPCR showing expresion of *Zfp521* (a) *Sox1* (b) *FgfR2* (c), *Pax3* (d) and *Gli1* (e). For each gene the average expression in the two clones in uninduced self-renewal conditions has been arbitrarily set to 1. For each clone one experiment performed in duplicates is shown. Error bars represent value range.

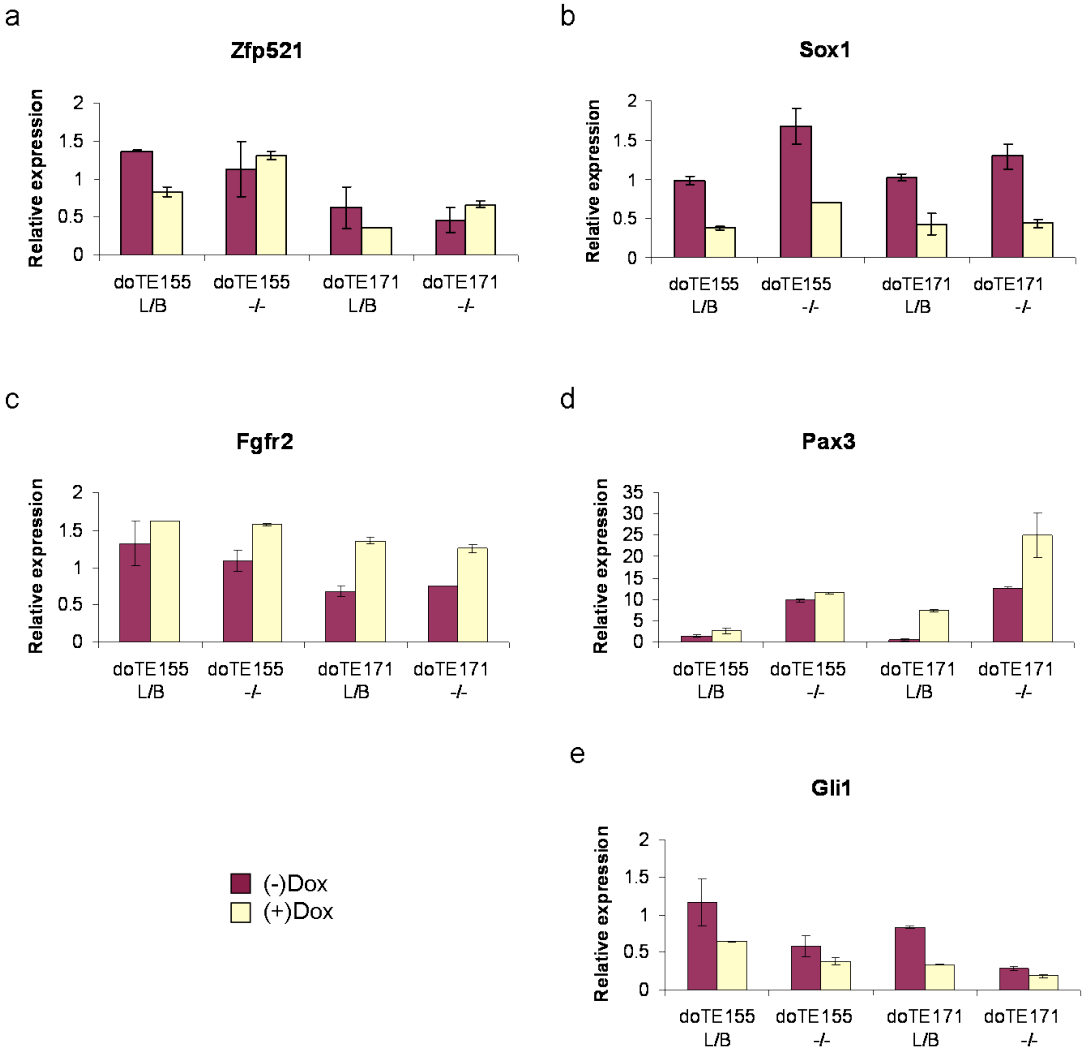
a
Zfp521
Relative expression
2
1.5
1
0.5
0
doTE155 L/B
doTE155 -/-
doTE171 L/B
doTE171 -/-
b
Sox1
Relative expression
2
1.5
1
0.5
0
doTE155 L/B
doTE155 -/-
doTE171 L/B
doTE171 -/-
c
Fgfr2
Relative expression
2
1.5
1
0.5
0
doTE155 L/B
doTE155 -/-
doTE171 L/B
doTE171 -/-
d
Pax3
Relative expression
35
30
25
20
15
10
5
0
doTE155 L/B
doTE155 -/-
doTE171 L/B
doTE171 -/-
(-)Dox
(+)Dox
e
Gli1
Relative expression
2
1.5
1
0.5
0
doTE155 L/B
doTE155 -/-
doTE171 L/B
doTE171 -/-

In summary, TwE has early negative effects on pluripotency and neural differentiation as shown by the negative regulation of *Klf4* and *Sox1* at 9 hours post induction. Other complex differentiation events might be the combined result of early and late TwE effects, but it is also possible that some of the reported genes like: *Zeb2, Pax3* and *Gli1,* have an early role in this process.

R3.5 TwE Can Block Neural Differentiation.

In Results_1 I correlated premature downregulation of *Sox1* in response to TwE with early formation of post mitotic neurons as indicated by formation of TUBB3 positive cells. Here I asked the question if formation of such early neurons can result in response to higher levels of TwE as well.

When TwE high expressing clones were subject to 4 days neural differentiation, a marked difference, between the two clones tested, could be observed. While, in the case of doTE155, microscopic fields with premature neurites could be observed, for clone doTE171 neuron formation was inhibited compared to –Dox control. **Fig R3.9** presents the fields with the highest number of TUBB3 positive cells for each condition.

R3.6. High TwE Effects on Neural Differentiation

R3.6.1 TwE Induction during Neural Differentiation

The above experiment supports the idea that perhaps high TWIST1 activity favours non-neural fates as, indicated by suppression of neuron formation in the clone with the highest TwE expression and lowest silencing. Such a hypothesis is consistent with the *Twist1* pattern of expression, which was observed at high levels only in the mesenchyme and not in the neural tissue. However, there was a possibility that the reported suppression was only the result of early effects of high level TwE. This might have biological significance considering that in the embryo I could only

observe Twist1 in the neural tissue after the head fold stage, a time point when neural fate is already protected against other suppressive signals, like BMP.

To test whether high levels of TwE could no longer suppress neural fate after the initial differentiation events an experiment was designed where Dox was added only after the first two days of differentiation. This time point was chosen considering the fact that in the in vitro system I was using, at day 3, few postmitotic neurons could already be observed [**Fig R1.8**]. Moreover, at day 3 of differentiation upregulation of neural markers had been reported [Kamiya et al., 2011], indicating that neural fate was established. As control, were used the conditions where Dox was either not added at all, or added throughout the experiment. Differentiation was assessed by marker expression at day 4.

First, Twist1 induction was tested. It was observed that in this context for clone doTE155 induction does not decrease as severely as in self renewal condition, indicating that during differentiation the selective pressure against TwE expressing cells is less important [**Fig R3.10**].

Next, neural differentiation was assessed based on four classes of markers: early neural markers *Sox1* and *Zfp521*, late neural marker *Atoh1*, EMT marker *Zeb1* and, neural crest markers *Sox9* and *Msx1*.

R3.6.2 High TwE Induction Effects on Neural Differentiation Markers

In the previous experiments involving lower TwE induction level in clone doTE77 suppression of *Sox1* and enhancement of *Zfp521* upregulation during neural differentiation was observed [**Fig R1.10b and c**]. In the present experiments these observation were generally confirmed [**Fig R3.11a and b**]. Interestingly, *Sox1* upregulation was curbed, but still permitted to some extent in both Dox treatments in the case of clone doTE155. On the other hand, for doTE171 expression was completely blocked in Dox continuous treatment and, almost completely blocked in Dox late treatment [**Fig R3.11a**] and, this complete block of *Sox1* correlates with the block in neuron formation for this clone [**Fig R3.9**].

Figure R3.9. TwE induction has clonal dependent effects on neural differentiation.

4 days of monolayer neural differentiation in N2B27 under Dox induction: lower row; and in the absence of Dox: upper row. Left panels: phase contrast, right panels immunofluorescence: TUBB3 staining: green; with nuclei counterstained with DAPI. Scale bars represent 50 μm.

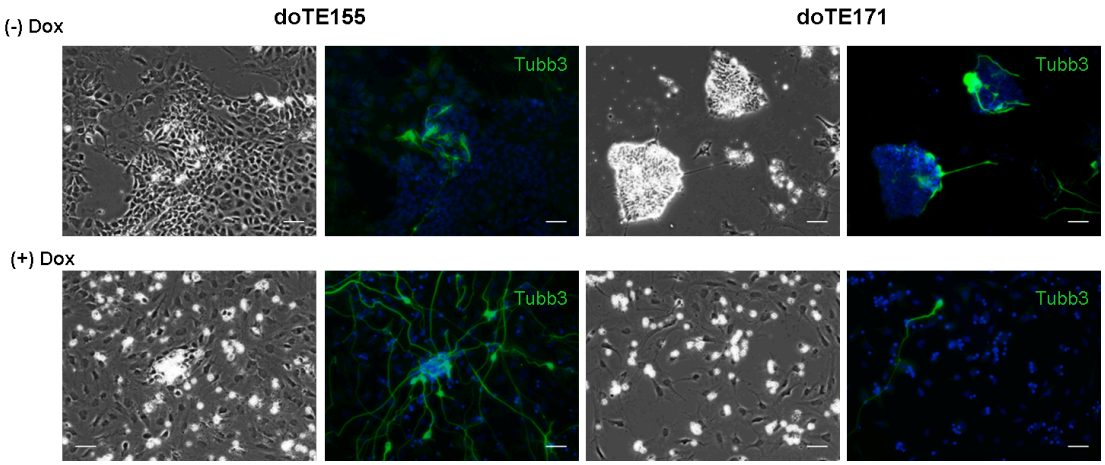
doTE155
doTE171
(-) Dox
(+) Dox
Tubb3
Tubb3
Tubb3
Tubb3

Figure R3.10. TwE induction during neural differentiation

qPCR showing *Twist1* expression in ES cells and cells at day 4 of neural differentiation in monolayer protocol. Cells were either not induced: -Dox, induced for the last 2 days of differentiation: +Dox Day 2-4, or induced throughout differentiation: +Dox Day 0-4. Expression of clone doTE171 in uninduced self-renewal conditions has been arbitrarily set to 1. For each clone one experiment performed in duplicates is shown. Error bars represent value range.

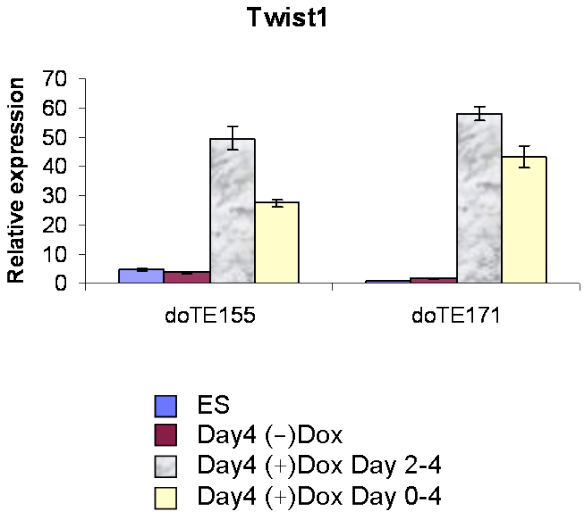
Twist1
Relative expression
70
60
50
40
30
20
10
0
doTE155
doTE171
ES
Day4 (−)Dox
Day4 (+)Dox Day 2-4
Day4 (+)Dox Day 0-4

Figure R3.11. Time of TwE induction influence on differentiation markers expression

qPCR showing expression of *Sox1* (a), *Zfp521* (b), *Atoh1* (c), *Sox9* (d), *Msx1* (e) and *Zeb1* (f) in ES cells and cells at day 4 of neural differentiation in monolayer protocol. Cells were either not induced: -Dox, induced for the last 2 days of differentiation: +Dox Day 2-4, or induced throughout differentiation: +Dox Day 0-4. For each gene the average expression in the two clones at ES cell stage has been arbitrarily set to 1. For each clone one experiment performed in duplicates is shown. Error bars represent value range.

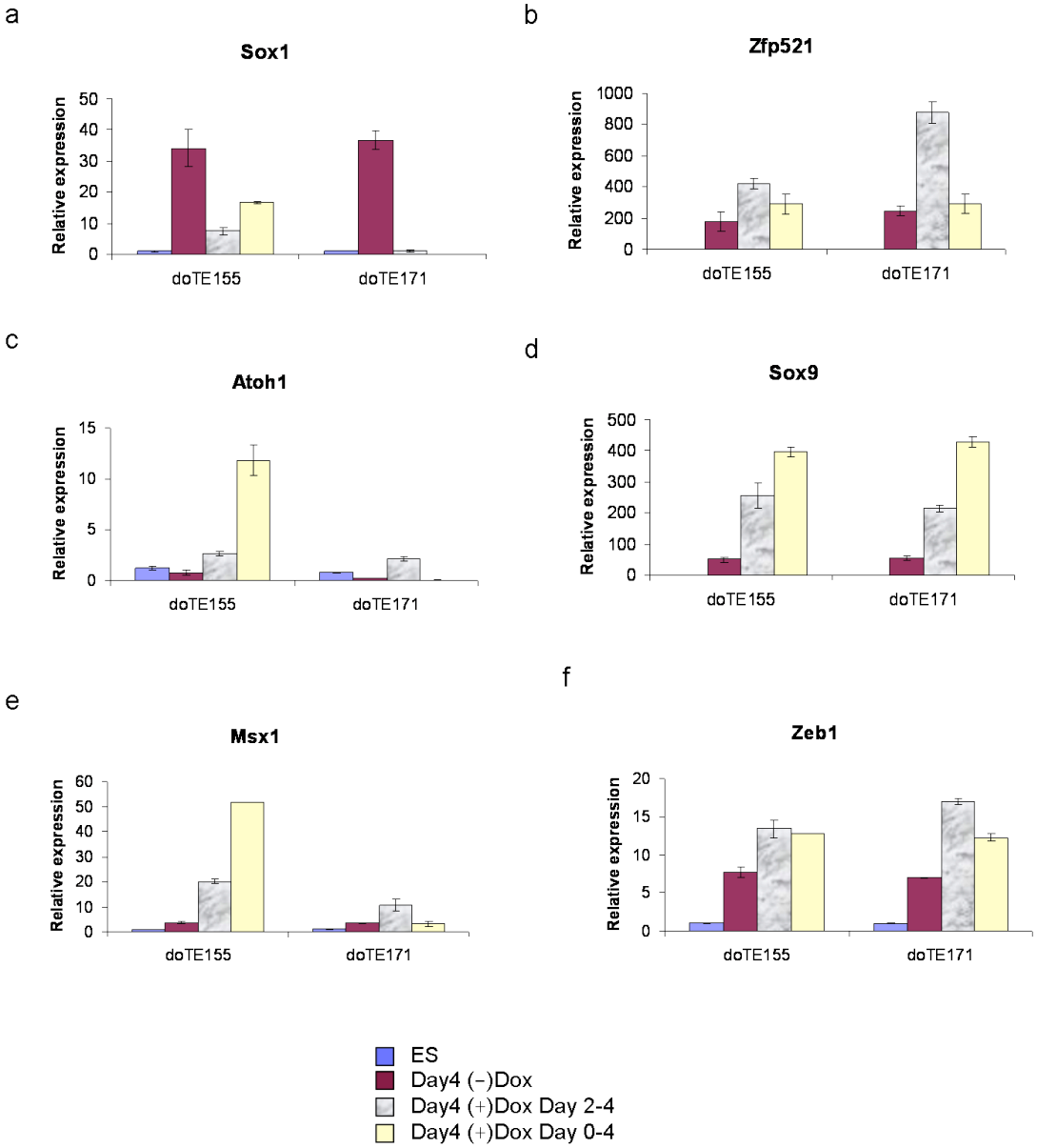
a
Sox1
Relative expression
50
40
30
20
10
0
doTE155
doTE171
b
Zfp521
Relative expression
1000
800
600
400
200
0
doTE155
doTE171
c
Atoh1
Relative expression
15
10
5
0
doTE155
doTE171
d
Sox9
Relative expression
500
400
300
200
100
0
doTE155
doTE171
e
Msx1
Relative expression
60
50
40
30
20
10
0
doTE155
doTE171
f
Zeb1
Relative expression
20
15
10
5
0
doTE155
doTE171
ES
Day4 (−)Dox
Day4 (+)Dox Day 2-4
Day4 (+)Dox Day 0-4

The later marker *Atoh1* was not upregulated in either clone in the absence of Dox. *Atoh1* was highly upregulated only by continuous Dox treatment and, only in the case of clone doTE155. Its expression was completely blocked for doTE171 in the case of continuous Dox treatment [**Fig R3.11c**]. This correlates with the complete block of *Sox1* for that clone and condition. Thus, it can be concluded that *Atoh1* requires for its upregulation, in this in vitro protocol, both prolonged TwE stimulation and *Sox1* presence.

Collectively the data presented above indicates that formation of neurons correlates well with *Sox1* and *Atoh1* expression but not with that of *Zfp521*. It seems that this latter marker responds to TwE even when differentiation is diverted from the neural pathway.

It should be noted that high TwE blocks overt neural differentiation by accentuating *Sox1* suppression, as it can be observed in clone doTE171. On the other hand in clone doTE77 where TwE is induced at lower levels and in clone doTE155 where TwE is downregulated *Sox1* expression is permitted and TUBB3 positive neurons can be observed.

R3.6.3 High TwE Induction Effects on EMT

Zeb2 is an EMT effector specifically expressed in the developing neuroepithelium and neural crest [Van de Putte et al., 2003]. In previous experiments I found that this gene's expression is upregulated by TwE. However, this enhancement tended to plateau towards the end of the differentiation [**Fig R1.14b**]. The related gene *Zeb1* (also known as *δEF1*) is less specific, being expressed only in a subset of neural progenitors, as well as in neural crest and axial and paraxial mesoderm. I found this marker to be enhanced by TwE during neural differentiation and the difference between +Dox and –Dox conditions was maintained throughout the experiment [**Fig R1.14a**]. For this reason I tested *Zeb1* expression in this experiment, at day 4 of differentiation. *Zeb1* was enhanced in both clones by Dox treatment, the highest level being observed for the late Dox treatment in the case of doTE171 [**Fig R3.11f**]. This data indicates that *Zeb1* stimulation stands in direct relation with TwE and is not a consequence of neural facilitation.

R3.6.4 High TwE Induction Effects on Dorsal Neural Markers

The neural crest marker *Sox9* [Sauka-Spengler and Bronner-Fraser, 2008, Lee and Saint-Jeanette, 2011] was upregulated in both clones and in both induction conditions. It was highest in continuous Dox treatment [**Fig R3.11d**]. This may indicate that *Sox9* upregulation in response to TwE is independent of progression through neural differentiation.

Msx1 (also known as Hox-7) is a neural crest marker [Hill et al., 1989; Robert et al., 1989] which was not upregulated in the previous experiments involving clone doTE77 (data not shown). In the current experiment it was upregulated strongly by clone doTE155, especially in the continuous treatment condition. On the other hand in the case of clone doTE171 it was only upregulated in the late induction condition [**Fig R3.11e**]. This inconsistency between clones might indicate that this marker requires other unpredictable differentiation events in order to respond to TwE.

In conclusion, the data presented here confirms the idea that high levels of TwE are detrimental to neural induction and that delaying the time of induction at 48 hours after the start of in vitro differentiation is not enough to preserve the neural fate. However, most transcriptional effects observed previously for low TwE induction could also be observed in the case of high TwE induction. Divergent differentiation effects could be ascribed to levels of regulation. Most notably, the block on neural differentiation by high TwE correlated with the block in *Sox1* expression.

R3.7 TwE Block on Neural Differentiation Is Dose and Not Clone Dependent.

R3.7.1. Modulating The Levels of TwE Induction

The previous experiments indicated that the neural differentiation can only be preserved if TwE induction is reduced to lower levels, as is the case of clone doTE155. There was a possibility that this phenomenon was dependent on some individual clonal phenotypical adaptations and not directly connected with TwE levels. However, based on Twist1 levels of expression in the embryo, as well as on TwE effects of neural differentiation reported in Results_1 I am proposing that: "low levels of TwE help induce a dorsal neural fate whilst higher levels of TwE induce a mesenchymal fate". If this hypothesis is correct, than low levels of TwE, should replicate the observed effects on neural differentiation in all clones.

In order to establish the optimal level of induction I carried a dose dependence test, as shown in **Fig R3.12**. Considering the results shown and the fact that clone doTE77 had a usual induction pattern of 7 fold or more, I concluded that the Dox doses which would be most likely to produce the desired induction are 10 and 30 ng/ml Dox.

However, for the next experiments, I modified the doses to 10 and 40 ng/ml Dox, for the following reasons. I thought important to have a very low dose of Dox, for the possibility that the tiniest amount of TwE might have a phenotypic effect. On the other hand, if a higher dose was required 40 ng/ml was a minimal increase which would enhance the chances of unravelling the active dimer effects. As controls, 0 and 800 ng/ml Dox were used. The treatment was carried for the entire duration of the experiment: day 0 to day 4.

Figure R3.12. Correlation of TwE induction with Dox concentration

qPCR showing Twist1 expression after 9 hours induction with Dox in self renewing conditions at stated concentrations. Expression in uninduced cells for clone doTE171 has been arbitrarily set to 1. For each clone one experiment performed in duplicates is shown. Error bars represent value range.

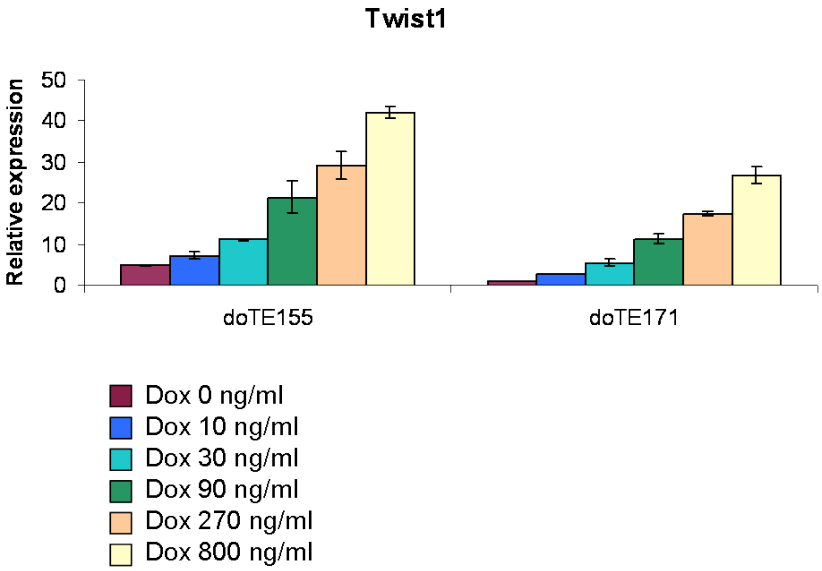
Twist1
Relative expression
50
40
30
20
10
0
doTE155
doTE171
Dox 0 ng/ml
Dox 10 ng/ml
Dox 30 ng/ml
Dox 90 ng/ml
Dox 270 ng/ml
Dox 800 ng/ml

R3.7.2 Premature Neurons Can Be Observed in All Clones in The Case of Low TwE Induction.

When cells were differentiated for four days in the described conditions and neural differentiation assessed by TUBB3 staining the two clones (doTE155 and 171) behaved consistently for 0, 10 and 40 ng/ml Dox conditions. Thus, the presence of TUBB3 cells was minimal on day 2 for all conditions tested. Then, on days 3 and 4, premature neurites could be observed especially at 40 ng/ml for both clones. At 800 ng/ml TUBB3 upregulation is almost completely blocked for clone doTE171. Furthermore, even for clone doTE155, where neurons can be observed, there is a suppression of formation of TUBB3 positive neurites compared to 40 ng/ml [**Fig R3.13**].

R3.7.3. Quantification of Neurite Formation in Response to TwE

To better assess these effects of TwE on neuronal differentiation, I developed a system for quantifying neurite number and length as described in Material and Methods (M4.1.2); at day four of neural differentiation, a time point when neurites could be best observed. Briefly, total cell numbers were counted using a nuclear segmentation algorithm based on DAPI nuclear staining. Then, neurons were counted and the length of the neurites for each neuron were measured based on TUBB3 staining.

Regarding efficiency of neuronal formation no difference was observed between 0 and 10 ng/ul of Dox for both clones studied. However, a dose dependent suppression of neuron formation could be observed for 40 and 800 ng/ml Dox. The only notable difference between clones could be observed at 800 ng/ml Dox, a treatment for which neural formation as assessed by TUBB3 was completely blocked in the case of clone doTE171, while for doTE155 rare neurons could still be observed [**Fig R3.14**].

Furthermore, when TUBB3 positive cells were separated between immature neurons with short processes and, more mature neurons, with longer processes, it was observed that up to 40 ng/ml Dox neural suppression, for both clones, was generated

solely on the expense of immature neurons, while formation of more mature neurons was slightly increased. At 800 ng/ml Dox formation of all neurons was suppressed [**Fig R3.14**].

These data is consistent with the idea that at high levels TwE blocks neural differentiation while at lower levels it is permissive for this process and, accelerates it. Furthermore, it should be noted that reduction in total neuron numbers at 40 ng/ml Dox, does not refute my hypothesis, as acceleration of neural differentiation reduces the pool of proliferating progenitors and thus, the final number of differentiated cells.

Since there was a high degree of correlation between the two clones, the data was pooled together for statistical analysis. Using One-way ANOVA, followed by Tukey HSD post hoc test, as described in M4.1.2, it was determined that suppression of neural formation was significant both at 40 ng/ml Dox compared with 0 and 10 ng/ml Dox as well as, at 800 ng/ml Dox compared with 40 ng/ml Dox [**Fig R3.15a**]. Furthermore, formation of neurons with short neurites was significantly suppressed at 40 ng/ml Dox compared with 0 and 10 ng/ml and, at 800 ng/ml compared with 0 and 10 ng/ml [**Fig R3.15b**]. On the other hand there was a significant enhancement of generation of neurons with long neurites at 40 ng/ml Dox compared with 0 ng/ml and a significant suppression of at 800 ng/ml compared with 40 ng/ml [**Fig R3.15c**]. It should be noted that the large error bars in this case represent normal field to field variation.

R3.7.4 Neural Marker Expression Modulation by Different Levels of TwE Induction

In the previous section I inferred transcriptional effects of different levels of TwE based on results obtained in different clones. I wanted to confirm these observations by assessing the influence on neural differentiation of different levels of TwE within the same clones. By using this method I was able to confirm all the previous observations, namely that Sox1 downregulation and, *Zfp521, Zeb2, Sox9* and *Wnt1* upregulation correlated with TwE induction levels.

Figure R3.13. Only high TwE induction blocks neural differentiation.

Immunofluoresce for TUBB3: green, with nuclei counterstained with DAPI of cells differentiated for 4 days in monolayer protocol and induced with the stated concentration of Dox. Cells were fixed at Day 2 of differentiation (a), Day 3 (b) and Day 4 (c). Scale bars represent 50 μm.

a – **Day2**

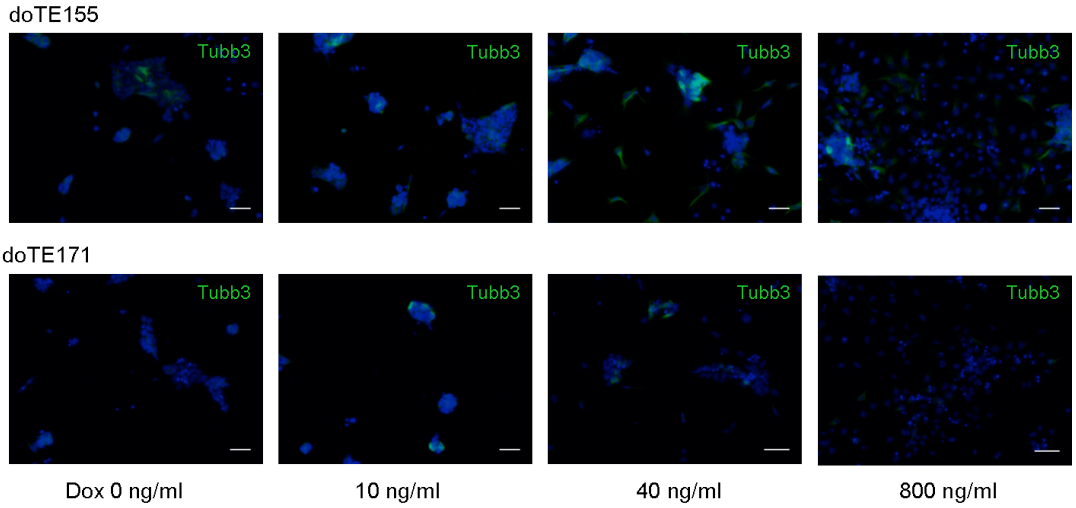

b – **Day3**

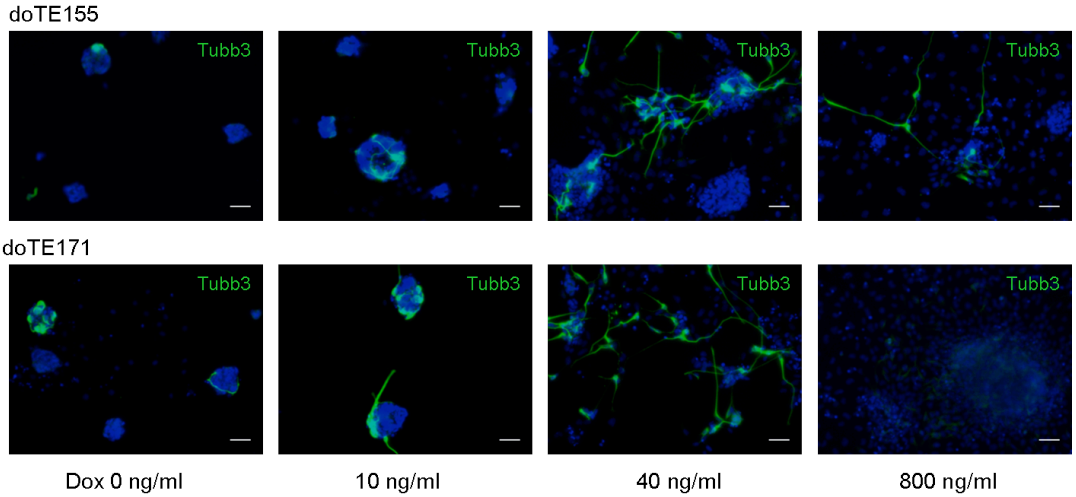

c – **Day4**

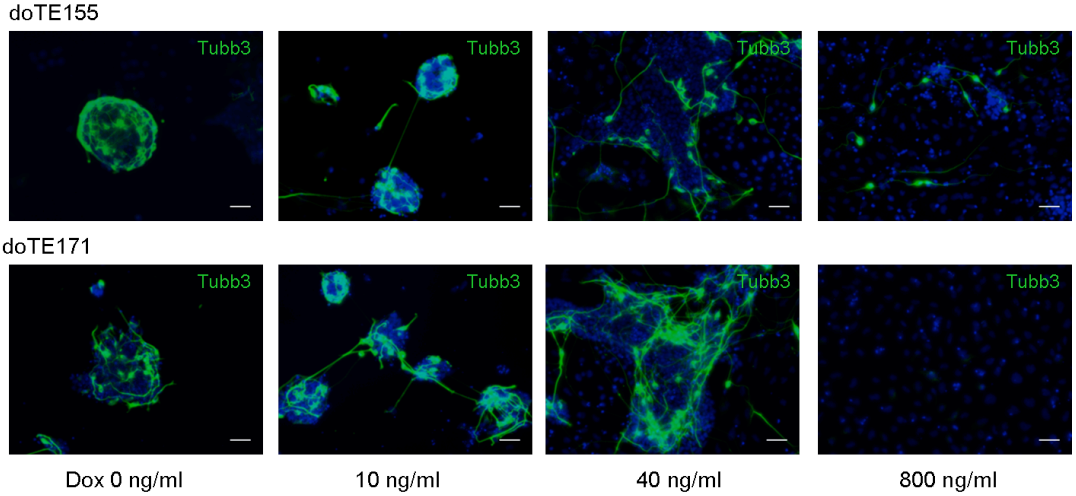

Figure R3.14. Quantification of neuron formation under TwE influence

Representation of total number of TUBB3 positive cells per 100 cells: clone doTE155 (a) and doTE171 (b). Representation of neurons with short and long neurites respectively per 100 cells: clone doTE155 (c) and doTE171 (d). An arbitrary threshold has been set considering a neurite as being long if its length equalled or exceeded 7 mean nuclear diameters. Data collected at day four of neural differentiation. Dox doses used: 0, 10, 40 and 800 ng/ml respectively. Error bars represent standard deviation of the mean for three microscopic fields for each clone and condition.

a

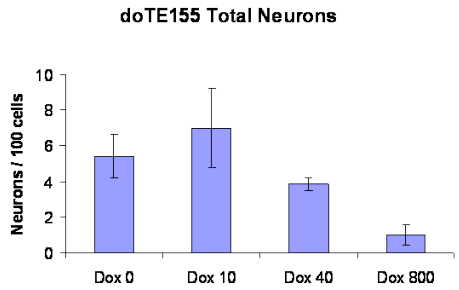
doTE155 Total Neurons
Neurons / 100 cells
10
8
6
4
2
0
Dox 0
Dox 10
Dox 40
Dox 800

b

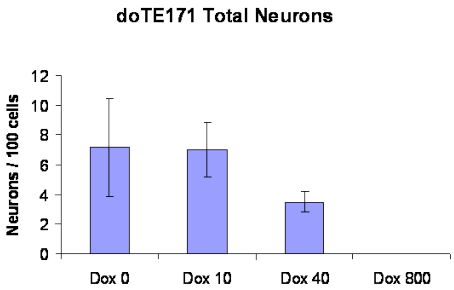
doTE171 Total Neurons
Neurons / 100 cells
12
10
8
6
4
2
0
Dox 0
Dox 10
Dox 40
Dox 800

c

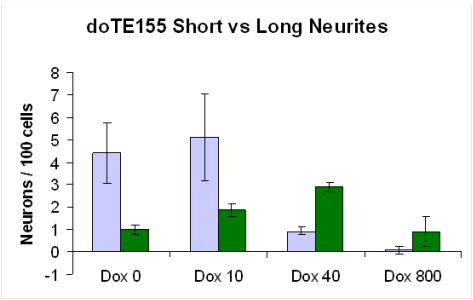
doTE155 Short vs Long Neurites
Neurons / 100 cells
8
7
6
5
4
3
2
1
0
-1
Dox 0
Dox 10
Dox 40
Dox 800

d

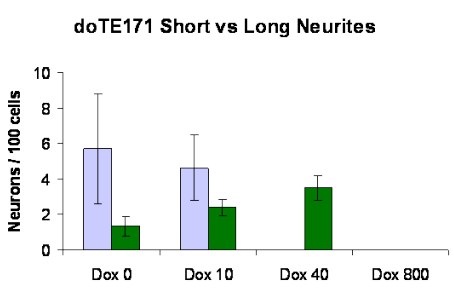
doTE171 Short vs Long Neurites
Neurons / 100 cells
10
8
6
4
2
0
Dox 0
Dox 10
Dox 40
Dox 800

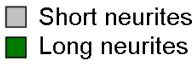
Short neurites
Long neurites

Figure R3.15. Statistical analysis of neuron formation quantification

For statistical analysis data from the two clones has been pooled together. Total neurons quantification (a). 40 ng/ml Dox significantly suppress neuron formation both compared to no Dox $p = 0.043$ and to 10 ng/ml Dox $p = 0.007$. 800 ng/ml Dox induced a further supression compared to 40 ng/ml Dox condition $p = 0.011$. Furthermore, suppression at 800 ng/ml Dox was highly significant compared to 0 and 10 ng/ml Dox; $p = 2x10^{-5}$ and $p = 3x10^{-6}$ respectively. Short and Long neurite formation (b) and (c) respectively. Formation of neurons with short neurites has been significantly suppressed by 40 ng/ml Dox compared to the lower induction doses 0 and 10 ng/ml $p = 2x10^{-7}$ and $p = 4x10^{-8}$ respectively. It was also highly significant for 800 ng/ml Dox compared with 0 and 10 ng/ml, $p = 1x10^{-7}$ for both conditions. Formation of neurons with long neurites has been significantly stimulated by 40 ng/ml Dox compared with no Dox induction $p = 0.042$. At 800 ng/ml it was significantly suppressed compared with 40 ng/ml $p = 0.002$ Data collected at day four of neural differentiation. Dox doses used: 0, 10, 40 and 800 ng/ml respectively. Error bar represent standard deviation of the mean for six microscopic fields from two clones.

a

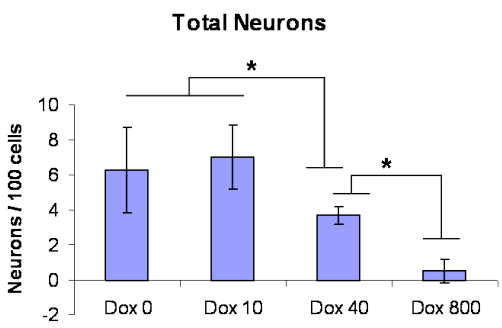
Total Neurons
Neurons / 100 cells
10
8
6
4
2
0
-2
*
*
Dox 0
Dox 10
Dox 40
Dox 800

b

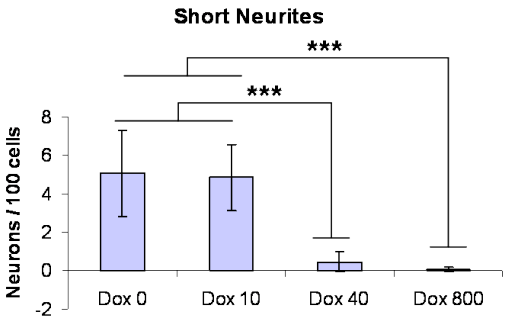
Short Neurites
Neurons / 100 cells
8
6
4
2
0
-2
***
***
Dox 0
Dox 10
Dox 40
Dox 800

c

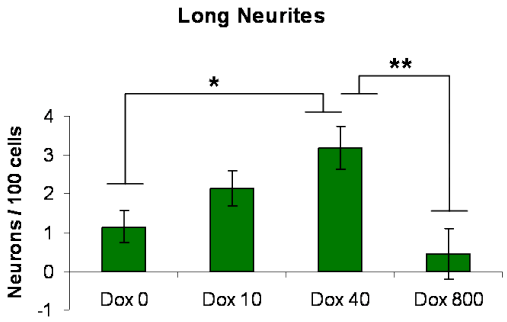
Long Neurites
Neurons / 100 cells
4
3
2
1
0
-1
*
**
Dox 0
Dox 10
Dox 40
Dox 800

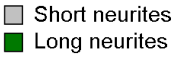
Short neurites
Long neurites

For both clones 40 ng/ml produced an induction of TwE within desired levels: above 10 fold. 800 ng/ml produced a high induction, while 10 ng/ml produced a very weak induction [**Fig R3.16**]. Interestingly, for this experiment, a steep reduction in induction was observed for both clones for both 800 and 40 ng/ml Dox.

When neural differentiation was investigated it was observed that for clone doTE171, 800 ng/ml completely blocked *Sox1*, at all time points tested. On the other hand, 40 ng/ml produced only a mild downregulation, more notable on day 4. By contrast, clone doTE155 suffered only downregulation, but not block, at 800 ng/ml Dox for *Sox1* expression and, no influence for 10 and 40 ng/ml doses. These data confirm the previous results and explains neural inhibition by high levels of TwE through block in *Sox1* upregulation. Furthermore, the differences in *Sox1* expression at 40 ng/ml Dox, a dose at which induction was similar for both clones points to the fact that not only doTE155 can silence the transgene more efficiently, but that it is also less sensitive to lower levels of induction [**Fig R3.17a and b**].

The early marker *Zfp521* had an expression which correlated directly with the level of induction for both clones, though upregulation by TwE was very moderate. This is in line with previous data, showing that important upregulation of *Zfp521* in response to TwE in the case of clone doTE77 was observed as a rescue against BMP inhibition, while in basal neural conditions this effect was less obvious [**Fig R3.17c, d;** see also **Fig R1.10b and Fig 1.17b**].

Furthermore, for the EMT marker *Zeb2* both clones the highest upregulation was seen at day 2. Interestingly, the most important difference was seen for doTE155 when shifting Dox dose from 40 to 800 ng/ml, while for doTE171 when shifting from 10 to 40 ng/ml [**Fig R3.18a and b**].

The upregulation of the neural crest marker *Sox9* was for both clones was directly dependent on Dox dose. However, it should be noted that 40 ng/ml Dox for clone doTE171 achieved an upregulation similar with 800 ng/ml for doTE155. The upregulation of the nest neural crest marker *Wnt1* was less consistent. For clone doTE155 it was dose dependent, with the highest upregulation for 800 ng/ml Dox.

Figure R3.16. Induction of TwE during neural differentiation in response to various concentrations of Dox

qPCR showing *Twist1* expression in self renewal conditions, or during differentiation at the stated time points and Dox concentrations. Clone doTE155 (a and c), clone doTE171 (b and d). Bottom row shows expression only for lower Dox concentrations. *Twist1* expression for clone doTE171 in self renewal conditions was arbitrarily set to 1. For each clone one experiment performed in duplicates is shown. Error bars represent value range.

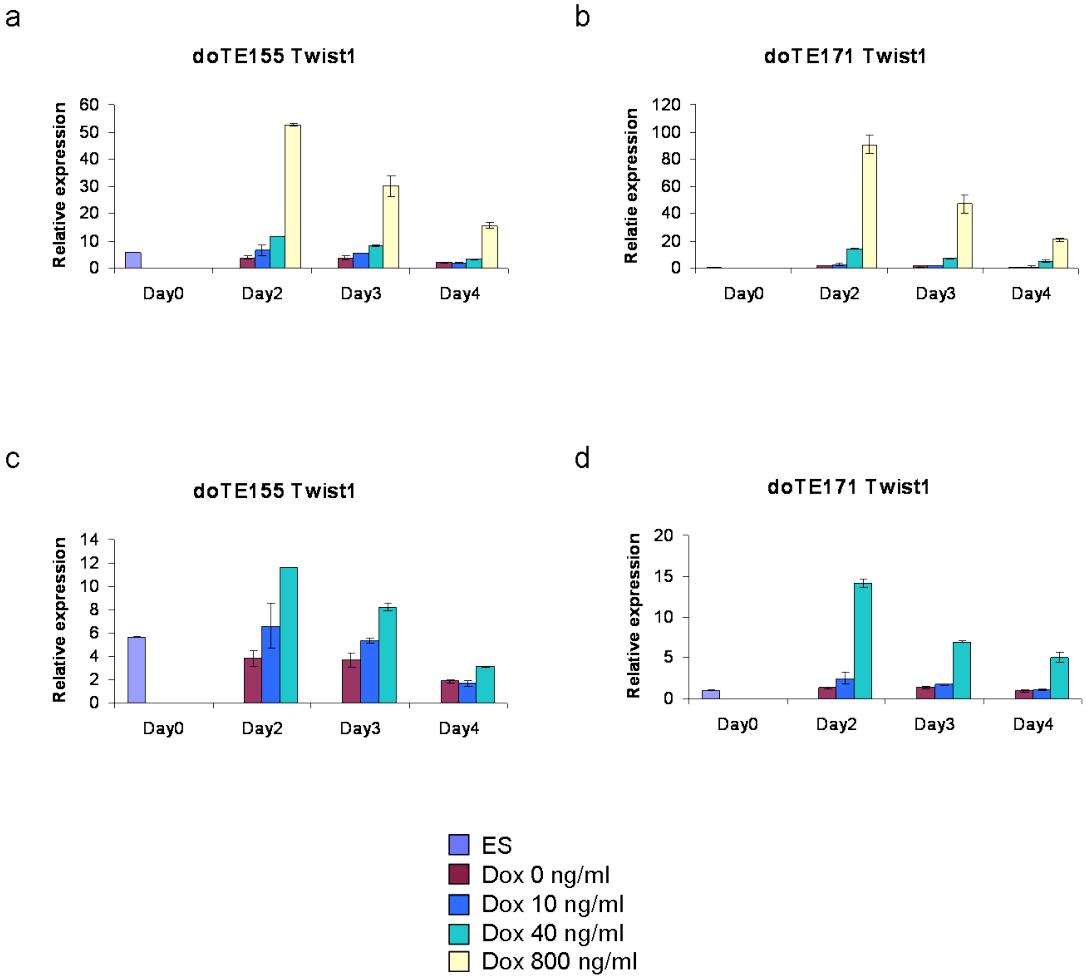
a
doTE155 Twist1
Relative expression
60
50
40
30
20
10
0
Day0
Day2
Day3
Day4
b
doTE171 Twist1
Relatie expression
120
100
80
60
40
20
0
Day0
Day2
Day3
Day4
c
doTE155 Twist1
Relative expression
14
12
10
8
6
4
2
0
Day0
Day2
Day3
Day4
d
doTE171 Twist1
Relative expression
20
15
10
5
0
Day0
Day2
Day3
Day4
ES
Dox 0 ng/ml
Dox 10 ng/ml
Dox 40 ng/ml
Dox 800 ng/ml

Figure R3.17. Upregulation of early neural markers in response to various concentrations of Dox

qPCR showing Sox1 and Zfp521 expression in self renewal conditions, or during differentation at the stated time points and concentrations of Dox. Sox1 (a and b), Zfp521 (c and d). For each gene the average expression in the two clones at ES cell stage has been arbitrarily set to 1. For each clone one experiment performed in duplicates is shown. Error bars represent value range.

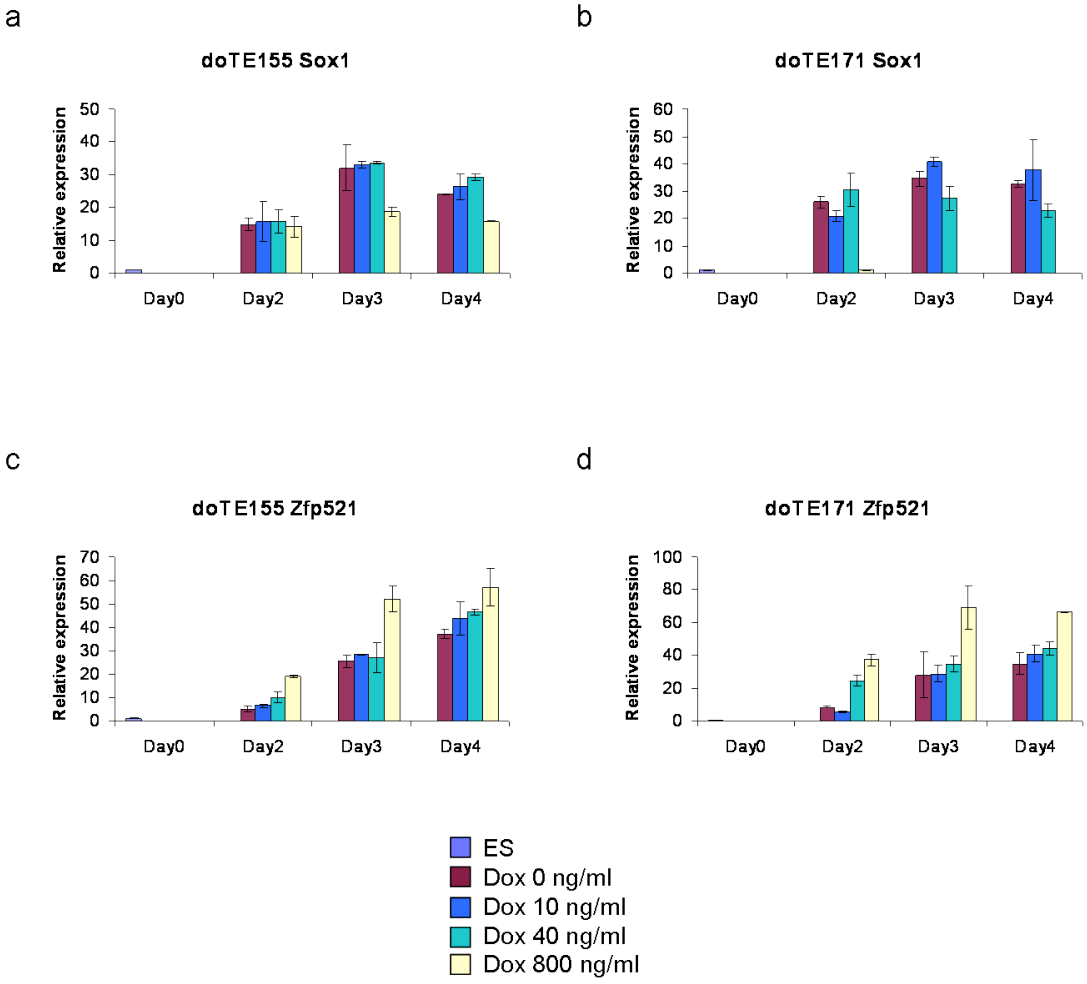
a
doTE155 Sox1
Relative expression
50
40
30
20
10
0
Day0
Day2
Day3
Day4
b
doTE171 Sox1
Relative expression
60
50
40
30
20
10
0
Day0
Day2
Day3
Day4
c
doTE155 Zfp521
Relative expression
70
60
50
40
30
20
10
0
Day0
Day2
Day3
Day4
d
doTE171 Zfp521
Relative expression
100
80
60
40
20
0
Day0
Day2
Day3
Day4
ES
Dox 0 ng/ml
Dox 10 ng/ml
Dox 40 ng/ml
Dox 800 ng/ml

Figure R3.18. Upregulation of EMT and neural crest markers in response to various concentrations of Dox

qPCR showing Zeb2 (a and b), Sox9 (c and d) and Wnt1 (e and f) expression in self renewal conditions, or during differentiation at the stated time points and concentrations of Dox for clone doTE155 and doTE171 respectively. For each gene the average expression in the two clones at ES cell stage has been arbitrarily set to 1. For each clone one experiment performed in duplicates is shown. Error bars represent value range.

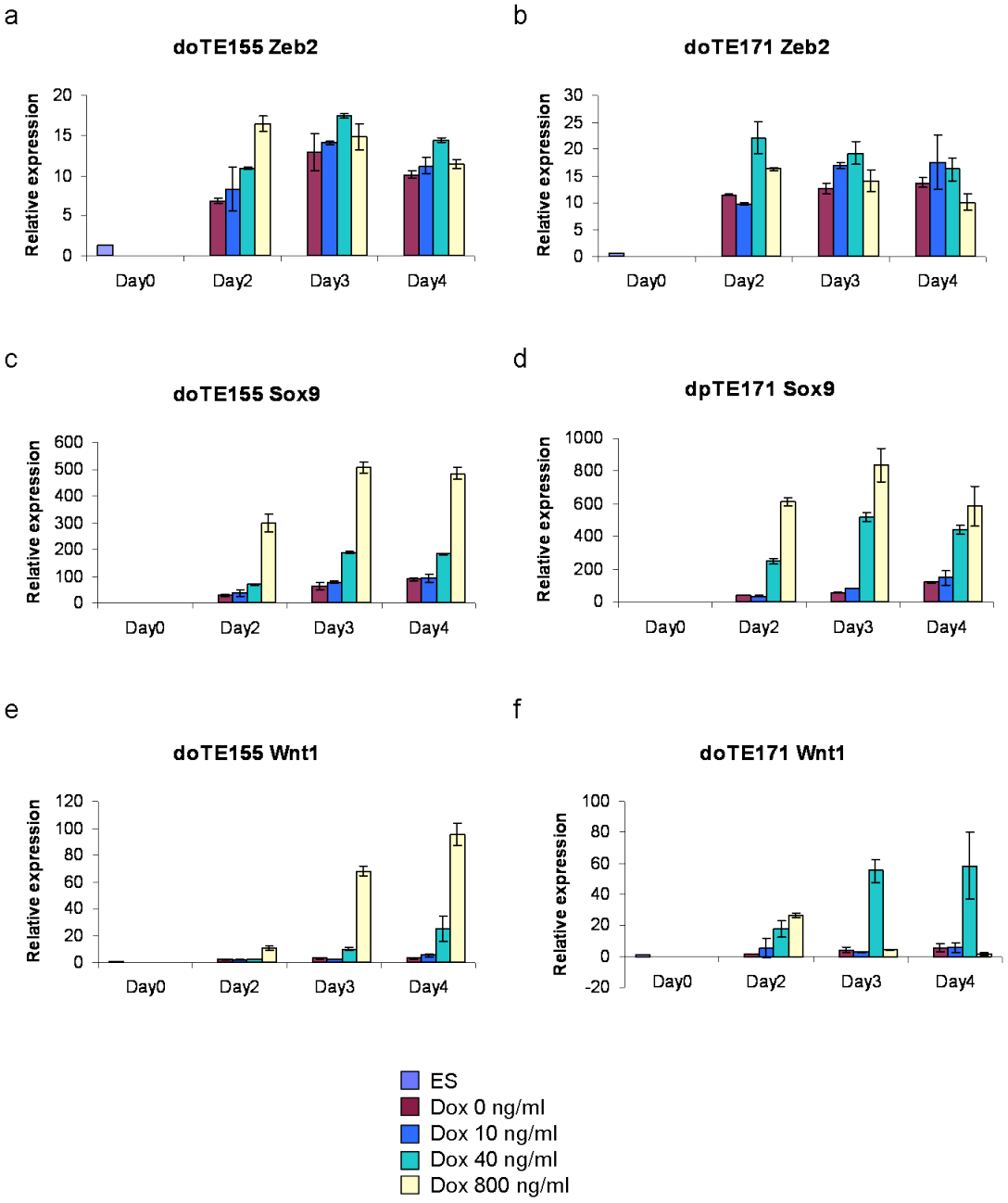
a
doTE155 Zeb2
Relative expression
20
15
10
5
0
Day0
Day2
Day3
Day4
b
doTE171 Zeb2
Relative expression
30
25
20
15
10
5
0
Day0
Day2
Day3
Day4
c
doTE155 Sox9
Relative expression
600
500
400
300
200
100
0
Day0
Day2
Day3
Day4
d
dpTE171 Sox9
Relative expression
1000
800
600
400
200
0
Day0
Day2
Day3
Day4
e
doTE155 Wnt1
Relative expression
120
100
80
60
40
20
0
Day0
Day2
Day3
Day4
f
doTE171 Wnt1
Relative expression
100
80
60
40
20
0
-20
Day0
Day2
Day3
Day4
ES
Dox 0 ng/ml
Dox 10 ng/ml
Dox 40 ng/ml
Dox 800 ng/ml

However, for doTE171 800 ng/ml was inhibitory almost completely blocking the expression of this marker. By contrast, 40 ng/ml Dox induced a good upregulation of *Wnt1*, superior to the upregulation produce by the same dose in doTE155. These data indicate that while *Wnt1* is responsive to TwE, it is also dependent of neural differentiation and that cellular context can alter TwE effect on this marker [**Fig R3.18c to f**].

Together the data presented in this section indicate that the levels of TwE are more important than the time of induction and that, high levels of TwE are incompatible with neural differentiation.

R3.8 TWIST1 Dimer Choice Relevance

R3.8.1 Generation and Characterization of Tw-Tw Inducible Clones

Since as shown in the previous chapter *Twist1* is expressed in the dorsal region of the neural folds there is a possibility that BMP signalling is strong enough in that region to bias TWIST1 towards homodimer formation. Previously, it was proposed that TW-E and TW-TW dimers have opposing roles, at least in the certain fate choice decisions [Connerney et al., 2006]. Furthermore, TW-E and TW-TW dimers regulate different genes [Laursen et al., 2007]. Considering that ID proteins block formation of TW-E dimers and thus favour TW-TW dimers, and that IDs act downstream neural negative regulator BMP, it is conceivable that TW-TW should block neural differentiation. On the other hand TW-TW formed under the BMP influence in the dorsal neural fold could participate in inducing the neural crest fate. Therefore, the influence of TWIST1-TWIST1 forced dimer on neural differentiation should be investigated.

For this reason I generated a plasmid similar with the TetO-TwE plasmid described in Results_1, in which Twist1-linker-E construct has been replaced with Twist1-linker-Twist1 construct [**Fig R3.19**]. The active dimer produced by this plasmid will be called in this thesis TwTw.

TwTw clones were isolated as before for TwE using PD0325901 as an anti-differentiating molecule. Using this method, stable inducible clones, expressing the transgene at high levels, could be obtained [**Fig R3.20**].

R3.8.2 Tw-Tw Influence on Neuron Formation

First, I tested TwTw influence on neural differentiation and its dependence on induction levels. For this purpose I used the same doses of Dox as in the TwE experiment: 0 ng/ml, 10 ng/ml, 40 ng/ml and 800 ng/ml respectively. Neural differentiation was assessed by TUBB3 staining form day 2 to day 4. It can be seen that in the case of 800 ng/ml Dox, neurites are never formed, indicating a very efficient block in neural differentiation. However, at 10 and 40 ng/ml rare TUBB3 positive neurites are formed, but they are never bundled around the originating colony, as in control, but rather have a tendency to connect to the neighbouring colony, as is the case for TwE induced neurons [**Fig R3.21**].

When neural formation was quantified, as described in M4.1.2, the same genral pattern as for TwE clones was observed. Namely, there was a dose dependent suppression of neural formation, with complete neural block at 800 ng/ml Dox [**Fig R3.22a**]. Furthermore, up to the dose of 40 ng/ml Dox neural suppression was produced on the expense of neurons with short neurites, while formation of neurons with long neurites was slightly increased compared to no Dox treatment [**Fig R3.22b**].

R3.8.3 Tw-Tw Influence on Neural Marker Expression

Next, I tested TwTw influence on neural differentiation based on marker expression. Again, I considered the possibility that after the initial differentiation events TwTw could be more permissive for neural fate. Thus, Dox was added either throughout the experiment or only at day 2. The differentiation was assessed by marker expression at day 4.

It was observed that in these conditions the transgene is expressed at higher level than TwE, while some downregulation was present after four days of induction, compared to two days [**Fig R3.23**].

When neural markers were tested, *Sox1* upregulation at day 4 of differentiation was strongly suppressed by Dox treatment in all conditions [**Fig R3.24**a]. On the other hand, *Zfp521* was not significantly influenced, except for a slight downregulation induced by late Dox treatment [**Fig R3.24b**]. The recovery of this marker expression to control level in the case of Dox continuous treatment indicates that the observed downregulation does not have major influence on cell fate. *Atoh1* is expressed in all conditions, including control, at levels significantly lower than in the ES cells [**Fig R3.24c**]. Together, these data indicates that TwTw has a negative influence on neural differentiation regardless of the moment of expression.

When other markers upregulated by TwE were investigated a more consistent picture appeared. TwTw upregulated *Sox9*, and the upregulation depended directly on the length of induction [**Fig R3.24d**]. Furthermore, *Msx1* was upregulated, but only by stimulation for the entire differentiation [**Fig R3.24e**]. *Zeb1* was upregulated in all conditions in a manner very similar with the upregulation induced by TwE [**Fig R3.24f**]. These data indicates that while TwE and TwTw are considered transcriptional effectors with divergent roles they might share at least some of their actions in certain contexts.

The data presented here is somewhat in agreement with my initial hypothesis, in the sense that at high levels Tw-Tw a dimer though to be favoured by BMP/ID signalling, has a negative influence on neural differentiation. However, since no striking difference can be observed between TwTw and TwE I have to conclude that BMP/ID influence on TWIST1 dimer choice is not a major mechanism for regulating the neural fate. Moreover, the level of *Twist1* expression holds the fundamental fate choice decision, with high levels favouring mesenchymal fates and low levels favouring dorsal neural fates. It can also be inferred that *Twist1* upregulation might be involved in the transition from dorsal neural to neural crest.

Figure R3.19. Schematics of Doxycyclin inducible TWIST1 homodimer

Diagram of TwTw Doxycyclin inducible construct and plasmid (a and b respectively).

a


PGK
Puro
pA
CMV-TetO
Flag
Twist1
linker
Twist1
pA

b

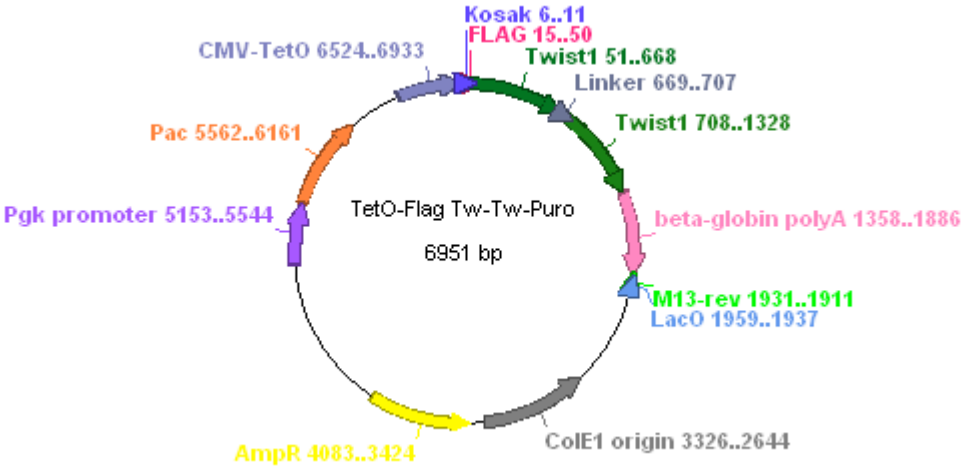
Kosak 6..11
FLAG 15..50
Twist1 51..668
Linker 669..707
Twist1 708..1328
beta-globin polyA 1358..1886
M13-rev 1931..1911
LacO 1959..1937
ColE1 origin 3326..2644
AmpR 4083..3424
Pgk promoter 5153..5544
Pac 5562..6161
CMV-TetO 6524..6933
TetO-Flag Tw-Tw-Puro
6951 bp

Figure R3.20. Screening of TWIST-TWIST cell lines

Immunofluorescence for two clones: doTT202 and doTT219, after 24 hours of induction showing heterogeneous expression, including brightly stained cells. Red: Flag staining, blue DAPI. Scale bars represent 50 μm (a). qPCR showing expression of Twist1 after 24 hours of induction compared to parental cell line. Expression in parental cell line has been arbitrarily set to 1. For each clone one experiment performed in duplicates is shown. Error bars represent value range (b). Western blot for Flag for 3 clonal lines showing induction of the transgene in response to Dox (c).

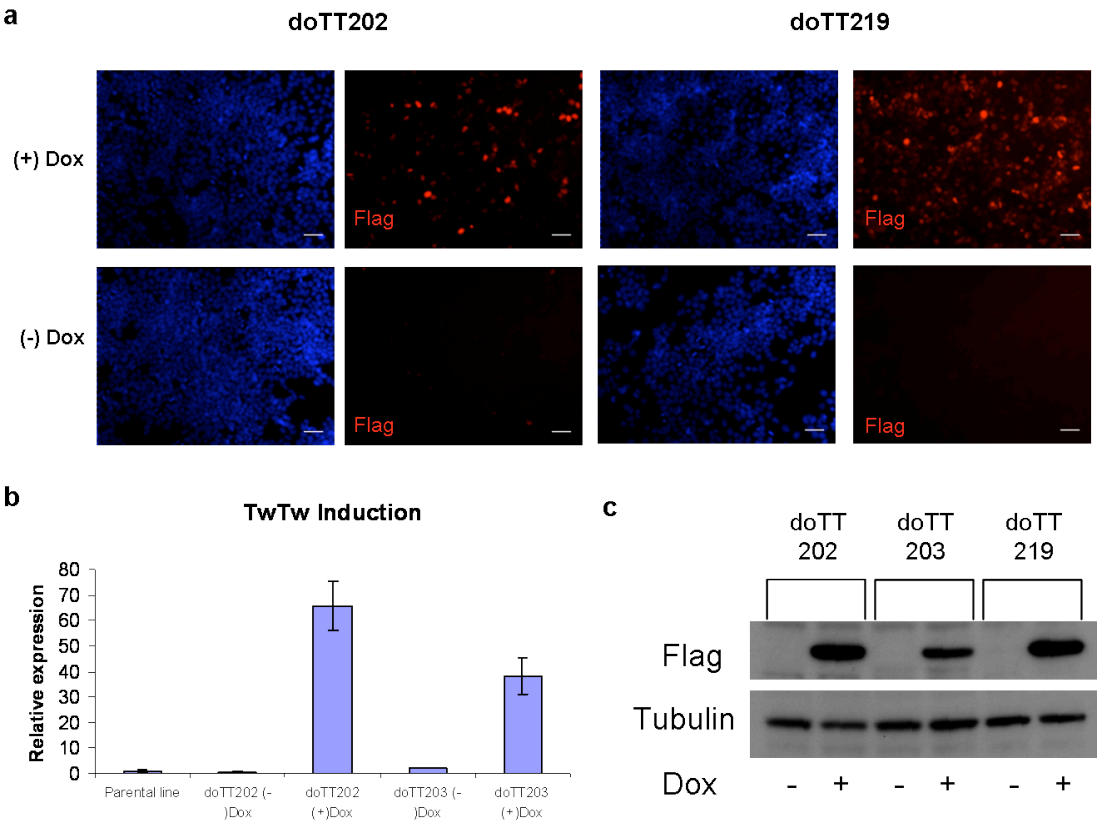
a
doTT202
doTT219
(+) Dox
(-) Dox
Flag
Flag
Flag
Flag
b
TwTw Induction
Relative expression
80
70
60
50
40
30
20
10
0
Parental line
doTT202 (-)Dox
doTT202 (+)Dox
doTT203 (-)Dox
doTT203 (+)Dox
c
doTT 202
doTT 203
doTT 219
Flag
Tubulin
Dox
- + - + - +

Figure R3.21. TwTw effects on neural differentiation based on induction levels

Immunofluorescence for TUBB3: green; nuclei counterstained with DAPI for cells from clone doTT202 differentiated for 4 days in monolayer protocol and induced with the stated concentration of Dox. Cells were fixed at Day 2 of differentiation (a), day 3 (b) and day 4 (c). Scale bars represent 50 μm.

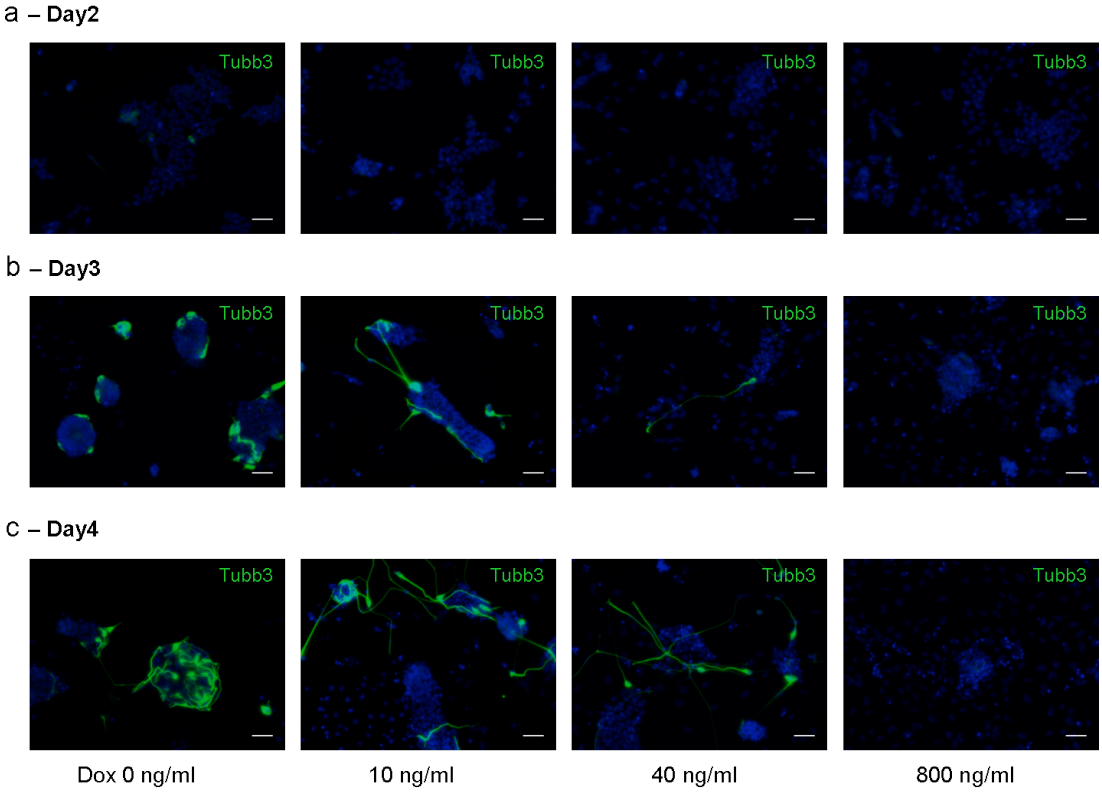
a – Day2
Tubb3
Tubb3
Tubb3
Tubb3
b – Day3
Tubb3
Tubb3
Tubb3
Tubb3
c – Day4
Tubb3
Tubb3
Tubb3
Tubb3
Dox 0 ng/ml
10 ng/ml
40 ng/ml
800 ng/ml

Figure R3.22. Quantification of neuron formation under TwTw influence

Representation of total number of TUBB3 positive cells per 100 cells for clone doTT202 (a). Representation of neurons with short and long neurites respectively per 100 cells (b). An arbitrary threshold has been set considering a neurite as being long if its length equalled or exceeded 7 mean nuclear diameters. Data collected at day four of neural differentiation. Dox doses used: 0, 10, 40 and 800 ng/ml respectively. Error bar represent standard deviation of the mean for three microscopic fields for each condition.

a

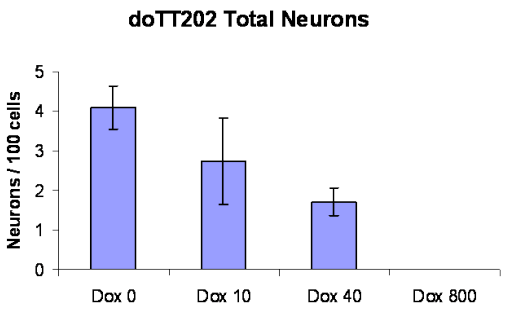
doTT202 Total Neurons
Neurons / 100 cells
5
4
3
2
1
0
Dox 0
Dox 10
Dox 40
Dox 800

b

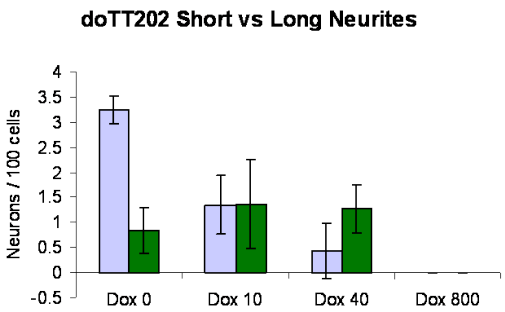
doTT202 Short vs Long Neurites
Neurons / 100 cells
4
3.5
3
2.5
2
1.5
1
0.5
0
-0.5
Dox 0
Dox 10
Dox 40
Dox 800

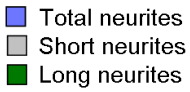
Total neurites
Short neurites
Long neurites

Figure R3.23. TwTw induction during neural differentiation

qPCR showing Twist1 expression in ES cells and cells at day 4 of neural differentiation in monolayer protocol. Cells were either not induced: -Dox, induced for the last 2 days of differentiation: +Dox Day 2-4, or induced throughout differentiation: +Dox Day 0-4. Expression in ES cells for clone doTE171 has been arbitrarily set to 1, to allow full comparison with TwE results. Then, the resulting levels have been divided by 2 to compensate for the presence of 2 Twist1 sequences in the TwTw construct. Error bars represent standard deviation of the mean for two biological replicates. One experiment performed in duplicates is shown. Error bars represent value range.

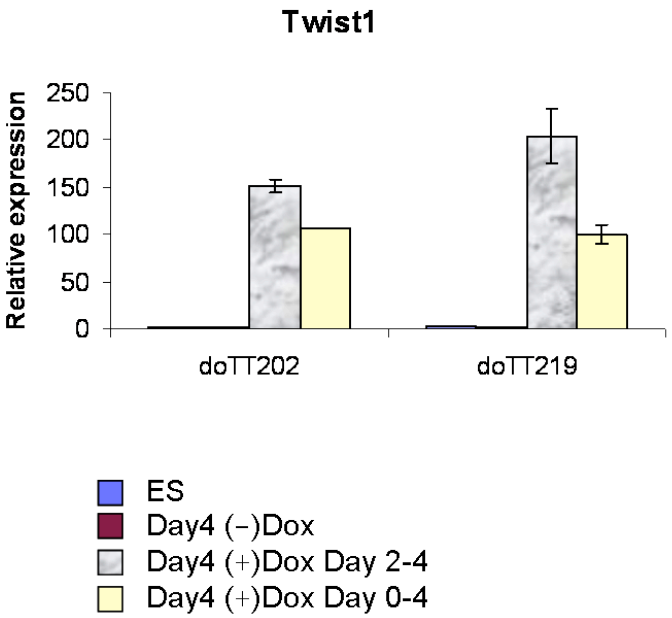
Twist1
Relative expression
250
200
150
100
50
0
doTT202
doTT219
ES
Day4 (−)Dox
Day4 (+)Dox Day 2-4
Day4 (+)Dox Day 0-4

Figure R3.24. Time of TwTw induction influence on differentiation markers expression

qPCR showing expression of Sox1 (a), Zfp521 (b), Atoh1 (c), Sox9 (d), Msx1 (e) and Zeb1 (f) in ES cells and cells at day 4 of neural differentiation in monolayer protocol. Cells were either not induced: -Dox, induced for the last 2 days of differentiation: +Dox Day 2-4, or induced throughout differentiation: +Dox Day 0-4. For each gene the average expression in the two clones at ES cell stage has been arbitrarily set to 1. One experiment performed in duplicates is shown. Error bars represent value range.

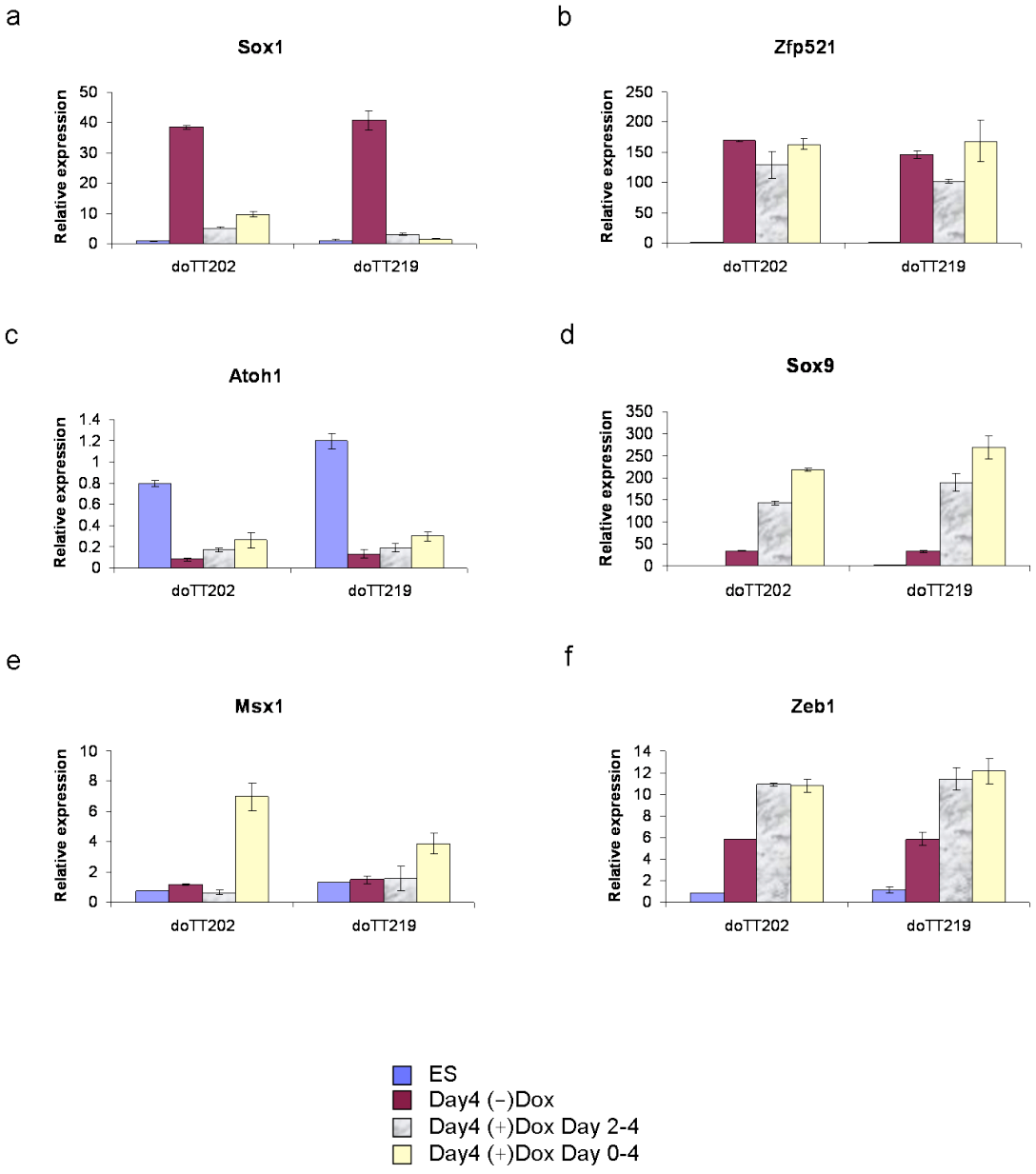
a
Sox1
Relative expression
50
40
30
20
10
0
doTT202
doTT219
b
Zfp521
Relative expression
250
200
150
100
50
0
doTT202
doTT219
c
Atoh1
Relative expression
1.4
1.2
1
0.8
0.6
0.4
0.2
0
doTT202
doTT219
d
Sox9
Relative expression
350
300
250
200
150
100
50
0
doTT202
doTT219
e
Msx1
Relative expression
10
8
6
4
2
0
doTT202
doTT219
f
Zeb1
Relative expression
14
12
10
8
6
4
2
0
doTT202
doTT219
ES
Day4 (-)Dox
Day4 (+)Dox Day 2-4
Day4 (+)Dox Day 0-4

R3.9 Conclusions

In this chapter I started from the observation that *Twist1* is expressed at low levels in a subset of cells from the neuroectoderm, but is highly expressed in cells that have recently exited the epiblast to become mesoderm, as well as in cells which exited the neuroectoderm to become neural crest. Therefore I proposed that *Twist1* might regulate fate decisions depending on its levels; namely, that at low levels it favours dorsal neural fates and at high levels it favours mesenchymal fates.

When I tested relatively high TwE expressing clones I found out that they have a variable phenotype. I assigned this variability to a process of adaptation due to selective pressure. I showed that TwE can override the selfrenewing program controlled by LIF and BMP. I also showed that this process of exit from pluripotency is accompanied by EMT and formation of a mesenchymal like cell type.

Furthermore, I showed that TwE blocks neural differentiation when expressed at high levels and accelerates formation of postmitotic neurons when expressed at low levels. I confirmed the fact that TwE upregulates neural crest markers and that, for clone doTE171 which is more responsive to TwE, moderate levels of expression are sufficient for the upregulation of these markers.

I indicate a number of early responsive genes, which most likely, cooperate in generating the later effects. TwE has an early effect on pluripotency and EMT genes though not on Cadherins. On neural differentiation TwE is a two edge sword, upregulating some dorsal neural markers while having a marked negative effect on more genral neural markers, most notably *Sox1*. Furthermore, *Sox1* has been shown to maintain the pool of undifferentiated neural progenitors by counteracting pro-neural bHLH factors [Bylund et al., 2003]. Here, I report the complementary effect, where a bHLH factor accelerates neural differentiation by inhibiting *Sox1*.

Next I investigated the putative roles of TwTw on neural differentiation. The significance of this question had already been weakened by the observation that high TwE blocks neural differentiation. Thus, it could no longer be argued that we are

dealing with a binary fate switch were TwE favours neural differentiation while TwTw blocks it.

Surprisingly, there was a high level of similarity between TwE and TwTw. TwTw, just like TwE blocks neural differentiation when expressed at high levels. At moderate levels, again, it promotes formation of premature neurons, while upregulating similar EMT and neural crest markers. Thus, it is possible that *Twist1* roles in CNS depend primarily of its expression, while being protected against BMP dynamic by the irrelevance of dimer choice in this context, independent of the battle for supremacy between various BMP activators and inhibitors in the dorsal neural tube.

Figure R3.25. Schematic Conclusions

TwE induction of cell fate depends on its level of activity. Both high and low TwE divert a cell from the pluripotent compartment, but at high levels a cell is directed towards non-neural fates, while at low levels neural differentiation is permitted and accelerated. Furthermore, both high and low levels of TwE induce EMT, including upregulation of *Zeb2*, a neural EMT marker. It should be noted that *Twist1, Zfp521, Pax3* and *Sox9* are expressed both in certain neural and mesenchymal cells, and could form a transcriptional network involved in cell fate decision depending on developmental context.

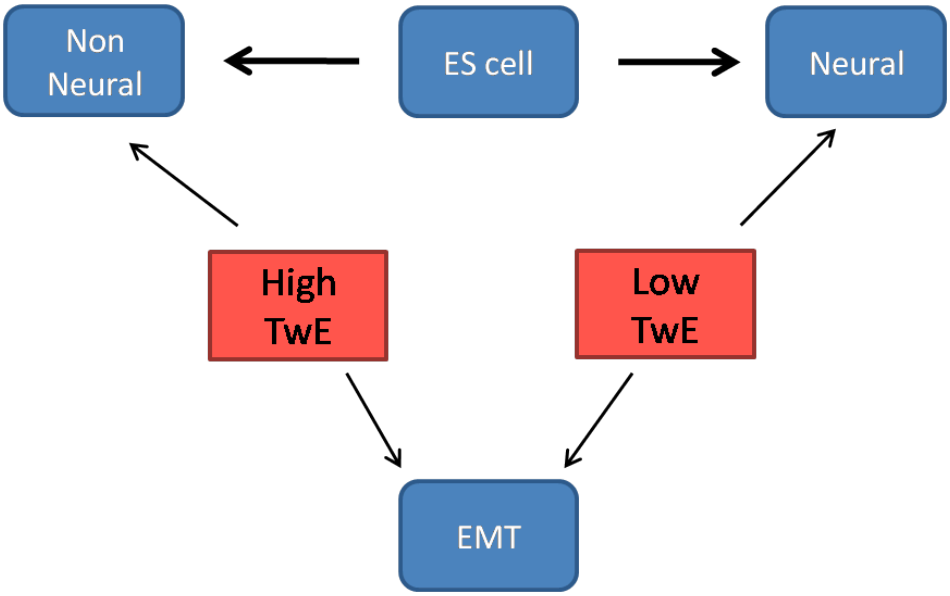
Non Neural
ES cell
Neural
High TwE
Low TwE
EMT

VI. DISCUSSION

D1 Finding a Place in Time: TWIST1 and Neural Differentiation

From a large body of work which started with Spemann and Mangold's seminal experiments of axis induction by the organizer and culminated with the discovery of BMP antagonists as the key effectors of the organizer, BMP has been firmly established as the most important anti-neural signalling molecule [Spemann and Mangold, 1924; Smith and Harland, 1992; Sasai et al, 1994; Hemmati-Brivanlou and Melton, 1994; Bouwmeester et al, 1996]. As is always the case in science, here too, the situation has been proven to be more complicated, with many signalling pathways collaborating to correctly establish the neural fate [Streit et al, 2000; Lowell et al, 2006; Stavridis et al, 2007; Marchal et al, 2009]. Nevertheless, these later investigations could not challenge the importance of BMP inhibition in neural specification, while ID proteins have been proposed as the main antineural effectors downstream BMP [Ying et al, 2003a].

Our lab continued the work presented above aiming at defining more precisely the events associated with the entry to neural progenitor fate. Owen Davies identified TWIST1, TCF15 and NEUROD1 as partners of E proteins in ES cells, which might be subject to ID inhibition.

Judging TWIST1 as the most likely candidate I tested it under the form of an ID insensitive, E forced partner: TwE. The results presented in this thesis, while exciting in certain aspects do not support the notion that TWIST1 and, more notably, TWIST1-E dimer is the key transcription factor required for neural induction; TwE at high levels was incompatible with neural differentiation and at low levels accelerated it. However, acceleration was not the expected outcome; rather induction and maintenance of the neural progenitor pool should be the roles of an early neural gene. Furthermore, experimental knockdown of *Twist1* does not seem to impair neural

differentiation, while gene expression analysis indicated that *Twist1* is expressed only at later stages of development in the prospective neural tissue. It should also be noted, that *Twist1* expression in ES and early differentiating cells could be entirely artifactual, a consequence of specific culture conditions.

What then might be the ID target, relevant to neural induction? The other two proposed bHLH factors have been tested in the Lowell lab (manuscripts in preparation). NEUROD1 does not seem to be the appropriate choice for this task, as it is very poorly tolerated by pluripotent cells and has been implicated in the terminal differentiation of mature neurons [Lee et al., 1995]. *Tcf15* is expressed at higher levels in ES cells and seems to be a very early facilitator of neural induction. However, induction of TCF15-E forced dimer could not be shown yet to overcome neural BMP inhibition. Overall, no ID target found so far has a comparable strong effect with either ID1 or BMP.

One confounding issue might be that we are not aware of the exact moment of neural induction [Di Gregorio et al., 2007; Stern C.D., 2006]. Since ES cells can be maintained undifferentiated by LIF and BMP4, it was assumed that, at this stage, BMP4 already acts to inhibit neural inducing factors. However, this is not necessarily the case. It is possible that BMP4 has a dual role, one in ES cells where it inhibits priming factors, and another in epiblast like cells, where it inhibits the true neural inducers, which might be present only at this stage. It should also be noted that the term “epiblast cells” encompasses a rather large pool of cell fates and stages. In the embryo epiblast cells undergo rapid changes, both in marker expression and spatial position. Furthermore, there is no guarantee, that differentiation in the tissue culture dish, progresses at the same rate as in the embryo. In fact, we can almost be sure of the contrary. Thus, we are the victims of a double uncertainty: for one we are not entirely sure when neural specification starts in vivo [Puelles et al, 2005] and, for the other, the limited knowledge we have from the embryo can not be easily extrapolated to our in vitro models. The data presented here for early TwE induction argue that key events take place in the first 24 hours of withdrawal of pluripotency factors, an idea which correlates with the previous finding that FGF signalling is critical for neural induction in the first 24 hours of differentiation [Kunath et al., 2007; Stavridis et al., 2007]. However, since Twist1 physiological roles might be pertinent to later stages,

the phenomenon observed could represent just a rapid phenotypic change of the cells towards a stage when Twist1 should normally act.

D2 TWIST1 a Surprising Neural Effector

D2.1 Can TWIST1 Be Neural?

TwE was consistently found to hasten the exit from neural progenitor state. An effect which can be explained by its negative influence on transcription factors associated with neural progenitors like *Sox1* and SOX2 [Fig R1.11c; Fig R1.12]. This could be consistent with the idea that *Twist1* might not be a neural factor at all, in the sense, that it should not be normally active in neural progenitors and, that its forced expression deeply perturbs the neural program.

However data from multiple directions contradict such a simplistic hypothesis.

First, I found *Twist1* to be expressed in a subset of neural progenitors in vivo.

Second, TwE induces early upregulation of *Sox1*. This is most likely an indirect effect and, probably represents an indication that the cells have entered the neural program, as pointed out by upregulation of other early neural markers: *Zfp521*, *Pax3* and *Zeb2* [Fig R1.15; Fig R1.16].

Third, TwE upregulates *Zfp521*, a molecule reported to induce *Sox1* [Kamiya et al., 2011]. Importantly, TwE most clear effect on *Zfp521* expression can be observed against BMP inhibition [Fig R1.20b]. Thus, *Twist1* could act to safeguard neural differentiation in very specific contexts, for instance, in the lateral regions of the neural plate.

D2.2 TWIST1 Joins The Fight for Neural against BMP.

Previous worked showed that BMP signalling from the surface ectoderm specifies neural crest cells in the lateral most regions of the neural plate. One idea would be that neural crest cells act as a buffer region between surface ectoderm and the "strictly neural cells", as defined by Puelles and colleagues, namely cells which are fated to become part of CNS [Puelles et al, 2005]. Thus, the "strictly neural cells" are spatially determined in the region where BMP signalling is low enough for their fate to be permitted. Nevertheless, it is more reasonable to think that once the neural fate has been initiated, specific effectors start to act, which stabilize this program against inherent fluctuations in signalling levels. We know that at early stages, neural progenitors are still responsive to antineural BMP signalling [Yang and Klingensmith, 2006], but this does not deny the very likely possibility, that some resistance against low BMP levels is set in place.

The *in vitro* data presented here, argues that TWIST1 could be one of the factors involved in such stabilization [Fig D1]. On one hand, TwE can rescue neural program against moderate levels of BMP. On the other hand, high levels BMP can still block neural differentiation. This is consistent with the idea that TwE is not part of the master switch between neural and non-neural, but rather acts as a context dependent regulator.

Figure D1. Schematics of the proposed role of TWIST1 in neural plate

A BMP gradient decreasing from lateral to medial influences the epiblast. Medial from the point where this gradient is low enough to be permissive for neural induction (dotted line A) neural plate is being specified. Medial from dotted line B, the BMP signalling is so low that it has no biologic significance. In between lines A and B neural crest cells are formed and *Twist1* expressing cells (blue dots) act.

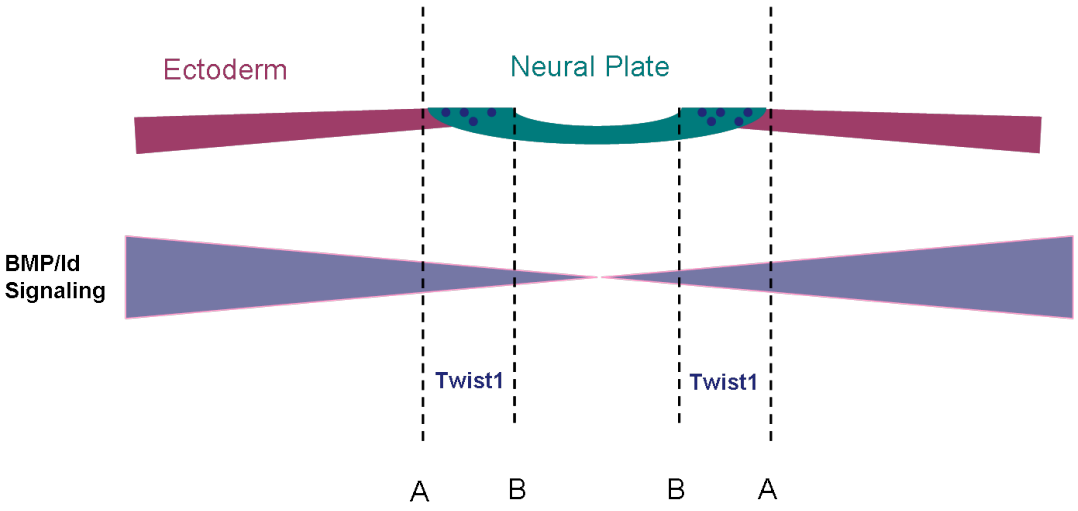
Ectoderm
Neural Plate
BMP/Id
Signaling
Twist1
Twist1
A
B
B
A

D2.3 TWIST1, EMT and The Neural Program

One question raised by the current project is: what role, if any, might TWIST1 have in the neural program? An obvious idea would be to connect TWIST1 role in epithelial to mesenchymal transition (EMT) with neural differentiation. Epiblast cells start as an epithelial sheet and early neural markers are upregulated before any morphological changes can be observed [Puelles et al., 2005; Arnold & Robertson, 2009]. Then, before the formation of the closed neural tube, neural cells undergo an EMT like event when OCCLUDIN is lost and CDH1 is replaced with CDH2 at the cell surface, resulting in the loss of tight junctions [Aaku-Saraste et al., 1996; Van de Putte et al., 2003]. Nevertheless, at this stage, cells maintain morphological and structural epithelial characteristics, based on the presence of adherens junctions. "This change may represent the first step in a program by which neuroepithelial cells gradually loose their epithelial characteristics, culminating in the generation of nonepithelial cells, the neurons." [Aaku-Saraste et al., 1996]

It is conceivable that CDH1 downregulation, which is one of the actions for which TWIST1 is known [Yang et al, 2004], facilitates the neural program and thus explains, at least in part, the observed effects of TwE. However, previously *Zeb2* and not *Twist1* has been implicated in Cdh1 downregulation during neural differentiation [Van de Putte et al., 2003]. Interestingly, TwE was found to enhance *Zeb* factors upregulation during *in vitro* neural differentiation [Fig R1.16a and b]. From the data presented here it is not possible to distinguish if CDH1 is downregulated in response to TWIST1 or, as a consequence of ZEB factors induction. Perhaps, it is more useful to simply consider the phenomenons observed: namely that during neural differentiation, both in vitro and in vivo. CDH1 is downregulated and *Zeb2* is upregulated and that TwE facilitates both this processes. Thus, TwE induces EMT associated events during early in vitro differentiation of pluripotent cells, in a manner which is consistent with the neural program.

It should be noted that TWIST1 early roles cannot be limited to EMT induction. On one hand, TwE induces the expression of early neural markers, which are normally present before the downregulation of CDH1, like *Pax3* [Basch et al., 2006].

On the other hand, TwE induces a dorsal bias in neural identity, while CDH1 is downregulated fully throughout the neural tube [Aaku-Saraste et al, 1996; and Lowell lab unpublished data]. Together these data indicate that TWIST1 could integrate EMT induction with specific transcriptional activities to affect neural differentiation.

D3 Twist1 and Neural Crest

D3.1 Neural Crest a Dorsal Cell Type and Twist1 Activity

Since most of the dorsal neural markers, reported here, are shared with the neural crest, an interesting question would be if TWIST1 has only a general role in establishing dorsal identity, or a more specific role in cell fate. *Snai2* (also known as Slug or Snail2, in Xenopus snai2-a) marks the pre-migratory neural crest cells in Xenopus [Mayor et al, 1995] and is essential for the induction of these cells [Shi et al, 2011]. However, in mouse *Snai2* is only expressed in migratory neural crest cells and is not required for their formation [Jiang et al., 1998]. Furthermore, *Snai2* and *Twist1* were found to cooperate in EMT induction [Casas et al., 2011]; hence *Twist1* could play a role in mouse neural crest specification.

Given the previously reported marker overlap [Puelles et al, 2005], it is difficult to distinguish a putative role for TWIST1 in establishing either the neural crest or dorsal neural fate, by means of *in vitro* neural differentiation. However, prospective dorsal neurons and neural crest cells, are both neural in a larger sense, and there is yet, no conclusive evidence, to show that this two fates are strictly separated before neural crest delamination. Therefore, it can be proposed that TWIST1 imparts a dorsal identity to cells residing in the neural folds and, that specific signals which further segregate the cell fates within this developmental niche are to be uncovered by future research,

D3.2 Could Twist1 Be an Early Neural Crest Marker?

A role for Twist1 in establishing the neural crest fate should also be considered. *Twist1* is expressed very strongly in the neural crest cells and has functional significance in neural crest differentiation and migration [Bildsoe et al., 2009; Das & Crump, 2012; Soo et al., 2002; Vincentz et al., 2008; Zhang et al., 2012]. However, since *Twist1* was thought not to be expressed at the level of neural plate/neural tube its relevance in neural crest specification and delamination was less studied.

The only direct, albeit not very strong evidence, regarding Twist1 expression in early neural crest comes from Fuchtabauer's in situ data [Fuchtabuer E.M., 1995]. The author found that *Twist1* is expressed in a few cells in the neural tube and since, those cells seemed to have a round morphology, with little cell to cell contact with the surrounding cells, they were deemed as delaminating neural crest cells. If this observation is correct, it indicates that *Twist1* is upregulated in neural crest before or, to the very least, at the time of delamination and points to a possible role *Twist1* might have in the process of delamination.

One question here would be: why wasn't this process described more consistently? It would be reasonable to infer that if *Twist1* is indeed upregulated in all delaminating neural crest cells this would have been reported and clearly documented. On the other hand, neural crest cells do delaminate from the neural tube in *Twist1* null mice [Soo et al., 2002]. Furthermore, *Twist1*-negative neural crest cells migrate relatively normally when directed by *Twist1* expressing mesoderm. Collectively, these observations make a strong argument against a role for *Twist1* in neural crest specification and delamination. At minimum they indicate that even if *Twist1* has a role in these processes, it can be well compensated by other factors.

Interestingly, challenging the above arguments, evidence for a role of *Twist1* in neural crest delamination was presented by Firulli and colleagues [Vincenz et al, 2008]. They found that in the case of *Twist1* null mice dorsal neural tube becomes enlarged, being populated with *Wnt1* expressing cells which fail to migrate out of the neural tube. Thus, it seems that indeed neural crest delamination is impaired in the

absence of *Twist1* even if it is not completely blocked. The point, should also be considered, that due to growth retardation in *Twist1* null embryos an overall reduction in neural crest domain would have been difficult to assess. Consequently, one can imagine, that in this context, only a fraction of neural crest cells delaminate and possibly, that this partial failure in delamination contributes to the global growth retardation.

Nevertheless, the above proposition does not clarify why *Twist1* has not been consistently observed in the neural tube residing neural crest, although it seems to have an influence on delamination. There are three possible explanations and I will discuss them in turn.

1. The neural tube surrounding mesenchyme, which expresses *Twist1* at high levels, has a positive influence on neural crest delamination. However, such an influence cannot be achieved by cell to cell contact, since if that were the case, only the cells placed at the very edge of the neural tube/mesenchyme interface would be able to enter this process, which is not the case [Nichols D.H., 1981]. Consequently, it follows, that mesenchymal cells would have to secrete chemotactic factors to which neural crest and neural crest cells alone could respond. On one hand, there is no evidence for the existence of such factors, on the other hand, there is positive evidence that neural crest specified cells can delaminate in the absence of any inductive signals [Basch et al., 2006].

2. *Twist1* acts specifically on cranial neural crest cells. Such a possibility would explain many, as yet, unanswered questions. Twist1 knockout has a striking cranial phenotype, resulting in exencephaly while the neural tube forms normally at the level of spinal cord. Furthermore, patterning defects were identified only at the level of forebrain and midbrain [Soo et al., 2002]. Thus, *Twist1* role seems to be limited to rostral regions of the neural tube. This notion can further be corroborated with the idea that most likely neural crest cells employ different mechanism to delaminate from the rostral and caudal regions respectively, as indicated by the different manners in which this process is produced. *Twist1* acting only at the level of prospective brain neural crest delamination would explain how it could have easily been missed in expression studies. At this level, delamination is an abrupt process, limited in time and neural crest cells could upregulate *Twist1* only shortly before their delamination. However, a migration defect was found in the spinal cord, at a level where neural

tube formed and closed apparently normally [Vincenz et al, 2008]. Therefore, this explanation is not completely satisfactory either.

3. *Twist1* is expressed at very low levels in neural crest cells before delamination. This explanation is consistent with the *Twist1* expression pattern reported here at the level of the spinal cord. I cannot draw any conclusions for the cranial neural crest as all embryos sectioned were at a stage either before or after the time of cranial neural crest delamination. The fact that low levels of *Twist1* expression could be observed in the dorsal parts of spinal cord correlates with the reported role in neural crest delamination at this level. However, a careful analysis on neural crest delamination and correlation with *Twist1* expression needs to be carried out before the question of *Twist1* role in early neural crest can be clearly answered.

D3.3 Neural Crest Specification: Lessons from Evolution

Cephalochordates, represented by the extant amphioxus, considered a living fossil, are closely related with the vertebrata subphylum. They lack the vertebrate characteristic tissue: neural crest. However, in this model organism, cells at the neural plate border express homologues of some of the neural crest related markers like *Pax3*, *Pax7* [AmphiPax3/7; Holland et al., 1999], *Msx* [AmphiMsx; Sharman et al., 1999], *Snai* [amphioxus snail; Langeland et al., 1998] and *Zic* genes [AmphiZic; Gostling & Shimeld, 2003]. In chick, *Id*s are expressed in the pre-migratory neural crest (*Id1* and *Id2*) and migratory neural crest (*Id2* and *Id4*) [Kee et al., 2001]. Notably, *Id* homologues are not expressed in the neural plate border of the amphioxus, but they are expressed in the same region of lamprey, one of the most basic extant vertebrate [Meulemans et al., 2003]. This indicates that *Id* genes are essential for neural crest specification, as *Id* expression and neural crest formation appear together in evolution and, points to a role for bHLH factors in this process.

Twist1 homologue is absent from the neural plate border in amphioxus [Yasui et al., 1998], but present in Xenopus [Hopwood et al., 1989]. Interestingly, a more recent report, proposed based on genomic sequencing, that the urochordates (tunicates) and, not the cephalochordate, are most closely related to vertebrates

[Delsuc et al., 2006], a finding which suggests that the simpler structure of tunicates might be a result of a process of involution [Gee H., 2006]. A critical study, reports the finding in tunicates, of a rudimentary neural crest like cell line, which express *Id* but not *Twist* homologues [Abitua et al., 2012]. These cells, which form at the neural plate border, differentiate into melanocytes, but do not migrate away from the dorsal midline. However, it is sufficient to misexpress the tunicate's closest homologue of *Twist1*, in these cells, to reprogram them into "migrating mesenchymal cells, reminiscent of vertebrate ectomesenchyme" [Abitua et al., 2012]. Collectively, these data suggest that neural crest "invention" was a gradual process in which expression of *Twist1* might have been the final and critical event.

D4 *Twist1* in The Patterning of The Neural Tube

D4.1 A Putative Role for *Twist1* in Specification of Dorsal Neurons and Neural Crest Cells

A role for *Twist1* in the patterning of anterior neural tube has long been established. *Twist1* mice fail to close the neural tube in the cephalic region and, in the open neural tube ventral markers are displaced dorsally [Chen and Behringer, 1995; Soo et a, 2002]. However, until now no mechanism of action has been proposed, except for the diffuse idea that it acts non-autonomously from the surrounding mesoderm.

Here, I provide in vitro evidence for a putative autonomous mechanism of action. I propose that low levels of *Twist1* expressed in the neural progenitors can bias the neural program towards a dorsal phenotype. TwE induced cells, upregulate markers common for dorsal neural and neural crest. I also propose that the decision a cell has to make between remaining in the neural tube as a dorsal neural cell, or leaving the neural tube as a neural crest cell might be a late decision, probably taken not long before delamination and, might be dependent on *Twist1* expression. More precisely, dorsal neural cells express *Twist1* at low level up around the neural tube

closure. Cells which are to reside in the neural tube, downregulate *Twist1* and, undergo the full neural program. Cells which are to delaminate, upregulate *Twist1*, at which point they rapidly lose their adherens junctions and begin their migration [Fig D2].

D4.2 TWIST1 Non-autonomous Roles

I provide evidence that TWIST1 could non-autonomously stabilize the neural program. For instance, TwE expressing cells can downregulate surface ectoderm marker *Gata2* in neighbouring cells [Fig R16b and d]. This is significant for two reasons. One, not all cells need to express *Twist1* in order to be protected against differentiation uncertainty. Two, correlation between in vitro and in vivo data indicates, for the first time, how TWIST1 could act non-autonomously from within the neural tube. The importance of this should be considered against the old idea that TWIST1 acts non-autonomously from the neighbouring mesoderm. I showed here that *Twist1* has a pattern of expression in the neural tube, limited temporally and spatially, which is consistent with its proposed role. On the other hand, *Twist1* strong, but rather uniform expression throughout the mesoderm cannot easily explain its effects on neural tube patterning.

D4.3 TWIST1 and Late Dorsal Progenitors

The idea of TWIST1 being favourable for the neural and neural crest programs is strongly supported by the early in vitro neural differentiation events in response to TwE induction; especially, the continuous upregulation of *Pax3* by early induction and the absence of a negative influence on *Sox1* in these conditions. However, for upregulation of other dorsal markers, like *Atoh1*, the in vitro experiments showed a requirement for TwE induction at later time points, as well [Fig R1.15a, c and d].

Atoh1 expression in the neural tube was reported starting at 9.5 dpc [Helms et al. 1998], a time point which coincides with the moment *Twist1* stops being expressed in the discussed location [Fig R2.9]. Furthermore, *Atoh1* has been linked with neural

progenitor differentiation, at least in a subset of cells [Helms et al. 1998; Lyden et al., 1999; Flora et al., 2007]. Thus, *Twist1* and *Atoh1* coincide in their role in neural progenitor maturation, but not in their expression in time. So far, I considered acceleration of neural differentiation by TWIST1 as an *in vitro* artefact without physiological relevance. I concentrated on explaining how *in vivo*, such an acceleration is circumvented by timely downregulation of *Twist1*. Nevertheless, TWIST1 might have a role in generating a subset of more differentiated progenitors. In chick, the first post-mitotic, TUBB3 positive cells, were observed only hours after neural tube closure and, the majority of these cells appeared in the dorsal most regions of the midbrain neural tube [Aaku-Saraste et al, 1996], a region which coincides with the D-V domain of both *Twist1* and *Atoh1*. Thus, it is conceivable that Twist1 may mark an early differentiating neuron population and, that it is present long enough in these cells, to be able to affect both the D-V marker expression and, to accelerate their differentiation.

D4.4 *Twist1* and Anterior Neural Tube Fusion

One of the most striking observation reported here is that shortly before forebrain closure *Twist1* expression is restricted within each section, to just one or two cells placed at the very tip of each neural fold, most likely the cells which are going to initiate the fusion. This may suggest, for the first time, that *Twist1* role in cephalic neural tube closure is a very direct one and not an indirect consequence of dorsal patterning perturbations. While, I did not investigate the mechanism by which *Twist1* might produce this effects it is easy to conceive that regulation of cell adhesion is involved. Possibly, these cells connect less tightly with their neighbours and have an enhanced ability to generate new intercellular contacts. It is also possible that these cells, placed on the two approaching neural folds, express a specific marker and thus “recognize” each other.

D5. *Twist1* Affects Development – A Model

The work presented here indicates that at early stages of development *Twist1* level of expression is the most important modulator of its actions. High levels of *Twist1* are incompatible with the neural program. However, current evidence suggests that this is a mechanism not employed by the embryo to decide for or, against the neural fate, since *Twist1* is never expressed in the epiblast.

An attractive idea had been that *Twist1* expressing cells are fated to become mesoderm. However, such a hypothesis is not supported either by *Twist1* expression or rather lack of it, in the Primitive Streak nor, by the apparently normal formation of mesoderm in *Twist1* mutants [Chen and Behringer, 1995; Soo et al, 2002]. It seems more appropriate to consider that *Twist1* has a role after the mesodermal fate has been established as indicated by the data showing that in *Twist1* null mutants the somitic compartments are differentially affected [Chen and Behringer, 1995] and that teratomas from *Twist1* null cells have an altered compositions, with very little muscle, tooth or trabecular bone [Soo et al., 2002]. Furthermore, at the time of mesoderm differentiation cell fate is differentially regulated by the two main TWIST1 dimer choices TW-E and TW-TW [Connerney at al., 2006].

Interestingly, *Zfp521*, before being reported as an early neural inducer, was considered, just like *Twist1* a mesenchymal effector [Bond et al, 2007; Wu et al, 2009]. Nature has a well known tendency to recycle its means, to use the same mechanisms or molecules to achieve different goals, or to regulate various processes. Thus, depending on the cellular context, TWIST1 and ZFP521 could either regulate mesenchymal or neural differentiation. These factors could also represent means by which a cell could easily transit from one state to another. The example of neural crest cells is very significant. They start in the region of neural epithelium, from which initially can hardly be distinguished, then, they undergo EMT and acquire a mesenchymal phenotype, leave the neural tissue and migrate to the tissue of destination. Here, some of them undergo neural differentiation as they become part of the peripheral nervous system.

In the neural tissue *Twist1* is expressed at low levels in a subset of progenitors which are fated to become either dorsal neurons or, neural crest cells. One could even speculate that the reason why *Twist1* is not expressed in early mesoderm cells is that this transcription factor has been reserved for the induction of neural crest cells. An interesting experiment would be to express TwE or TwTw in a mesoderm differentiation protocol and see if cells are not diverted to a phenotype resembling more neural crest cells.

From in vitro experiments I made the observation that induction of TwE leads to abrupt loss of epithelial integrity and formation of loose mesenchyme-like structures [Fig R1.19, Fig R3.2]. An interesting area of investigation, could involve the mechanisms employed by neural progenitors to maintain the integrity of the neural epithelium at the time of neural crest migration. These could involve either rapid proliferation of the neural progenitors to fill the gaps, or formation of new adherens junctions between remaining epithelial cells. Significantly, if cells fated to become strict neural progenitors do indeed downregulate *Twist1*, this would amount to a MET (mesenchymal to epithelial transition) event which would strengthen the epithelial structure in the wake of the neural crest delamination havoc.

It should be noted that formation of mesenchymal like cells was observed even in experiments with low TwE induction. Thus the question arise how could cells expressing *Twist1* maintain their neural fate. First, it is possible that the active TWIST1 levels in the embryo are even lower than the lowest levels used in the current *in vitro* experiments. Second, the observed patchy expression [Fig R2.8h and Fig D2] may arise from cells downregulating *Twist1*, after only a short exposure to this factor. Thus, the expression analysis could only indicate a heterogeneous population which expresses *Twist1* for variable time lengths while this time exposure, could have fate consequences, similarly to the levels of expression.

Another potential point of concern could be that induction of TwE, even at levels permissive for neural program, seems to have a differentiation acceleration effect. This is not necessarily detrimental, considering that some progenitors form post-mitotic neurons before others. Thus, the observation made here about of a few cells expressing *Twist1* in the dorsal neural tube could be correlated with the previous

observation of rare postmitotic neurons in the dorsal neural tube soon after closure [Aaku-Saraste et al, 1996]. In this interpretation TWIST1 would be one of the factors which ensure that not all progenitors differentiate at the same time.

A novel role, reported here for TWIST1 involves stabilization of the neural program at the junction between lateral neural plate and surface ectoderm. Thus, while expressing *Twist1* might be dangerous for neural progenitors, having some *Twist1* expressing cells might be useful for neighbouring cells. On the other hand *Twist1* expressing cells themselves have the option to downregulate this factor early enough, before their differentiation would be negatively affected. Alternatively they could either join the pool of cells which will form the earliest differentiating neurons or leave the neural tube as neural crest cells.

I found that *Twist1* expression domain becomes restricted in the neural tube more and more dorsally, until at the time of fusion, only the few cells directly involved in this process still express *Twist1*, a feature which can be linked with the reported phenotype of *Twist1* null mutants [Chen and Behringer, 1995].

In conclusion I propose four roles for TWIST1 in early development, summarized in Fig D2:

1. To act as an anti BMP and pro EMT neural modulator;
2. To participate in neural crest specification and delamination;
3. To employ both autonomous and non-autonomous mechanisms to pattern the neural tube;
4. To directly regulate neural tube fusion.

The work presented in this thesis proposes novel mechanisms for the regulation of neural differentiation and neural tube formation. Each of the mechanisms put forth could prove to be a fruitful area of research. For instance much could be gained from investigating the heterogeneous expressing of transcription factors in generation of progenitors which differentiate with different speeds. Dissecting the induction of dorsal neural and neural crest phenotypes will very likely reveal interesting target genes. The role of TWIST1 induced EMT could bring new insights in the process of

neural crest delamination as well as on what makes a cells to be neural crest. Finally, I provided a hypothesis regarding neural tube fusion which could be used to generate experiments that would clarify this delicate process.

Figure D2. Schematic representation of TWIST1 role in neural development

From formation of the neural folds (a) to closure (c). Initially *Twist1* expression can be seen as gradient from future ventral to dorsal. TWIST1 participates autonomously in establishing the dorsal neural phenotype and in blocking the surface ectoderm fate by downregulating CDH1 (a). As neural folds mature, *Twist1* expression becomes restricted to a few dorsal cells which non-autonomously block surface ectoderm fate in the surrounding neural cells. Some of the *Twist1* positive cells further upregulate this marker and delaminate as neural crest (b). Just before closure only cells involved in the process of fusion remain *Twist1* positive. All the other cells either downregulated this marker, or migrated out of the neural tube (c).

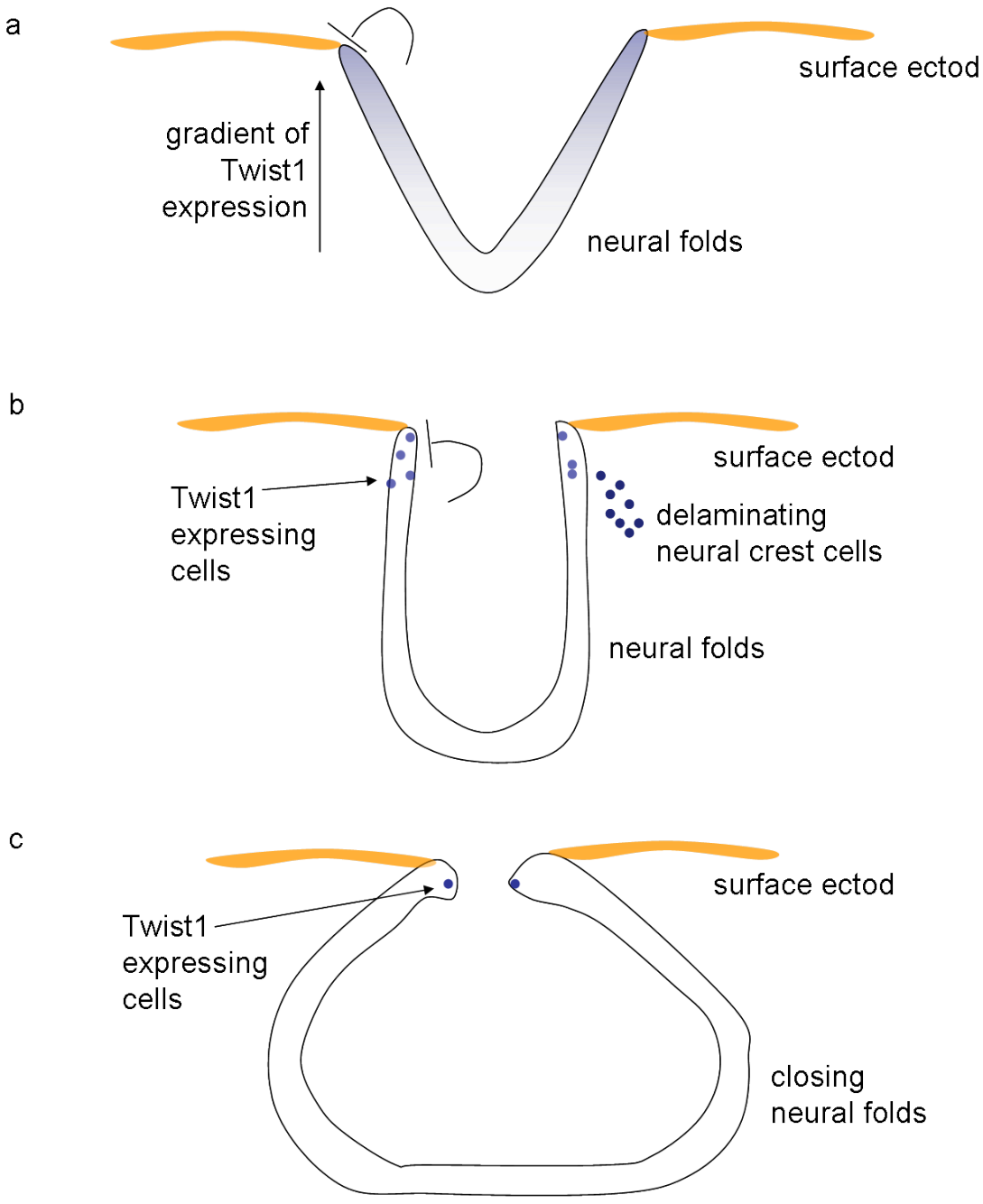
a
surface ectod
gradient of
Twist1
expression
neural folds
b
surface ectod
Twist1
expressing
cells
delaminating
neural crest cells
neural folds
c
surface ectod
Twist1
expressing
cells
closing
neural folds

VII. REFERENCES

Aaku-Saraste, E., A. Hellwig, and W.B. Huttner. 1996. Loss of occludin and functional tight junctions, but not ZO-1, during neural tube closure--remodeling of the neuroepithelium prior to neurogenesis. *Dev Biol*. 180:664-79.

Abitua, P.B., E. Wagner, I.A. Navarrete, and M. Levine. 2012. Identification of a rudimentary neural crest in a non-vertebrate chordate. *Nature*.

Agren, M., P. Kogerman, M.I. Kleman, M. Wessling, and R. Toftgard. 2004. Expression of the PTCH1 tumor suppressor gene is regulated by alternative promoters and a single functional Gli-binding site. *Gene*. 330:101-14.

Aiba, K., T. Nedorezov, Y. Piao, A. Nishiyama, R. Matoba, L.V. Sharova, A.A. Sharov, S. Yamanaka, H. Niwa, and M.S. Ko. 2009. Defining developmental potency and cell lineage trajectories by expression profiling of differentiating mouse embryonic stem cells. *DNA Res*. 16:73-80.

Alvarez-Medina, R., J. Cayuso, T. Okubo, S. Takada, and E. Marti. 2008. Wnt canonical pathway restricts graded Shh/Gli patterning activity through the regulation of Gli3 expression. *Development*. 135:237-47.

Anderson, R.M., R.W. Stottmann, M. Choi, and J. Klingensmith. 2006. Endogenous bone morphogenetic protein antagonists regulate mammalian neural crest generation and survival. *Dev Dyn*. 235:2507-20.

Ang, S.L., R.A. Conlon, O. Jin, and J. Rossant. 1994. Positive and negative signals from mesoderm regulate the expression of mouse Otx2 in ectoderm explants. *Development*. 120:2979-89.

Ang, S.L., and D.B. Constam. 2004. A gene network establishing polarity in the early mouse embryo. *Semin Cell Dev Biol*. 15:555-61.

Ang, S.L., and J. Rossant. 1994. HNF-3 beta is essential for node and notochord formation in mouse development. *Cell*. 78:561-74.

Arnold S.J., Hofmann U.K., Bikoff E.K., and E.J. Robertson 2008. Pivotal roles for eomesodermin during axis formation, epithelium-to-mesenchyme transition and endoderm specification in the mouse. *Development*. 135:501-11.

Arnold, S.J., and E.J. Robertson. 2009. Making a commitment: cell lineage allocation and axis patterning in the early mouse embryo. *Nat Rev Mol Cell Biol*. 10:91-103.

Atchley, W.R., and W.M. Fitch. 1997. A natural classification of the basic helix-loop-helix class of transcription factors. *Proc Natl Acad Sci U S A*. 94:5172-6.

Bachiller, D., J. Klingensmith, C. Kemp, J.A. Belo, R.M. Anderson, S.R. May, J.A. McMahon, A.P. McMahon, R.M. Harland, J. Rossant, and E.M. De Robertis. 2000. The organizer factors Chordin and Noggin are required for mouse forebrain development. *Nature*. 403:658-61.

Bai, C.B., W. Auerbach, J.S. Lee, D. Stephen, and A.L. Joyner. 2002. Gli2, but not Gli1, is required for initial Shh signaling and ectopic activation of the Shh pathway. *Development*. 129:4753-61.

Bai, C.B., D. Stephen, and A.L. Joyner. 2004. All mouse ventral spinal cord patterning by hedgehog is Gli dependent and involves an activator function of Gli3. *Dev Cell*. 6:103-15.

Bain, G., D. Kitchens, M. Yao, J.E. Huettner, and D.I. Gottlieb. 1995. Embryonic stem cells express neuronal properties in vitro. *Dev Biol*. 168:342-57.

Bain, G., E.C. Maandag, D.J. Izon, D. Amsen, A.M. Kruisbeek, B.C. Weintraub, I. Krop, M.S. Schlissel, A.J. Feeney, M. van Roon, and et al. 1994. E2A proteins are required for proper B cell development and initiation of immunoglobulin gene rearrangements. *Cell*. 79:885-92.

Baker, C.V., and M. Bronner-Fraser. 1997a. The origins of the neural crest. Part I: embryonic induction. *Mech Dev*. 69:3-11.

Baker, C.V., and M. Bronner-Fraser. 1997b. The origins of the neural crest. Part II: an evolutionary perspective. *Mech Dev*. 69:13-29.

Banaszynski, L.A., L.C. Chen, L.A. Maynard-Smith, A.G. Ooi, and T.J. Wandless. 2006. A rapid, reversible, and tunable method to regulate protein function in living cells using synthetic small molecules. *Cell*. 126:995-1004.

Barnes, R.M., and A.B. Firulli. 2009. A twist of insight - the role of Twist-family bHLH factors in development. *Int J Dev Biol*. 53:909-24.

Barth, K.A., Y. Kishimoto, K.B. Rohr, C. Seydler, S. Schulte-Merker, and S.W. Wilson. 1999. Bmp activity establishes a gradient of positional information throughout the entire neural plate. *Development*. 126:4977-87.

Basch, M.L., M. Bronner-Fraser, and M.I. Garcia-Castro. 2006. Specification of the neural crest occurs during gastrulation and requires Pax7. *Nature*. 441:218-22.

Battiste J., Helms A.W., Kim E.J., Savage T.K., Lagace D.C., Mandyam C.D., Eisch A.J., G., Miyoshi, and J.E., Johnson. 2007. Ascl1 defines sequentially generated lineage-restricted neuronal and oligodendrocyte precursor cells in the spinal cord. *Development*. 134:285-93.

Beck, S., J.A. Le Good, M. Guzman, N. Ben Haim, K. Roy, F. Beermann, and D.B. Constam. 2002. Extraembryonic proteases regulate Nodal signalling during gastrulation. *Nat Cell Biol*. 4:981-5.

Beddington, R.S. 1994. Induction of a second neural axis by the mouse node. *Development*. 120:613-20.

Beddington, R.S., and E.J. Robertson. 1989. An assessment of the developmental potential of embryonic stem cells in the midgestation mouse embryo. *Development*. 105:733-7.

Bellus, G.A., K. Gaudenz, E.H. Zackai, L.A. Clarke, J. Szabo, C.A. Francomano, and M. Muenke. 1996. Identical mutations in three different fibroblast growth factor receptor genes in autosomal dominant craniosynostosis syndromes. *Nat Genet*. 14:174-6.

Benezra, R., R.L. Davis, D. Lockshon, D.L. Turner, and H. Weintraub. 1990. The protein Id: a negative regulator of helix-loop-helix DNA binding proteins. *Cell*. 61:49-59.

Ben-Haim, N., C. Lu, M. Guzman-Ayala, L. Pescatore, D. Mesnard, M. Bischofberger, F. Naef, E.J. Robertson, and D.B. Constam. 2006. The nodal precursor acting via activin receptors induces mesoderm by maintaining a source of its convertases and BMP4. *Dev Cell*. 11:313-23.

Bildsoe, H., D.A. Loebel, V.J. Jones, Y.T. Chen, R.R. Behringer, and P.P. Tam. 2009. Requirement for Twist1 in frontonasal and skull vault development in the mouse embryo. *Dev Biol*. 331:176-88.

Blanchet, M.H., J.A. Le Good, D. Mesnard, V. Oorschot, S. Baflast, G. Minchiotti, J. Klumperman, and D.B. Constam. 2008. Cripto recruits Furin and PACE4 and controls Nodal trafficking during proteolytic maturation. *EMBO J*. 27:2580-91.

Bond, H.M., M. Mesuraca, N. Amodio, T. Mega, V. Agosti, D. Fanello, D. Pelaggi, L. Bullinger, M. Grieco, M.A. Moore, S. Venuta, and G. Morrone. 2008. Early hematopoietic zinc finger protein-zinc finger protein 521: a candidate regulator of diverse immature cells. *Int J Biochem Cell Biol*. 40:848-54.

Bonner, J., S.L. Gribble, E.S. Veien, O.B. Nikolaus, G. Weidinger, and R.I. Dorsky. 2008. Proliferation and patterning are mediated independently in the dorsal spinal cord downstream of canonical Wnt signaling. *Dev Biol*. 313:398-407.

Bourgeois, P., A.L. Bolcato-Bellemin, J.M. Danse, A. Bloch-Zupan, K. Yoshiba, C. Stoetzel, and F. Perrin-Schmitt. 1998. The variable expressivity and incomplete penetrance of the twist-null heterozygous mouse phenotype resemble those of human Saethre-Chotzen syndrome. *Hum Mol Genet*. 7:945-57.

Bouwmeester, T., S. Kim, Y. Sasai, B. Lu, and E.M. De Robertis. 1996. Cerberus is a head-inducing secreted factor expressed in the anterior endoderm of Spemann's organizer. *Nature*. 382:595-601.

Bradley, A., M. Evans, M.H. Kaufman, and E. Robertson. 1984. Formation of germ-line chimaeras from embryo-derived teratocarcinoma cell lines. *Nature*. 309:255-6.

Bradley, T.R., and D. Metcalf. 1966. The growth of mouse bone marrow cells in vitro. *Aust J Exp Biol Med Sci*. 44:287-99.

Breau, M.A., T. Pietri, O. Eder, M. Blanche, C. Brakebusch, R. Fassler, J.P. Thiery, and S. Dufour. 2006. Lack of beta1 integrins in enteric neural crest cells leads to a Hirschsprung-like phenotype. *Development*. 133:1725-34.

Brennan, J., C.C. Lu, D.P. Norris, T.A. Rodriguez, R.S. Beddington, and E.J. Robertson. 2001. Nodal signalling in the epiblast patterns the early mouse embryo. *Nature*. 411:965-9.

Brons, I.G., L.E. Smithers, M.W. Trotter, P. Rugg-Gunn, B. Sun, S.M. Chuva de Sousa Lopes, S.K. Howlett, A. Clarkson, L. Ahrlund-Richter, R.A. Pedersen, and L. Vallier. 2007. Derivation of pluripotent epiblast stem cells from mammalian embryos. *Nature*. 448:191-5.

Brunelli, S., E. Silva Casey, D. Bell, R. Harland, and R. Lovell-Badge. 2003. Expression of Sox3 throughout the developing central nervous system is dependent on the combined action of discrete, evolutionarily conserved regulatory elements. *Genesis*. 36:12-24.

Burdon, T., I. Chambers, C. Stracey, H. Niwa, and A. Smith. 1999a. Signaling mechanisms regulating self-renewal and differentiation of pluripotent embryonic stem cells. *Cells Tissues Organs*. 165:131-43.

Burdon, T., Stracey, C., Chambers, I, Nichols, J., Smith, A., 1999b. Suppression of SHP-2 and ERK signalling promotes self-renewal of mouse embryonic stem cells. *Dev Biol*. 210:30-43.

Burgess, R., P. Cserjesi, K.L. Ligon, and E.N. Olson. 1995. Paraxis: a basic helix-loop-helix protein expressed in paraxial mesoderm and developing somites. *Dev Biol*. 168:296-306.

Burke, R., D. Nellen, M. Bellotto, E. Hafen, K.A. Senti, B.J. Dickson, and K. Basler. 1999. Dispatched, a novel sterol-sensing domain protein dedicated to the release of cholesterol-modified hedgehog from signaling cells. *Cell*. 99:803-15.

Buscher, D., B. Bosse, J. Heymer, and U. Ruther. 1997. Evidence for genetic control of Sonic hedgehog by Gli3 in mouse limb development. *Mech Dev*. 62:175-82.

Buxton, P., P. Hunt, P. Ferretti, and P. Thorogood. 1997. A role for midline closure in the reestablishment of dorsoventral pattern following dorsal hindbrain ablation. *Dev Biol*. 183:150-65.

Bylund, M., E. Andersson, B.G. Novitch, and J. Muhr. 2003. Vertebrate neurogenesis is counteracted by Sox1-3 activity. *Nat Neurosci*. 6:1162-8.

Cajal, M., K.A. Lawson, B. Hill, A. Moreau, J. Rao, A. Ross, J. Collignon, and A. Camus. 2012. Clonal and molecular analysis of the prospective anterior neural boundary in the mouse embryo. *Development*. 139:423-36.

Campuzano, S., L. Carramolino, C.V. Cabrera, M. Ruiz-Gomez, R. Villares, A. Boronat, and J. Modolell. 1985. Molecular genetics of the achaete-scute gene complex of D. melanogaster. *Cell*. 40:327-38.

Camus, A., A. Perea-Gomez, A. Moreau, and J. Collignon. 2006. Absence of Nodal signaling promotes precocious neural differentiation in the mouse embryo. *Dev Biol*. 295:743-55.

Casas, E., J. Kim, A. Bendesky, L. Ohno-Machado, C.J. Wolfe, and J. Yang. 2011. Snail2 is an essential mediator of Twist1-induced epithelial mesenchymal transition and metastasis. *Cancer Res*. 71:245-54.

Caudy, M., H. Vassin, M. Brand, R. Tuma, L.Y. Jan, and Y.N. Jan. 1988. daughterless, a Drosophila gene essential for both neurogenesis and sex determination, has sequence similarities to myc and the achaete-scute complex. *Cell*. 55:1061-7.

Chai, Y., X. Jiang, Y. Ito, P. Bringas, Jr., J. Han, D.H. Rowitch, P. Soriano, A.P. McMahon, and H.M. Sucov. 2000. Fate of the mammalian cranial neural crest during tooth and mandibular morphogenesis. *Development*. 127:1671-9.

Chambers, I., D. Colby, M. Robertson, J. Nichols, S. Lee, S. Tweedie, and A. Smith. 2003. Functional expression cloning of Nanog, a pluripotency sustaining factor in embryonic stem cells. *Cell*. 113:643-55.

Chambers, I., J. Silva, D. Colby, J. Nichols, B. Nijmeijer, M. Robertson, J. Vrana, K. Jones, L. Grotewold, and A. Smith. 2007. Nanog safeguards pluripotency and mediates germline development. *Nature*. 450:1230-4.

Chambers, S.M., C.A. Fasano, E.P. Papapetrou, M. Tomishima, M. Sadelain, and L. Studer. 2009. Highly efficient neural conversion of human ES and iPS cells by dual inhibition of SMAD signaling. *Nat Biotechnol*. 27:275-80.

Chappell, S.A., G.M. Edelman, and V.P. Mauro. 2000. A 9-nt segment of a cellular mRNA can function as an internal ribosome entry site (IRES) and when present in linked multiple copies greatly enhances IRES activity. *Proc Natl Acad Sci U S A*. 97:1536-41.

Chazaud, C., and J. Rossant. 2006. Disruption of early proximodistal patterning and AVE formation in Apc mutants. *Development*. 133:3379-87.

Chen, J.K., J. Taipale, M.K. Cooper, and P.A. Beachy. 2002. Inhibition of Hedgehog signaling by direct binding of cyclopamine to Smoothened. *Genes Dev*. 16:2743-8.

Chen, T., D. Yuan, B. Wei, J. Jiang, J. Kang, K. Ling, Y. Gu, J. Li, L. Xiao, and G. Pei. 2010. E-cadherin-mediated cell-cell contact is critical for induced pluripotent stem cell generation. *Stem Cells*. 28:1315-25.

Chen, Z.F., and R.R. Behringer. 1995. twist is required in head mesenchyme for cranial neural tube morphogenesis. *Genes Dev*. 9:686-99.

Chesnutt, C., L.W. Burrus, A.M. Brown, and L. Niswander. 2004. Coordinate regulation of neural tube patterning and proliferation by TGFbeta and WNT activity. *Dev Biol*. 274:334-47.

Cheung, M., and J. Briscoe. 2003. Neural crest development is regulated by the transcription factor Sox9. *Development*. 130:5681-93.

Cheung, M., M.C. Chaboissier, A. Mynett, E. Hirst, A. Schedl, and J. Briscoe. 2005. The transcriptional control of trunk neural crest induction, survival, and delamination. *Dev Cell*. 8:179-92.

Chiang, C., Y. Litingtung, E. Lee, K.E. Young, J.L. Corden, H. Westphal, and P.A. Beachy. 1996. Cyclopia and defective axial patterning in mice lacking Sonic hedgehog gene function. *Nature*. 383:407-13.

Chizhikov, V.V., and K.J. Millen. 2004. Control of roof plate formation by Lmx1a in the developing spinal cord. *Development*. 131:2693-705.

Chng, Z., A. Teo, R.A. Pedersen, and L. Vallier. 2010. SIP1 mediates cell-fate decisions between neuroectoderm and mesendoderm in human pluripotent stem cells. *Cell Stem Cell*. 6:59-70.

Clay, M.R., and M.C. Halloran. 2010. Control of neural crest cell behavior and migration: Insights from live imaging. *Cell Adh Migr*. 4:586-94.

Conlon, F.L., K.M. Lyons, N. Takaesu, K.S. Barth, A. Kispert, B. Herrmann, and E.J. Robertson. 1994. A primary requirement for nodal in the formation and maintenance of the primitive streak in the mouse. *Development*. 120:1919-28.

Connerney, J., V. Andreeva, Y. Leshem, M.A. Mercado, K. Dowell, X. Yang, V. Lindner, R.E. Friesel, and D.B. Spicer. 2008. Twist1 homodimers enhance FGF responsiveness of the cranial sutures and promote suture closure. *Dev Biol*. 318:323-34.

Connerney, J., V. Andreeva, Y. Leshem, C. Muentener, M.A. Mercado, and D.B. Spicer. 2006. Twist1 dimer selection regulates cranial suture patterning and fusion. *Dev Dyn*. 235:1345-57.

Conti, L., S.M. Pollard, T. Gorba, E. Reitano, M. Toselli, G. Biella, Y. Sun, S. Sanzone, Q.L. Ying, E. Cattaneo, and A. Smith. 2005. Niche-independent symmetrical self-renewal of a mammalian tissue stem cell. *PLoS Biol*. 3:e283.

Couly, G.F., and N.M. Le Douarin. 1985. Mapping of the early neural primordium in quail-chick chimeras. I. Developmental relationships between placodes, facial ectoderm, and prosencephalon. *Dev Biol*. 110:422-39.

Couly, G.F., and N.M. Le Douarin. 1987. Mapping of the early neural primordium in quail-chick chimeras. II. The prosencephalic neural plate and neural folds: implications for the genesis of cephalic human congenital abnormalities. *Dev Biol*. 120:198-214.

Creuzet, S.E. 2009. Regulation of pre-otic brain development by the cephalic neural crest. *Proc Natl Acad Sci U S A*. 106:15774-9.

Creuzet, S.E., S. Martinez, and N.M. Le Douarin. 2006. The cephalic neural crest exerts a critical effect on forebrain and midbrain development. *Proc Natl Acad Sci U S A*. 103:14033-8.

Crisan, M., M. Corselli, C.W. Chen, and B. Peault. 2011. Multilineage stem cells in the adult: a perivascular legacy? *Organogenesis*. 7:101-4.

Crisan, M., S. Yap, L. Casteilla, C.W. Chen, M. Corselli, T.S. Park, G. Andriolo, B. Sun, B. Zheng, L. Zhang, C. Norotte, P.N. Teng, J. Traas, R. Schugar, B.M. Deasy, S. Badylak, H.J. Buhring, J.P. Giacobino, L. Lazzari, J. Huard, and B. Peault. 2008. A perivascular origin for mesenchymal stem cells in multiple human organs. *Cell Stem Cell*. 3:301-13.

Dahlstrand J., M. Lardelli, and U. Lendahl. 1995. Nestin mRNA expression correlates with the central nervous system progenitor cell state in many, but not all, regions of developing central nervous system. *Brain Res Dev Brain Res.* 84:109-29.

Dai, P., H. Akimaru, Y. Tanaka, T. Maekawa, M. Nakafuku, and S. Ishii. 1999. Sonic Hedgehog-induced activation of the Gli1 promoter is mediated by GLI3. *J Biol Chem*. 274:8143-52.

Dale, J.K., C. Vesque, T.J. Lints, T.K. Sampath, A. Furley, J. Dodd, and M. Placzek. 1997. Cooperation of BMP7 and SHH in the induction of forebrain ventral midline cells by prechordal mesoderm. *Cell*. 90:257-69.

Das, A., and J.G. Crump. 2012. Bmps and id2a act upstream of Twist1 to restrict ectomesenchyme potential of the cranial neural crest. *PLoS Genet*. 8:e1002710.

Davidson, L.A., and R.E. Keller. 1999. Neural tube closure in Xenopus laevis involves medial migration, directed protrusive activity, cell intercalation and convergent extension. *Development*. 126:4547-56.

Davies O.R., C.Y. Lin, A. Radzisheuskaya, X. Zhou, J. Taube, G. Blin, A. Waterhouse, A.J. Smith, and S. Lowell. 2013. Tcf15 primes pluripotent cells for differentiation. *Cell Rep.* 3:472-84.

Davis, R.L., H. Weintraub, and A.B. Lassar. 1987. Expression of a single transfected cDNA converts fibroblasts to myoblasts. *Cell*. 51:987-1000.

De Robertis, E.M. 2009. Spemann's organizer and the self-regulation of embryonic fields. *Mech Dev*. 126:925-41.

Delaune, E., P. Lemaire, and L. Kodjabachian. 2005. Neural induction in Xenopus requires early FGF signalling in addition to BMP inhibition. *Development*. 132:299-310.

Dessaud, E., A.P. McMahon, and J. Briscoe. 2008. Pattern formation in the vertebrate neural tube: a sonic hedgehog morphogen-regulated transcriptional network. *Development*. 135:2489-503.

Dickinson, M.E., R. Krumlauf, and A.P. McMahon. 1994. Evidence for a mitogenic effect of Wnt-1 in the developing mammalian central nervous system. *Development*. 120:1453-71.

Di-Gregorio, A., M. Sancho, D.W. Stuckey, L.A. Crompton, J. Godwin, Y. Mishina, and T.A. Rodriguez. 2007. BMP signalling inhibits premature neural differentiation in the mouse embryo. *Development*. 134:3359-69.

Ding, Q., J. Motoyama, S. Gasca, R. Mo, H. Sasaki, J. Rossant, and C.C. Hui. 1998. Diminished Sonic hedgehog signaling and lack of floor plate differentiation in Gli2 mutant mice. *Development*. 125:2533-43.

Dong, J., S. Huang, M. Caikovski, S. Ji, A. McGrath, M.G. Custorio, C.J. Creighton, P. Maliakkal, E. Bogoslovskaia, Z. Du, X. Zhang, M.T. Lewis, F. Sablitzky, C. Brisken, and Y. Li. 2011. ID4 regulates mammary gland development by suppressing p38MAPK activity. *Development*. 138:5247-56.

Dottori, M., M.K. Gross, P. Labosky, and M. Goulding. 2001. The winged-helix transcription factor Foxd3 suppresses interneuron differentiation and promotes neural crest cell fate. *Development*. 128:4127-38.

Duncan, M., E.M. DiCicco-Bloom, X. Xiang, R. Benezra, and K. Chada. 1992. The gene for the helix-loop-helix protein, Id, is specifically expressed in neural precursors. *Dev Biol*. 154:1-10.

Echelard, Y., D.J. Epstein, B. St-Jacques, L. Shen, J. Mohler, J.A. McMahon, and A.P. McMahon. 1993. Sonic hedgehog, a member of a family of putative signaling molecules, is implicated in the regulation of CNS polarity. *Cell*. 75:1417-30.

Echelard, Y., G. Vassileva, and A.P. McMahon. 1994. Cis-acting regulatory sequences governing Wnt-1 expression in the developing mouse CNS. *Development*. 120:2213-24.

el Ghouzzi, V., M. Le Merrer, F. Perrin-Schmitt, E. Lajeunie, P. Benit, D. Renier, P. Bourgeois, A.L. Bolcato-Bellemin, A. Munnich, and J. Bonaventure. 1997. Mutations of the TWIST gene in the Saethre-Chotzen syndrome. *Nat Genet*. 15:42-6.

Ephrussi, A., G.M. Church, S. Tonegawa, and W. Gilbert. 1985. B lineage--specific interactions of an immunoglobulin enhancer with cellular factors in vivo. *Science*. 227:134-40.

Erickson, C.A., and J.A. Weston. 1983. An SEM analysis of neural crest migration in the mouse. *J Embryol Exp Morphol*. 74:97-118.

Evan, G.I., A.H. Wyllie, C.S. Gilbert, T.D. Littlewood, H. Land, M. Brooks, C.M. Waters, L.Z. Penn, and D.C. Hancock. 1992. Induction of apoptosis in fibroblasts by c-myc protein. *Cell*. 69:119-28.

Evans, M.J., and M.H. Kaufman. 1981. Establishment in culture of pluripotential cells from mouse embryos. *Nature*. 292:154-6.

Evans, S.M., and T.X. O'Brien. 1993. Expression of the helix-loop-helix factor Id during mouse embryonic development. *Dev Biol*. 159:485-99.

Festuccia N., Osorno R., Halbritter F., Karwacki-Neisius V., Navarro P., Colby D., Wong F., Yates A., S.R. Tomlinson, and I. Chambers. 2012. Esrrb is a direct Nanog target gene that can substitute for Nanog function in pluripotent cells. *Cell*

Stem Cell. 11:477-90.

Finley, M.F., S. Devata, and J.E. Huettner. 1999. BMP-4 inhibits neural differentiation of murine embryonic stem cells. *J Neurobiol*. 40:271-87.

Fletcher, G., G.E. Jones, R. Patient, and A. Snape. 2006. A role for GATA factors in Xenopus gastrulation movements. *Mech Dev*. 123:730-45.

Flora, A., J.J. Garcia, C. Thaller, and H.Y. Zoghbi. 2007. The E-protein Tcf4 interacts with Math1 to regulate differentiation of a specific subset of neuronal progenitors. *Proc Natl Acad Sci U S A*. 104:15382-7.

Fraichard, A., O. Chassande, G. Bilbaut, C. Dehay, P. Savatier, and J. Samarut. 1995. In vitro differentiation of embryonic stem cells into glial cells and functional neurons. *J Cell Sci*. 108 (Pt 10):3181-8.

Frank-Kamenetsky, M., X.M. Zhang, S. Bottega, O. Guicherit, H. Wichterle, H. Dudek, D. Bumcrot, F.Y. Wang, S. Jones, J. Shulok, L.L. Rubin, and J.A. Porter. 2002. Small-molecule modulators of Hedgehog signaling: identification and characterization of Smoothened agonists and antagonists. *J Biol*. 1:10.

Friedenstein, A.J., R.K. Chailakhjan, and K.S. Lalykina. 1970. The development of fibroblast colonies in monolayer cultures of guinea-pig bone marrow and spleen cells. *Cell Tissue Kinet*. 3:393-403.

Friedenstein, A.J., K.V. Petrakova, A.I. Kurolesova, and G.P. Frolova. 1968. Heterotopic of bone marrow. Analysis of precursor cells for osteogenic and hematopoietic tissues. *Transplantation*. 6:230-47.

Frohman, M.A., M. Boyle, and G.R. Martin. 1990. Isolation of the mouse Hox-2.9 gene; analysis of embryonic expression suggests that positional information along the anterior-posterior axis is specified by mesoderm. *Development*. 110:589-607.

Fuchtbauer, E.M. 1995. Expression of M-twist during postimplantation development of the mouse. *Dev Dyn*. 204:316-22.

Fulda, S., W. Lutz, M. Schwab, and K.M. Debatin. 1999. MycN sensitizes neuroblastoma cells for drug-induced apoptosis. *Oncogene*. 18:1479-86.

Fuse, N., T. Maiti, B. Wang, J.A. Porter, T.M. Hall, D.J. Leahy, and P.A. Beachy. 1999. Sonic hedgehog protein signals not as a hydrolytic enzyme but as an apparent ligand for patched. *Proc Natl Acad Sci U S A*. 96:10992-9.

Gardner, R.L., and J. Rossant. 1979. Investigation of the fate of 4-5 day post-coitum mouse inner cell mass cells by blastocyst injection. *J Embryol Exp Morphol*. 52:141-52.

Gee, H. 2006. Evolution: careful with that amphioxus. *Nature*. 439:923-4.

Goldfarb, A.N., K. Lewandowska, and M. Shoham. 1996. Determinants of helix-loop-helix dimerization affinity. Random mutational analysis of SCL/tal. *J Biol Chem*. 271:2683-8.

Goodrich, L.V., R.L. Johnson, L. Milenkovic, J.A. McMahon, and M.P. Scott. 1996. Conservation of the hedgehog/patched signaling pathway from flies to mice: induction of a mouse patched gene by Hedgehog. *Genes Dev*. 10:301-12.

Goodrich, L.V., L. Milenkovic, K.M. Higgins, and M.P. Scott. 1997. Altered neural cell fates and medulloblastoma in mouse patched mutants. *Science*. 277:1109-13.

Gostling, N.J., and S.M. Shimeld. 2003. Protochordate Zic genes define primitive somite compartments and highlight molecular changes underlying neural crest evolution. *Evol Dev*. 5:136-44.

Goulding, M.D., G. Chalepakis, U. Deutsch, J.R. Erselius, and P. Gruss. 1991. Pax-3, a novel murine DNA binding protein expressed during early neurogenesis. *EMBO J*. 10:1135-47.

Goumans, M.J., G. Valdimarsdottir, S. Itoh, A. Rosendahl, P. Sideras, and P. ten Dijke. 2002. Balancing the activation state of the endothelium via two distinct TGF-beta type I receptors. *EMBO J*. 21:1743-53.

Gowan, K., A.W. Helms, T.L. Hunsaker, T. Collisson, P.J. Ebert, R. Odom, and J.E. Johnson. 2001. Crossinhibitory activities of Ngn1 and Math1 allow specification of distinct dorsal interneurons. *Neuron*. 31:219-32.

Granier, C., V. Gurchenkov, A. Perea-Gomez, A. Camus, S. Ott, C. Papanayotou, J. Iranzo, A. Moreau, J. Reid, G. Koentges, D. Saberan-Djoneidi, and J. Collignon. 2011. Nodal cis-regulatory elements reveal epiblast and primitive endoderm heterogeneity in the peri-implantation mouse embryo. *Dev Biol*. 349:350-62.

Gratsch, T.E., and K.S. O'Shea. 2002. Noggin and chordin have distinct activities in promoting lineage commitment of mouse embryonic stem (ES) cells. *Dev Biol*. 245:83-94.

Greber, B., P. Coulon, M. Zhang, S. Moritz, S. Frank, A.J. Muller-Molina, M.J. Arauzo-Bravo, D.W. Han, H.C. Pape, and H.R. Scholer. 2011. FGF signalling inhibits neural induction in human embryonic stem cells. *EMBO J*. 30:4874-84.

Greber, B., H. Lehrach, and J. Adjaye. 2007. Silencing of core transcription factors in human EC cells highlights the importance of autocrine FGF signaling for self-renewal. *BMC Dev Biol*. 7:46.

Greber, B., H. Lehrach, and J. Adjaye. 2008. Control of early fate decisions in human ES cells by distinct states of TGFbeta pathway activity. *Stem Cells Dev*. 17:1065-77.

Greber, B., G. Wu, C. Bernemann, J.Y. Joo, D.W. Han, K. Ko, N. Tapia, D. Sabour, J. Sterneckert, P. Tesar, and H.R. Scholer. 2010. Conserved and divergent roles of FGF signaling in mouse epiblast stem cells and human embryonic stem cells. *Cell Stem Cell*. 6:215-26.

Grunz, H., and L. Tacke. 1989. Neural differentiation of Xenopus laevis ectoderm takes place after disaggregation and delayed reaggregation without inducer. *Cell Differ Dev*. 28:211-7.

Guo, G., M. Huss, G.Q. Tong, C. Wang, L. Li Sun, N.D. Clarke, and P. Robson. 2010. Resolution of cell fate decisions revealed by single-cell gene expression analysis from zygote to blastocyst. *Dev Cell*. 18:675-85.

Guzman-Ayala, M., N. Ben-Haim, S. Beck, and D.B. Constam. 2004. Nodal protein processing and fibroblast growth factor 4 synergize to maintain a trophoblast stem cell microenvironment. *Proc Natl Acad Sci U S A*. 101:15656-60.

Hacker, C., R.D. Kirsch, X.S. Ju, T. Hieronymus, T.C. Gust, C. Kuhl, T. Jorgas, S.M. Kurz, S. Rose-John, Y. Yokota, and M. Zenke. 2003. Transcriptional profiling identifies Id2 function in dendritic cell development. *Nat Immunol*. 4:380-6.

Haldin, C.E., and C. LaBonne. 2010. SoxE factors as multifunctional neural crest regulatory factors. *Int J Biochem Cell Biol*. 42:441-4.

Hall, B.K. 2000. The neural crest as a fourth germ layer and vertebrates as quadroblastic not triploblastic. *Evol Dev*. 2:3-5.

Hatta, K., and M. Takeichi. 1986. Expression of N-cadherin adhesion molecules associated with early morphogenetic events in chick development. *Nature*. 320:447-9.

Hay, E.D. 1995. An overview of epithelio-mesenchymal transformation. *Acta Anat (Basel)*. 154:8-20.

Hayward, W.S., B.G. Neel, and S.M. Astrin. 1981. Activation of a cellular onc gene by promoter insertion in ALV-induced lymphoid leukosis. *Nature*. 290:475-80.

Helms, A.W., and J.E. Johnson. 1998. Progenitors of dorsal commissural interneurons are defined by MATH1 expression. *Development*. 125:919-28.

Hemmati-Brivanlou, A., and D.A. Melton. 1994. Inhibition of activin receptor signaling promotes neuralization in Xenopus. *Cell*. 77:273-81.

Hesse, E., H. Saito, R. Kiviranta, D. Correa, K. Yamana, L. Neff, D. Toben, G. Duda, A. Atfi, V. Geoffroy, W.C. Horne, and R. Baron. 2010. Zfp521 controls bone mass by HDAC3-dependent attenuation of Runx2 activity. *J Cell Biol*. 191:1271-83.

Hill, R.E., P.F. Jones, A.R. Rees, C.M. Sime, M.J. Justice, N.G. Copeland, N.A. Jenkins, E. Graham, and D.R. Davidson. 1989. A new family of mouse homeo box-containing genes: molecular structure, chromosomal location, and developmental expression of Hox-7.1. *Genes Dev*. 3:26-37.

His, W., 1868. Untersuchung über die ersteanlage des Wirbeltierleibes. Die erste entwickling des Hühnchens. Vogel, Leipzig.

Holland, L.Z., M. Schubert, Z. Kozmik, and N.D. Holland. 1999. AmphiPax3/7, an amphioxus paired box gene: insights into chordate myogenesis, neurogenesis, and the possible evolutionary precursor of definitive vertebrate neural crest. *Evol Dev*. 1:153-65.

Hollnagel, A., V. Oehlmann, J. Heymer, U. Ruther, and A. Nordheim. 1999. Id genes are direct targets of bone morphogenetic protein induction in embryonic stem cells. *J Biol Chem*. 274:19838-45.

Hong, C.S., B.Y. Park, and J.P. Saint-Jeannet. 2008. Fgf8a induces neural crest indirectly through the activation of Wnt8 in the paraxial mesoderm. *Development*. 135:3903-10.

Hong, C.S., and J.P. Saint-Jeannet. 2005. Sox proteins and neural crest development. *Semin Cell Dev Biol*. 16:694-703.

Hopwood, N.D., A. Pluck, and J.B. Gurdon. 1989. A Xenopus mRNA related to Drosophila twist is expressed in response to induction in the mesoderm and the neural crest. *Cell*. 59:893-903.

Hörstadius, S., 1950. The Neural Crest: Its Properties and Derivatives in the Light of Experimental Research. Oxford University Press, London.

Hu, Q., N. Ueno, and R.R. Behringer. 2004. Restriction of BMP4 activity domains in the developing neural tube of the mouse embryo. *EMBO Rep*. 5:734-9.

Huelsken, J., R. Vogel, V. Brinkmann, B. Erdmann, C. Birchmeier, and W. Birchmeier. 2000. Requirement for beta-catenin in anterior-posterior axis formation in mice. *J Cell Biol*. 148:567-78.

Hughes, D.C., J. Allen, G. Morley, K. Sutherland, W. Ahmed, J. Prosser, L. Lettice, G. Allan, M.G. Mattei, M. Farrall, and R.E. Hill. 1997. Cloning and sequencing of

the mouse Gli2 gene: localization to the Dominant hemimelia critical region. *Genomics*. 39:205-15.

Hui, C.C., D. Slusarski, K.A. Platt, R. Holmgren, and A.L. Joyner. 1994. Expression of three mouse homologs of the Drosophila segment polarity gene cubitus interruptus, Gli, Gli-2, and Gli-3, in ectoderm- and mesoderm-derived tissues suggests multiple roles during postimplantation development. *Dev Biol*. 162:402-13.

Hurtado, C., and E.M. De Robertis. 2007. Neural induction in the absence of organizer in salamanders is mediated by MAPK. *Dev Biol*. 307:282-9.

Hynes, M., D.M. Stone, M. Dowd, S. Pitts-Meek, A. Goddard, A. Gurney, and A. Rosenthal. 1997. Control of cell pattern in the neural tube by the zinc finger transcription factor and oncogene Gli-1. *Neuron*. 19:15-26.

Iavarone, A., P. Garg, A. Lasorella, J. Hsu, and M.A. Israel. 1994. The helix-loop-helix protein Id-2 enhances cell proliferation and binds to the retinoblastoma protein. *Genes Dev*. 8:1270-84.

Ille, F., S. Atanasoski, S. Falk, L.M. Ittner, D. Marki, S. Buchmann-Moller, H. Wurdak, U. Suter, M.M. Taketo, and L. Sommer. 2007. Wnt/BMP signal integration regulates the balance between proliferation and differentiation of neuroepithelial cells in the dorsal spinal cord. *Dev Biol*. 304:394-408.

Inoue, T., M. Hatayama, T. Tohmonda, S. Itohara, J. Aruga, and K. Mikoshiba. 2004. Mouse Zic5 deficiency results in neural tube defects and hypoplasia of cephalic neural crest derivatives. *Dev Biol*. 270:146-62.

Inoue, T., W. Shoji, and M. Obinata. 1999. MIDA1, an Id-associating protein, has two distinct DNA binding activities that are converted by the association with Id1: a novel function of Id protein. *Biochem Biophys Res Commun*. 266:147-51.

Israel, M.A., M.C. Hernandez, M. Florio, P.J. Andres-Barquin, A. Mantani, J.H. Carter, and C.M. Julin. 1999. Id gene expression as a key mediator of tumor cell biology. *Cancer Res*. 59:1726s-1730s.

Jen, Y., K. Manova, and R. Benezra. 1996. Expression patterns of Id1, Id2, and Id3 are highly related but distinct from that of Id4 during mouse embryogenesis. *Dev Dyn*. 207:235-52.

Jen, Y., H. Weintraub, and R. Benezra. 1992. Overexpression of Id protein inhibits the muscle differentiation program: in vivo association of Id with E2A proteins. *Genes Dev*. 6:1466-79.

Jiang, R., Y. Lan, C.R. Norton, J.P. Sundberg, and T. Gridley. 1998. The Slug gene is not essential for mesoderm or neural crest development in mice. *Dev Biol*. 198:277-85.

Johansson, B.M., and M.V. Wiles. 1995. Evidence for involvement of activin A and bone morphogenetic protein 4 in mammalian mesoderm and hematopoietic development. *Mol Cell Biol*. 15:141-51.

Johnson, C.E., B.E. Crawford, M. Stavridis, G. Ten Dam, A.L. Wat, G. Rushton, C.M. Ward, V. Wilson, T.H. van Kuppevelt, J.D. Esko, A. Smith, J.T. Gallagher, and C.L. Merry. 2007. Essential alterations of heparan sulfate during the differentiation of embryonic stem cells to Sox1-enhanced green fluorescent protein-expressing neural progenitor cells. *Stem Cells*. 25:1913-23.

Jones, S. 2004. An overview of the basic helix-loop-helix proteins. *Genome Biol*. 5:226.

Jostes, B., C. Walther, and P. Gruss. 1990. The murine paired box gene, Pax7, is expressed specifically during the development of the nervous and muscular system. *Mech Dev*. 33:27-37.

Kageyama, R., T. Ohtsuka, J. Hatakeyama, and R. Ohsawa. 2005. Roles of bHLH genes in neural stem cell differentiation. *Exp Cell Res*. 306:343-8.

Kamiya, D., S. Banno, N. Sasai, M. Ohgushi, H. Inomata, K. Watanabe, M. Kawada, R. Yakura, H. Kiyonari, K. Nakao, L.M. Jakt, S. Nishikawa, and Y. Sasai. 2011. Intrinsic transition of embryonic stem-cell differentiation into neural progenitors. *Nature*. 470:503-9.

Kang, H.B., J.S. Kim, H.J. Kwon, K.H. Nam, H.S. Youn, D.E. Sok, and Y. Lee. 2005. Basic fibroblast growth factor activates ERK and induces c-fos in human embryonic stem cell line MizhES1. *Stem Cells Dev*. 14:395-401.

Kang, Y., C.R. Chen, and J. Massague. 2003. A self-enabling TGFbeta response coupled to stress signaling: Smad engages stress response factor ATF3 for Id1 repression in epithelial cells. *Mol Cell*. 11:915-26.

Kee, Y., and M. Bronner-Fraser. 2001. Id4 expression and its relationship to other Id genes during avian embryonic development. *Mech Dev*. 109:341-5.

Keller, R., J. Shih, A.K. Sater, and C. Moreno. 1992. Planar induction of convergence and extension of the neural plate by the organizer of Xenopus. *Dev Dyn*. 193:218-34.

Kelly, O.G., K.I. Pinson, and W.C. Skarnes. 2004. The Wnt co-receptors Lrp5 and Lrp6 are essential for gastrulation in mice. *Development*. 131:2803-15.

Kelsh, R.N. 2006. Sorting out Sox10 functions in neural crest development. *Bioessays*. 28:788-98.

Khokha, M.K., J. Yeh, T.C. Grammer, and R.M. Harland. 2005. Depletion of three BMP antagonists from Spemann's organizer leads to a catastrophic loss of dorsal structures. *Dev Cell*. 8:401-11.

Kimura-Yoshida, C., H. Nakano, D. Okamura, K. Nakao, S. Yonemura, J.A. Belo, S. Aizawa, Y. Matsui, and I. Matsuo. 2005. Canonical Wnt signaling and its antagonist regulate anterior-posterior axis polarization by guiding cell migration in mouse visceral endoderm. *Dev Cell*. 9:639-50.

Kinder, S.J., T.E. Tsang, G.A. Quinlan, A.K. Hadjantonakis, A. Nagy, and P.P. Tam. 1999. The orderly allocation of mesodermal cells to the extraembryonic structures and the anteroposterior axis during gastrulation of the mouse embryo. *Development*. 126:4691-701.

Kinder, S.J., T.E. Tsang, M. Wakamiya, H. Sasaki, R.R. Behringer, A. Nagy, and P.P. Tam. 2001. The organizer of the mouse gastrula is composed of a dynamic population of progenitor cells for the axial mesoderm. *Development*. 128:3623-34.

Kleinsmith, L.J., and G.B. Pierce, Jr. 1964. Multipotentiality of Single Embryonal Carcinoma Cells. *Cancer Res*. 24:1544-51.

Klingensmith, J., S.L. Ang, D. Bachiller, and J. Rossant. 1999. Neural induction and patterning in the mouse in the absence of the node and its derivatives. *Dev Biol*. 216:535-49.

Knoetgen, H., C. Viebahn, and M. Kessel. 1999. Head induction in the chick by primitive endoderm of mammalian, but not avian origin. *Development*. 126:815-25.

Korchynskyi, O., and P. ten Dijke. 2002. Identification and functional characterization of distinct critically important bone morphogenetic protein-specific response elements in the Id1 promoter. *J Biol Chem*. 277:4883-91.

Kunath, T., M.K. Saba-El-Leil, M. Almousailleakh, J. Wray, S. Meloche, and A. Smith. 2007. FGF stimulation of the Erk1/2 signalling cascade triggers transition of pluripotent embryonic stem cells from self-renewal to lineage commitment. *Development*. 134:2895-902.

Kurabayashi, M., R. Jeyaseelan, and L. Kedes. 1994. Doxorubicin represses the function of the myogenic helix-loop-helix transcription factor MyoD. Involvement of Id gene induction. *J Biol Chem*. 269:6031-9.

Kuroda, H., L. Fuentealba, A. Ikeda, B. Reversade, and E.M. De Robertis. 2005. Default neural induction: neuralization of dissociated Xenopus cells is mediated by Ras/MAPK activation. *Genes Dev*. 19:1022-7.

Kwon, G.S., M. Viotti, and A.K. Hadjantonakis. 2008. The endoderm of the mouse embryo arises by dynamic widespread intercalation of embryonic and extraembryonic lineages. *Dev Cell*. 15:509-20.

LaBonne, C., and M. Bronner-Fraser. 1998. Neural crest induction in Xenopus: evidence for a two-signal model. *Development*. 125:2403-14.

Labosky, P.A., and K.H. Kaestner. 1998. The winged helix transcription factor Hfh2 is expressed in neural crest and spinal cord during mouse development. *Mech Dev*. 76:185-90.

Lamb, T.M., and R.M. Harland. 1995. Fibroblast growth factor is a direct neural inducer, which combined with noggin generates anterior-posterior neural pattern. *Development*. 121:3627-36.

Lamb, T.M., A.K. Knecht, W.C. Smith, S.E. Stachel, A.N. Economides, N. Stahl, G.D. Yancopolous, and R.M. Harland. 1993. Neural induction by the secreted polypeptide noggin. *Science*. 262:713-8.

Langeland, J.A., J.M. Tomsa, W.R. Jackman, Jr., and C.B. Kimmel. 1998. An amphioxus snail gene: expression in paraxial mesoderm and neural plate suggests a conserved role in patterning the chordate embryo. *Dev Genes Evol*. 208:569-77.

Laursen, K.B., E. Mielke, P. Iannaccone, and E.M. Fuchtbauer. 2007. Mechanism of transcriptional activation by the proto-oncogene Twist1. *J Biol Chem*. 282:34623-33.

Lawson, K.A., J.J. Meneses, and R.A. Pedersen. 1991. Clonal analysis of epiblast fate during germ layer formation in the mouse embryo. *Development*. 113:891-911.

Le Douarin, N.M., G. Couly, and S.E. Creuzet. 2012. The neural crest is a powerful regulator of pre-otic brain development. *Dev Biol*. 366:74-82.

Ledent, V., O. Paquet, and M. Vervoort. 2002. Phylogenetic analysis of the human basic helix-loop-helix proteins. *Genome Biol*. 3:RESEARCH0030.

Lee, J.J., S.C. Ekker, D.P. von Kessler, J.A. Porter, B.I. Sun, and P.A. Beachy. 1994. Autoproteolysis in hedgehog protein biogenesis. *Science*. 266:1528-37.

Lee, J.E., S.M. Hollenberg, L. Snider, D.L. Turner, N. Lipnick, and H. Weintraub. 1995. Conversion of Xenopus ectoderm into neurons by NeuroD, a basic helix-loop-helix protein. *Science*. 268:836-44.

Lee, J., K.A. Platt, P. Censullo, and A. Ruiz i Altaba. 1997. Gli1 is a target of Sonic hedgehog that induces ventral neural tube development. *Development*. 124:2537-52.

Lee, K.J., M. Mendelsohn, and T.M. Jessell. 1998. Neuronal patterning by BMPs: a requirement for GDF7 in the generation of a discrete class of commissural interneurons in the mouse spinal cord. *Genes Dev*. 12:3394-407.

Lee, Y.H., and J.P. Saint-Jeannet. 2011. Sox9 function in craniofacial development and disease. *Genesis*. 49:200-8.

Levine, A.J., and A.H. Brivanlou. 2007. Proposal of a model of mammalian neural induction. *Dev Biol*. 308:247-56.

Li, L., P. Cserjesi, and E.N. Olson. 1995. Dermo-1: a novel twist-related bHLH protein expressed in the developing dermis. *Dev Biol*. 172:280-92.

Li, M., L. Pevny, R. Lovell-Badge, and A. Smith. 1998. Generation of purified neural precursors from embryonic stem cells by lineage selection. *Curr Biol*. 8:971-4.

Li, X.J., Z.W. Du, E.D. Zarnowska, M. Pankratz, L.O. Hansen, R.A. Pearce, and S.C. Zhang. 2005. Specification of motoneurons from human embryonic stem cells. *Nat Biotechnol*. 23:215-21.

Liem, K.F., Jr., T.M. Jessell, and J. Briscoe. 2000. Regulation of the neural patterning activity of sonic hedgehog by secreted BMP inhibitors expressed by notochord and somites. *Development*. 127:4855-66.

Liem, K.F., Jr., G. Tremml, and T.M. Jessell. 1997. A role for the roof plate and its resident TGFbeta-related proteins in neuronal patterning in the dorsal spinal cord. *Cell*. 91:127-38.

Liem, K.F., Jr., G. Tremml, H. Roelink, and T.M. Jessell. 1995. Dorsal differentiation of neural plate cells induced by BMP-mediated signals from epidermal ectoderm. *Cell*. 82:969-79.

Litingtung, Y., and C. Chiang. 2000. Specification of ventral neuron types is mediated by an antagonistic interaction between Shh and Gli3. *Nat Neurosci*. 3:979-85.

Liu, A., A.L. Joyner, and D.H. Turnbull. 1998. Alteration of limb and brain patterning in early mouse embryos by ultrasound-guided injection of Shh-expressing cells. *Mech Dev*. 75:107-15.

Liu, A., and L.A. Niswander. 2005. Bone morphogenetic protein signalling and vertebrate nervous system development. *Nat Rev Neurosci*. 6:945-54.

Liu, P., M. Wakamiya, M.J. Shea, U. Albrecht, R.R. Behringer, and A. Bradley. 1999. Requirement for Wnt3 in vertebrate axis formation. *Nat Genet*. 22:361-5.

Lopez-Rovira, T., E. Chalaux, J. Massague, J.L. Rosa, and F. Ventura. 2002. Direct binding of Smad1 and Smad4 to two distinct motifs mediates bone morphogenetic protein-specific transcriptional activation of Id1 gene. *J Biol Chem*. 277:3176-85.

Loveys, D.A., M.B. Streiff, and G.J. Kato. 1996. E2A basic-helix-loop-helix transcription factors are negatively regulated by serum growth factors and by the Id3 protein. *Nucleic Acids Res*. 24:2813-20.

Lowell, S., A. Benchoua, B. Heavey, and A.G. Smith. 2006. Notch promotes neural lineage entry by pluripotent embryonic stem cells. *PLoS Biol*. 4:e121.

Lum, L., C. Zhang, S. Oh, R.K. Mann, D.P. von Kessler, J. Taipale, F. Weis-Garcia, R. Gong, B. Wang, and P.A. Beachy. 2003. Hedgehog signal transduction via Smoothened association with a cytoplasmic complex scaffolded by the atypical kinesin, Costal-2. *Mol Cell*. 12:1261-74.

Lyden, D., A.Z. Young, D. Zagzag, W. Yan, W. Gerald, R. O'Reilly, B.L. Bader, R.O. Hynes, Y. Zhuang, K. Manova, and R. Benezra. 1999. Id1 and Id3 are required for neurogenesis, angiogenesis and vascularization of tumour xenografts. *Nature*. 401:670-7.

Ma, Q., C. Kintner, and D.J. Anderson. 1996. Identification of neurogenin, a vertebrate neuronal determination gene. *Cell*. 87:43-52.

Maestro, R., A.P. Dei Tos, Y. Hamamori, S. Krasnokutsky, V. Sartorelli, L. Kedes, C. Doglioni, D.H. Beach, and G.J. Hannon. 1999. Twist is a potential oncogene that inhibits apoptosis. *Genes Dev*. 13:2207-17.

Malas, S., M. Postlethwaite, A. Ekonomou, B. Whalley, S. Nishiguchi, H. Wood, B. Meldrum, A. Constanti, and V. Episkopou. 2003. Sox1-deficient mice suffer from epilepsy associated with abnormal ventral forebrain development and olfactory cortex hyperexcitability. *Neuroscience*. 119:421-32.

Mancilla, A., and R. Mayor. 1996. Neural crest formation in Xenopus laevis: mechanisms of Xslug induction. *Dev Biol*. 177:580-9.

Mansouri, A., A. Stoykova, M. Torres, and P. Gruss. 1996. Dysgenesis of cephalic neural crest derivatives in Pax7-/- mutant mice. *Development*. 122:831-8.

Marchal, L., G. Luxardi, V. Thome, and L. Kodjabachian. 2009. BMP inhibition initiates neural induction via FGF signaling and Zic genes. *Proc Natl Acad Sci U S A*. 106:17437-42.

Marchant, L., C. Linker, P. Ruiz, N. Guerrero, and R. Mayor. 1998. The inductive properties of mesoderm suggest that the neural crest cells are specified by a BMP gradient. *Dev Biol*. 198:319-29.

Marigo, V., R.A. Davey, Y. Zuo, J.M. Cunningham, and C.J. Tabin. 1996a. Biochemical evidence that patched is the Hedgehog receptor. *Nature*. 384:176-9.

Marigo, V., R.L. Johnson, A. Vortkamp, and C.J. Tabin. 1996b. Sonic hedgehog differentially regulates expression of GLI and GLI3 during limb development. *Dev Biol*. 180:273-83.

Marigo, V., and C.J. Tabin. 1996. Regulation of patched by sonic hedgehog in the developing neural tube. *Proc Natl Acad Sci U S A*. 93:9346-51.

Marti, E., R. Takada, D.A. Bumcrot, H. Sasaki, and A.P. McMahon. 1995. Distribution of Sonic hedgehog peptides in the developing chick and mouse embryo. *Development*. 121:2537-47.

Martin, G.R. 1981. Isolation of a pluripotent cell line from early mouse embryos cultured in medium conditioned by teratocarcinoma stem cells. *Proc Natl Acad Sci U S A*. 78:7634-8.

Martin, V., G. Carrillo, C. Torroja, and I. Guerrero. 2001. The sterol-sensing domain of Patched protein seems to control Smoothened activity through Patched vesicular trafficking. *Curr Biol*. 11:601-7.

Martinsen, B.J., and M. Bronner-Fraser. 1998. Neural crest specification regulated by the helix-loop-helix repressor Id2. *Science*. 281:988-91.

Massari, M.E., and C. Murre. 2000. Helix-loop-helix proteins: regulators of transcription in eucaryotic organisms. *Mol Cell Biol*. 20:429-40.

Matise, M.P., D.J. Epstein, H.L. Park, K.A. Platt, and A.L. Joyner. 1998. Gli2 is required for induction of floor plate and adjacent cells, but not most ventral neurons in the mouse central nervous system. *Development*. 125:2759-70.

Matsuda, T., T. Nakamura, K. Nakao, T. Arai, M. Katsuki, T. Heike, and T. Yokota. 1999. STAT3 activation is sufficient to maintain an undifferentiated state of mouse embryonic stem cells. *EMBO J*. 18:4261-9.

Mayor, R., R. Morgan, and M.G. Sargent. 1995. Induction of the prospective neural crest of Xenopus. *Development*. 121:767-77.

McLarren, K.W., A. Litsiou, and A. Streit. 2003. DLX5 positions the neural crest and preplacode region at the border of the neural plate. *Dev Biol*. 259:34-47.

Megason, S.G., and A.P. McMahon. 2002. A mitogen gradient of dorsal midline Wnts organizes growth in the CNS. *Development*. 129:2087-98.

Mekki-Dauriac, S., E. Agius, P. Kan, and P. Cochard. 2002. Bone morphogenetic proteins negatively control oligodendrocyte precursor specification in the chick spinal cord. *Development*. 129:5117-30.

Mesnard, D., M. Guzman-Ayala, and D.B. Constam. 2006. Nodal specifies embryonic visceral endoderm and sustains pluripotent cells in the epiblast before overt axial patterning. *Development*. 133:2497-505.

Meulemans, D., D. McCauley, and M. Bronner-Fraser. 2003. Id expression in amphioxus and lamprey highlights the role of gene cooption during neural crest evolution. *Dev Biol*. 264:430-42.

Milet, C., and A.H. Monsoro-Burq. 2012. Neural crest induction at the neural plate border in vertebrates. *Dev Biol*. 366:22-33.

Millonig, J.H., K.J. Millen, and M.E. Hatten. 2000. The mouse Dreher gene Lmx1a controls formation of the roof plate in the vertebrate CNS. *Nature*. 403:764-9.

Mitchell, P.J., P.M. Timmons, J.M. Hebert, P.W. Rigby, and R. Tjian. 1991. Transcription factor AP-2 is expressed in neural crest cell lineages during mouse embryogenesis. *Genes Dev*. 5:105-19.

Miyazono, K., and K. Miyazawa. 2002. Id: a target of BMP signaling. *Sci STKE*. 2002:pe40.

Molkentin, J.D. 2000. The zinc finger-containing transcription factors GATA-4, -5, and -6. Ubiquitously expressed regulators of tissue-specific gene expression. *J Biol Chem*. 275:38949-52.

Monsoro-Burq, A.H., R.B. Fletcher, and R.M. Harland. 2003. Neural crest induction by paraxial mesoderm in Xenopus embryos requires FGF signals. *Development*. 130:3111-24.

Mori, S., S.I. Nishikawa, and Y. Yokota. 2000. Lactation defect in mice lacking the helix-loop-helix inhibitor Id2. *EMBO J*. 19:5772-81.

Morkel, M., J. Huelsken, M. Wakamiya, J. Ding, M. van de Wetering, H. Clevers, M.M. Taketo, R.R. Behringer, M.M. Shen, and W. Birchmeier. 2003. Beta-catenin regulates Cripto- and Wnt3-dependent gene expression programs in mouse axis and mesoderm formation. *Development*. 130:6283-94.

Morrisey E.E., Tang Z., Sigrist K., Lu M.M., Jiang F., H.S. Ip, and M.S. Parmacek.

1998. GATA6 regulates HNF4 and is required for differentiation of visceral endoderm in the mouse embryo. *Genes Dev.* 12:3579-90.

Munoz-Sanjuan, I., and A.H. Brivanlou. 2002. Neural induction, the default model and embryonic stem cells. *Nat Rev Neurosci*. 3:271-80.

Murre, C., G. Bain, M.A. van Dijk, I. Engel, B.A. Furnari, M.E. Massari, J.R. Matthews, M.W. Quong, R.R. Rivera, and M.H. Stuiver. 1994. Structure and function of helix-loop-helix proteins. *Biochim Biophys Acta*. 1218:129-35.

Murre, C., P.S. McCaw, and D. Baltimore. 1989. A new DNA binding and dimerization motif in immunoglobulin enhancer binding, daughterless, MyoD, and myc proteins. *Cell*. 56:777-83.

Nagai, T., J. Aruga, O. Minowa, T. Sugimoto, Y. Ohno, T. Noda, and K. Mikoshiba. 2000. Zic2 regulates the kinetics of neurulation. *Proc Natl Acad Sci U S A*. 97:1618-23.

Nagai, T., J. Aruga, S. Takada, T. Gunther, R. Sporle, K. Schughart, and K. Mikoshiba. 1997. The expression of the mouse Zic1, Zic2, and Zic3 gene suggests an essential role for Zic genes in body pattern formation. *Dev Biol*. 182:299-313.

Nagata, Y., and K. Todokoro. 1994. Activation of helix-loop-helix proteins Id1, Id2 and Id3 during neural differentiation. *Biochem Biophys Res Commun*. 199:1355-62.

Nakata, K., Y. Koyabu, J. Aruga, and K. Mikoshiba. 2000. A novel member of the Xenopus Zic family, Zic5, mediates neural crest development. *Mech Dev*. 99:83-91.

Nakata, K., T. Nagai, J. Aruga, and K. Mikoshiba. 1997. Xenopus Zic3, a primary regulator both in neural and neural crest development. *Proc Natl Acad Sci U S A*. 94:11980-5.

Nakata, K., T. Nagai, J. Aruga, and K. Mikoshiba. 1998. Xenopus Zic family and its role in neural and neural crest development. *Mech Dev*. 75:43-51.

Ng, L.J., S. Wheatley, G.E. Muscat, J. Conway-Campbell, J. Bowles, E. Wright, D.M. Bell, P.P. Tam, K.S. Cheah, and P. Koopman. 1997. SOX9 binds DNA, activates transcription, and coexpresses with type II collagen during chondrogenesis in the mouse. *Dev Biol*. 183:108-21.

Nichols, D.H. 1981. Neural crest formation in the head of the mouse embryo as observed using a new histological technique. *J Embryol Exp Morphol*. 64:105-20.

Nichols, D.H. 1987. Ultrastructure of neural crest formation in the midbrain/rostral hindbrain and preotic hindbrain regions of the mouse embryo. *Am J Anat*. 179:143-54.

Nichols, J., B. Zevnik, K. Anastassiadis, H. Niwa, D. Klewe-Nebenius, I. Chambers, H. Scholer, and A. Smith. 1998. Formation of pluripotent stem cells in the mammalian embryo depends on the POU transcription factor Oct4. *Cell*. 95:379-91.

Norton, J.D. 2000. ID helix-loop-helix proteins in cell growth, differentiation and tumorigenesis. *J Cell Sci*. 113 (Pt 22):3897-905.

Ogden, S.K., M. Ascano, Jr., M.A. Stegman, L.M. Suber, J.E. Hooper, and D.J. Robbins. 2003. Identification of a functional interaction between the transmembrane protein Smoothened and the kinesin-related protein Costal2. *Curr Biol*. 13:1998-2003.

Ohkawara, B., S. Iemura, P. ten Dijke, and N. Ueno. 2002. Action range of BMP is defined by its N-terminal basic amino acid core. *Curr Biol*. 12:205-9.

Ohtani, N., Z. Zebedee, T.J. Huot, J.A. Stinson, M. Sugimoto, Y. Ohashi, A.D. Sharrocks, G. Peters, and E. Hara. 2001. Opposing effects of Ets and Id proteins on p16INK4a expression during cellular senescence. *Nature*. 409:1067-70.

Oppenheimer, J.M. 1936 Structures developed in amphibians by implantation of living fish organizer. *Proc. Soc. Exp. Biol. Med*. 34:461–463

Ouyang, X.S., X. Wang, M.T. Ling, H.L. Wong, S.W. Tsao, and Y.C. Wong. 2002. Id-1 stimulates serum independent prostate cancer cell proliferation through inactivation of p16(INK4a)/pRB pathway. *Carcinogenesis*. 23:721-5.

Pan, L., S. Sato, J.P. Frederick, X.H. Sun, and Y. Zhuang. 1999. Impaired immune responses and B-cell proliferation in mice lacking the Id3 gene. *Mol Cell Biol*. 19:5969-80.

Panchision, D.M., J.M. Pickel, L. Studer, S.H. Lee, P.A. Turner, T.G. Hazel, and R.D. McKay. 2001. Sequential actions of BMP receptors control neural precursor cell production and fate. *Genes Dev*. 15:2094-110.

Park, H.L., C. Bai, K.A. Platt, M.P. Matise, A. Beeghly, C.C. Hui, M. Nakashima, and A.L. Joyner. 2000. Mouse Gli1 mutants are viable but have defects in SHH signaling in combination with a Gli2 mutation. *Development*. 127:1593-605.

Pelton T.A., Sharma S., Schulz T.C., J. Rathjen, and P.D. Rathjen. 2002. Transient pluripotent cell populations during primitive ectoderm formation: correlation of in vivo and in vitro pluripotent cell development. *J Cell Sci.* 115:329-39

Pepinsky, R.B., C. Zeng, D. Wen, P. Rayhorn, D.P. Baker, K.P. Williams, S.A. Bixler, C.M. Ambrose, E.A. Garber, K. Miatkowski, F.R. Taylor, E.A. Wang, and A. Galdes. 1998. Identification of a palmitic acid-modified form of human Sonic hedgehog. *J Biol Chem*. 273:14037-45.

Pera, E.M., A. Ikeda, E. Eivers, and E.M. De Robertis. 2003. Integration of IGF, FGF, and anti-BMP signals via Smad1 phosphorylation in neural induction. *Genes Dev*. 17:3023-8.

Pera, E.M., O. Wessely, S.Y. Li, and E.M. De Robertis. 2001. Neural and head induction by insulin-like growth factor signals. *Dev Cell*. 1:655-65.

Pera, M.F., J. Andrade, S. Houssami, B. Reubinoff, A. Trounson, E.G. Stanley, D. Ward-van Oostwaard, and C. Mummery. 2004. Regulation of human embryonic stem cell differentiation by BMP-2 and its antagonist noggin. *J Cell Sci*. 117:1269-80.

Pera, M.F., B. Reubinoff, and A. Trounson. 2000. Human embryonic stem cells. *J Cell Sci*. 113 (Pt 1):5-10.

Perea-Gomez, A., W. Shawlot, H. Sasaki, R.R. Behringer, and S. Ang. 1999. HNF3beta and Lim1 interact in the visceral endoderm to regulate primitive streak formation and anterior-posterior polarity in the mouse embryo. *Development*. 126:4499-511.

Perea-Gomez, A., F.D. Vella, W. Shawlot, M. Oulad-Abdelghani, C. Chazaud, C. Meno, V. Pfister, L. Chen, E. Robertson, H. Hamada, R.R. Behringer, and S.L. Ang. 2002. Nodal antagonists in the anterior visceral endoderm prevent the formation of multiple primitive streaks. *Dev Cell*. 3:745-56.

Persson, M., D. Stamataki, P. te Welscher, E. Andersson, J. Bose, U. Ruther, J. Ericson, and J. Briscoe. 2002. Dorsal-ventral patterning of the spinal cord requires Gli3 transcriptional repressor activity. *Genes Dev*. 16:2865-78.

Peverali, F.A., T. Ramqvist, R. Saffrich, R. Pepperkok, M.V. Barone, and L. Philipson. 1994. Regulation of G1 progression by E2A and Id helix-loop-helix proteins. *EMBO J*. 13:4291-301.

Pevny, L.H., S. Sockanathan, M. Placzek, and R. Lovell-Badge. 1998. A role for SOX1 in neural determination. *Development*. 125:1967-78.

Piccolo, S., E. Agius, L. Leyns, S. Bhattacharyya, H. Grunz, T. Bouwmeester, and E.M. De Robertis. 1999. The head inducer Cerberus is a multifunctional antagonist of Nodal, BMP and Wnt signals. *Nature*. 397:707-10.

Pinson, K.I., J. Brennan, S. Monkley, B.J. Avery, and W.C. Skarnes. 2000. An LDL-receptor-related protein mediates Wnt signalling in mice. *Nature*. 407:535-8.

Pollard, S.M., R. Wallbank, S. Tomlinson, L. Grotewold, and A. Smith. 2008. Fibroblast growth factor induces a neural stem cell phenotype in foetal forebrain progenitors and during embryonic stem cell differentiation. *Mol Cell Neurosci*. 38:393-403.

Porter, J.A., K.E. Young, and P.A. Beachy. 1996. Cholesterol modification of hedgehog signaling proteins in animal development. *Science*. 274:255-9.

Prabhu, S., A. Ignatova, S.T. Park, and X.H. Sun. 1997. Regulation of the expression of cyclin-dependent kinase inhibitor p21 by E2A and Id proteins. *Mol Cell Biol*. 17:5888-96.

Prelle, K., I.M. Vassiliev, S.G. Vassilieva, E. Wolf, and A.M. Wobus. 1999. Establishment of pluripotent cell lines from vertebrate species--present status and future prospects. *Cells Tissues Organs*. 165:220-36.

Puelles, L., P. Fernandez-Garre, L. Sanchez-Arrones, E. Garcia-Calero, and L. Rodriguez-Gallardo. 2005. Correlation of a chicken stage 4 neural plate fate map with early gene expression patterns. *Brain Res Brain Res Rev*. 49:167-78.

Redmer, T., S. Diecke, T. Grigoryan, A. Quiroga-Negreira, W. Birchmeier, and D. Besser. 2011. E-cadherin is crucial for embryonic stem cell pluripotency and can replace OCT4 during somatic cell reprogramming. *EMBO Rep*. 12:720-6.

Reversade, B., H. Kuroda, H. Lee, A. Mays, and E.M. De Robertis. 2005. Depletion of Bmp2, Bmp4, Bmp7 and Spemann organizer signals induces massive brain formation in Xenopus embryos. *Development*. 132:3381-92.

Ribes, V., and J. Briscoe. 2009. Establishing and interpreting graded Sonic Hedgehog signaling during vertebrate neural tube patterning: the role of negative feedback. *Cold Spring Harb Perspect Biol*. 1:a002014.

Rice, D.P., T. Aberg, Y. Chan, Z. Tang, P.J. Kettunen, L. Pakarinen, R.E. Maxson, and I. Thesleff. 2000. Integration of FGF and TWIST in calvarial bone and suture development. *Development*. 127:1845-55.

Richardson, L., M.E. Torres-Padilla, and M. Zernicka-Goetz. 2006. Regionalised signalling within the extraembryonic ectoderm regulates anterior visceral endoderm positioning in the mouse embryo. *Mech Dev*. 123:288-96.

Rivera-Perez, J.A., J. Mager, and T. Magnuson. 2003. Dynamic morphogenetic events characterize the mouse visceral endoderm. *Dev Biol*. 261:470-87.

Rivera-Perez, J.A., and T. Magnuson. 2005. Primitive streak formation in mice is preceded by localized activation of Brachyury and Wnt3. *Dev Biol*. 288:363-71.

Robb, L., and P.P. Tam. 2004. Gastrula organiser and embryonic patterning in the mouse. *Semin Cell Dev Biol*. 15:543-54.

Robert, B., D. Sassoon, B. Jacq, W. Gehring, and M. Buckingham. 1989. Hox-7, a mouse homeobox gene with a novel pattern of expression during embryogenesis. *EMBO J*. 8:91-100.

Roberts, E.C., R.W. Deed, T. Inoue, J.D. Norton, and A.D. Sharrocks. 2001. Id helix-loop-helix proteins antagonize pax transcription factor activity by inhibiting DNA binding. *Mol Cell Biol*. 21:524-33.

Rodriguez, T.A., S. Srinivas, M.P. Clements, J.C. Smith, and R.S. Beddington. 2005. Induction and migration of the anterior visceral endoderm is regulated by the extra-embryonic ectoderm. *Development*. 132:2513-20.

Roelink, H., J.A. Porter, C. Chiang, Y. Tanabe, D.T. Chang, P.A. Beachy, and T.M. Jessell. 1995. Floor plate and motor neuron induction by different concentrations of the amino-terminal cleavage product of sonic hedgehog autoproteolysis. *Cell*. 81:445-55.

Rogers, C.D., G.S. Ferzli, and E.S. Casey. 2011. The response of early neural genes to FGF signaling or inhibition of BMP indicate the absence of a conserved neural induction module. *BMC Dev Biol*. 11:74.

Rossant, J., and P.P. Tam. 2009. Blastocyst lineage formation, early embryonic asymmetries and axis patterning in the mouse. *Development*. 136:701-13.

Ruel, L., R. Rodriguez, A. Gallet, L. Lavenant-Staccini, and P.P. Therond. 2003. Stability and association of Smoothened, Costal2 and Fused with Cubitus interruptus are regulated by Hedgehog. *Nat Cell Biol*. 5:907-13.

Ruiz i Altaba, A. 1990. Neural expression of the Xenopus homeobox gene Xhox3: evidence for a patterning neural signal that spreads through the ectoderm. *Development*. 108:595-604.

Ruiz i Altaba, A. 1992. Planar and vertical signals in the induction and patterning of the Xenopus nervous system. *Development*. 116:67-80.

Ruiz i Altaba, A., and D.A. Melton. 1989. Interaction between peptide growth factors and homoeobox genes in the establishment of antero-posterior polarity in frog embryos. *Nature*. 341:33-8.

Rutishauser, U., A. Acheson, A.K. Hall, D.M. Mann, and J. Sunshine. 1988. The neural cell adhesion molecule (NCAM) as a regulator of cell-cell interactions. *Science*. 240:53-7.

Ruzinova, M.B., and R. Benezra. 2003. Id proteins in development, cell cycle and cancer. *Trends Cell Biol*. 13:410-8.

Sadaghiani, B., and C.H. Thiebaud. 1987. Neural crest development in the Xenopus laevis embryo, studied by interspecific transplantation and scanning electron microscopy. *Dev Biol*. 124:91-110.

Sasai, Y., B. Lu, H. Steinbeisser, and E.M. De Robertis. 1995. Regulation of neural induction by the Chd and Bmp-4 antagonistic patterning signals in Xenopus. *Nature*. 376:333-6.

Sasai, Y., B. Lu, H. Steinbeisser, D. Geissert, L.K. Gont, and E.M. De Robertis. 1994. Xenopus chordin: a novel dorsalizing factor activated by organizer-specific homeobox genes. *Cell*. 79:779-90.

Sasaki, H., and B.L. Hogan. 1994. HNF-3 beta as a regulator of floor plate development. *Cell*. 76:103-15.

Sasaki, H., Y. Nishizaki, C. Hui, M. Nakafuku, and H. Kondoh. 1999. Regulation of Gli2 and Gli3 activities by an amino-terminal repression domain: implication of Gli2 and Gli3 as primary mediators of Shh signaling. *Development*. 126:3915-24.

Sato, S.M., and T.D. Sargent. 1989. Development of neural inducing capacity in dissociated Xenopus embryos. *Dev Biol*. 134:263-6.

Sauka-Spengler, T., and M. Bronner-Fraser. 2008. A gene regulatory network orchestrates neural crest formation. *Nat Rev Mol Cell Biol*. 9:557-68.

Schulz, H., R. Kolde, P. Adler, I. Aksoy, K. Anastassiadis, M. Bader, N. Billon, H. Boeuf, P.Y. Bourillot, F. Buchholz, C. Dani, M.X. Doss, L. Forrester, M. Gitton, D. Henrique, J. Hescheler, H. Himmelbauer, N. Hubner, E. Karantzali, A. Kretsovali, S. Lubitz, L. Pradier, M. Rai, J. Reimand, A. Rolletschek, A. Sachinidis, P. Savatier, F. Stewart, M.P. Storm, M. Trouillas, J. Vilo, M.J. Welham, J. Winkler, A.M. Wobus, and A.K. Hatzopoulos. 2009. The FunGenES database: a genomics resource for mouse embryonic stem cell differentiation. *PLoS One*. 4:e6804.

Schwab, K.E., and C.E. Gargett. 2007. Co-expression of two perivascular cell markers isolates mesenchymal stem-like cells from human endometrium. *Hum Reprod*. 22:2903-11.

Sela-Donenfeld, D., and C. Kalcheim. 1999. Regulation of the onset of neural crest migration by coordinated activity of BMP4 and Noggin in the dorsal neural tube. *Development*. 126:4749-62.

Selleck, M.A., and M. Bronner-Fraser. 1995. Origins of the avian neural crest: the role of neural plate-epidermal interactions. *Development*. 121:525-38.

Selleck, M.A., M.I. Garcia-Castro, K.B. Artinger, and M. Bronner-Fraser. 1998. Effects of Shh and Noggin on neural crest formation demonstrate that BMP is required in the neural tube but not ectoderm. *Development*. 125:4919-30.

Serafini, M., and C.M. Verfaillie. 2006. Pluripotency in adult stem cells: state of the art. *Semin Reprod Med*. 24:379-88.

Sharman, A.C., S.M. Shimeld, and P.W. Holland. 1999. An amphioxus Msx gene expressed predominantly in the dorsal neural tube. *Dev Genes Evol*. 209:260-3.

Sharpe, C.R., and J.B. Gurdon. 1990. The induction of anterior and posterior neural genes in Xenopus laevis. *Development*. 109:765-74.

Shen, M.M., and A.F. Schier. 2000. The EGF-CFC gene family in vertebrate development. *Trends Genet*. 16:303-9.

Sheng, G., M. dos Reis, and C.D. Stern. 2003. Churchill, a zinc finger transcriptional activator, regulates the transition between gastrulation and neurulation. *Cell*. 115:603-13.

Sheng, G., and C.D. Stern. 1999. Gata2 and Gata3: novel markers for early embryonic polarity and for non-neural ectoderm in the chick embryo. *Mech Dev*. 87:213-6.

Shi, J., C. Severson, J. Yang, D. Wedlich, and M.W. Klymkowsky. 2011. Snail2 controls mesodermal BMP/Wnt induction of neural crest. *Development*. 138:3135-45.

Shoji, W., T. Inoue, T. Yamamoto, and M. Obinata. 1995. MIDA1, a protein associated with Id, regulates cell growth. *J Biol Chem*. 270:24818-25.

Smith, A.G., J.K. Heath, D.D. Donaldson, G.G. Wong, J. Moreau, M. Stahl, and D. Rogers. 1988. Inhibition of pluripotential embryonic stem cell differentiation by purified polypeptides. *Nature*. 336:688-90.

Smith, A.G., and M.L. Hooper. 1987. Buffalo rat liver cells produce a diffusible activity which inhibits the differentiation of murine embryonal carcinoma and embryonic stem cells. *Dev Biol*. 121:1-9.

Smith, D.E., F. Franco del Amo, and T. Gridley. 1992. Isolation of Sna, a mouse gene homologous to the Drosophila genes snail and escargot: its expression pattern

suggests multiple roles during postimplantation development. *Development*. 116:1033-9.

Smith, W.C., and R.M. Harland. 1992. Expression cloning of noggin, a new dorsalizing factor localized to the Spemann organizer in Xenopus embryos. *Cell*. 70:829-40.

Smukler, S.R., S.B. Runciman, S. Xu, and D. van der Kooy. 2006. Embryonic stem cells assume a primitive neural stem cell fate in the absence of extrinsic influences. *J Cell Biol*. 172:79-90.

Soncin, F., L. Mohamet, D. Eckardt, S. Ritson, A.M. Eastham, N. Bobola, A. Russell, S. Davies, R. Kemler, C.L. Merry, and C.M. Ward. 2009. Abrogation of E-cadherin-mediated cell-cell contact in mouse embryonic stem cells results in reversible LIF-independent self-renewal. *Stem Cells*. 27:2069-80.

Soncin, F., L. Mohamet, S. Ritson, K. Hawkins, N. Bobola, L. Zeef, C.L. Merry, and C.M. Ward. 2011. E-cadherin acts as a regulator of transcripts associated with a wide range of cellular processes in mouse embryonic stem cells. *PLoS One*. 6:e21463.

Soo, K., M.P. O'Rourke, P.L. Khoo, K.A. Steiner, N. Wong, R.R. Behringer, and P.P. Tam. 2002. Twist function is required for the morphogenesis of the cephalic neural tube and the differentiation of the cranial neural crest cells in the mouse embryo. *Dev Biol*. 247:251-70.

Sosic, D., J.A. Richardson, K. Yu, D.M. Ornitz, and E.N. Olson. 2003. Twist regulates cytokine gene expression through a negative feedback loop that represses NF-kappaB activity. *Cell*. 112:169-80.

Spemann, H. & Mangold, H. 1924. Uber Induktion von Embryonanlagen durch Implantation artfremder Organisatoren. *Arch. Mikrosk. Anat. Entwickl. Mech*. 100:599–638.

Srinivas, S., T. Rodriguez, M. Clements, J.C. Smith, and R.S. Beddington. 2004. Active cell migration drives the unilateral movements of the anterior visceral endoderm. *Development*. 131:1157-64.

Stamataki, D., F. Ulloa, S.V. Tsoni, A. Mynett, and J. Briscoe. 2005. A gradient of Gli activity mediates graded Sonic Hedgehog signaling in the neural tube. *Genes Dev*. 19:626-41.

Stavridis, M.P., B.J. Collins, and K.G. Storey. 2010. Retinoic acid orchestrates fibroblast growth factor signalling to drive embryonic stem cell differentiation. *Development*. 137:881-90.

Stavridis, M.P., J.S. Lunn, B.J. Collins, and K.G. Storey. 2007. A discrete period of FGF-induced Erk1/2 signalling is required for vertebrate neural specification. *Development*. 134:2889-94.

Stern, C.D. 2006. Neural induction: 10 years on since the 'default model'. *Curr Opin Cell Biol*. 18:692-7.

Sterneckert, J., M. Stehling, C. Bernemann, M.J. Arauzo-Bravo, B. Greber, L. Gentile, C. Ortmeier, M. Sinn, G. Wu, D. Ruau, M. Zenke, R. Brintrup, D.C. Klein, K. Ko, and H.R. Scholer. 2010. Neural induction intermediates exhibit distinct roles of Fgf signaling. *Stem Cells*. 28:1772-81.

Steventon, B., C. Araya, C. Linker, S. Kuriyama, and R. Mayor. 2009. Differential requirements of BMP and Wnt signalling during gastrulation and neurulation define two steps in neural crest induction. *Development*. 136:771-9.

Stoetzel, C., B. Weber, P. Bourgeois, A.L. Bolcato-Bellemin, and F. Perrin-Schmitt. 1995. Dorso-ventral and rostro-caudal sequential expression of M-twist in the postimplantation murine embryo. *Mech Dev*. 51:251-63.

Stone, D.M., M. Hynes, M. Armanini, T.A. Swanson, Q. Gu, R.L. Johnson, M.P. Scott, D. Pennica, A. Goddard, H. Phillips, M. Noll, J.E. Hooper, F. de Sauvage, and A. Rosenthal. 1996. The tumour-suppressor gene patched encodes a candidate receptor for Sonic hedgehog. *Nature*. 384:129-34.

Stottmann, R.W., and J. Klingensmith. 2011. Bone morphogenetic protein signaling is required in the dorsal neural folds before neurulation for the induction of spinal neural crest cells and dorsal neurons. *Dev Dyn*. 240:755-65.

Streit, A., A.J. Berliner, C. Papanayotou, A. Sirulnik, and C.D. Stern. 2000. Initiation of neural induction by FGF signalling before gastrulation. *Nature*. 406:74-8.

Streit, A., K.J. Lee, I. Woo, C. Roberts, T.M. Jessell, and C.D. Stern. 1998. Chordin regulates primitive streak development and the stability of induced neural cells, but is not sufficient for neural induction in the chick embryo. *Development*. 125:507-19.

Stuhlmiller, T.J., and M.I. Garcia-Castro. 2012. FGF/MAPK signaling is required in the gastrula epiblast for avian neural crest induction. *Development*. 139:289-300.

Sugai, M., H. Gonda, T. Kusunoki, T. Katakai, Y. Yokota, and A. Shimizu. 2003. Essential role of Id2 in negative regulation of IgE class switching. *Nat Immunol*. 4:25-30.

Sun, X., E.N. Meyers, M. Lewandoski, and G.R. Martin. 1999. Targeted disruption of Fgf8 causes failure of cell migration in the gastrulating mouse embryo. *Genes Dev*. 13:1834-46.

Tabata, T., and T.B. Kornberg. 1994. Hedgehog is a signaling protein with a key role in patterning Drosophila imaginal discs. *Cell*. 76:89-102.

Taga, T., and T. Kishimoto. 1997. Gp130 and the interleukin-6 family of cytokines. *Annu Rev Immunol*. 15:797-819.

Takada, S., K.L. Stark, M.J. Shea, G. Vassileva, J.A. McMahon, and A.P. McMahon. 1994. Wnt-3a regulates somite and tailbud formation in the mouse embryo. *Genes Dev*. 8:174-89.

Takagi T., H. Moribe, H. Kondoh, and Y. Higashi. 1998. DeltaEF1, a zinc finger and homeodomain transcription factor, is required for skeleton patterning in multiple lineages. *Development*. 125:21-31.

Takaoka, K., M. Yamamoto, H. Shiratori, C. Meno, J. Rossant, Y. Saijoh, and H. Hamada. 2006. The mouse embryo autonomously acquires anterior-posterior polarity at implantation. *Dev Cell*. 10:451-9.

Talikka, M., S.E. Perez, and K. Zimmerman. 2002. Distinct patterns of downstream target activation are specified by the helix-loop-helix domain of proneural basic helix-loop-helix transcription factors. *Dev Biol*. 247:137-48.

Tam, P.P., K.A. Steiner, S.X. Zhou, and G.A. Quinlan. 1997. Lineage and functional analyses of the mouse organizer. *Cold Spring Harb Symp Quant Biol*. 62:135-44.

Tanaka, T.S., R.E. Davey, Q. Lan, P.W. Zandstra, and W.L. Stanford. 2008. Development of a gene-trap vector with a highly sensitive fluorescent protein reporter system for expression profiling. *Genesis*. 46:347-56.

Tang, F., C. Barbacioru, S. Bao, C. Lee, E. Nordman, X. Wang, K. Lao, and M.A. Surani. 2010. Tracing the derivation of embryonic stem cells from the inner cell mass by single-cell RNA-Seq analysis. *Cell Stem Cell*. 6:468-78.

Tesar, P.J., J.G. Chenoweth, F.A. Brook, T.J. Davies, E.P. Evans, D.L. Mack, R.L. Gardner, and R.D. McKay. 2007. New cell lines from mouse epiblast share defining features with human embryonic stem cells. *Nature*. 448:196-9.

Theveneau, E., J.L. Duband, and M. Altabef. 2007. Ets-1 confers cranial features on neural crest delamination. *PLoS One*. 2:e1142.

Theveneau, E., and R. Mayor. 2012. Neural crest delamination and migration: from epithelium-to-mesenchyme transition to collective cell migration. *Dev Biol*. 366:34-54.

Thomas, P.Q., A. Brown, and R.S. Beddington. 1998. Hex: a homeobox gene revealing peri-implantation asymmetry in the mouse embryo and an early transient marker of endothelial cell precursors. *Development*. 125:85-94.

Thomson, J.A., J. Itskovitz-Eldor, S.S. Shapiro, M.A. Waknitz, J.J. Swiergiel, V.S. Marshall, and J.M. Jones. 1998. Embryonic stem cell lines derived from human blastocysts. *Science*. 282:1145-7.

Till, J.E., and C.E. Mc. 1961. A direct measurement of the radiation sensitivity of normal mouse bone marrow cells. *Radiat Res*. 14:213-22.

Tischfield M.A., Baris H.N., Wu C., Rudolph G., Van Maldergem L., He W., Chan W.M., Andrews C., Demer J.L., Robertson R.L., Mackey D.A., Ruddle J.B., Bird T.D., Gottlob I., Pieh C., Traboulsi E.I., Pomeroy S.L., Hunter D.G., Soul J.S., Newlin A., Sabol L.J., Doherty E.J., de Uzcátegui C.E., de Uzcátegui N., Collins M.L., Sener E.C., Wabbels B., Hellebrand H., Meitinger T., de Berardinis T., Magli A., Schiavi C., Pastore-Trossello M., Koc F., Wong A.M., Levin A.V., Geraghty M.T., Descartes M., Flaherty M., Jamieson R.V., Møller H.U., Meuthen I., Callen D.F., Kerwin J., Lindsay S., Meindl A., Gupta M.L. Jr., D. Pellman, and E.C. Engle. 2010. Human TUBB3 mutations perturb microtubule dynamics, kinesin interactions, and axon guidance. *Cell.* 140:74-87.

Tole, S., C.W. Ragsdale, and E.A. Grove. 2000. Dorsoventral patterning of the telencephalon is disrupted in the mouse mutant extra-toes(J). *Dev Biol*. 217:254-65.

Tropepe, V., S. Hitoshi, C. Sirard, T.W. Mak, J. Rossant, and D. van der Kooy. 2001. Direct neural fate specification from embryonic stem cells: a primitive mammalian neural stem cell stage acquired through a default mechanism. *Neuron*. 30:65-78.

Tzouanacou, E., A. Wegener, F.J. Wymeersch, V. Wilson, and J.F. Nicolas. 2009. Redefining the progression of lineage segregations during mammalian embryogenesis by clonal analysis. *Dev Cell*. 17:365-76.

Urlinger, S., U. Baron, M. Thellmann, M.T. Hasan, H. Bujard, and W. Hillen. 2000. Exploring the sequence space for tetracycline-dependent transcriptional activators: novel mutations yield expanded range and sensitivity. *Proc Natl Acad Sci U S A*. 97:7963-8.

Vallier, L., T. Touboul, Z. Chng, M. Brimpari, N. Hannan, E. Millan, L.E. Smithers, M. Trotter, P. Rugg-Gunn, A. Weber, and R.A. Pedersen. 2009. Early cell fate

decisions of human embryonic stem cells and mouse epiblast stem cells are controlled by the same signalling pathways. *PLoS One*. 4:e6082.

Valsesia-Wittmann, S., M. Magdeleine, S. Dupasquier, E. Garin, A.C. Jallas, V. Combaret, A. Krause, P. Leissner, and A. Puisieux. 2004. Oncogenic cooperation between H-Twist and N-Myc overrides failsafe programs in cancer cells. *Cancer Cell*. 6:625-30.

Van de Putte, T., M. Maruhashi, A. Francis, L. Nelles, H. Kondoh, D. Huylebroeck, and Y. Higashi. 2003. Mice lacking ZFHX1B, the gene that codes for Smad-interacting protein-1, reveal a role for multiple neural crest cell defects in the etiology of Hirschsprung disease-mental retardation syndrome. *Am J Hum Genet*. 72:465-70.

van Straaten, H.W., F. Thors, L. Wiertz-Hoessels, J. Hekking, and J. Drukker. 1985. Effect of a notochordal implant on the early morphogenesis of the neural tube and neuroblasts: histometrical and histological results. *Dev Biol*. 110:247-54.

Vincentz, J.W., R.M. Barnes, R. Rodgers, B.A. Firulli, S.J. Conway, and A.B. Firulli. 2008. An absence of Twist1 results in aberrant cardiac neural crest morphogenesis. *Dev Biol*. 320:131-9.

Voiculescu, O., F. Bertocchini, L. Wolpert, R.E. Keller, and C.D. Stern. 2007. The amniote primitive streak is defined by epithelial cell intercalation before gastrulation. *Nature*. 449:1049-52.

Voronova, A., and D. Baltimore. 1990. Mutations that disrupt DNA binding and dimer formation in the E47 helix-loop-helix protein map to distinct domains. *Proc Natl Acad Sci U S A*. 87:4722-6.

Waddington, C. H. 1933. Induction by the primitive streak and its derivatives in the chick. *J. Exp. Biol*. 10:38-48.

Waddington, C. H. 1936. Organizers in Mammalian Development. *Nature*. 138:125.

Waldrip, W.R., E.K. Bikoff, P.A. Hoodless, J.L. Wrana, and E.J. Robertson. 1998. Smad2 signaling in extraembryonic tissues determines anterior-posterior polarity of the early mouse embryo. *Cell*. 92:797-808.

Wang, B., J.F. Fallon, and P.A. Beachy. 2000. Hedgehog-regulated processing of Gli3 produces an anterior/posterior repressor gradient in the developing vertebrate limb. *Cell*. 100:423-34.

Wang, Y., R. Benezra, and D.A. Sassoon. 1992. Id expression during mouse development: a role in morphogenesis. *Dev Dyn*. 194:222-30.

Weston, J.A. 1963. A radioautographic analysis of the migration and localization of trunk neural crest cells in the chick. *Dev Biol*. 6:279-310.

Wijgerde, M., J.A. McMahon, M. Rule, and A.P. McMahon. 2002. A direct requirement for Hedgehog signaling for normal specification of all ventral progenitor domains in the presumptive mammalian spinal cord. *Genes Dev*. 16:2849-64.

Williams, R.L., D.J. Hilton, S. Pease, T.A. Willson, C.L. Stewart, D.P. Gearing, E.F. Wagner, D. Metcalf, N.A. Nicola, and N.M. Gough. 1988. Myeloid leukaemia inhibitory factor maintains the developmental potential of embryonic stem cells. *Nature*. 336:684-7.

Wilson, P.A., and A. Hemmati-Brivanlou. 1995. Induction of epidermis and inhibition of neural fate by Bmp-4. *Nature*. 376:331-3.

Wilson, S.I., E. Graziano, R. Harland, T.M. Jessell, and T. Edlund. 2000. An early requirement for FGF signalling in the acquisition of neural cell fate in the chick embryo. *Curr Biol*. 10:421-9.

Wine-Lee, L., K.J. Ahn, R.D. Richardson, Y. Mishina, K.M. Lyons, and E.B. Crenshaw, 3rd. 2004. Signaling through BMP type 1 receptors is required for development of interneuron cell types in the dorsal spinal cord. *Development*. 131:5393-403.

Winnier, G., M. Blessing, P.A. Labosky, and B.L. Hogan. 1995. Bone morphogenetic protein-4 is required for mesoderm formation and patterning in the mouse. *Genes Dev*. 9:2105-16.

Wood, H.B., and V. Episkopou. 1999. Comparative expression of the mouse Sox1, Sox2 and Sox3 genes from pre-gastrulation to early somite stages. *Mech Dev*. 86:197-201.

Wu, M., E. Hesse, F. Morvan, J.P. Zhang, D. Correa, G.C. Rowe, R. Kiviranta, L. Neff, W.M. Philbrick, W.C. Horne, and R. Baron. 2009. Zfp521 antagonizes Runx2, delays osteoblast differentiation in vitro, and promotes bone formation in vivo. *Bone*. 44:528-36.

Xu, C., M.S. Inokuma, J. Denham, K. Golds, P. Kundu, J.D. Gold, and M.K. Carpenter. 2001. Feeder-free growth of undifferentiated human embryonic stem cells. *Nat Biotechnol*. 19:971-4.

Yamada, T., M. Placzek, H. Tanaka, J. Dodd, and T.M. Jessell. 1991. Control of cell pattern in the developing nervous system: polarizing activity of the floor plate and notochord. *Cell*. 64:635-47.

Yamagata, M., and M. Noda. 1998. The winged-helix transcription factor CWH-3 is expressed in developing neural crest cells. *Neurosci Lett*. 249:33-6.

Yamaguchi T.P., R.A. Conlon, and J. Rossant. 1992. Expression of the fibroblast growth factor receptor FGFR-1/flg during gastrulation and segmentation in the mouse embryo. *Dev Biol*. 152:75-88.

Yamaguchi, T.P., K. Harpal, M. Henkemeyer, and J. Rossant. 1994. fgfr-1 is required for embryonic growth and mesodermal patterning during mouse gastrulation. *Genes Dev*. 8:3032-44.

Yamanaka, Y., O.J. Tamplin, A. Beckers, A. Gossler, and J. Rossant. 2007. Live imaging and genetic analysis of mouse notochord formation reveals regional morphogenetic mechanisms. *Dev Cell*. 13:884-96.

Yan, W., A.Z. Young, V.C. Soares, R. Kelley, R. Benezra, and Y. Zhuang. 1997. High incidence of T-cell tumors in E2A-null mice and E2A/Id1 double-knockout mice. *Mol Cell Biol*. 17:7317-27.

Yang, J., S.A. Mani, J.L. Donaher, S. Ramaswamy, R.A. Itzykson, C. Come, P. Savagner, I. Gitelman, A. Richardson, and R.A. Weinberg. 2004. Twist, a master regulator of morphogenesis, plays an essential role in tumor metastasis. *Cell*. 117:927-39.

Yang, L., H. Zhang, G. Hu, H. Wang, C. Abate-Shen, and M.M. Shen. 1998. An early phase of embryonic Dlx5 expression defines the rostral boundary of the neural plate. *J Neurosci*. 18:8322-30.

Yang, Y.P., and J. Klingensmith. 2006. Roles of organizer factors and BMP antagonism in mammalian forebrain establishment. *Dev Biol*. 296:458-75.

Yao, S., S. Chen, J. Clark, E. Hao, G.M. Beattie, A. Hayek, and S. Ding. 2006. Long-term self-renewal and directed differentiation of human embryonic stem cells in chemically defined conditions. *Proc Natl Acad Sci U S A*. 103:6907-12.

Yasui, K., S.C. Zhang, M. Uemura, S. Aizawa, and T. Ueki. 1998. Expression of a twist-related gene, Bbtwist, during the development of a lancelet species and its relation to cephalochordate anterior structures. *Dev Biol*. 195:49-59.

Yates, P.R., G.T. Atherton, R.W. Deed, J.D. Norton, and A.D. Sharrocks. 1999. Id helix-loop-helix proteins inhibit nucleoprotein complex formation by the TCF ETS-domain transcription factors. *EMBO J*. 18:968-76.

Ybot-Gonzalez, P., C. Gaston-Massuet, G. Girdler, J. Klingensmith, R. Arkell, N.D. Greene, and A.J. Copp. 2007. Neural plate morphogenesis during mouse neurulation is regulated by antagonism of Bmp signalling. *Development*. 134:3203-11.

Ying, Q.L., J. Nichols, E.P. Evans, and A.G. Smith. 2002. Changing potency by spontaneous fusion. *Nature*. 416:545-8.

Ying, Q.L., J. Nichols, I. Chambers, and A. Smith. 2003a. BMP induction of Id proteins suppresses differentiation and sustains embryonic stem cell self-renewal in collaboration with STAT3. *Cell*. 115:281-92.

Ying, Q.L., M. Stavridis, D. Griffiths, M. Li, and A. Smith. 2003b. Conversion of embryonic stem cells into neuroectodermal precursors in adherent monoculture. *Nat Biotechnol*. 21:183-6.

Ying, Q.L., J. Wray, J. Nichols, L. Batlle-Morera, B. Doble, J. Woodgett, P. Cohen, and A. Smith. 2008. The ground state of embryonic stem cell self-renewal. *Nature*. 453:519-23.

Yokota, Y., A. Mansouri, S. Mori, S. Sugawara, S. Adachi, S. Nishikawa, and P. Gruss. 1999. Development of peripheral lymphoid organs and natural killer cells depends on the helix-loop-helix inhibitor Id2. *Nature*. 397:702-6.

Yu, W., K. McDonnell, M.M. Taketo, and C.B. Bai. 2008. Wnt signaling determines ventral spinal cord cell fates in a time-dependent manner. *Development*. 135:3687-96.

Yun, K., A. Mantani, S. Garel, J. Rubenstein, and M.A. Israel. 2004. Id4 regulates neural progenitor proliferation and differentiation in vivo. *Development*. 131:5441-8.

Zechner, D., T. Muller, H. Wende, I. Walther, M.M. Taketo, E.B. Crenshaw, 3rd, M. Treier, W. Birchmeier, and C. Birchmeier. 2007. Bmp and Wnt/beta-catenin signals control expression of the transcription factor Olig3 and the specification of spinal cord neurons. *Dev Biol*. 303:181-90.

Zernicka-Goetz, M. 2002. Patterning of the embryo: the first spatial decisions in the life of a mouse. *Development*. 129:815-29.

Zhang, K., L. Li, C. Huang, C. Shen, F. Tan, C. Xia, P. Liu, J. Rossant, and N. Jing. 2010. Distinct functions of BMP4 during different stages of mouse ES cell neural commitment. *Development*. 137:2095-105.

Zhang, S.C., M. Wernig, I.D. Duncan, O. Brustle, and J.A. Thomson. 2001. In vitro differentiation of transplantable neural precursors from human embryonic stem cells. *Nat Biotechnol*. 19:1129-33.

Zhang, Y., E.L. Blackwell, M.T. McKnight, G.R. Knutsen, W.T. Vu, and L.B. Ruest. 2012. Specific inactivation of Twist1 in the mandibular arch neural crest cells affects the development of the ramus and reveals interactions with hand2. *Dev Dyn*. 241:924-40.

Zhao, S., J. Nichols, A.G. Smith, and M. Li. 2004. SoxB transcription factors specify neuroectodermal lineage choice in ES cells. *Mol Cell Neurosci*. 27:332-42.

Zhuang, Y., C.G. Kim, S. Bartelmez, P. Cheng, M. Groudine, and H. Weintraub. 1992. Helix-loop-helix transcription factors E12 and E47 are not essential for skeletal or cardiac myogenesis, erythropoiesis, chondrogenesis, or neurogenesis. *Proc Natl Acad Sci U S A*. 89:12132-6.

Zhuang, Y., P. Soriano, and H. Weintraub. 1994. The helix-loop-helix gene E2A is required for B cell formation. *Cell*. 79:875-84.

Zohn, I.E., Y. Li, E.Y. Skolnik, K.V. Anderson, J. Han, and L. Niswander. 2006. p38 and a p38-interacting protein are critical for downregulation of E-cadherin during mouse gastrulation. *Cell*. 125:957-69.

VIII. APPENDICES

Appendix 1. Doxycycline does not influence differentiation of non-inducible cells.

4 days of monolayer neural differentiation of rtTA parental cell line in N2B27 under Dox (800 ng/ml) and/or BMP4 (5 ng/ml) influence respectively (a). Left panels phase contrast, right panels immunofluorescence: TUBB3 staining; green. At this time point few TUBB3 positive neurons can be seen only in the absence of BMP4 and their presence is not influenced by Dox. Scale bars represent 50 μm. qPCR showing expression of *Twist1, Sox1* and *Zfp521* in ES cells and cells at day 3 and 4 of neural differentiation in monolayer protocol for rtTA parental cell line (b). The expression of the tested markers is not influenced by Dox in this cell line. One experiment performed in duplicates is shown. Error bars represent value range. Expression in ES cells has been arbitrarily set to 1. Similar control experiments have been performed extensively during other projects in the lab that make use of the same parental lines as controls for experiments where Dox is used to induce other transcription factors (for example *Tcf15* – Davies et al., 2013). It is well established from the results of these experiments that Dox does not influence the rate or direction of neural differentiation from ES cells

a

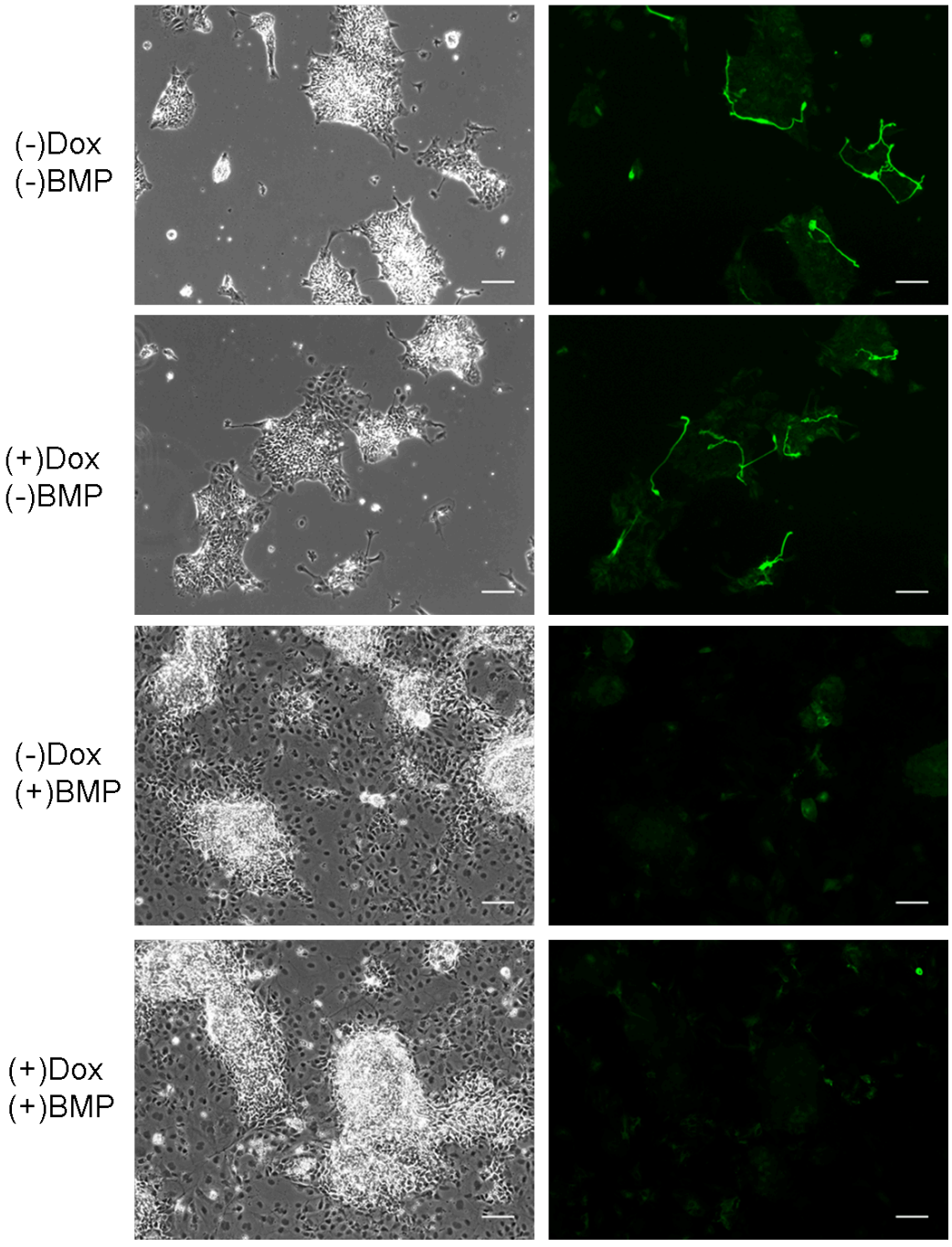

b

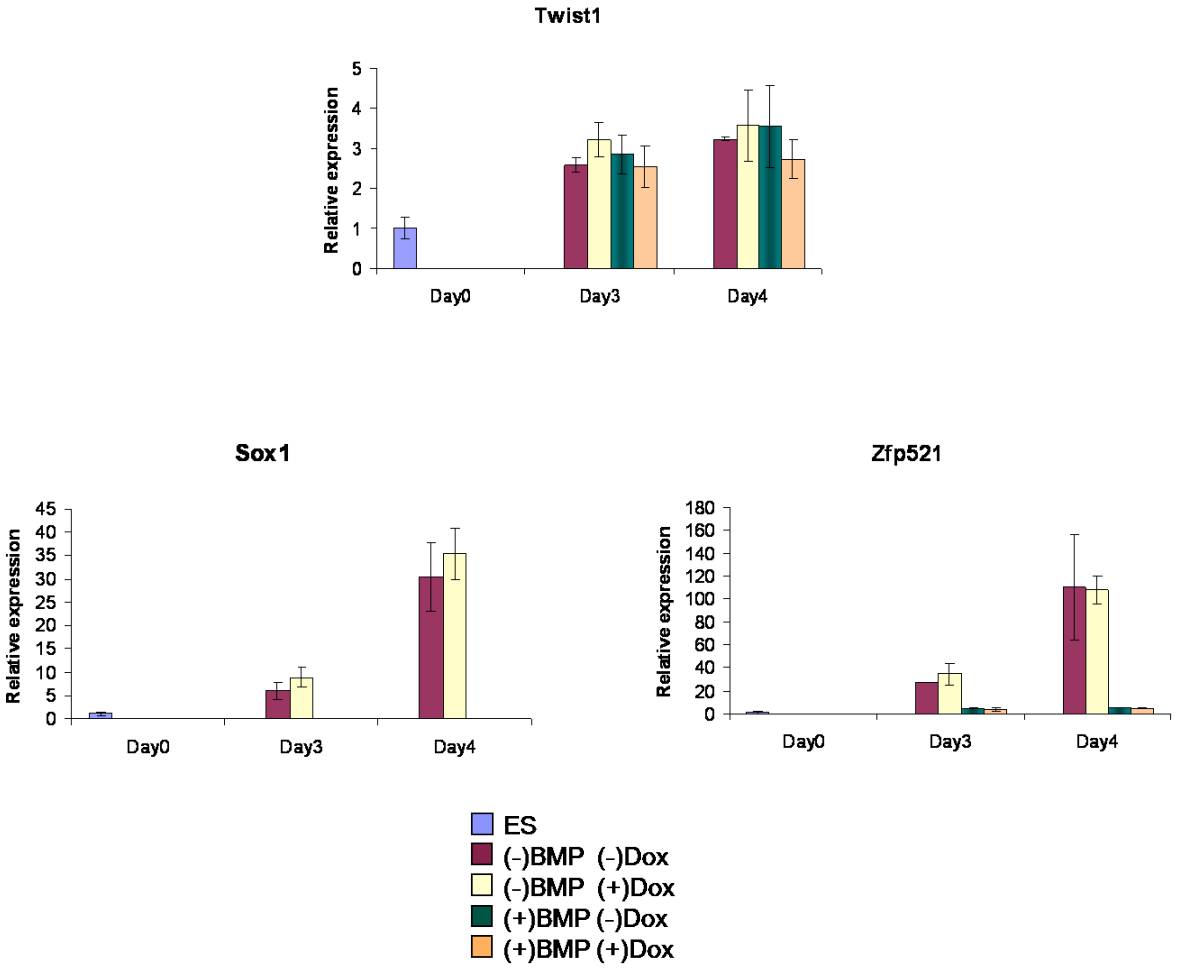
Twist1
Relative expression
5
4
3
2
1
0
Day0
Day3
Day4
Sox1
Relative expression
45
40
35
30
25
20
15
10
5
0
Day0
Day3
Day4
Zfp521
Relative expression
180
160
140
120
100
80
60
40
20
0
Day0
Day3
Day4
ES
(-)BMP (-)Dox
(-)BMP (+)Dox
(+)BMP (-)Dox
(+)BMP (+)Dox

Appendix 2. List of markers:

Marker	Expression	Used as
Ascl1	In a subset of dorsal neural cells and oligodendrocytes	Dorsal neural marker (Battiste et al., 2007)
Atoh1	Dorsal neural marker, marks the DI1 interneurons	Dorsal neural marker (Flora et al., 2007)
Brachyury	Primite streak	Primitive streak marker (Rivera-Perez & Magnuson, 2005)
Cdh1	Epiblast, surface ectoderm, other epithelial tissues	Epithelial marker (Aaku-Saraste et al., 1996; Van de Putte et al., 2003)
Cdh2	Neural epithelium, briefly expressed in the primitive streak and in certain subpopulations in the heart and lens	Marker of the switch from epiblast to neural epithelium (Aaku-Saraste et al., 1996; Van de Putte et al., 2003)
Eomes	in differentiating trophoblast cells, during gastrulation is expressed in the primitive streak and, later on it has important roles in the hematopoietic system	Primitive streak marker (Arnold et al., 2003)
Esrrb	ES cells	Marker of undifferentiated cells (Festuccia et al., 2012)
Fgf5	Highly upregulated during the transition from ES to epiblast cells. Subsequently, expressed at various levels in multiple cell types and organs.	Marker of epiblast cells (Pelton et al., 2002)
Fgfr1	in multiple cells and organs	To investigate its modulation by TW-E (Yamaguchi et al., 1992)
Gata2	early in development in the surface ectoderm, later expressed in a subset of mesenchymal cells, notably hematopoietic progenitors	Surface ectoderm marker (Sheng & Stern, 1999)

Gata6	In primitive endoderm, definitive endoderm and a subset of mesodermal cells	Endoderm marker (Morrisey et al., 1998)
Gli1	In response to SHH	Readout of SHH activity modulation (Lee et al., 1997)
Id1	In response to BMP4	Readout of BMP4 activity modulation (Lopez-Rovira et al., 2002)
Klf4	ES cells, later in development it is expressed in various cells and organs	Marker of undifferentiated cells (Guo et al., 2010)
Msx1	Early neural crest marker	Neural crest marker (Hill et al., 1989)
Nanog	ES cells	Marker of undifferentiated cells (Chambers et al., 2003)
Ncam1	Expressed in neural and neural crest cells	Marker of the switch from epiblast to neural epithelium (Rutishauser et al., 1988)
NESTIN	Neural progenitors	Neural progenitor marker (Dahlstrand et al., 1995)
Pax3	Expressed early in prospective dorsal neural and neural crest domains, and then in dorsal neural and neural crest cells and their derivates as well as in the somites	Dorsal neural and neural crest marker (Goulding et al., 1991)
Pax6	Dorsal neural tube	Dorsal neural marker immediately ventral to the domain specified by Twist1 (Liu & Niswander, 2005)
Pou5f1	ES cells	Marker of undifferentiated cells (Nichols et al., 1998)
Shh	In various cells and tissues. In development is actively involved in morphogenesis	Marker of ventral neural progenitors (Ang & Rossant, 1994)

Sox1	Neural progenitors	Marker of neural progenitors (Pevny et al., 1998)
SOX2	ES cells, epiblast and neural progenitors	Marker of neural progenitors differentiation (Wood & Episkopou, 1999)
Sox9	Early in neural crest precursor cells and in migrating neural crest cells, dorsal neural tube. It is also expressed in a subpopulation of the somitic mesoderm.	Dorsal neural and neural crest marker (Cheung & Briscoe, 2003)
Tcf15	ES cells, and early epiblast cells. During gastrulation its expression is restricted to the somitic compartment.	Somitic marker (Burgess et al., 1995)
TUBB3	Postmitotic neurons	Marker of postmitotic neurons (Tischfield et al., 2010)
Wnt1	Prospective midbrain progenitors, pre-delaminating and delaminating neural crest cells	Marker of neural crest (Echelard et al., 1994)
Zeb1	specifically expressed in the developing neuroepithelium	Marker of the switch from epiblast to neural epithelium (Takagi et al., 1998)
Zeb2	a subset of neural progenitors, as well as in neural crest and axial and paraxial mesoderm	Marker of the switch from epiblast to neural epithelium (Van de Putte et al., 2003)
Zfp521	Early in development in neural progenitors. Subsequently it is expressed in various cells of mesenchymal origin	Marker of neural progenitors (Kamiya et al., 2011)

Appendix 3. *Twist1* expression data from the literature

(a to d) published in Stoetzel et al, 1995. (a) primitive streak stage, (b) allantoic bud stage, (c) head fold stage, (d) somitic stage embryo. The expression pattern is very similar with the one reported here. The primitive streak expression can be observed in (b and c) as a very fine line which appears to be on top of the epiblast. (d to j) published in Fuchtbauer et al, 1995. (d to g) embryo considered at the primitive streak stage shown form anterio, posterior view, transverse and sagital section respectively. The presence of the allantois and of the head mesenchyme, which can be clearly seen in (a) indicate that this is probably an older embryo, closer to head fold. The expression is veri consistent with the present report. (h to j) transverse sections of somitic stage embryo. The neural tube seems clear and the signal can be only observed in the somites. In (j) the author reports a few positive cells in the neural tissue (black arrows) which he deems as delaminating neural crest. (k) published in Ang and Rossant, 1994. Head fold stage showing strong signal in the head mesenchyme and allantois.

a

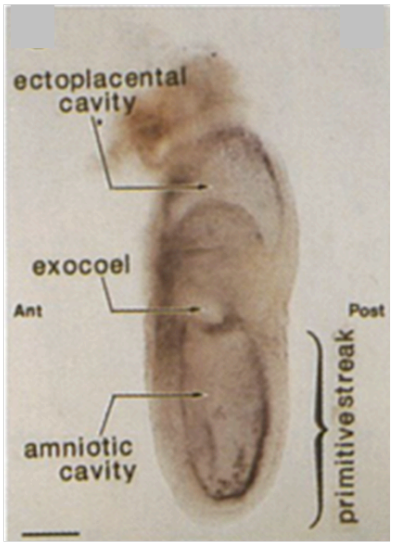

b

c

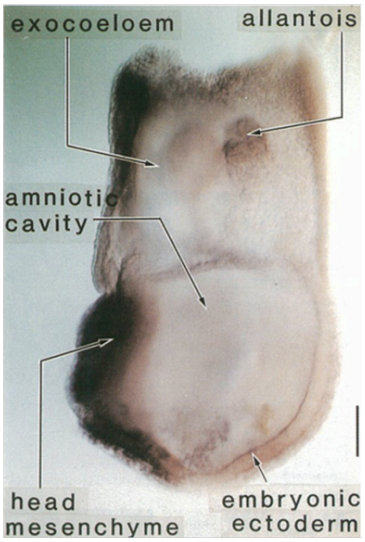

c

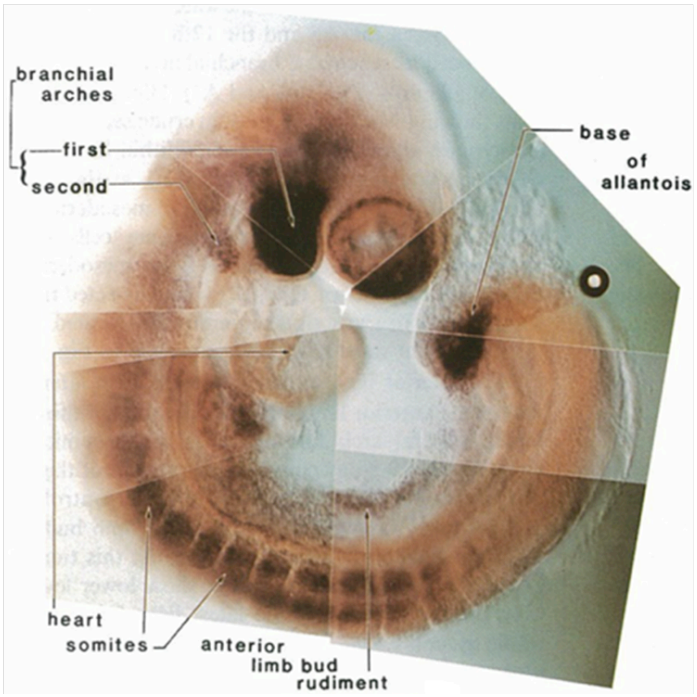

See next page:

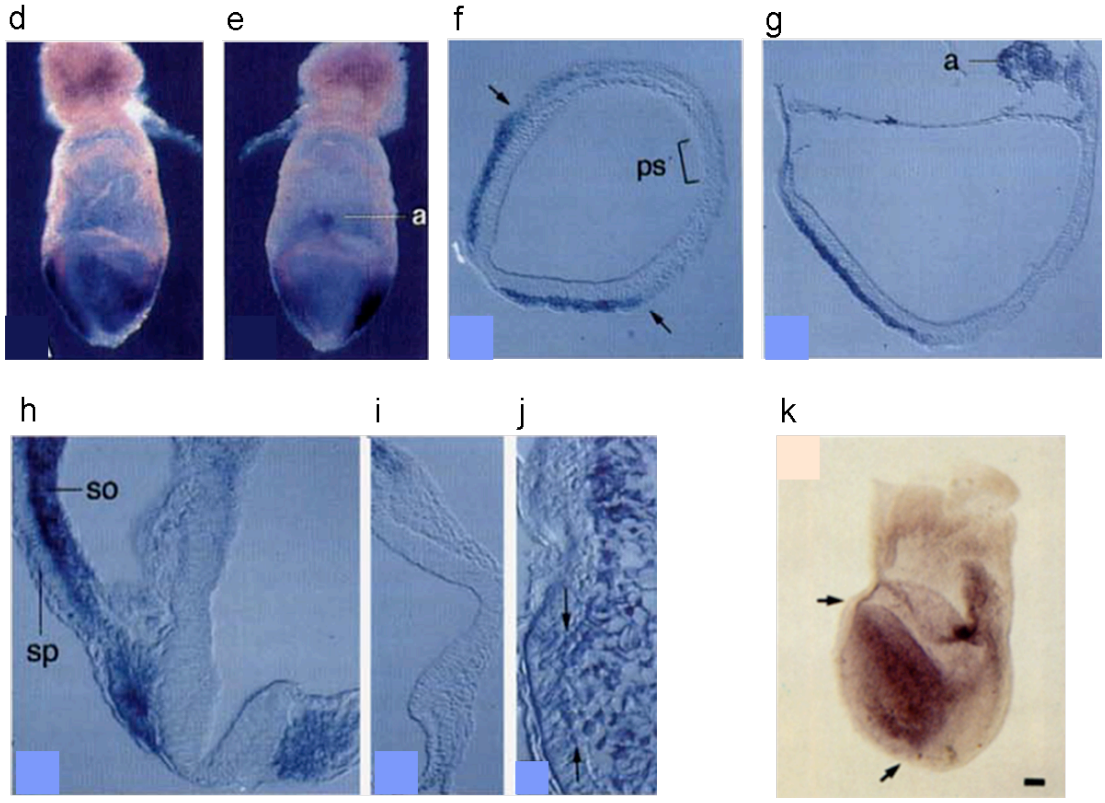
d
e
a
f
ps
g
a
h
so
sp
i
j
k

Appendix 4. Schematic map of the results presented in this thesis